Determining Long-Term Ecological Baselines in the Tropical Andes

Thesis

The Open University

Determining long-term ecological baselines in the tropical Andes

Bryan G. Valencia Castillo
B.Sc. Universidad Nacional de San Antonio Abad del Cusco
MSc. Florida Institute of Technology

Submitted in accordance with the requirements for the degree of Doctor of Philosophy

November 2014

Department of Environment, Earth & Ecosystems
Centre for Earth, Planetary, Space and Astronomical Research
The Open University
United Kingdom

DATE OF SUBMISSION: 10 APRIL 2014
DATE OF AWARD: 27 NOVEMBER 2014

ProQuest LLC.
789 East Eisenhower Parkway
P.O. Box 1346
Ann Arbor, MI 48106 – 1346

Determining long-term ecological baselines in the tropical Andes

A thesis presented for the degree of Doctor of Philosophy

by

Bryan Guido Valencia Castillo

MSc. (Florida Institute of Technology)

April 2014

Department of Environment, Earth & Ecosystems

Centre for Earth, Planetary, Space and Astronomical Research

The Open University

Milton Keynes

UK

Abstract

Conservation, restoration and management strategies are employed to maintain Earth's biological diversity and environment to a near "natural" state. But "natural" has included degraded landscapes.

The tropical Andes is a hotspot identified as a global conservation priority because of their high biodiversity, and threat to ecosystems by human activity and climate change. Our understanding of long-term (100-1000's year) natural ecological baselines is limited due to a paucity of studies in the Andes. In this thesis ecological baselines are identified for tropical Andean vegetation by comparing multi-proxy palaeoecological reconstructions (pollen, diatoms, charcoal, loss-on-ignition and magnetic susceptibility) derived from three lakes; Miski, Huamanmarca and Pacucha. These sites experience different levels of human impact today; Miski and Huamanmarca are undisturbed, Pacucha is disturbed.

The trajectory of vegetation change at the three lakes over the last *c.*12ka was determined, and compared, using Detrended Correspondence Analysis of multi-proxy data. The sites share a similar trajectory of vegetation change prior to *c.*7 ka. After *c.*7 ka Pacucha diverges from the other sites due to anthropogenic disturbance. Therefore natural ecological baselines for the tropical Andes can be determined from undisturbed sites from the last 3-2 ka, and disturbed sites from the last *c.*10 ka.

Fossilized tree pollen from across the tropical Andes was then used to test the hypothesis that, prior to human disturbance woodlands (dominated by Polylepis) formed a continuous 'belt' from Ecuador to Bolivia. A MaxEnt model based on 22 modern environmental variables and data derived from 13 Andean records were used to determine the spatial arrangement of Polylepis woodlands and suggests that they can naturally occur as a mosaic. The palaeoecological reconstructions confirmed that woodland mosaic predates human arrival (*c.*14 ka) and disturbances (*c.*7 ka). After *c.*7 ka, human disturbances further accentuated the woodland patchiness generating a hyper-fragmented landscape.

Acknowledgments

I would like to thank my supervisors William Gosling, Angela Coe, and Mark Bush for their guidance, support, and for sharing with me their time and wisdom. Mark and Will, I am grateful for your sincere advice, patience, and friendship. I have learned so much from you and hopefully I will remember enough to escape the hall of shame. I truly enjoyed the time we spend together in the lab, camping under a sea of stars and snow on the highest peak of the Andes or sitting on the roadside waiting for the police to report that our gear was stolen. Mark, Will, thank you so much... I whish I could be more eloquent! With some luck, we will keep working together, sharing ideas, and of course, those mythical stories with the power of hitting cows at high speed or making horses disappear in a blink of the eye.

I am thankful for the support and encouragement of past and current members of the mighty Paleolab, especially Crystal McMichael, Angela Rozas-Dávila, Dunia Urrego, Guaria Cardenes, Nicole Mosblech, Aaron Collins and Marco Raczka. Special thanks to Anne Rockholt, Majoi Nascimento, and Robert Van for counting the diatoms from Lake Miski; I really appreciate your help. Thank you Guillermo Jordan Garza (Golden Memo) for your friendship, help, jokes, R-chats, and the coffee that kept us awake when working after midnight. I shall not forget my brave friends that would have accompanied me to the end of the world to work, core lakes, or just to talk nonsense: Darcy Galiano, Marlene Mamani, Javier Silva, Patricia Guerra, Walter Huaraca, Bryan Rado, Lucy Vargas, Juan Tito, and Jorge Vargas. ¡Gracias!

Nothing would be possible without the following people that represent my own life:
Teito, quien me regaló la vida y me arrulló con voz de primavera aunque fuese invierno.
Guido, que me enseñó a sonreir y seguir adelante aunque todo parezca perdido.
Mi Mamá Epi, quien estuvo conmigo sin claudicar, incluso en los momentos más dificiles.
Angie, quien es la razón de mi vida, lo mas preciado que tengo, mis días de sol, lluvia mi musa y poesía.

Table of contents

List of figures

List of tables, scripts and equations

Chapter 1) Introduction

Conservation, restoration, and management practice in biodiversity hotspots aim to maintain the ecological value of these areas and mitigate threats from anthropogenic activities and ongoing climate change (Sanderson et al. 2002). However, for conservation, restoration and management efforts to be effective knowledge of the long-term (100-1000's years) natural ecological baseline conditions are required (Pauly 1995, Willis and Birks 2006, Willis et al. 2007). Without an understating of what the natural ecological baseline conditions are means that previously human modified environments could be mistaken as "natural". An absence of baseline ecological data could affect conservation, restoration and management in two key ways, by resulting in:

(i) A continuous recalibration of targets (ecological baselines) as perception of "what is natural" is modified through time; a phenomenon known as shifting baselines *sensu* Pauly (1995), and

(ii) A setting of 'false' targets (conservation/restoration goals), and consequently wasted effort, if human modified baselines are mistaken for natural baselines.

The main objective of this thesis is therefore to determine ecological baselines (i.e. natural vegetation assemblages) for the tropical high Andes (>3000 m above sea level [asl]) that can be applied to conservation, restoration and management of biodiverse ecosystems. New past environmental change data (e.g., pollen, diatoms, charcoal, and chemical analysis) for the last *c.*17 thousand years (ka) derived from three lake sediment cores, Miski, Huamanmarca and Pacucha, are presented. The concept of baselines is then applied to 13 records of past environmental change; the three new study sites, and reanalysis of 10 additional sites from the literature (Hansen and Rodbell 1995, Colinvaux et al. 1997, Hansen et al. 2003, Mourguiart and Ledru 2003, Paduano et al. 2003, Bush et al. 2005, Weng et al. 2006, Valencia et al. 2010b, Urrego et al. 2011, Williams et al. 2011a, www.ncdc.noaa.gov/paleo/lapd.html).

The overarching aim of this research is therefore to use the combined palaeoecological data to determine the ecological baselines for the high central Andes, and show how

they have varied through time. To achieve the overarching aim four specific research questions are addressed:

1. Temporal variation. Can any time period in the Holocene, i.e. last *c.*11,700 years (Walker et al. 2009), be used as representative of a natural ecological baseline for the high tropical Andean vegetation? (i.e. identify if there is a period of time without, or with minimal, human impact).

2. Spatial variation (climate). Are the study sites representative of climate change across the high central Andes? (i.e. evaluate if Miski and Huamanmarca were sensitive enough to record regional climatic events).

3. Spatial variation (vegetation). Is the observed modern woodland-grassland vegetation mosaic in the high central Andes a long-term feature of the landscape? (i.e. determine if there is evidence for continuous woodland or grassland across the region in the past).

4. Environmental parameters. What are the environmental factors that control the temporal and spatial distribution of vegetation in the high tropical Andes?

The geographic focus for the research presented in this thesis is the high tropical Andes which has been identified as being of high ecological value (biodiversity hotspot), and at risk losing its diversity due to direct human pressure and on-going climatic change (Orme et al. 2005, Malcolm et al. 2006, Feeley and Silman 2010). The current work focuses on palaeoecological reconstructions that provide insights regarding past alternate states of high Andean ecosystems under human influence. Palaeoecological reconstructions are not intended to generate conservation goals themselves but to provide a historical framework of past processes that should aid additional disciplines used in conservation in designing management plans. It is therefore hoped that the findings presented here will be useful for guiding ecological conservation, restoration and management practice in the region. Ensuring that this improved understanding of natural ecological baselines is communicated to policy makers is important to ensure

that: (i) realistic conservation, restoration and management goals are set, and (ii) the 'trap' of shifting baselines (trying to restore anthropogenic landscapes) is avoided.

1.1) Ecology of the tropical Andes

1.1.1) Overview

The tropical Andes[1] is a biodiversity hotspot that contains the largest number of endemic plants and vertebrates on the planet that are threatened due to habitat loss (Table 1.1, Myers 1988, Mittermeier et al. 1998, Myers et al. 2000). The tropical Andes spans from the north of Colombia and Venezuela to the north west of Argentina and north east of Chile, above 500m the area covering *c.*1.5 million km^2 (Fig. 1-1A). The Tropical Andes are also considered one of the most vulnerable hotspots to projected climate change and increasing anthropogenic activities (Myers et al. 2000, Orme et al. 2005, Malcolm et al. 2006, Feeley and Silman 2010).

Taxonomic Group	Species	Endemic Species	Percent Endemism
Plants	30,000	15,000	50
Mammals	570	75	13.2
Birds	1,724	579	33.6
Reptiles	610	275	45.1
Amphibians	981	673	68.6
Freshwater Fishes	380	131	34.5

Table 1-1 Biodiversity and endemism in the Tropical Andes. Data source: Conservation International (www.conservation.org).

The global distribution of plant species in the Neotropics is influenced by environmental and landscape heterogeneity (Gentry 1988, Pitman et al. 2001, Condit et al. 2002, Anderson et al. 2011). The complex topography of the Andes generates a variety of local environmental and micro-climatic conditions that favours speciation and

[1] Andean biodiversity hotspot located within the tropics

endemism (Hughes and Eastwood 2006). For instance, the local environment may be responsible for 70-75% of the floristic variability of a site highlighting the importance of climate variability linked to landscape heterogeneity (Tuomisto et al. 2003). In general, patterns of species occurrence and distribution can be predicted based on the environmental conditions of a given site; although the frequencies of particular occurrence of any species cannot (Terborgh and Andresen 1998, Tuomisto et al. 2003). Empirical data indicate that sites having similar environmental conditions are likely to share the same diversity patterns (Pitman et al. 2001) suggesting that environmental determinism has a strong influence of species distribution and diversity (ter Steege et al. 2013).

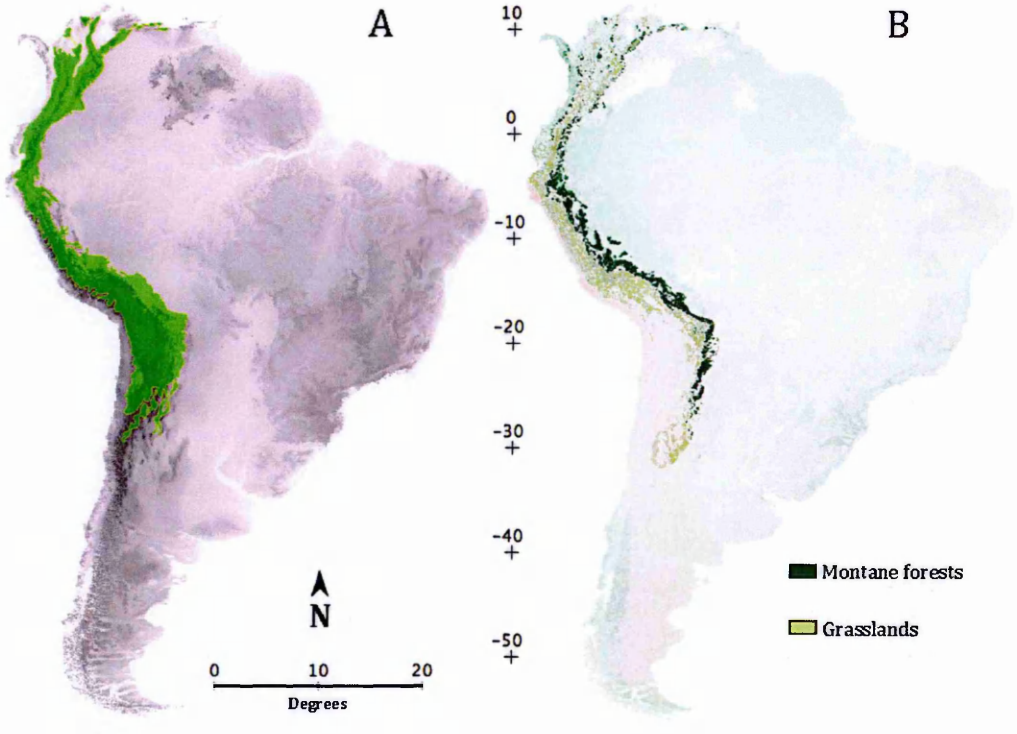

Fig. 1-1 Map of South America depicting the tropical Andes as a green contour (A) The montane forest and grassland biomes are depicted by olive and dark green contours (B). Panel B was modified from Eva *et al.*, (2004).

1.1.1.1) *Moisture availability and species distribution*

Species richness (number of species per unit area) is strongly correlated with annual precipitation and inversely correlated with increasing elevation (Gentry 1988). Gentry (1988) observed that the positive correlation of richness and precipitation was practically linear but that the relationship levelled off when precipitation was *c.*>4000 mm yr^{-1} (Fig. 1-2A). Precipitation patterns in the Andes are uneven at regional (e.g. eastern Andes[1]) or local (e.g. in a particular inter-Andean valley) scales and therefore favour the formation of discontinuous wet and dry spots, each one with a characteristic flora (Killeen et al. 2007, Bookhagen 2013). For instance, montane forests are mostly restricted to the eastern cordillera of the Andes and receive more rain than the central or western cordillera (Eva et al. 2004, Killeen et al. 2007). The tropical mountain forest (Fig. 1-1B) is one of the most important biomes based on land cover and diversity in the Eastern Andes (Eva et al. 2004). This biome is one of the wettest in South America because it is located in the eastern Andean slope. The Andes intercepts the moisture arriving from the Amazonia and the Atlantic Ocean favouring orographic precipitation in the eastern cordillera (Bookhagen and Strecker 2008).

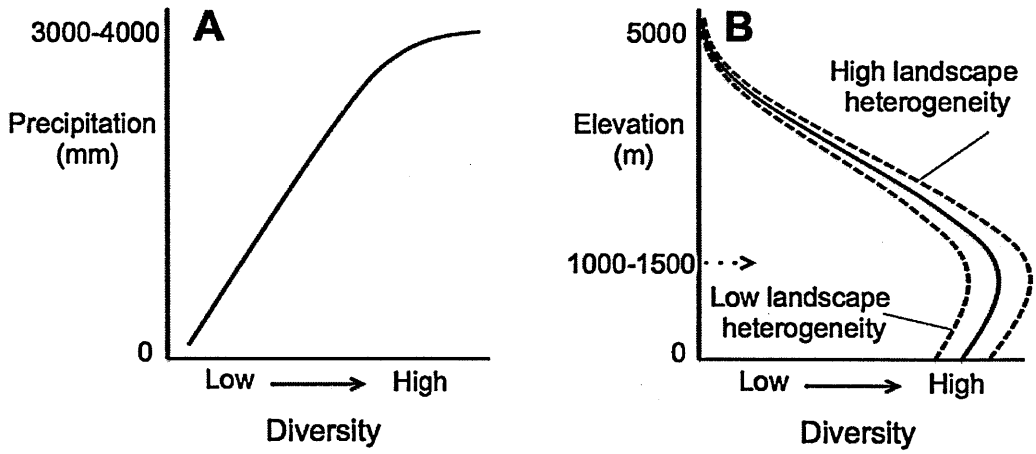

Fig. 1-2 Conceptual model of changes in diversity as a function of precipitation (A), elevation (B), and landscape heterogeneity (B); (Concepts derived from Gentry 1988, Rahbek 1995, Terborgh and Andresen 1998, Körner 2003, Tuomisto et al. 2003)

[1] Andean mountain chain that faces the Amazon basin

Cloud cover is also an important source of moisture in the Andes particularly during the austral winter when precipitation is low. Cloud cover generally persists throughout the year at elevations between 2000 and 3500 m in the eastern cordillera and induces horizontal precipitation (Hildebrandt and Eltahir 2008, Halladay et al. 2012). Ground-level cloud cover contributes with 20% of the water input in montane forests, but under extreme conditions may provide up to 40% (Hildebrandt and Eltahir 2008, Kessler et al. 2011). This additional moisture can play a critical role in shaping local habitats and biodiversity (Bendix et al. 2004, Sklenar et al. 2011). Orographic interception of wet Amazonian air masses underlies precipitation, cloud cover, and moisture availability on the eastern flank of the Andes, with a rainshadow effect building in the central Andean valleys. Essentially, the diminishing gradient in moisture availability can be used to predict overall biodiversity and the occurrence of endemic species (Gentry 1988).

1.1.1.2) *Temperature, elevation and species distribution*

Species richness is also affected by changes in elevation that drives temperature changes. On average, temperature in the Neotropics decreases by 5.5 °C with every 1000 metres of ascent (Bush et al. 2004b). Nevertheless, lapse rates ranging from 5.2 °C•1000 m^{-1} in everwet regions of Ecuador and 6.6 °C•1000 m^{-1} in the valleys of Colombia have been reported (Van der Hammen and Gonzalez 1965, Bendix et al. 2008). The sensitivity of lapse rates to the dryness of air is well-established (Brunt 1933). Consequently, elevation modulated by atmospheric humidity determines the temperature of any given site, which in turn influences the species distribution (Fig 1-2B). Although each species has its own particular elevation range (temperature range), maximum ecosystem richness is generally observed between 1000 and 2000 m asl (Rahbek 1995, Kessler 2000).

The continuous woodland cover generally has an upper elevation range of *c.*3500 m where mean annual temperature (*c.*15 °C) is *c.*17-19 °C colder than in the Amazon lowlands. Above 3500 m the continuous woodland cover transitions into the grassland biome (Fig. 1-1B) that can be climatically characterized by extreme temperature fluctuations (e.g. frost damage), high solar irradiance (UV damage) and low moisture content. Extreme climate conditions could be responsible of the diversity decline at high

elevations because they are beyond the tolerance for many species physiological limitations (Körner 2003, Hoch and Körner 2005, Bader et al. 2007).

1.1.1.3) *Soils and species distribution*

Complex soil dynamics may further contribute to habitat heterogeneity and be related to high species turnover. For instance, soil types were correlated with the distribution and composition of the vegetation in Neotropical forests (Terborgh and Andresen 1998, Phillips et al. 2003, Tuomisto et al. 2003, ter Steege et al. 2013). An exceptional example of habitat specialization related to species distribution was described by ter Steege (2013) where the commonest tree species (hyper dominants) in the Amazon were mostly adapted to a particular habitat (i.e. terra firme, várzea, white-sand forest, swamps, and igapó) or region (Guiana Shield and northwest, southwest, south, east, and central Amazonia) (ter Steege et al. 2013). Soil dynamics are closely related to topography and geology because topographic features control the redistribution of eroded material, soil formation and soil fertility (Quesada et al. 2009). Ultimately, soil patchiness and topographic features may influence the vegetation composition at local or even regional scales. For instance, at small scale, rich soils from river beds in Andean valleys rich in alluvial sediments can be interspersed with poor soils derived from landslides (Körner 2003). In inter Andean valleys is also common to find areas covered exclusively in herbaceous vegetation or mosses because shrubby and woody vegetation has been excluded by waterlogging. Woodlands are generally restricted to the edges of these water-saturated areas that are generally richer in organics forming inverted treelines (Young and León 2007).

1.1.1.4) *Landscape heterogeneity and species distribution*

Several of the endemic species in the tropical Andes are adapted to narrow altitudinal ranges or have patchy habitats (Terborgh 1977). For instance mountaintops could behave as discontinuous "sky islands" that are separated by deep valleys (Brown 1971, Warshall 1995, Foster 2001, Powledge 2003). Consequently landscape transformation

and fragmentation may have a strong impact on population dynamics especially when local extinctions further limits the step-stone connectivity between patches (Cochrane 2001, Renison et al. 2004, Young 2009). Ongoing climate change may exacerbate species extinctions, as species migrations may not cope with the projected changes within this heterogeneous landscape (Parmesan and Yohe 2003, Malcolm et al. 2006, Feeley et al. 2010, Larsen et al. 2011). Species vulnerability and widespread extinctions could be enhanced for high Andean endemics especially if desertification thresholds are reached (Kessler 2002, Bush et al. 2010, Larsen et al. 2011).

Overall, the Tropical Andes can be described as complex and heterogeneous in terms of species distributions, habitat, climate and topography. These characteristics accompanied by high vulnerability to projected climate change and anthropogenic impacts suggest that current assemblages are very likely to be degraded (Willis et al. 2004, Hastorf 2008). Palaeoecological information should be used to determine baselines and provide additional insights to assess vulnerability when designing or implementing conservation and management strategies (Willis et al. 2007, Dawson et al. 2011).

1.2) Climatic components in the tropical high Andes

1.2.1) Precipitation and clouds

Precipitation changes in the Andes result from the combination of different mechanisms that influence the distribution of moist air masses derived from the Atlantic Ocean. The moisture availability and transport is influenced over orbital (1000's years) to inter-annual timescales (Moy et al. 2002, Fritz et al. 2007). Precipitation at orbital timescales is mostly related to the amount of energy (insolation) that the Earth receives due to the Earth's orbital pathway (eccentricity) and orientation relative to the Sun (obliquity and precession, Hays et al. 1976, Imbrie et al. 1984, Berger 1992). During the late Pleistocene (20 ka) and the Holocene (modern time) insolation maxima have led to

increased precipitation in the Central Andes[1], the Altiplano[2], the western Amazon, and the southeast of Brazil (Baker et al. 2001, Gosling et al. 2008). These regions were out of phase relative to the central and eastern Brazil (Fig. 1-3) and known as the South American Precipitation Dipole derived from 27 precipitation reconstructions based on speleothems, lake, and ice core records (Cheng et al. 2013). In contrast, insolation minima were correlated with droughts and were less conspicuous than events produced at insolation maxima (Seltzer et al. 1998, Abbott et al. 2003, Hillyer et al. 2009). Precipitation changes at centennial or multi-decadal timescales were also related to variations in Sea Surface Temperature (SST) in the Northern tropical Atlantic (Marengo et al. 2008a, Baker et al. 2009). Low SSTs in the Atlantic were correlated with increased precipitation in Amazonia and the Andes (Peterson et al. 2000, Vuille et al. 2000b). Furthermore, the decline of the SST during Bond events was also coincident with enhanced precipitation in the central Andes during the Holocene (Bond et al. 2001, Baker et al. 2009). At interannual timescales precipitation in the central Andes was mostly controlled by El Niño Southern Oscillation (ENSO) activity (Moy et al. 2002, Bookhagen and Strecker 2010). The negative phase of ENSO brought additional moisture into the system while positive ENSO was related to dry episodes (Vuille et al. 2000b, Nepstad et al. 2004b, Haylock et al. 2006, Bookhagen and Strecker 2010). The onset or demise of events such ENSO can vary at millennial timescales (Moy et al. 2002). For instance, it was suggested that ENSO activity (i.e. 3-8 year periodicity) started around *c.*6 ka (Moy et al. 2002). The possibility that ENSO-human interactions had a synergistic effect on Andean settings is described in Chapter 5.

[1] Andean region between 10 °S and 30 °S
[2] Andean plateau located between Bolivia and Peru at c.3800 m asl

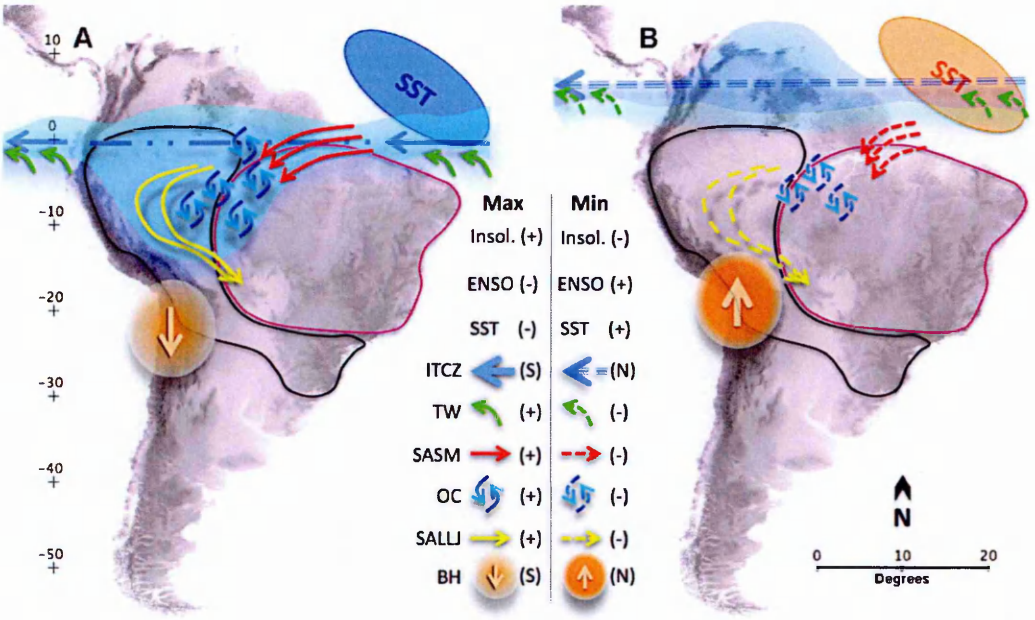

Fig. 1-3 Precipitation changes in the Andes based on multiple climate parameters. Conditions that theoretically enhance precipitation are depicted in panel A and conditions that theoretically diminish precipitation are depicted in panel B. Symbols "+" and "-" indicate a positive or negative state for each climate parameter while N and S indicate a northward or southward displacements respectively. The following abbreviations were used: Insolation (Insol.), El Niño Southern Oscillation (ENSO), North Atlantic Sea Surface Temperature (SST), Intertropical Convergence Zone (ITCZ), Trade winds (TW), South American Summer Monsoon (SASM), Organized Convection (OC), South American Low Level Jet (SALLJ), and Bolivian High (BH). The black and purple lines represent the South American Precipitation Dipole sensu Cheng (2013).

At any given timescale, precipitation changes in the Andes were closely related to the activity of Trade Winds, Amazonian organized convection, the South American Summer Monsoon (SASM), the South American Low Level Jet (SALLJ), the position of the Inter Tropical Convergence Zone (ITCZ), and the position of the Bolivian High (Lenters and Cook 1997, Zhou and Lau 1998, Peterson et al. 2000, Garreaud and Aceituno 2001, Haug et al. 2001, Garreaud et al. 2003, Bush and Silman 2004, Marengo et al. 2004, Wang and Fu 2004). Each of these processes can occur in a positive (enhanced) or negative (diminished) phase depending on the timescale and their mutual interactions. Because multiple combinations are possible, it becomes more convenient to define their behaviour based on a theoretical maximum or minimum output (Fig. 1-3). Periods of maximum precipitation in the Central Andes would result

from the combination of maximum insolation, Negative ENSO, low SST, enhanced trade winds, southward displacement of the ITCZ, enhanced SASM, enhanced organized convection, enhanced SALLJ, and southward displacement of the Bolivian High (Fig. 1-3A); conversely maximum drought would follow the opposite phase for each of the listed factors (Fig. 1-3B).

In general, multiple South American records highlight the southward displacement of the ITCZ with the strengthening of the SASM and the Trade Winds as drivers of increased precipitation (Wang et al. 2004, Sylvestre 2009, Bush et al. 2010, Urrego et al. 2010). Moisture transport is mostly restricted to the austral summer and coupled to positive easterly airflow (Vuille et al. 2000b, Garreaud and Aceituno 2001). Some studies portrayed dry scenarios when precipitation was at its forcing-mechanism maxima (wet conditions) generating active debate about precipitation patterns in the Andes related to driving forces, sources and timing at millennial timescales (Thompson et al. 1998, Betancourt et al. 2000, Mourguiart and Ledru 2003). However, the complex topography of the Andean chain may explain the coexistence of simultaneous wet and dry conditions independent of the total moisture available at any given time. For example, the Andes is a topographic barrier that intercepts moisture derived from the Atlantic. Furthermore heating differences due to irregular Andean landscapes may induce a preferential moist distribution depicted as wet and dry spots at regional scales (Killeen et al. 2007). At local scales, differences in moisture availability can favour the occurrence of two or more neighbouring vegetation types. For instance, xerophytic vegetation could be present in areas adjacent to cloud forests.

1.2.2) Temperature and climate

Insolation can be regarded as the pacemaker for temperature change at millennial timescales (Hays et al. 1976, Shackleton 2000). During the Last Glacial Maximum (LGM) temperatures in the high Andes[1] were about 5-7 °C cooler than modern (Hooghiemstra 1984, Paduano et al. 2003, Valencia et al. 2010b). Depending on the

[1] Andes above *c.*3000 m asl

moisture availability glaciers expanded to their maximum extent by *c.*21 ka reaching elevations of *c.*1.5 km below their modern location (Porter 2001, Smith et al. 2005). The onset of the deglaciation started between *c.*23 and 21 ka producing a glacial retreat highly dependent on the local geographic conditions (Seltzer et al. 2002a, Smith et al. 2005). Vegetation changed gradually influenced by the warming starting at *c.*21 ka although the warming signal became more evident after *c.*18 ka (Bush et al. 2004b, Bush et al. 2005, Valencia et al. 2010b). The vegetation shift was unidirectional changing from grassland to forest types suggesting that temperature rose gradually (Paduano et al. 2003). Evidence of abrupt thermal reversals like the Younger Dryas (YD) (Steig et al. 1998, Thompson et al. 1998) were absent in Andean vegetation records (Paduano et al. 2003, Bush et al. 2004b, Williams et al. 2011a). However, temperature fluctuations were perceived prior the YD but never reaching LGM-like conditions, i.e. cooling of 5-7 °C (Paduano et al. 2003). In contrast, data derived from ice cores suggested that the Andes experienced the YD almost synchronously with records from the northern hemisphere (Thompson et al. 1998, Thompson 2000, Hodell et al. 2008). These changes suggested a thermal decline analogous to full glacial conditions. Finally, during the Holocene, temperatures were fairly constant.

1.2.3) Temperature and elevation

Temperature and elevation are strongly correlated and can effectively be used interchangeably. Today temperature decreases by 5.5 °C for every 1000 metres of ascent in the Central Andes (Bush et al. 2004b). This thermal change is known as the moist-air adiabatic lapse rate (hereafter lapse rate). Lapse rates are relatively insensitive to change if moisture conditions remain constant (Blandford et al. 2008), else, lapse rates would constantly change with time of the day and season (Bendix et al. 2004). Therefore, while lapse rates should vary between regions, e.g. Andes of Peru versus Andes of Colombia (Van der Hammen and Gonzalez 1965, Bush et al. 2004b, Bendix et al. 2008), at a given location, without strong alteration of relative humidity, they are generally assumed to be constant through time (Webster and Streten 1978, Rind and Peteet 1985). Elevation is also related to changes in atmospheric pressure that reduces the partial pressure of the atmospheric components. The concentration of atmospheric

gases such as oxygen and CO_2 decline as elevation increases although their proportions will remain the same at any elevation due to homogeneous atmosphere mixing. Changes in moisture availability can also be expressed as a function of elevation. The reduction of temperature as elevation increases reduces the saturation vapour pressure limiting air moisture content (Körner 2003). Moisture content may also be dependent on surface heating as a function of solar radiation (Körner 2003). Consequently moisture circulation patterns may change at seasonal or daily scales (Rapp and Silman 2012). Atmosphere thinning is related with extreme thermal fluctuations at high elevations. Rapid nocturnal heat-loss is common especially during the austral winter when reduced atmospheric moisture favours night time frost (Bush and Silman 2004). Above the treeline, the differences between maximum and minimum daily temperatures can reach values between *c.*20 and 30 °C (Kessler 2006, Bader et al. 2007). In contrast, seasonal changes may only influence a fraction (few degrees) of the daily variation through the year. The incidence of ultraviolet radiation at higher elevations is also an effect of atmospheric thickness. High irradiation is typical of paramo and puna settings that increases with elevation (Bader et al. 2007). For instance, radiation may exceed the extra-terrestrial solar constant (1360 W m^{-2}) in areas where direct and diffuse light beams overlap (Thekaekara and Drummond 1971, Körner 2003).

1.2.4) Vegetation and climate change

Vegetation in the tropical high Andes is expected to change as Earth's climate change. However, the synergic effect of projected climate scenarios and landscape transformation should limit species migrations and favour extinctions as land and water resources became actively managed (Hannah et al. 2002, Malcolm et al. 2006, IPCC 2013). Anthropogenic impacts were particularly detrimental for species with narrow spatial distributions, typical of tropical Andean species (Bradley et al. 2006, Anderson et al. 2011, Young 2011). General and regional circulation models (GCM, RCM), despite the uncertainties, predicted species migration due to warming (2.5-3.5 m yr^{-1}), a pattern currently observed in tropical plant species (Feeley et al. 2010, Bae et al. 2011, Chen et al. 2011). Although GCMs provide insights at lower spatial resolution than RCM, GCM can be fully coupled (ocean, atmosphere, land, and vegetation interactions) (Cox et al.

2000, Raper and Giorgi 2005). Coupling provides a complete spectrum of future scenarios that can be used by policymakers to implement strategies in fields like conservation or management (IPCC 2013). Although downscaling methods are currently being implemented (e.g. CORDEX, http://wcrp-cordex.ipsl.jussieu.fr), downscaling methods in RCM may increase result uncertainties and should be evaluated with caution (Chen et al. 2011). Species extinctions due to the synergistic effects of climate and human activities were also predicted by GCMs (Orme et al. 2005, Malcolm et al. 2006). However, models generally lack of enough resolution to depict the complex climatic heterogeneity of the tropical Andes as a reflection of its topography (Killeen et al. 2007, Urrutia and Vuille 2009). Uncertain climatic scenarios and the poor knowledge of the biological richness of tropical Andean species make any assessment difficult.

Climate change may alter the hydrological budget of the high Andes, particularly if, as projected, ENSO becomes more frequent and induces an increasing number of droughts that favour fire events (Asbjornsen et al. 2005). The synergistic effect of climate change and land use may also boost the intensity and frequency of fire events promoting fragmentation (Cochrane 2001, Laurance et al. 2001, Nepstad et al. 2004a). Fragmentation changes the forest structure and composition increasing tree mortality, temperature variability, light, desiccation, and wind disturbance, inducing the formation of edges that become fire prone (Laurance et al. 2001, Barlow 2002, Cochrane and Laurance 2002, Laurance 2004). In the eastern flank fires were associated with shifts in family importance and diversity (Oliveras et al. 2013). As fire becomes more recurrent, due to a positive feedback, it reduces seed availability, pollination and seed dispersal preventing the recovery of fire-intolerant species (Cochrane et al. 1999, Barlow 2002, Cochrane 2003).

Moisture deficit in the Andes is not exclusively related to ENSO events. Modern anomalies in the north Atlantic SST (warming events) were also responsible of droughts in Amazonia and the Andes (Marengo et al. 2008b, Zeng et al. 2008). Although the mechanisms driving this event are yet to be identified, anomalous warming in the north Atlantic SST prevents the southward migration of the ITCZ (Fig. 1-3B). Consequently

past moisture decline in Amazonia and the Eastern flank of the Andes could also be related to the incidence of SST anomalies.

High Andean ecosystems are very sensitive to climate change and species are currently migrating upslope due to increasing temperatures (Feeley et al. 2010). However, the high incidence of anthropogenic fires and the enhanced flammability of vegetation due to moisture reduction prevent the actual migration of species above current treelines (Bush et al. *in rev.*) showed that transitional areas between woodlands and grasslands were expanding and areas that in the past had a woodland signal also became transitional. In general the projected climate may favour droughts; therefore, induce the fragmentation of Andean woodlands due to increasing fire events. The contraction and alteration of Andean ecosystems may also produce economic and social problems related to ecosystem services (Anderson et al. 2011).

1.2.5) Ecosystem services

Historically, people from the high Andes benefitted from a wide range of ecosystem services. A full review is beyond the scope of this thesis, but examples of the four categories of ecosystem service identified by the UNEP Millennium Ecosystem Assessment report (2001) are provided.

1) Provisioning Services: These services supply food, water and the essentials of life. Water and wood supply have been essential and, at times it has been suggested, scarce resources for Andean communities. In the mid-Holocene a dry event that caused lakes to dry up resulted in much of the Atacama Desert being abandoned by its human occupants (Nunez et al. 2002). Currently, Quito and Bogota (capitals of Ecuador and Colombia) maintain a combined population of 10 million (Anderson et al. 2011) and are reliant upon water derived from glaciers and the paramo. Ice caps are retreating rapidly in the high Andes due to rising temperatures with reported warming rates of +0.34 °C/decade (Vuille et al. 2008). Ice cap retreat should reduce the amount of water available through gradual melting with impacts on water direct consumption, hydropower generation, agriculture, diversity maintenance, and ecosystem integrity especially for Bolivia, Colombia, Ecuador and Peru (Buytaert et al. 2006, Anderson et

al. 2011). High Andean woodlands have long been used as a source of wood and charcoal. An apparent fuel shortage has been suggested as the cause of Incan regulations that prohibited the citizens of Cusco from clearing Polylepis woodland (Chepstow-Lusty and Winfield 2000).

2) Regulating Services: These are services that regulate large biogeochemical cycles. Organic-rich soils in the montane forests and Puna are responsible for substantial carbon sequestration. Despite the aboveground biomass being lower than in lowland evergreen forest, the belowground carbon stocks are so high that montane ecosystems can store as much or more carbon than an equivalent area of lowland forest (Leuschner et al. 2013). Similarly, precipitation effectively regulates the annual formation of snowpack, which in turn contributes to the formation of glaciers, and water supply.

3) Cultural Services: These services cover the spectrum of non-use values of a system ranging from aesthetics to spirituality. The indigenous traditions of Andean cultures centered upon their relationship to the Andes, e.g. the Incan Goddess Pachamama. Nowadays, ecotourism is one of the fastest growing industries, which draws heavily on the aesthetic appeal of Andean landscapes.

4) Supporting Services: These services provide value to more remote locations. An Andean example would be the erosion of Andean rocks to provide the clays that wash downstream to form the white-water rivers of the Amazon (Jordan 1985). These rivers, also known as varzea systems, are the most fertile of Amazonian systems, because of the nutrients provided by the Andes.

Despite the importance of the ecosystem services provided by the high Andean woodlands, only small woodland areas are protected. For instance in 2009, only 15% of the high Andean *Polylepis* woodlands in the Andes (Venezuela, Colombia, Ecuador, Peru and Bolivia) were reported as protected, compromising the provision of ecosystem services (Josse et al. 2009). Landscape transformation and the extraction of mineral resources could further compromise the ecosystem services provided by the high Andean woodlands especially when occurring in Andean headwaters (Rodbell et al. 2013). These issues may force the relocation of cultivation fields and cities into new areas leading to the replacement of Andean woodlands.

1.3) Human activities in the Andes

1.3.1) Prehistoric landscapes

The origin of the human occupation in South America and the Andes is constrained to the Pleistocene-Holocene transition. Evidence of human occupation predating the Holocene has been found at low elevations and coastal sites such as Monte Verde at *c.*14 ka, or Monte Alegre at *c.*12 ka (Roosevelt et al. 1996a, Haynes 1997, Dillehay et al. 2008, Fig. 1-4). The archaeological evidence of human occupation in the Andes that predates the Holocene is limited to few sites and the dating of these has been questioned (Bryan and Gruhn 2003, Piperno 2007, Aldenderfer 2008, Dillehay 2008). The earliest occupation of the Andes probably started with intermittent incursions of coastal people at or below 2600 m in sites like Guitarrero, Puente and Toquepala centred at 12 ka (Fig. 1-4) (Lynch 1980, Lynch 1985, Aldenderfer 2008). Sites between 3400 and 4200 m like Lauricocha, Jiskayrumoko, Asana, Telarmachay and Pachamachay became occupied during the early Holocene i.e. between *c.*10 and 8 ka (Pires-Ferreira et al. 1976, Lavallée 1987, Aldenderfer 2008).

During the early stage of human occupation of the highlands landscape modification can be related to low-density human populations clustered in small mobile groups. Human adaptive radiation at high elevations was suggested to be slow due to physiological constraints (hypoxia) combined with harsh climate, limited resources and landscape heterogeneity (Aldenderfer 2008, Dillehay 2008). Despite the assumed low population densities, early hunters could have modified large woodland landscapes if fire was regularly used for hunting (Kessler 2002). Consequently, high Andean woodlands could have contracted or fragmented modifying the position of the treeline as fire events became frequent. In the driest sections of the Andes, e.g. the Altiplano, fire has been a natural component of the landscape for >350,000 years (Hanselman et al. 2011b).

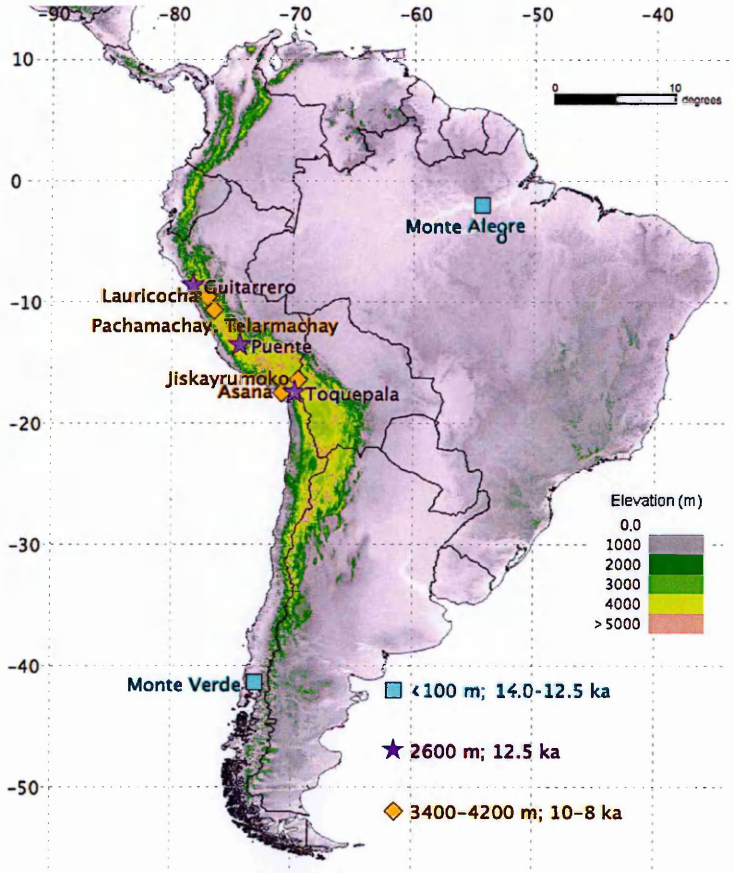

Fig. 1-4 Map showing the sites where there is evidence of the earliest human occupation of the South American High Andes.

The inability to differentiate between natural and anthropogenic fires in charcoal records requires that both fire records and independent climate records are considered when determining the onset of human activity at a location. An uncertain impact of early human colonists was the eradication of the megafauna. The uncertainty comes from the scale of the extinction caused by climatic change versus human hunters (Barnosky and Lindsey 2010). The loss of at least 57 genera of megafauna is anticipated to have had profound effects on communities, fire frequencies, and the balance of plant functional types (Gill et al. 2009, 2012, Rozas-Davila 2012).

The development of agricultural practices during the mid- and late-Holocene may have altered substantially the landscape. For instance, the origins of cultivation, early

horticulture and plant domestication are considered to start around *c.*10 ka (Piperno and Stothert 2003, Stothert et al. 2003, Dillehay et al. 2007, Pearsall 2008). Plant domestication was probably synchronous between the Northern and Central Andes. The recovery of a variety of edible lowland species such as capsicum, lima beans and lucuma at Guitarrero Cave (Lynch 1980) suggest that human were transporting goods between lowlands and highlands. Although plant domestication started around *c.*10 ka, early agriculture and the use of irrigation systems dates between *c.*6 and 5 ka and was restricted to coastal river valleys (Shady-Solis et al. 2001, Dillehay et al. 2005). However, cultivation may have being practiced in the High Andes at a scale large enough to be conspicuously registered in the pollen record despite the paucity of earthworks at *c.*6 ka, e.g. around Lake Pacucha (3100 m asl).

Small villages and hamlets were evident by *c.*3.5 ka in the Cusco area (Chávez 1980, Bauer et al. 2010) and Apurimac (Grossman 1972, Bauer et al. 2010) during the formative period (Fig 1-5). Cultivation in these regions was probably based on quinoa or amaranth crops before switching to maize around 3 ka (Mosblech et al. 2012). Later occupation is related with cultures such as the Wari, Tiwanaku and Chanka starting at *c.*1.4 ka followed by the Inca between *c.*700 and 550 years BP (Fig. 1-5) (Chepstow-Lusty et al. 2003). Historical and palynological records suggest that forest resources were actively managed by the Inca (Chepstow-Lusty et al. 2009). However, the managing practice probably originated during the period of the Wari dominance (Sublette et al. 2012).

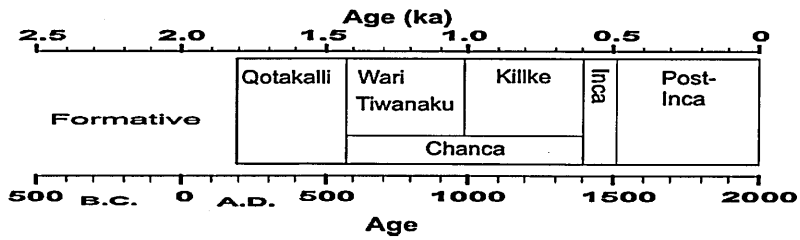

Fig. 1-5 Cultural stratigraphy for the Central Andes (Bauer 2004) modified from Chepstow-Lusty (2009).

In general, landscape modification became evident with the development of civilizations probably influenced by climate during the last four millennia. The onset or demise of civilizations such as the Wari and Tiwanaku were related to major climate fluctuations (Binford et al. 1997, deMenocal 2001). As civilizations expanded and populations became larger, requirements for food and construction resources increased (Hastorf et al. 2005, Hastorf 2008). Landscapes were modified as cultivation areas expanded. The use of wood for fuel, construction or tool manufacturing implies that woodlands were under constant human pressure. The depletion of wood resources may have triggered the onset of agroforestry practices and active management of the woodlands that probably started with the Wari (Mosblech et al. 2012). The post management woodland recovery should have had a positive impact on the fauna, enhanced water retention and minimize slope the erosion besides providing a sustainable wood supply. However, the interaction between resource availability and resource utilization was likely paced by climate change modulating the ecosystem services (e.g. water availability) (Gosling and Williams 2013). For instance, the collapse of the Wari culture at *c.*1.1-1.0 ka hindered the woodland management as the population of this civilization collapsed due to a drought. During the same period woodlands, mostly represented by *Alnus*, experienced a decline recorded in the Huaypo record (Mosblech et al. 2012). Therefore, ecosystem services gained through landscape management were diminished as the drought progressed at *c.*1.1-1.0 ka and showed the close interaction of climate over resource availability and ecosystem services (Gosling and Williams 2013). Woodland management was also observed during the expansion of the Inca Empire. Pollen records from lakes Marcacocha, Huaypo and Pacucha registered peaks of *Alnus* pollen and support the idea of agroforestry woodlands expansion prior the conquest of the Inca (*c.*0.5 ka) in hands of Europeans (Chepstow-Lusty et al. 1996).

1.3.2) Modern Andean landscapes

Most contemporary landscapes at elevations above 3000 meters above sea level (m asl) are heavily modified by human activities (Paduano 2001, Paduano et al. 2003, Valencia 2006). In general, native woodlands are restricted to areas unsuitable for agriculture, construction, (Fjeldså 2002b, Kessler 2002). The dominance of grasslands over

woodlands is also considered an artefact of periodic burning that promotes resprouting for livestock grazing (Kessler 2002). Modern human-made landscapes are mostly represented by scattered native trees immersed in a grassland matrix (Fig. 1-6).

The introduction of exotic tree species such as *Eucalyptus* and *Pinus* among others species, further constrained the distribution of native Andean woodlands in areas not suitable for agriculture. The fast-growing *Eucalyptus* introduced the during 1960's (Luzar 2007) was preferred over the native species such as *Alnus, Polylepis, Escallonia, Podocarpus* and *Buddleja* that are slow growing (Hoch and Körner 2005). Native trees have lower net primary productivity than introduced or lowland trees (Girardin et al. 2010). Consequently, exotic species are generally planted replacing the native woodlands. In high Andean rural areas, native woodlands are regarded mostly as fuel source (Wunder 1996) as they cannot be used in construction. For instance, native tree species like *Polylepis,* and *Escallonia* have a twisted and short trunk in contrast to *Eucalyptus* that has a long and straight one. Consequently, *Eucalyptus* plantations are generally viewed as more advantageous than native trees. Currently plantations of exotic trees are extremely common in the Andes and locals generally assume they are a native species.

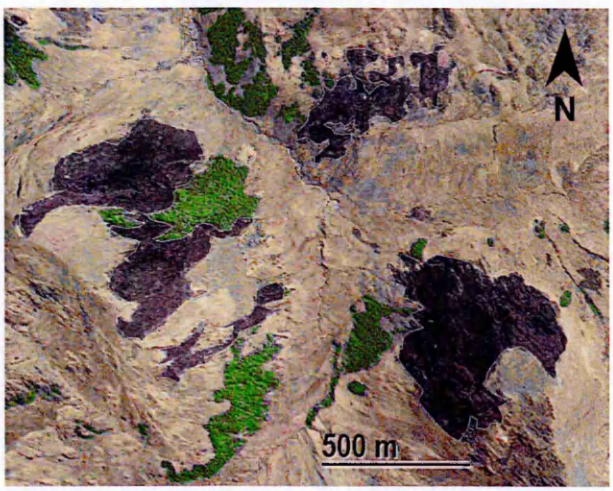

Fig. 1-6 Example of Andean landscape in the Central Andes. Woodlands (green) are surrounded by grasslands (brown) and burned areas (black). Image derived from Google Earth 7.0.3.8 centred at 8.553°S, 76.904°W at 3600 m.

The arboreal vegetation in sites with minimal human impacts can be divided into humid and dry woodlands. Most of the humid woodlands are located in the Eastern cordillera and inter-andean valleys that receive more than 800 mm of annual precipitation (Young 2006). Tree species of humid woodlands mainly belong to the following families: Rosaceae (*Polylepis, Hesperomeles*), Podocarpaceae (*Podocarpus*), Chloranthaceae (*Hedyosmum*), Buddlejaceae (*Buddleja*), Betulaceae (*Alnus*), Myrtaceae (*Myrcianthes*), Cunnoniaceae (*Weinmannia*), Aquifoliaceae (*Ilex*), Escalloniaceae (*Escallonia*), Myrsinaceae (*Myrsine*), Symplocaceae (*Symplocos*), and Elaeocarpaceae (*Vallea*). On the other hand, dry woodlands are mostly restricted to the Central cordillera and inter-andean valleys that receive less than 800 mm of precipitation per year. The following families are well represented in dry woodlands: Mimosaceae (*Mimosa*), Caesalpinaceae (*Senna, Caesalpinea*), Fabaceae (*Erythrina*), Bignoniaceae (*Delostoma, Tecoma*), Bombacaceae (*Eriotheca*), Anacardiaceae (*Schinus*) (Aguirre et al. 2006).

Most of the continuous woodlands generally reach elevations between 3300 and 3800 m asl (metres above sea level) due to environmental and physiological constraints besides the human disturbances (Hensen 2002, Körner 2003, Cierjacks et al. 2007a). Above the treeline occur the grasslands separated from the continuous woodlands by a narrow transition zone composed by a mixture of woodlands and grasslands species or few ecotone specialists like *Bejaria* or Melastomataceae. The most representative grassland species belong to the following families: Poaceae, Asteraceae, Caryophyllaceae, Apiaceae and Gentianaceae (Troll 1968, Graf 1981, Young and Leon 1990). Grasslands can also be divided into humid and dry types. Humid grasslands occur mostly in the northern Andes and composed of species from the families Asteraceae (*Espeletia, Chuquiraga, Pentacalia*), Gentianaceae (*Halenia, Gentianella*), Plantaginaceae (*Plantago*), Valerianaceae (*Valeriana*), Hypericaceae (*Hypericum*), Melastomataceae (*Disterigma*), Ericaceae (*Vaccinium)* Apiaceae (*Azorella*), Rosaceae (*Lachemilla, Potentilla*), Poaceae (*Paspalum, Calamagrostis, Neurolepis*). In contrast, dry grasslands were mostly represented by species of the family Poaceae (*Stipa*, *Calamagrostis*, *Festuca*) and xerophytic taxa.

all of them mainly driven by high demographic growth rates) of

1.4) Andean treelines

Treelines are represented by the upper elevational limit of arboreal species beyond which physiological and climatic limitations impair their successful biological development. Andean treelines in the Central Andes generally occur between c 3300 to 3800 m asl. The treeline position results from the interaction of climatic elements, topography, substrate, vegetation dynamics and human intervention (Young and León 2007). Consequently, single factors are unable to explain or define the treeline position at regional or even at local scales (Holtmeier and Broll 2005). Treelines should be viewed with caution as they are not fixed belts along the Andes (van der Hammen and González 1960, Hooghiemstra and van der Hammen 1993) but transitional zones between continuous woodlands and grasslands with assemblages that may vary over time. Overall, specific causes that control treeline elevation are yet to be identified. Below I define a list of possible parameters that influence the formation of Andean treelines.

- Mean temperatures: Körner (Körner 2003) hypothesized that minimum mean temperatures could be responsibly of the formation of treelines as growth is inhibited at cellular level in seedling populations constraining and upward expansion of the treeline.
- Frost: At and above treeline elevations night frost is a common event that increases in frequency and intensity with elevation. Frost is responsible for tissue damage that may limit the dispersal of tree species above treeline elevation (Bush and Silman 2004, Piper et al. 2006).

- Sun damage: The solar constant (*c.*1360 W m^{-2}) above treeline may be exceeded in *c.*150 W m^{-2} when direct sunlight is enhanced by diffuse (cloud diffuse transmittance) incidence. Sunlight may produce desiccation, overheat, photoinhibition, and UV cell damage reducing seedling survival at and above treeline elevation (Barber and Andersson 1992, Körner 2003, Bader et al. 2007).

- Precipitation: moisture availability generally decreases with elevation and could become a limiting factor at treeline elevation (Morales et al. 2004).
- Topography: The relief and slope orientation of Andean mountains should control temperatures (i.e. elevation), sunlight and shade that influence temperatures, and orographic moisture interception (e.g. rain) that produces runoff and leads to soil formation (Brown 1994, Killeen et al. 2007, Bookhagen and Strecker 2008, Stueve et al. 2009). Therefore, topography may indirectly influence treelines through its influence on other factors.
- Fires: Natural or anthropogenic fires could also delineate the treeline position (Stueve et al. 2009). Fires can depress treelines altering the woodland species composition (Oliveras et al. 2013). Anthropogenic fires in particular were considered detrimental and the main cause for fragmentation in high Andean ecosystems (Ellenberg 1958, Kessler 1995).
- Humans: Multiple anthropogenic activities can induce the treeline depression. Fires and change in land use (e.g. agriculture) are probably the most common ones.

1.5) Treeline and *Polylepis*

Polylepis is a genus of the family Rosaceae with 26 species distributed along the tropical Andes from Venezuela to the north of Chile and Argentina (Bitter 1911, Simpson 1979, Kessler and Schmidt-Lebuhn 2005). The current taxonomy of the genus is based on morphologic, biogeographic and ecological characters that exclude molecular analysis due to inconsistent results deriving from the high degree of hybridization in the genus (Kerr 2004, Kessler and Schmidt-Lebuhn 2005, Schmidt-Lebuhn et al. 2006). For instance two different species growing close were genetically more similar than two individuals of the same species growing distant from each other. Furthermore, the hybridization of *Polylepis* with the herbaceous *Acaena* was also suggested as a possibility (Kerr 2004, Kessler and Schmidt-Lebuhn 2005).

Polylepis is distributed between *c.*2000 and 5000 m asl. However, most species are generally found between 3000 and 4000 m asl (Fjeldså and Kessler 1996, Navarro et al. 2005). Some species of *Polylepis* are highly specialized to specific environmental conditions. e.g. *P. tarapacana* occurs in dry locations with precipitation <200 mm yr^{-1} and is able to reach elevations above 5000 m asl (Jordan 1983). Other species are generalists and have wider tolerance ranges (Kessler 1995, Kessler 2002).

As no other tree species reach elevations above the treeline, *Polylepis* forest becomes essential habitat for a number of birds and mammals (Kessler et al. 2001, Yensen and Tarifa 2002). Indeed a disproportionate number of endemic species live in *Polylepis* woodlands (Fjeldså and Kessler 1996). Consequently, a reduction of *Polylepis* forest could be related to loss of diversity due to local and regional extinctions.

Polylepis woodlands are usually reported as small groups of individuals scattered in the landscape. Initially this distribution pattern was considered to be natural (Raimondi 1874) but an emerging view suggests that fire incidence influences this pattern (Ellenberg 1958, Kessler 1995). The vulnerability of *Polylepis* increased through time as human populations expanded. According to Fjeldsa and Kessler more than 80% of the *Polylepis* forests evaluated in 1996 were eliminated by 2004 in Cordillera Real, Bolivia due to human pressure (Purcell and Brelsford 2004). Consequently it was considered that *Polylepis* only occupies a small fraction of the potential area it could have covered in the absence of human activity (Fjeldså and Kessler 1996, Cierjacks et al. 2007b).
Pollen data showed that *Polylepis* decreased in abundance (pollen production) with the onset of fire events (Urrego et al. 2011). Consequently, palaeoecological reconstructions of *Polylepis* woodlands and fire could be used to evaluate *Polylepis* responses to fire at regional at regional scales (Valencia et al. 2010b, Hanselman et al. 2011a).

1.6) Selecting vegetation assemblages as baselines

In general it is very tempting to use multi-centennial historical data to define ecological baselines (pristine-like conditions) for disturbed areas or define baselines from

geographically remote areas away from populated centres. However, these assumptions could be misleading, as pristine-like settings (counterfeit baselines) could be already the product of previous anthropogenic disturbances. The development of paleoecological proxies provides the opportunity to reconstruct past vegetation and climate changes at millennial timescales (Bush et al. 2004a, Fritz et al. 2007, Groot et al. 2011, Hanselman et al. 2011a). These reconstructions can be used as a historical background to be applied in modern conservation and management of Andean ecosystem (Gosling et al. 2009).

The concept of shifting baselines (Pauly 1995) highlights the importance of excluding degraded assemblages as baselines and can be evaluated adopting an equilibrium or neutral view (see section 1.6). If community stasis or equilibrium is assumed, then baselines should have the environmental conditions as similar as possible to the site that baselines are defined for. Baselines should also predate human disturbances. Because the high Andes were heavily transformed due to human activities after 4 ka; (Isbell 2008, Bauer et al. 2010) and experienced droughts mainly between 8 and 4 ka in multiple sites (Seltzer et al. 1998, Cross et al. 2000b, Abbott et al. 2003, Mayle and Power 2008, Hillyer et al. 2009), the early Holocene (c 10 ka) becomes the most suitable time to define baselines from.

Conversely, assuming neutrality (Kimura and Crow 1964, Hubbell 2001) implies that community changes were continuous and assemblages drifted naturally over time influenced by climate. Under this scenario baselines should only predate the influence of humans in the landscape because multiple vegetation assemblages would exist for any particular climate and landscape setting.

It would be tempting to use modern species distribution models to define the most likely assemblages for a site. However, the reconstruction of past assemblages may is still be required. For instance, if a site does not have any arboreal vegetation due to deforestation but has all the conditions to support it; then: (i) The restoration of this site under a null approach, would use the most likely species that could be present in this site. However in absence of vegetation baselines, exotic species to this particular site may be introduced. (ii) Under an equilibrium approach, restoration of this site would

exactly reproduce a past assemblage (baseline) ignoring that alternate states for the assemblage are possible (i.e. under a null approach). Furthermore, soil or any other parameter may have changed remaining unnoticed. Then, the restoration based on a fixed baseline may fail as it ignores the actual differences between past and modern assemblages. Whether a null or equilibrium approach is adopted, past assemblage reconstructions are required for restoration or management purposes. Ignoring the historical background of a site could be potentially dangerous and may lead to the restoration of a site with exotic species.

When defining baselines, glacial periods had to be excluded because of their low temperatures relative to modern times. During the last glacial period temperatures between 5 and 8 °C below modern were associated with species displacements of about one kilometre in elevation with respect to Holocene distributions (Groot et al. 2011). Previous interglacials could also be used to derive baselines from; however, the small number of records registering previous interglacials may limit this option (van der Hammen and Hooghiemstra 2003, Hanselman et al. 2011b). Furthermore, the presence of non-analogue communities developing between interglacials suggested that differences relative to modern assemblages should increased with time (Edwards et al. 2005, Williams and Jackson 2007). Consequently, baselines derived from previous interglacials are more likely to be dissimilar in terms of species composition and structure relative to the Holocene assemblages. Overall, baselines should postdate the Last Glacial Maximum (20 ka) and the influence of low temperatures of during deglacial times (roughly from 20 ka to 13 ka).

1.7) Thesis structure

Including the introductory chapter (Chapter 1) this thesis is composed of six chapters. Chapter 2 provides a detailed description of the studied sites and the rationale for the site selection. The modern vegetation and human impacts are also discussed in Chapter 2. Chapter 3 contains a detailed description of the methodology used including field and laboratory techniques besides step-by-step protocols (appendix sections). Background is

provided for the standard techniques of pollen, charcoal, diatoms, loss-on-ignition, magnetic susceptibility, statistical analysis, and for newly developed techniques. Chapters 4 and 5 represent the main data chapters of the thesis, which are formatted for submission to Ecological Monographs and Quaternary Science Reviews respectively. These chapters contain a multi-proxy paleoecological reconstruction for Lakes Miski and Huamanmarca based on pollen, diatoms, charcoal, loss-on-ignition, and magnetic susceptibility. Chapter 6 (section 1 to 3) considers the main conclusions from chapters 4 and 5 in the light of modern conservation and management. Chapter 6 (section 4) shows preliminary results based on newly developed methodology that includes Energy dispersive spectroscopy as an analogous technique to x-ray fluorescence, and scanning electron microscopy to improve the identification of pollen taxonomy and charcoal particle identification (e.g. differentiation of forest versus grasses). Chapter 6 (section 5) shows my contribution in the publication of additional scientific articles. Appendices I-VI provide a compendium of laboratory protocols used in this thesis. Appendix VII contains the data used in the thesis.

Chapter 2) Site description

This chapter describes the three study sites (Miski, Huamanmarca, and Pacucha) providing a rationale of site selection based on the physical settings, vegetation, climate, and human activity. A general description of the Pacucha site and climatic reconstruction was already published (Hillyer et al. 2009, Valencia et al. 2010b).

2.1) Site selection

The aim of this study was to characterize vegetation baselines based on the comparison of "natural" and "human disturbed" sites. Therefore, the studied sites had to be located in areas with contrasting probabilities for modern and past human occupation.

First, for the natural baseline characterization, the selected sites had to be in modern unoccupied and forested areas. The selection rationale was founded on the following assumptions: (i) Sites currently unoccupied are intrinsically unappealing for human settlement due to harsh climate (e.g. low temperatures and high humidity) or limited resources, and (ii) the characteristics that made these sites unappealing for modern settlement probably made them unappealing in the past. (iii) It would be unlikely for people to remain in areas with limited resources and harsh climate when better sites can be reach in 1-2 days walk. Therefore, based on the cited criteria, lakes occurring in the Eastern Andes were selected from satellite images using Google Earth. From the list of target lakes Miski and Huamanmarca were chosen as the best candidates for providing "natural" sites (Fig. 2-1). Specifically, they had no modern human populations close to the lake. Furthermore, access to the lakes was at the logistical limit of the field time available, i.e. Miski and Huamanmarca were the remotest sites that could be reached carrying the coring gear, with travel time to and from the lake 2-day walk (22 walking hours).

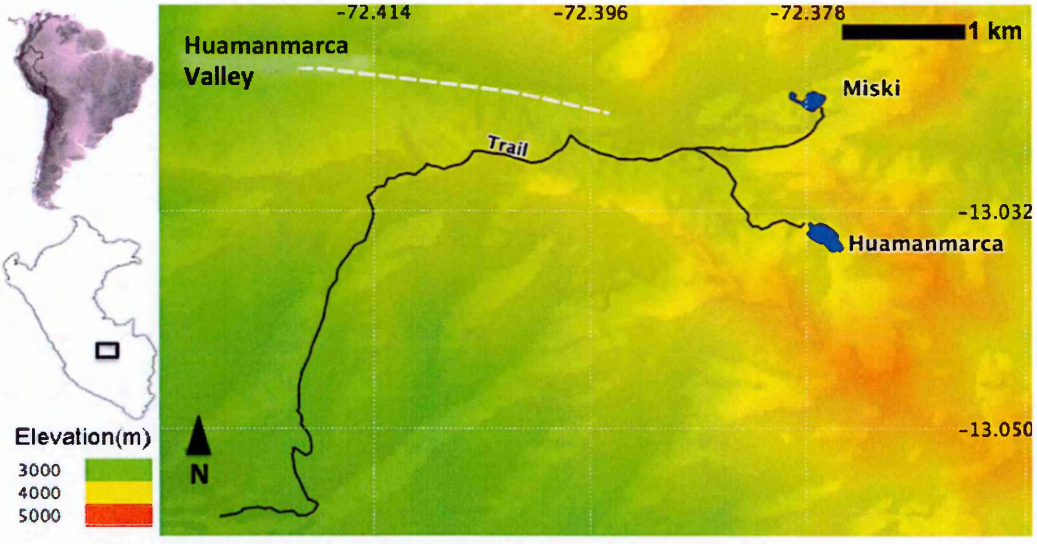

Fig. 2-1 Map of Miski and Huamanmarca.

Second, for the characterization of human disturbed areas, a site with long history of human occupation had to be used. The selection rationale was founded on the following assumptions: (i) Sites with a long history of human occupation (multiple millennial) should have favourable conditions to enable an early human settlement. (ii) The characteristics that favoured the settlement and occupation during multiple millennia indicate that the first Andean inhabitants could have preferred this site. Therefore, sites with a long history of occupation are likely to register the earliest human impacts.

Lake Pacucha was selected because it provided a record of continuous human occupation for near 5 thousand years (Valencia et al. 2010a). Furthermore, Lake Pacucha is located within a landscape rich in archaeological evidence that suggests it lay at the heart of the Chanka (*c.*1.4 - 0.5 ka) civilization and was within the geographical field of influence of the Wari (*c.*1.4 – 0.5 ka), Tiwanaku (date), and Inca (*c.*0.7 – 0.5 ka) civilizations.

2.2) Physical settings

2.2.1) Main Huamanmarca valley (Lakes Miski and Huamanmarca)

The Huamanmarca valley is a glacial valley located at 13°1'32.18"S, 72°23'40.95"W with an elevation between 2000 and 4000 m asl (Fig. 2-2). Hanging valleys with waterfalls feed by pater noster lakes occurred mostly on the northern side of the valley. The main Huamanmarca valley bifurcates at 3700 m. Each new section of the valley ended up in an unglaciated cirque that represents the catchment area for Lakes Miski and Huamanmarca respectively (Fig 2-2 and 2-3). Lakes Miski (13°1'23"S, 72°22'4"W) and Huamanmarca (13°2'1.29"S, 72°22'38.48"W) were formed as the glacials retreat in these valleys about *c.*13 ka. Terminal, medial and lateral moraines were evident above 3600 m asl. The lowest terminal moraine was located at *c.*3600 m asl followed by moraines at *c.*3700 and 3800 m asl. The moraines above the bifurcated section of the valley were present at the same elevation suggesting that deglaciation was synchronous and not delayed locally by shading.

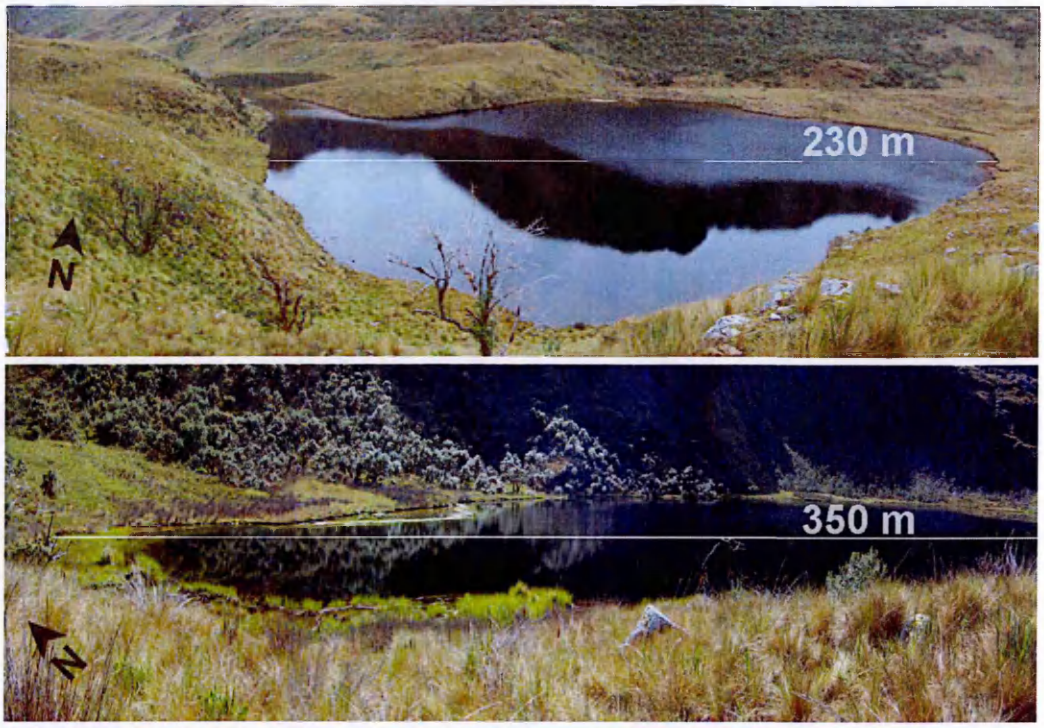

Fig. 2-2 Photograph of Lakes Miski (top, 3000 m asl) and Huamanmarca (bottom, 3900 m asl).

Lakes Miski and Huamanmarca lie above the bifurcation of the main Huamanmarca valley. The Miski valley is u-shaped with gentler slopes than Huamanmarca that has a v-shaped valley (Fig. 2-2 and 2-3). A dense fog continuously covers the sites. The streams feeding both lakes are probably maintained by orographic interception of fog. Lakes Miski and Huamanmarca have a catchment area of about 1.6 km^2 each. Both catchments were covered in woodlands (49.6% and 26% respectively), marshes or bogs (16.2% and 3%), and glacial-eroded rocks and grasslands (32.3% and 68%). The lakes represent only 2 and 4% of their respective catchment area.

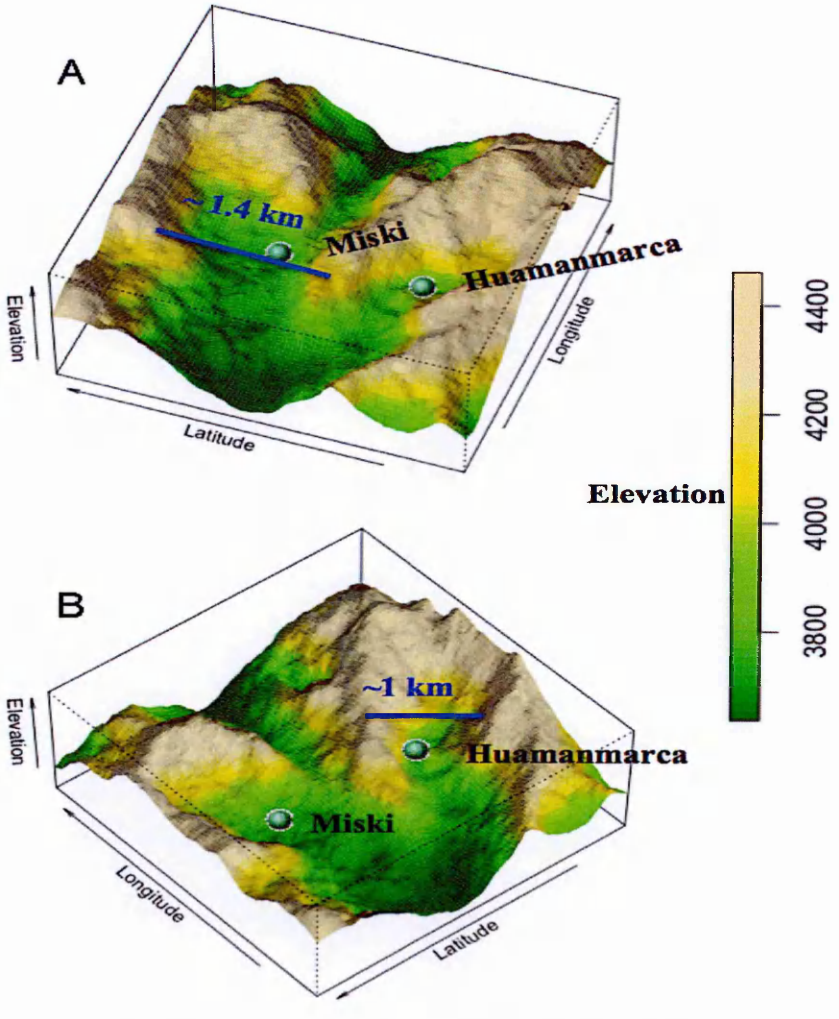

Fig. 2-3 Perspective plots showing the valley shape for Lakes Miski (u-shaped, A) and Huamanmarca (v-shaped, B). The plots were rotated and shaded to show the width and steepness of each valley.

2.2.2) Pacucha valley (Lake Pacucha)

Lake Pacucha (13°36'26"S, 73°19'42"W) lies at 3095 m asl of an unglaciated valley formed on Jurassic limestone, intrusive rocks, and Quaternary alluvial material (Valencia et al. 2010b, INGEMMET 2013). The closest moraines that indicate glacial activity around Pacucha occur in an adjacent valley 5 km to the southwest of the lake. More than 50 lakes were also formed in this area due to glacial activity. These lakes supply underground water to Lake Pacucha that has outflow but not inflow streams. Besides precipitation, no other water sources for Pacucha are available in this area.

The stream flowing out of Pacucha carved a narrow valley in the northern side of the lake sectioning a small mountain made of Jurassic limestone. It is very unlikely that a landslide blocking the lake outlet formed Pacucha because this area does not contain disaggregated material. Therefore, the most likely scenario is that Pacucha was formed in a solution hollow.

2.3) Modern local vegetation

2.3.1) Miski and Huamanmarca vegetation

The continuous cloud cover in this section of the Andes favours the presence of epiphytes (i.e. Bromeliaceae and *Tristerix*, Fig. 2-4) that were abundant up to 3900m. Above 3700m most of the epiphytes were represented by mosses and branching lichens, however few individuals of *Tristerix* (Loranthaceae) were also observed.

Fig. 2-4 *Polylepis* trees covered in mosses and parasitic plants i.e. *Tristerix* (epiphyte with elongated red and greenish flowers)

As part of this study, a total of 12 belt-transects of 200 m^2 each (4 x 50) were surveyed between 3730 and 4030 m asl around Lakes Miski and Huamanmarca (local woodlands). A total of 442 stems divided in arboreal (86%) and shrub (14%) types were counted. The genus and families recorded were: *Polylepis* (Rosaceae, 47%), *Gynoxys* (Asteraceae, 26%), *Hesperomeles* (Rosaceae, 12%), and Melastomataceae (14%). The genus *Solanum* (Solanaceae) and *Ilex* (Aquifoliaceae) were very rare representing 1% of the inventoried stems. *Polylepis*, *Gynoxys*, and *Hesperomeles* dominated the elevational range between 3700 and 4050 m asl. Few arboreal individuals of the family Araliaceae and the genus *Buddleja* (Buddlejaceae) were found at the same elevation of the surveys.

Some areas mostly below the catchment of Lakes Miski and Huamanmarca were burned. Tree regrowth in burned areas was limited, as *Chusquea* (an Andean bamboo) seemed to be outcompeting some of the trees forming a matrix of *Chusquea* with few and sparse tress within this matrix. The woodlands in Miski and Huamanmarca valleys are unsuitable for wood production. Wood from all the fallen trees we observed was decomposing because of the high soil-humidity and therefore useless for burning. Most of the dead woody material was covered in fungi and epiphytes.

2.3.2) Pacucha vegetation

Although the Pacucha valley lies below the continuous treeline (3300 – 3600 m asl; see chapter 1, section 1.4) this area has lost most of the natural vegetation. *Eucalyptus* trees and agricultural fields of potatoes, barley, and corn dominate the landscape replacing the native and diverse plant communities; nearby vegetation located at similar elevations supports near 100 woody species (Young and León 1999, Young 2006). The Pacucha area is drier than Huamanmarca and Miski valleys as Pacucha lacks a near continuous cloud cover. However, the three sites share similar genera although the actual species are sometimes different. *Podocarpus*, *Alnus*, *Polylepis*, and *Vallea* are among the most abundant genera present in the Pacucha valley. Shrubs and herbaceous species unpalatable to livestock are also very common (e.g. *Baccharis* and *Colletia*) around Pacucha due to the grazing pressure.

2.3.3) Local climate conditions

2.3.3.1) *Huamanmarca Valley (Miski and Huamanmarca)*

The closest meteorological station, Huyro (managed by the Peruvian national meteorological agency SENAMHI), lies at 1700 m asl, 18 km from Miski and Huamanmarca. Data derived from Huyro, shows that annual precipitation reaches *c.*2000 mm. Approximately, 80% of the annual precipitation occurs during the rainy season (November-April) peaking in the middle of the austral summer (Fig. 2-5). Reconstructed precipitation derived from calibrated TRMM 2B31 shows that precipitation patterns were similar in Huyro and Miski (Bookhagen 2013) and is consistent with other reconstruction for this section of the Andes (Zimmermann et al. 2010).

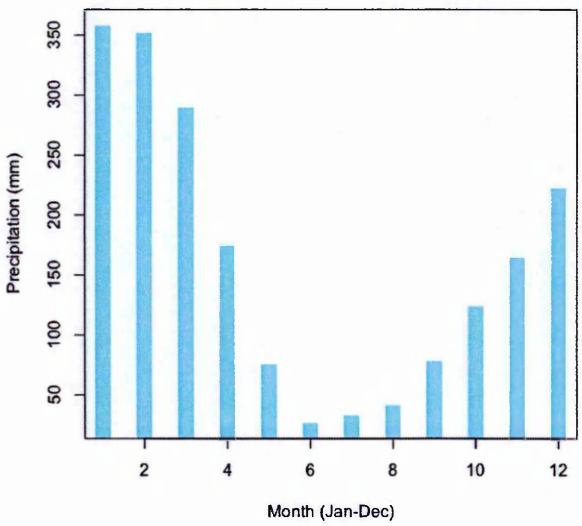

Fig. 2-5 Annual precipitation derived from the meteorological station of Huyro provided by SENAMHI at http://www.senamhi.gob.pe/.

The annual mean temperature at Huyro is 23.4 °C and considering the adiabatic lapse rate of 5.5 °C per 1000m of ascent, the annual mean temperatures at Miski and Huamanmarca should be close to 12 °C (Bush et al. 2004b). In general monthly mean

temperatures have small fluctuations relative to the annual mean in tropical latitudes. At Huyro, monthly mean temperatures rarely differs in more than 1.5°C relative to the annual mean (*c.*23.4 °C, Fig. 2-6). At the elevation of Lake Miski and Huamanmarca monthly variations should have a similar pattern. In contrast, the difference between diurnal maxima and minima temperatures can be large. At Huyro, the daily temperature fluctuation may reach *c.* >14 °C especially in wintertime. Thermal differences between maxima and minima increase with elevation, and for Miski and Huamanmarca, this difference should almost double.

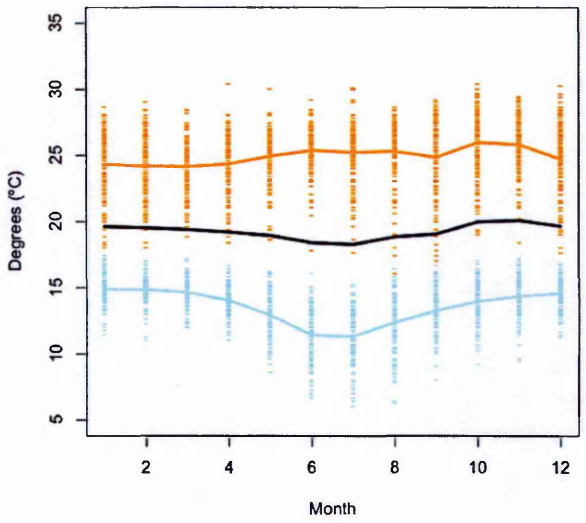

Fig. 2-6 Annual temperatures derived from the meteorological station of Huyro. The original data were retrieved from SENAMHI (http://www.senamhi.gob.pe/) and plotted as monthly means (black line), maximum temperature means (orange line), and minimum temperature means (blue line).

2.3.3.2) *Pacucha Valley (Lake Pacucha)*

The meteorological data for Pacucha derives from the Andahuaylas city located 6 km southwest from the lake and 150 m below Pacucha (3090 m asl). This region experiences a wet season from April to September that brings >80 % of the annual precipitation (*c.*610 mm yr^{-1}, Fig. 2-7). The dry season occur between October and March. The mean annual temperature for Andahuaylas is *c.*13 °C that should also be

representative for Pacucha (Fig. 2-8). Daily thermal fluctuations (> 15 °C) are greater than seasonal fluctuations (*c.* ± 2) e.g. winter versus summer month averages.

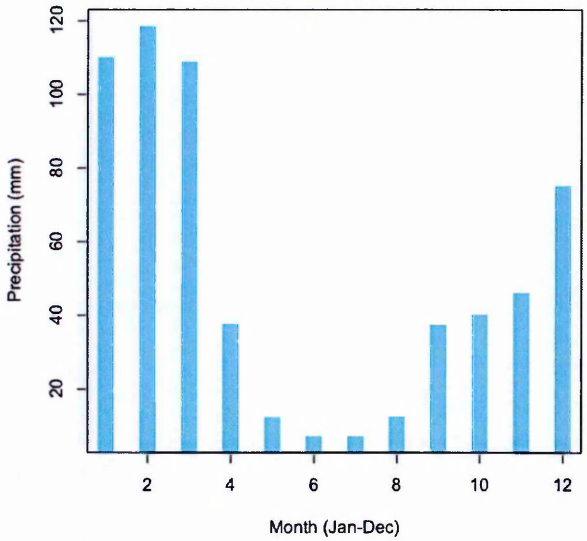

Fig. 2-7 Annual precipitation for Andahuaylas and Pacucha estimated from the period between 1964 and 1980. Data derived from www.met.igp.gob.pe/clima.

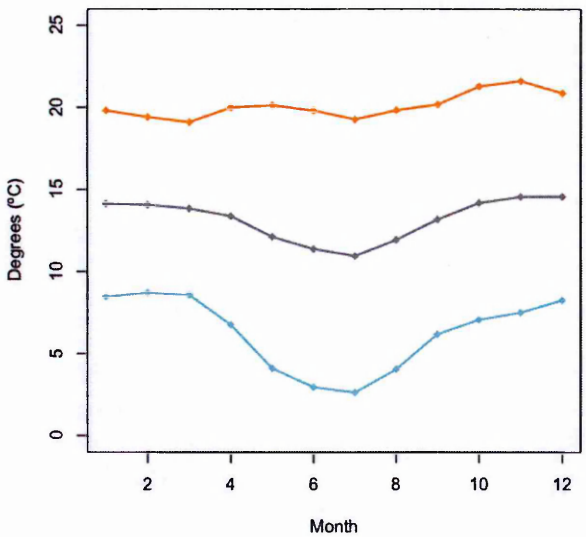

Fig. 2-8 Annual temperatures for Andahuaylas and Pacucha estimated from the period between 1964 and 1980. Data derived from www.met.igp.gob.pe/clima.

2.4) Local human activity

2.4.1) Miski and Huamanmarca human activity

The valleys of Miski and Huamanmarca are unoccupied today. A small hut built on a medial moraine was the only construction found in these valleys. According to the local people, the hut was used few times each year to control the livestock that graze this area. The number of cows was estimated to be between 25 and 30.

Some patches below the catchment of lakes Miski and Huamanmarca (i.e. < 3800 m) show some evidence of recent fires (Fig. 2-9). The burned areas had gentle slopes and were parallel to the main valley. During the fieldwork (December 2008) it was observed that fires were common on lateral moraines and the land contiguous to the moraines. The high Andean bamboo *Chusquea* was replacing the small trees and *Polylepis* seedlings on slopes that showed a signal of fire activity.

Fig. 2-9 Burned forest patches. Lateral moraines below Huamanmarca (left) and Miski (right).

Cultivation is not practiced in this valley, probably due to the difficult access to the site, complex topography and continuous cloud cover. These sites are too wet to cultivate potatoes or crops like quinoa or amaranth that require periods for grains drying prior harvest. Furthermore the sites are at an unsuitable elevation to cultivate maize and the paucity of earthworks suggests this area was not previously used for agriculture either.

The closest evidence of pre-Columbian (AD 1491) activity is the major archaeological Incan constructions such as Machu Picchu and Ollantaytambo are located *c.*23 km south from Miski and Huamanmarca in the Sacred Valley of the Incas (Fig. 2-10). Terraces are common at these archaeological sites and along the Sacred Valley providing unmistakable evidence of human occupation. Such conspicuous landscape features are absent in the immediate surroundings of Miski and Huamanmarca.

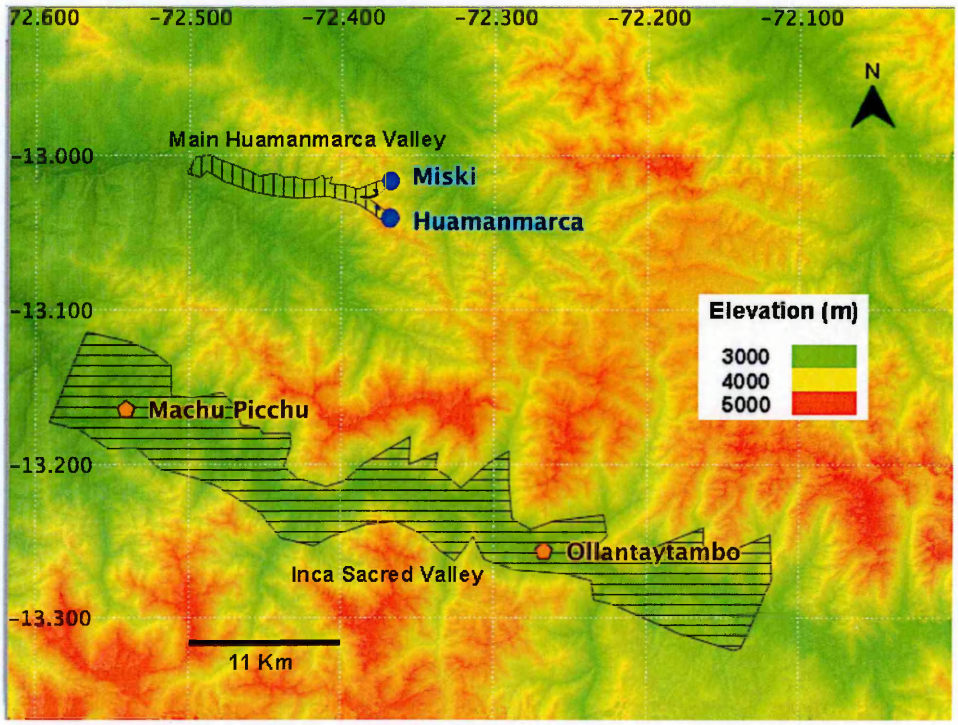

Fig. 2-10 Map depicting the position of Lakes Miski and Huamanmarca relative to main archaeological sites like Machupicchu and Ollantaytambo. Additional archaeological sites occur along the sacred valley

2.4.2) Human activity in Pacucha.

People currently occupy the valley of Pacucha. A small town composed of *c.*200 houses lie in the western side of the lake. Agricultural fields and *Eucalyptus* plantations surround the lake (Fig. 2-11). The most common crops are maize, amaranth, barley and potatoes. Most of the native vegetation around Pacucha was eliminated as land use changed.

Grazing further enhanced the pressure on native species and favoured the dominance of unpalatable species.

Fig. 2-11 Agricultural fields and *Eucalyptus* plantations around Lake Pacucha. Image modified from www.peru.travel.com

The near continuous abundance of cultivated species in Pacucha today indicates that this site is good for human populations and was therefore potentially occupied since humans settled in the Pacucha area *c.*6 ka. Archaeological excavations in the Pacucha area identified multiple human occupation sites after *c.*4.1 ka corresponding to the occupation phases of Muyu Moqo, Qasawirka prior *c.*1.4 ka (Fig. 2-12), Wari (*c.*1.4 - 1 ka), and Chanka (*c.*1 - 0.6 ka). The past regional climatic conditions probably favoured the cultivation of Amaranthaceae since *c.*6 ka shifting to maize cultivation about 3 ka (Valencia et al. 2010b, Sublette et al. 2012). The crop shift was a pattern observed in other records in the Cusco region (Sublette et al. 2010).

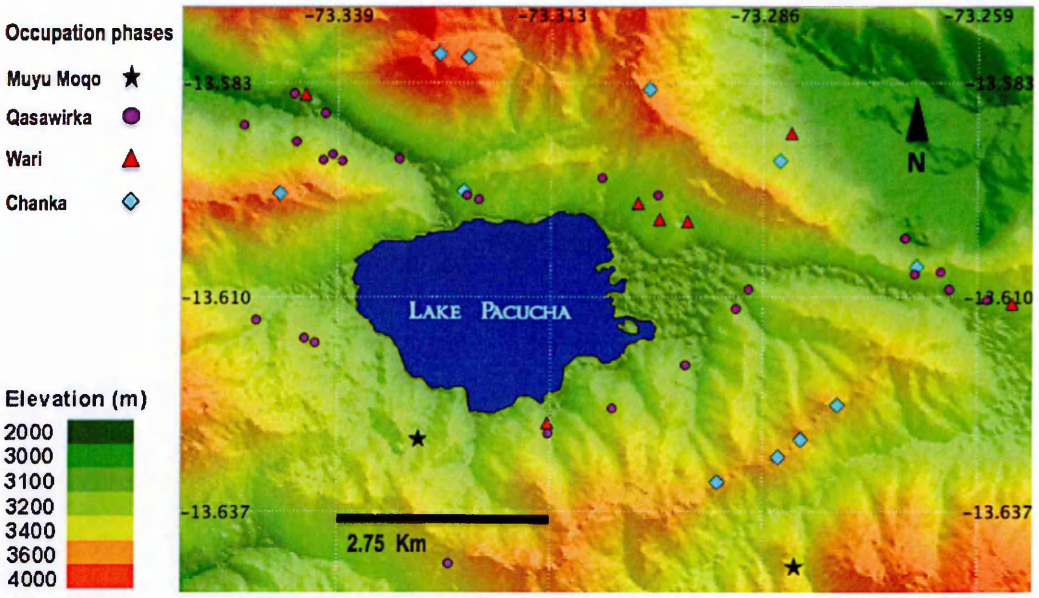

Fig. 2-12 Map of the Andahuaylas region showing human occupied sites around Lake Pacucha over the last 4.1 ka. Data modified from Bauer *et al.*, (2010).

2.5) Summary

This chapter provides a description and the rationale for selecting the study sites (Miski, Huamanmarca and Pacucha). The aim of this chapter was to identify areas with unfavourable conditions for human settlement to be compared with heavily transformed areas. The physical settings, local vegetation, local climate, and, archaeological evidence were taken into account for selecting Lakes Miski and Huamanmarca as sites with fewer favourable conditions than Lake Pacucha.

Chapter 3) Materials and Methods

This Chapter describes the field techniques used to survey and core Lakes Miski Huamanmarca and Pacucha. The laboratory sampling, physical characterization and analysis of ecological proxies is also portrayed. A detailed description of the age modelling and rationale for selecting statistical analysis is also explained in this chapter. Note that pollen and diatoms records were already published for Lake Pacucha (Hillyer et al. 2009, Valencia et al. 2010b). However additional pollen samples (31) were counted for this thesis following the methodology detailed in section 3.4.

3.1) Lake survey

Prior coring, the deepest and flattest area of the lake was located using a handheld sonar. Deep pockets with steep slopes that could be susceptible to sediment slumping were excluded as coring sites as they may produce reversals when dating the sediment. Shallow areas were also excluded because they are susceptible to desiccation during dry periods and yield a discontinuous record. Additional areas with signs of instantaneous deposition (e.g. landslides close to the lake edge) or fast sediment accumulation were also avoided.

3.1.1) Bathymetric survey

Georeferenced water depths (257 from Miski, 123 from Huamanmarca, and 40 from Pacucha) were obtained to generate a bathymetric map of each lake. The depths were surveyed using a depth sounder (Garmin GPSMAP 400; Miski and Huamanmarca) or a handheld sounder and a regular GPS unit (Garmin GPSMAP 60CSx; Huamanmarca, and Pacucha). The lakes were traversed multiple times and several stops were made to register the depths as well as the coordinates when using a handheld GPS. When using a depth sounder the recording intervals were set up at constant time intervals (e.g. 5-10 seconds) and stops were not required. The coordinates of the lake shoreline were recorded as the bathymetric data was going to be overlaid on satellite imagery.

3.1.2) Bathymetric maps.

The field measurements were downloaded from the GPS units and plotted over satellite images satellite images provided as a plugin-layer in QGIS version 1.8.0. The field measurements were aligned with satellite imagery. For example, the coordinates of Lake Miski were shifted 30 m westward and 10 m northward (Fig. 3-1). Additional lake contour-coordinates were extracted from satellite images (i.e. depth = 0) to define a precise lake contour for Miski and Huamanmarca and improve the accuracy of the interpolations when generating a map.

Fig. 3-1 Correcting the alignment of GPS coordinates and background images for Lake Miski derived from Google Earth. Left panel shows raw GPS data (purple dots) with a yellow arrow indicating the shifting direction. Right panel shows GPS data already shifted. The image of the right panel was subsequently corrected for the y-axis (not shown).

When coordinates of the lake edge are missing, sections of the bathymetric map become distorted. The lake edge represents a contour of depth equal to zero in the map and provide anchor points for the interpolations. In addition to the contours, coordinates outside the lake were used and were given arbitrary values of zero (i.e. corners of the plotted map were assigned depth= 0 for display purposes). This procedure enabled the display of the contours at the edge of the lake (zero) and contours in deeper sections. Digital elevation models can also be used to supply the data outside the lake; however, this procedure does not improve the quality of the bathymetric map. The coordinates

obtained in the field and the ones retrieved from satellite images were organized in a table as shown in Fig. 3-2. R-code was written to perform the interpolation using the package akima (Script 3-1) and to generate a bathymetric map (Fig. 3-3 and 3-4). If degrees are used instead of UTM coordinates, the entries should be formatted as decimal degrees e.g. use 10.5 instead of 10°30' 00"N. Coordinates in the southern hemisphere are negative e.g. 8°30' 00"S should be entered as -8.5.

	A	B	C	D
1	x	y	Depth	depth
2	784350	8558882	0.5	-0.5
3	784525	8558890	0.6	-0.6
4	784507	8558867	0.6	-0.6
5	784499	8558923	0.7	-0.7
6	784508	8558869	0.7	-0.7

Fig. 3-2 Structure of the GPS data required used to generate bathymetric map with the R-script 3-1. The x and y in the table header represents the longitude and latitude respectively but expressed in UTM. Depths were entered as positive or negative values just for plotting purposes.

Script 3-1 R-script for Lake Miski bathymetry

```
library(akima)                                    #loads the library akima
read.table("miskib.txt",header=TRUE)->miski       # reading coordinates
miski.li<-interp(miski$x,miski$y,miski$depth, duplicate="mean")  # interpolation
image(miski.li,xlab="UTM 18",ylab="UTM L",main="Lake Miski")     #Heatmap
contour(miski.li,nlevels=5,add=TRUE)              #Contours
points(miski$x[1:257],miski$y[1:257], pch=8)      #plot coordinates used (*)
points(miski$x[258:355],miski$y[258:355])         # coordinates derived from Google.
```

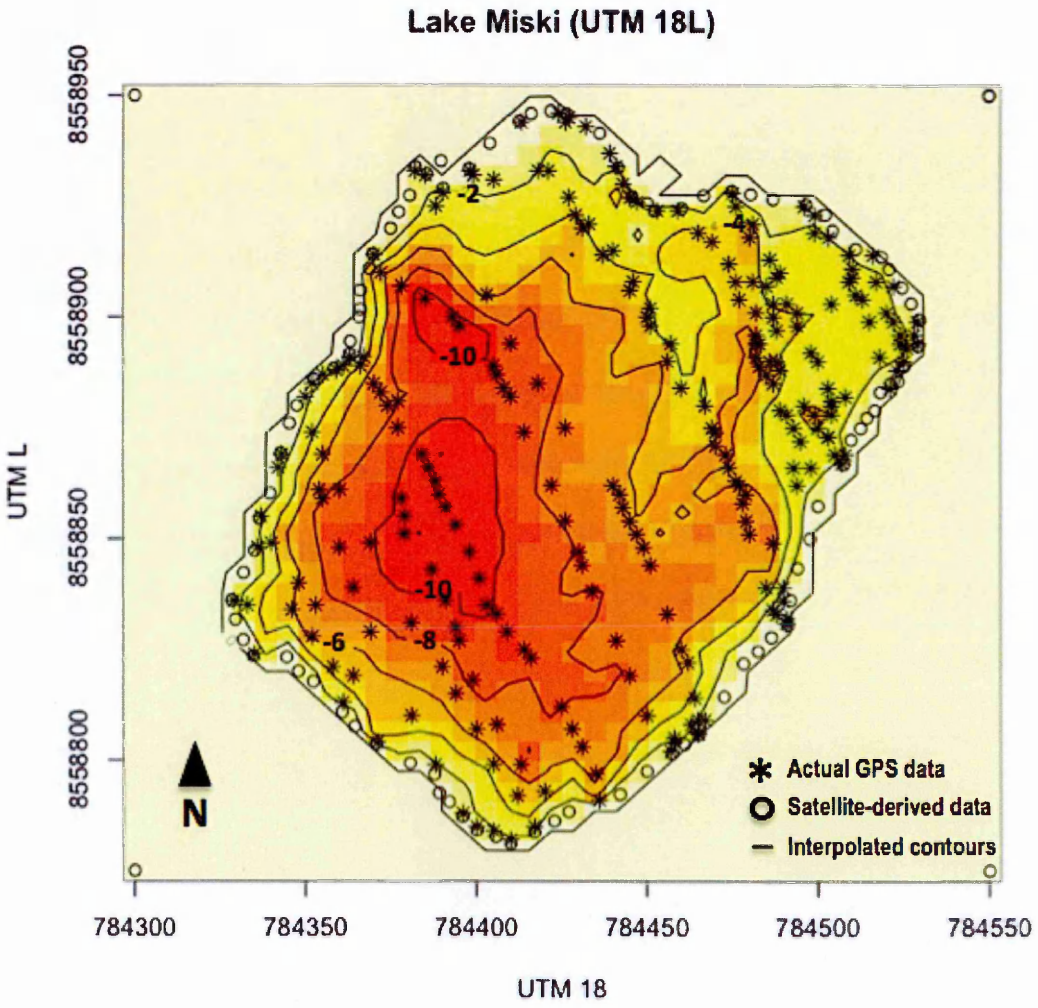

Fig. 3-3 Bathymetric map of the largest basin of Lake Miski. Asterisks depict GPS field measurements and the empty circles satellite-derived coordinates. Note that each UTM unit is equivalent to 1 m.

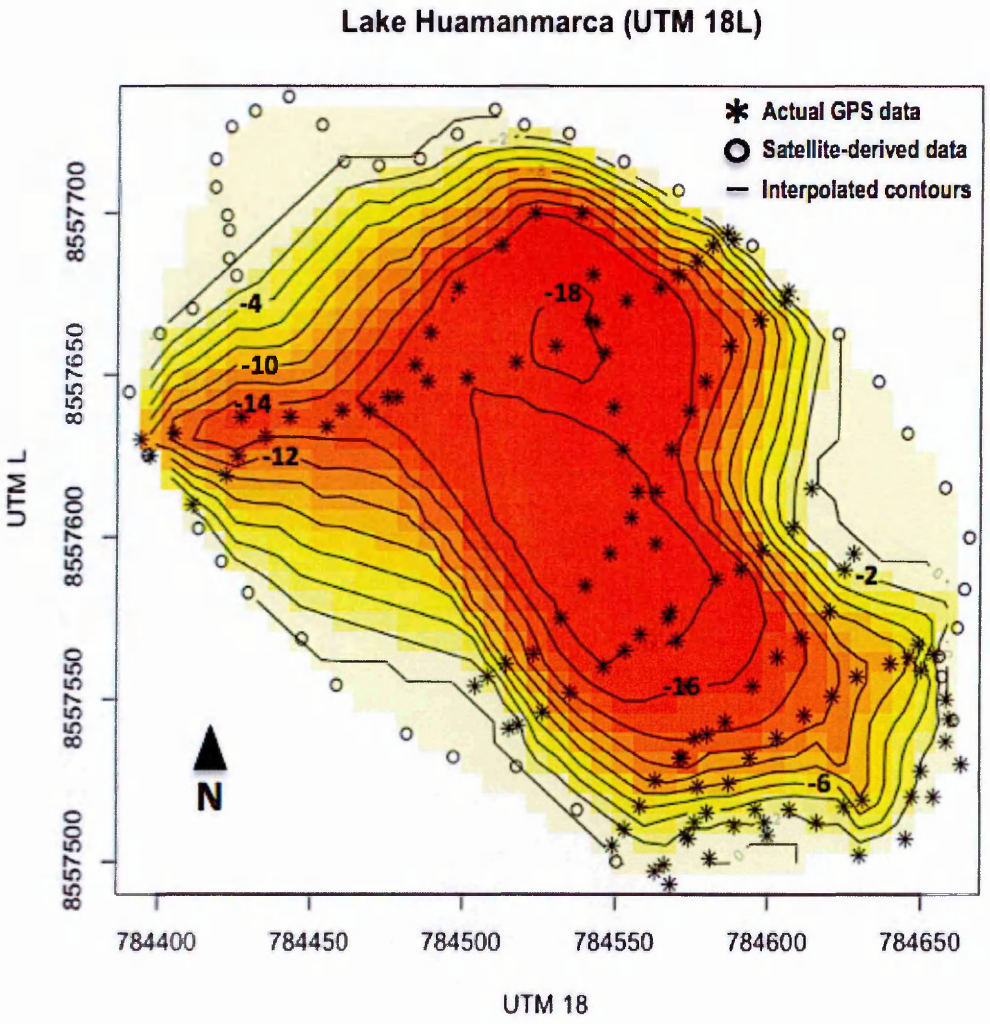

Fig. 3-4 Bathymetric map of Lake Huamanmarca. Asterisks depict GPS field measurements and the empty circles satellite-derived coordinates. Note that each UTM unit is equivalent to 1 m.

3.2) Sediment recovery

3.2.1) Principles of lake coring

Sediment cores were taken from Lakes Miski, Huamanmarca, and Pacucha between 2003 and 2008. The cores were raised using a Colinvaux-Vohnout piston corer (Colinvaux et al. 1999) from a platform supported by inflatable boats anchored in the deepest portion of the lake. The platform and the boats were securely kept in place

using three anchors of about 30 kg each. Two of the anchors were placed 60 degrees relative to the direction of incoming wind to minimize wind dragging. The third angle was placed parallel to the wind flow and opposite the first two anchors (Fig. 3-5).

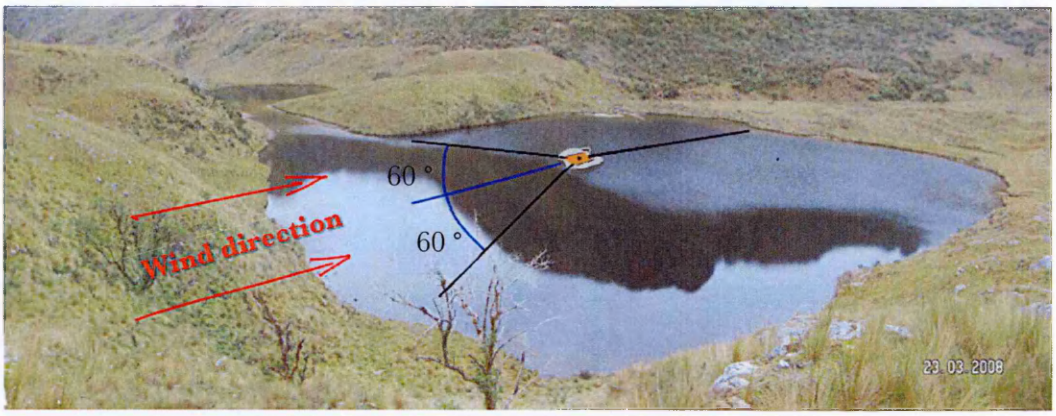

Fig. 3-5 Platform anchoring at Lake Miski showing two anchor lines (black) at 60° relative to the wind direction (blue), and a last line parallel to the wind direction. (Photograph by Bryan Rado).

Lake coring (Fig. 3-6) was performed retrieving sediment in sections of 1 metre at a time using lexan and aluminium tubes. At each site a second parallel core was taken 1-2 m apart from the first core. The second core was taken starting half a meter deeper than the first one to recover sections that may have been missed in the first core due to breaks in the between the core tubes. Each one of the retrieved 1m sections was labelled marking the top and bottom of the tube. Empty sections of the tube were cut to minimize the movement of the sediment during transportation. Subsequently the tubes were sealed. Finally the tubes were packed and shipped to the Paleoecology laboratory at Florida Institute of Technology and were kept in a cold room at 4 °C.

3.2.2) Huamanmarca coring

Sediments from Lake Huamanmarca were retrieved in 8 m of water depth (13° 2' 1.37" S, 72° 22' 39.10" W). A total of nine drives (sections) were recovered from Lake Huamanmarca (Table 3-1). Core 2 was taken 2 meters away from core 1 and started 0.5

m deeper than core 1. Mud water interface was recovered in core 2; consequently, no sediment was lost on the surface of the core. In general sediments were dark and slightly laminated through all drives. However, the sediment oxidized and some laminations were no longer evident when the tubes were split. The transition from organic to glacial silts was evident in drive 4 in both cores. Because of the ease of penetration noticed while coring it was assumed that the sediment had a low content of clays or peat. Hammering was required to retrieve drive 4 and stopped when the bedrock was hit.

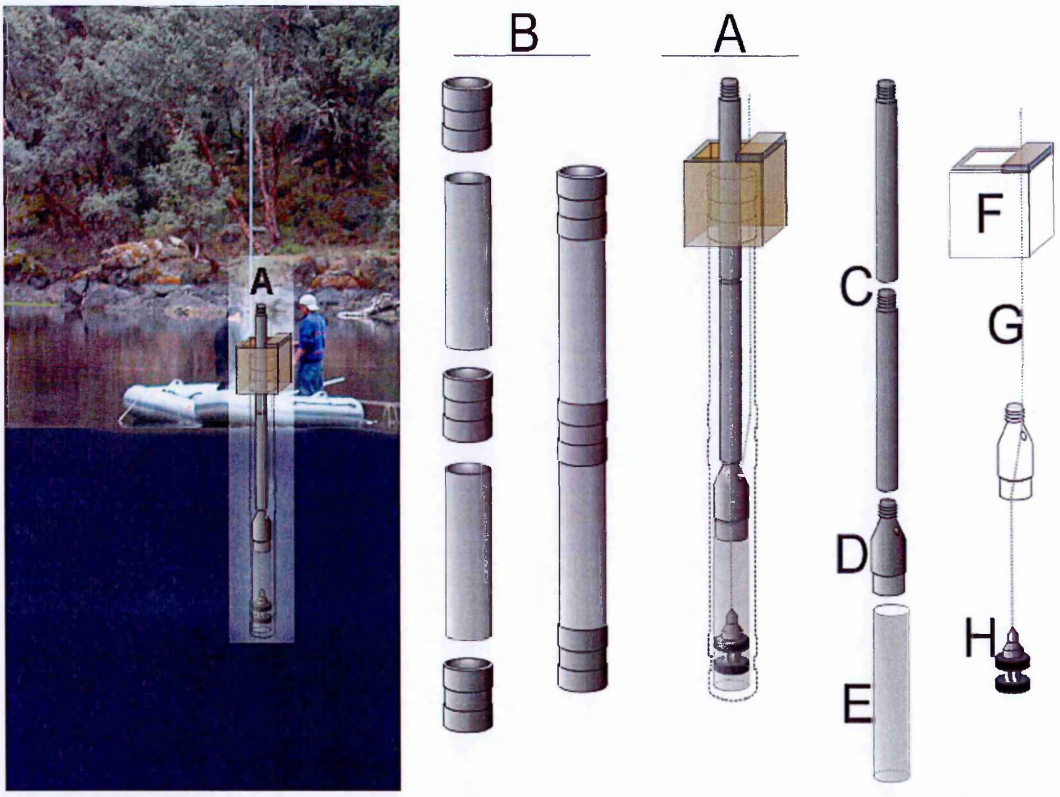

Fig. 3-6 Lake coring and coring equipment. A, assembled coring rig and placement on the platform supported by rafts; B, casing; C, coring rods; D piston and coring tube holder; E, coring tube (aluminium or Lexan); F, coring box; G, piston cable; H, piston. F,G, and H depict the cable set up that remains locked to the box when coring.

Core 1	Sediment	Length (cm)	Tube material
	Drive 1	85	Lexan
	Drive 2	95	Lexan
	Drive 3	100	Lexan
	Drive 4	37	Lexan
Core 2	Sediment	Length (cm)	Tube material
	Drive 1	100	Lexan
	Drive 2	98	Lexan
	Drive 3	95	Lexan
	Drive 4	77	Lexan
	Drive 5	39.5	Lexan

Table 3-1 Huamanmarca core details. Number of cores and drives retrieved from Lake Huamanmarca.

3.2.3) Miski coring

Sediments from Lake Miski were retrieved in 8 m of water depth (13° 1' 23.45" S, 72° 22' 40.89" W). Two cores of six drives each were raised using lexan and aluminium tubes (Table 3-2). Sediment was slightly laminated and easy to core. Silts were hit on drive 5 in cores 1 and 2 and aluminium tubes were used afterwards. It was noticed that some silts slumped inside the coring hole when using the aluminium tubes, i.e. drive 6 in cores 1 and 2. The sections that were likely influenced by slumping were not used. The coring stopped when bedrock was reached.

Core 1	Sediment	Length (cm)	Tube material
	Drive 1	78	Lexan
	Drive 2	98	Lexan
	Drive 3	100	Lexan
	Drive 4	100	Lexan
	Drive 5	40	Lexan
	Drive 6	15	Aluminium
Core 2	Sediment	Length (cm)	Tube material
	Drive 1	60	Lexan
	Drive 2	100	Lexan
	Drive 3	100	Lexan
	Drive 4	100	Lexan
	Drive 5	20	Lexan
	Drive 6	<15	Aluminium

Table 3-2 Miski core details. Number of cores and drives retrieved from Lake Miski.

3.2.4) Pacucha coring

Lake Pacucha (13°36'26 S, 73°19'42" W; 3095 m elevation) was cored multiple times in 30 m of water depth between 2003 and 2005. A composite sedimentary section of 14.5 m was reconstructed using cores Pac-B, Pac-D and Pac-E. Sediments were retrieved in aluminium tubes and coring stopped when the functional limit of the drilling rig was reached (Hillyer et al. 2009, Valencia et al. 2010b).

3.2.5) Vegetation survey

A total of 12 belt-transects of 200 m^2 each (4 x 50) were surveyed around Lakes Miski and Huamanmarca. The transects were 50 m long to remain within the woodland patches at elevations between 3730 and 4030 m asl. Transects were oriented radially relative to the lake centre and against the steepest slope to maximize the elevational range sampled. Transects of 200 m^2 were used as they provide reliable estimates of the species composition in areas represented by few species (Mueller-Dombois and Ellenberg 1974). The use of 12 transects was aimed to encompass the spatial variability of the area.

3.3) Laboratory procedures

3.3.1) Core splitting and description

The sediment cores were cut using a sliding saw at Florida Institute of Technology. Subsequently, the cores were split in two sections: an "archive" and a "working" half (Fig. 3-7). The sediment was measured and a stratigraphic description performed taking into account laminations, colour change and conspicuous features (e.g. presence of macrofossils). Subsequently, samples were taken from the working half to analyse pollen, diatoms, carbonates and charcoal.

3.3.2) Sample extraction

The amount of sediment for each proxy was dependent on the abundance of the microfossil of interest. For instance, smear slides were made to evaluate if 0.5 or 1 cm^3 contained enough material to analyse pollen, charcoal or any other proxy. Powder free gloves were used to handle the cores prior and during sampling to avoid contamination in the sample especially for radiocarbon dating. The surface of the sediment was carefully cleaned prior sample retrieval. A total of 12 samples, each with a minimum weight of 0.2 grams (dry weight), were taken for radiocarbon dating. Subsequently, samples for pollen, diatoms, charcoal and loss on ignition were taken at intervals of 10 cm. Once the age model was elaborated, additional samples were retrieved to have an equally spaced temporal sampling.

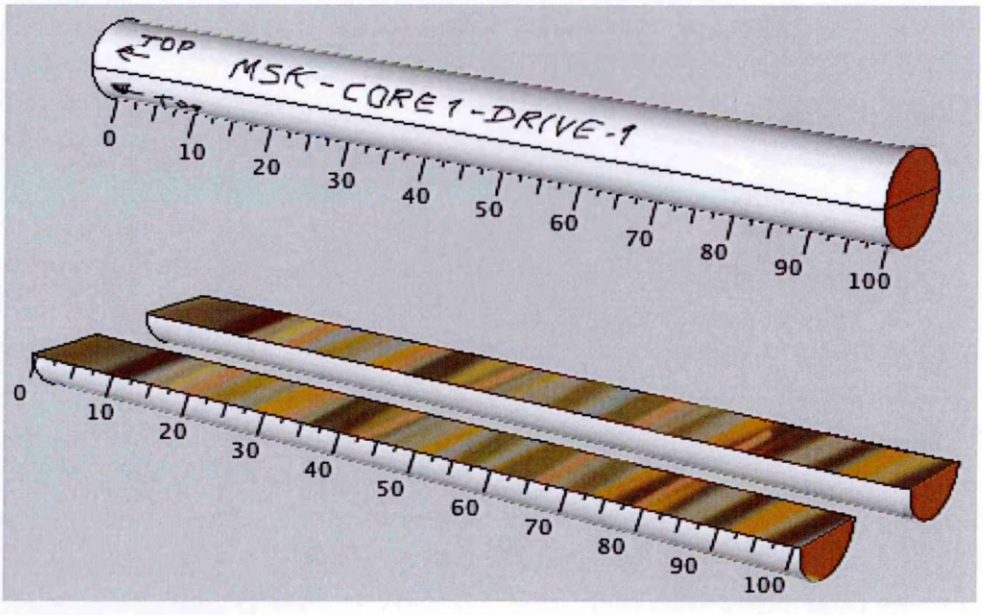

Fig. 3-7 Core labelling and splitting.

3.3.3) Physical and chemical characterization

3.3.3.1) *Magnetic susceptibility*

Lake sediments sometimes contain particles that react (magnetize) when exposed to a magnetic field (Roberts 2008). Magnetic susceptibility (MS) is a quantitative measurement of the magnetization observed in sediments or any other particular substrate (Murdock et al. 2013). Usually, magnetic susceptible materials encountered in lake sediments are the product of glacial activity (i.e. glacial silts also known as glacial flours). Glacial silts should be common when glaciers are continuously abrading the rock underneath them (Seltzer et al. 2002b). Consequently this technique was used to identify the onset of deglaciation in multiple Andean sites (Baker et al. 2001, Seltzer et al. 2002b). The glacial retreat is not unidirectional but a sequence of contraction-expansion events that favours the formation of small terminal moraines above a lake e.g. moraines above Lake Miski (Fig. 3-8). During deglacial periods, the small terminal moraines generally trap most of the glacial silts that no longer reach the lake. At this point, the magnetic susceptibility in the lake sediments should experience a rapid decline.

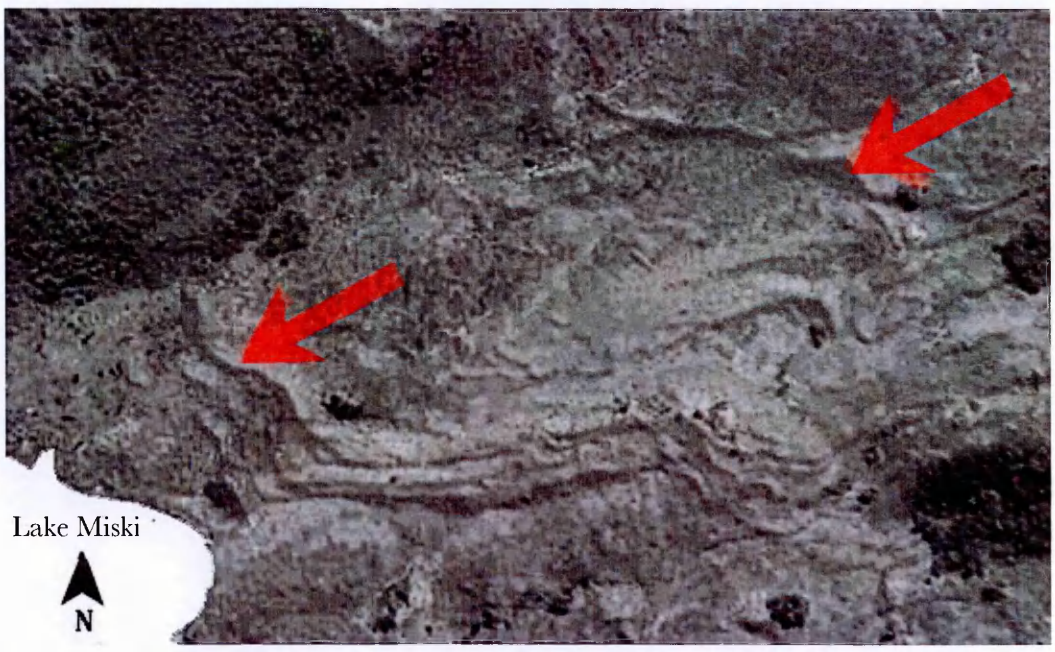

Fig. 3-8 Moraines (red arrows) above Lake Miski (white contour)

Magnetic susceptibility is generally measured before the sediment cores are cut and split. However, this is only possible when coring tube are made of lexan, plexiglass or any other acrylic glass that is free of minerals that may affect the MS readings. The sediment cores are passed through a Bartington loop MS2C that quantifies the magnetization observed in the sediment relative to the tube diameter (Fig. 3-9A). This measurement generally integrates the measurement over large areas (i.e. few centimetres before and after the point measured). This problem can be solved using a Bartington point sensor MS2E (Fig. 3-9B) that measures the MS on the sediment (opened core). The Bartington point sensor provides a better resolution but is less sensitive than the Bartington loop. Magnetic susceptibility was measured in a Geotek core logger (www.geotek.co.uk) at University of Florida using unopened lexan tubes. Details about the procedure are listed in the appendix I.1.

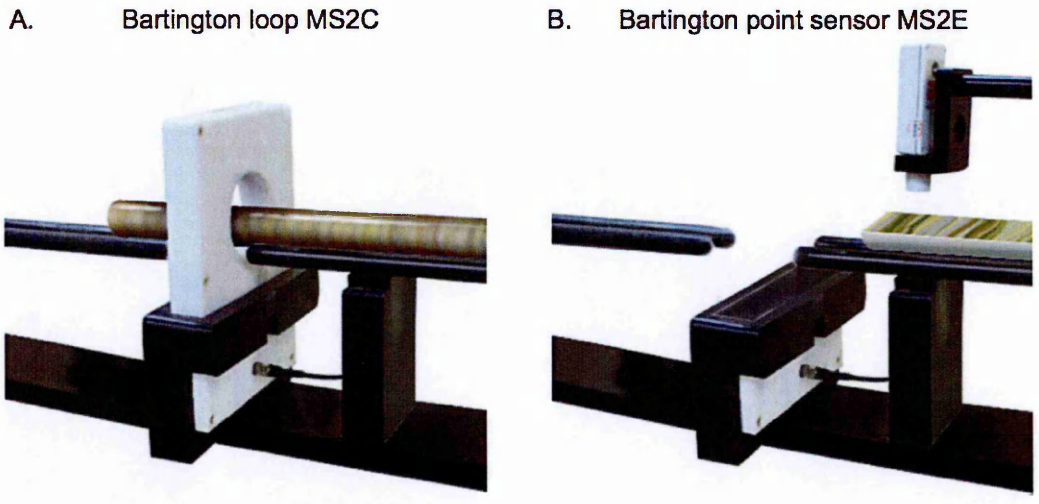

Fig. 3-9 Magnetic susceptibility sensors

The cores retrieved from Lake Miski were logged to determine the MS. The core material was mostly diamagnetic, i.e. the induced magnetic field was weakened by the content of the sediment therefore most of the susceptibility results were negative. A table derived from the Geotek site (www.geotek.co.uk, Table 3-3) was inserted to show the magnetic susceptibility of some common compounds.

Mineral	Magnetic Susceptibility (x 10-6) SI
Water	9
Calcite	-7.5 to -39
Quartz, Feldspar	-13 to -17
Kaolinite	-50
Halite, Gypsum	-10 to -60
Illite, Montmorillonite	330 to 410
Biotite	1,500 to 2,900
Pyrite	5 to 3,500
Haematite	500 to 40,000
Magnetite	1,000,000 to 5,700,000

Table 3-3 Magnetic susceptibility in some common compounds. Data derived from the Geotek MSCL manual (www.geotek.co.uk).

The logged files were opened in EXCEL to remove sections that corresponded to gaps or areas between 2 scanned cores. Once these sections were removed, the depth was corrected and matched to the actual depth registered in the opened cores.

3.3.3.2) *Loss-on-ignition*

Loss on ignition (Dean 1974) is a technique that permits the calculation of carbonate and organic content in sediment samples. The technique relies in successive burnings to eliminate progressively certain compounds in the sample (formulas listed in Table 3-4). For instance, sediment samples are desiccated at 105°C for 6 to 12 hours to eliminate the water content. The weight difference of the sample prior and after the desiccation treatment is used to estimate the water content by weight. The weight difference is used to estimate the organic, carbonate and silica content of the sample in successive burnings. For instance, a second burning at 550°C for 4 hours eliminates the organic material in the sample (eliminated as CO_2 and water). However, 550°C is not enough to raise the partial pressure of the sample to eliminate carbonates. A third burning is performed at 950°C for 2 hours to eliminate the carbonates from the sample. The remaining amount represents silica and other non-volatile elements (i.e. at 950°C). The protocol proposed by Dean (1974) reviewed by Heiri (2001) is based on equations 1 to 3

(below) to estimate the organic, carbonate and silica content of the sample. Appendix I.2 contains detailed description of the procedure.

$OWP = [(W_{105} - W_{550})/W_{105}] * 100$	(Equation 1)
$CWP = [(W_{550} - W_{950})/W_{105}]*100$	(Equation 2)
$SWP = 100 - (OWP+CWP)$	(Equation 3)

Table 3-4 Loss-on-ignition formulas. Where :

OWP: Percentage weight of organic matter

CWP: Percentage weight of $CaCO_3$.

SWP: Percentage weight of silica.

W105 : Dry weight of the sample after treatment at 105°C

W550 : Dry weight of the sample after treatment at 550°C

W950 : Dry sample weight after treatment at 950°C

Since the results are expressed as percentages, a specific volume is not required. However, when a constant volume is used, the results could also be expressed as weight per unit of volume. Additionally the use of a constant volume is useful to verify the accuracy of the measurements, as the weights should have a narrower range than samples with aliquot volumes. The theoretical carbonate weight could be estimated by multiplying the weight loss after the 950°C treatment by 1.36 (Bengtsson and Enell 1986).

3.4) Analysis of ecological proxies

3.4.1) The pollen proxy: background

Palynology is the study of pollen grains and palynomorphs such as spores. The analysis of palynomorphs can be applied in multiple fields such as taxonomy, forensic sciences, history of human occupation, and tracing vegetation and climate change through time among others. The reconstruction of vegetation change through time that initiated with von Post (1946) relies in the fact that the vegetation produces constantly pollen and spores. Pollen assemblages constitute a mirror for the vegetation and therefore can track

vegetation changes under natural (climate) or anthropogenic influences. A disadvantage of the pollen proxy is that pollen grains are well preserved only in anoxic conditions. Consequently substrates suitable for palynological studies are few, e.g. sediments from Delta Rivers, permanent lakes, peat lands, ice cores, and sometimes in water-saturated soils. These substrates record the history of vegetation and climate change through temporal changes in the pollen composition.

Pollen data offer a snapshot of the vegetation at different local and regional scales. The topography and geology of the site may also influence the taphonomic processes that control the pollen accumulation and composition in a given site (Fig. 3-10). Understanding the local topography and possible sources of pollen for the studied sites should not be neglected as it may improve or change how the pollen data is interpreted

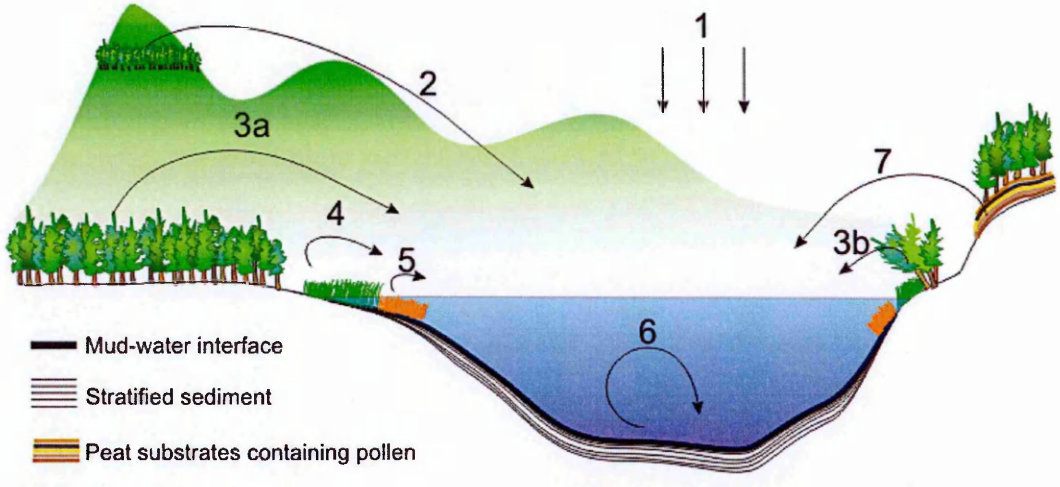

Fig. 3-10 Conceptual model of pollen deposition. Figure modified from Moore *et al.*, (1991) to depict pollen deposition and data interpretation for lakes Miski and Huamanmarca (Chapter 5). The image shows the following components: rain component (1), non-adjacent vegetation (2), Local vegetation (3); Marsh vegetation (4); aquatic vegetation (5); and recirculation (6). Further details are provided in the main text.

The conceptual model in Fig. 3-10 portrays deposition, taphonomic and topographic processes involved in the deposition of pollen grains including:

1 Rain component (regional signal). In the studied sites, e.g. Miski (3800 m), pollen grains derived from lowland species (below 2000 m) or inter montane valleys were grouped as low montane types e.g. *Cecropia* or Anacardiaceae species.
2 Non-adjacent vegetation (transition regional to local signal). In the studied sites this area is represented by cloud forest types i.e. species occurring below 3600 m that are rare in the pollen record.
3 Local vegetation (local signal). These species were surrounding the lakes and were grouped as local taxa e.g. *Polylepis*. The pollen signal of the species in this group is also influenced by how close the species grow relative to the lake e.g. 3a versus 3b.
4 Marsh vegetation (Local signal). Mostly represented by Cyperaceae. This group is extremely susceptible to lake level changes.
5 Aquatic vegetation (Local signal). Mostly represented by *Isoëtes*. This group is extremely susceptible to lake level changes.
6 Recirculation and bioturbation. Pollen grains may recirculate prior sedimentation. If winds are strong enough may produce mixing of the mud water interface with the surface water reducing the possibility of sediment stratification. Bioturbation is also possible when large living organisms are present in the lake. The laminated sediment in the study sites suggests that mixing or bioturbation did not take place.

3.4.2) Pollen preparation and analysis

Samples for pollen analysis were processed using standard palynological techniques described by Faegri and Iversen (1989). A detailed procedure and modifications to the protocol proposed by Faegri and Iversen (1989) is included in appendix II. A constant volume of sediment was measured per sample (0.5 cm^3). All the samples were spiked with a *Lycopodium* tablet containing *c.*18530 *Lycopodium* spores. The spike was used to tally the number of pollen grains contained in one cubic centimetre (Stockmarr 1972) and to estimate the pollen influx (pollen grains per cm^3 per year). Prepared samples were counted with Zeiss Axioskop microscope employing magnifications of 400 × and 1000 ×. A minimum of 300 terrestrially derived pollen grains or 2000 markers (*Lycopodium* spores) was counted per sample. Pollen grains were identified using

published pollen catalogues and descriptions (Markgraf 1978, Hooghiemstra 1984, Roubik and Moreno 1991, Velasquez 1999), the Neotropical Pollen Database and neotropical reference collection housed at the Florida Institute of Technology (Bush and Weng 2007). Pollen grains were also counted using a tally-counter coded in R (appendix II.3) where the commonest pollen types were assigned to a specific keyboard key. The taxa recorded using the R-code generates a csv-file recognized by Excel. The R tally-counter originally admitted a maximum of 62 pollen types; however, the code (appendix II.3) can be modified to include additional types. All the pollen diagrams were generated in C2 (Juggins 1991). Detailed instructions are provided in appendix II.4.

3.4.3) The diatom proxy: background

Diatoms are unicellular algae from the Division Bacillariophyta that produce a silica shell named frustule used for identification in modern and palaecological reconstructions (Battarbee et al. 2001).

Diatoms are globally distributed in water bodies, and lakes in the Andes are no exception (Finlay et al. 2002, Fritz et al. 2004, Hillyer et al. 2009). Once diatoms die, the silica frustules fall to the bottom of the lake and accumulate with the lake sediments, storing climatological information from the time when the diatoms were alive. As with pollen, diatom data provide snapshots of past environmental conditions but at finer spatial and temporal scales than pollen (Schlüter et al. 2012). Diatoms respond quickly (e.g. seasonally) to shifts in nutrient abundance, light, and other environmental variables (Kilharn et al. 1996, Schlüter et al. 2012). Deriving limnological data from diatoms goes back more than a century (Battarbee et al. 2001). Knowledge of the ecology of diatoms was applied in the identification of polluted waters in the early 1900s (Kolkwitz 1908). During the 1920s, diatoms were used as potential palaeoecological indicators (Battarbee et al. 2001). The implementation of statistical and numerical techniques, e.g. multivariate analysis and transfer functions, promoted quantitative diatom-based environmental reconstructions (Flower 1986, Birks et al. 1990, Fritz et al. 1991, Juggins 2013). Currently, diatoms can be used to infer changes in lake levels, (Kilharn et al. 1996, Racca et al. 2004, Fritz et al. 2007, Hillyer et al. 2009), salinity (Baker et al. 2001,

Tapia et al. 2003), pH (Flower 1986, Birks et al. 1990, Jones and Birks 2004), nutrients (Bigler and Hall 2002, Werner and Smol 2005), and temperature (Roseacute et al. 2000, Bigler and Hall 2002, Bigler and Hall 2003).

3.4.4) Diatom preparation and analysis

Samples for diatom analysis were processed using standard techniques described by (Battarbee 1986, Battarbee et al. 2001). A detailed procedure and modifications to the protocol proposed by Battarbee (1986) is included in appendix III. 1 and III.2. Approximately 0.1 cm^3 of sediment was measured per sample. The organic matter in the samples was digested with H_2O_2. Prepared samples were mounted in Naphrax® and counted with Zeiss Axioskop microscope at the magnification of 1000 ×. A minimum of 300 valves was counted per sample. Diatom frustules were identified using published diatom catalogues and descriptions (Patrick and Reimer 1966, Lange-Bertalot and Metzeltin 1996, 1998, Lange-Bertalot 2000).

Diatom diagrams were elaborated using C2 (Juggins 1991) following the instructions detailed in appendix II.4.

3.4.5) The charcoal proxy: background

3.4.5.1) *Standard technique*

Charcoal is a proxy that permits the reconstruction of fire history of a given site. This technique is fairly recent and was developed during the late 80's (Clark 1988, Clark and Patterson 1997a). Lacustrine sediments, and soils are the most common substrates used for charcoal analysis.

When a fire is produced charcoal will be produced in different sizes. The distance that a charcoal particle can be transported relative to the fire origin is inversely proportional to the charcoal particle size. For instance, large particles (> 180 µm) generally remain *in situ* or may be transported a few meters. In contrast, small particles are susceptible to

long distance transport (> 100 m). Consequently when lacustrine sediment contains charcoal particles, these should be categorized by size to differentiate between the signal of local and regional fires. Although fire events are discrete, the signal of the charcoal data in lacustrine sediments may not reproduce each fire event in detail. For instance, when a fire is produced, not all the charcoal fragments become immediately incorporated into the lake sediment. Charcoal transport could be active many years after the original fire was produced. Therefore, a charcoal peak represents a fire event that followed by declining charcoal concentrations year by year until the charcoal source becomes depleted.

The interpretation of charcoal data improves whenever used in combination with other proxies such as pollen, Loss-on-ignition and diatoms among others. For example, fire incidence can be attributed to periods of drought if charcoal peaks coincide with high concentrations of carbonates (lake desiccation) and increasing abundances of saline diatoms (lake desiccation). Without carbonate and diatoms proxies, the charcoal peaks remain as periods of intensified fires without further explanation. Charcoal samples were prepared using a protocol tailored to the sediment type in the records used. A detailed charcoal preparation procedure was inserted in appendix IV.

3.4.5.2) *Charcoal SEM identification*

Charcoal particles can also be identified using a scanning electron microscope (SEM, Fig. 3-11). This technique detailed in appendix IV.2 could be useful to identify which vegetation types were burned (e.g. forest versus grasslands). The charcoal ratio grassland/forest could be used as a fire intensity proxy because low intensity fires may not necessarily burn trees (Chapter 4 discussion). The size of the charcoal particle is probably the main limiting factor for charcoal identification using a SEM. Charcoal fragments from lake sediments rarely exceed 500 μm. Consequently, cleaning the recovered particles without smashing them becomes a challenge. Once the samples are clean, the charcoal particles suspended in water are decanted over the mounting medium. Although the particles can be rotated to the desired position before the water

evaporates, some particles can still rotate due to the water surface tension. The final position of the charcoal fragment in the mounting medium is random. An additional issue when working with SEM samples is the presence of small debris covering the charcoal particles. The debris is hard to remove when they are translucent (e.g. attached plant tissues are unnoticeable) or well attached to the charcoal particles (e.g. clays).

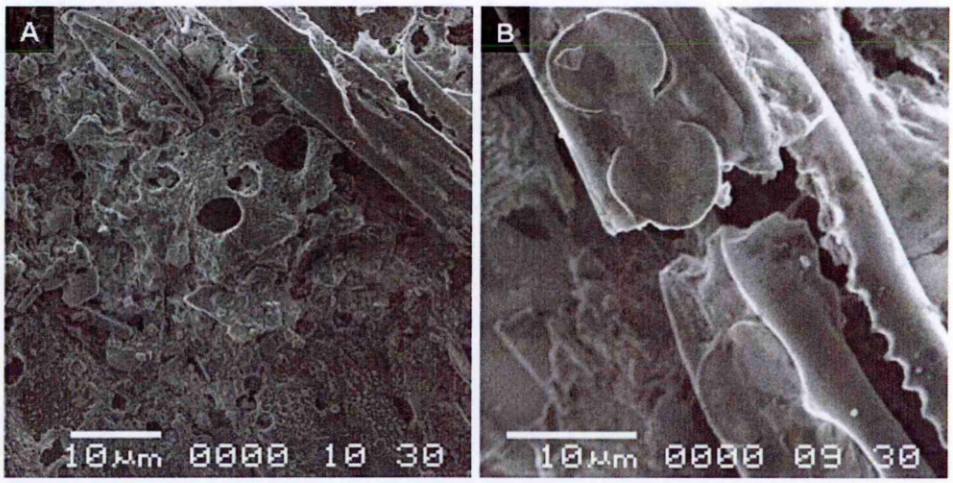

Fig. 3-11 SEM images of charcoal fragments from Lake Miski. A fragment covered in debris. B grass blade with phytoliths.

3.5) Radiocarbon dating

The interaction of nitrogen atoms and neutrons (by-product of high-energy cosmic rays hitting the upper atmosphere) are responsible for the natural formation of radiocarbon (^{14}C). Radiocarbon is an unstable radioactive isotope of carbon that has a half-life of 5730 years and decays into nitrogen. The formation of radiocarbon is fairly constant as it depends on solar irradiation. ^{14}C reacts with oxygen forming CO_2 molecules that are evenly mixed in the atmosphere. An assumption about radiocarbon dating is that plants constantly assimilate CO_2 via photosynthesis; therefore, the $^{14}C/^{12}C$ ratio in their tissues is in equilibrium with the atmospheric values. However, during the photosynthesis the CO_2 containing ^{12}C is preferentially fixed rather than CO_2 containing ^{14}C. Therefore, the proportion of ^{14}C relative to ^{12}C in the plant can reach 5% depletion relative to atmospheric values. This preferential intake of a particular isotope is called fractionation

and varies among organisms. A correction for the ^{14}C fractionation can be made measuring the ^{13}C in the sample because ^{14}C fractionation is twice that of ^{13}C. Such corrections are routine, and was made in this case for all reported ages by the Woods Hole Oceanographic Institute Radiocarbon Laboratory.

The $^{14}C/^{12}C$ ratio in animal tissues is also in equilibrium with the atmospheric $^{14}C/^{12}C$ ratio as they feed on plants (or herbivores). Once an organism dies, no additional ^{14}C is assimilated. Over time, the $^{14}C/^{12}C$ would decrease as ^{14}C atoms decay into nitrogen. Therefore the $^{14}C/^{12}C$ ratio can be used to estimate the time elapsed since an organism died. Lacustrine sediments can be subjected to ^{14}C dating when they contain enough organic material of terrestrial origin. The theoretical limit of radiocarbon is close to 70,000 years; however, actual limits are close to 40,000 years. In general radiocarbon dates above 40,000 are considered unreliable.

3.5.1) Age model

The age model for Lakes Miski and Huamanmarca was generated using six ^{14}C AMS dates for each lake. All the material was dated at The National Ocean Sciences Accelerator Mass Spectrometry Facility (NOSAMS). The ^{14}C results were calibrated using the online version of Calib 6.0 and the R-code provided in Blaauw (2010) selecting the SHcal curve (Table 3-5). The best calibration curve for the age model (black solid and dotted lines in Fig. 3-12) was selected to plot the stratigraphic diagrams for pollen and diatoms in chapter 5. One of the dates for lake Huamanmarca was rejected as it represented a reversal, i.e. did not fit with the stratigraphic order of the other dates.

The age model for Lake Pacucha was constructed from 18 ^{14}C AMS (Table 3-6) calibrated using Calib 5.0.2 (Stuiver et al. 2005) and Fairbanks (Fairbanks et al. 2005) and has been published (Hillyer et al. 2009, Valencia et al. 2010b).

Sample Number	Depth (cm)	14C age	Calibrated age	Mean calibrated age (bold) and (minimum-maximum ranges)	Sigma range	OS- Lab Code
HMC 1	35	2550 ± 70	2594 ± 141	**2594** (2453 - 2735)	2σ	OS-79412
HMC 2 *	117	4060 ± 70	4493.5 ± 88.5	**4493.5** (4405 - 4582)	2σ	OS-77624
HMC 3	202	3940 ± 50	4325 ± 93	**4325** (4232 - 4418)	2σ	OS-77516
HMC 4	287	5980 ± 80	6759.5 ± 102.5	**6759.5** (6657 - 6862)	2σ	OS-77517
HMC 5	328	7540 ± 60	8327.5 ± 52.5	**8327.5** (8275 - 8380)	2σ	OS-77532
HMC 6	350	10800 ± 200	12738.5 ± 185.5	**12738.5** (12553 - 12924)	2σ	OS-79431
HMC 7	406	11050 ± 320	12939.0 ± 303.0	**12939.0** (12636 - 13242)	2σ	OS-86833
MSK 1	62	2250 ± 45	2219.5 ± 117.5	**2219.5** (2102 - 2337)	2σ	OS- 72741
MSK 2	102	3610 ± 35	3823.5 ± 107.5	**3823.5** (3716 - 3931)	2σ	OS- 79411
MSK 3	192.7	6810 ± 55	7599 ± 94	**7599** (7505 - 7693)	2σ	OS- 72742
MSK 4	271	8080 ± 60	8838 ± 194	**8838** (8644 - 9032)	2σ	OS- 72743
MSK 5	318	10700 ± 80	2652 ± 132	**12652** (12520 - 12784)	2σ	OS- 72744
MSK 6	355.5	10800 ± 22.5	12707 ± 129	**12707** (12578 - 12836)	2σ	OS- 79554

Table 3-5 Radiocarbon dates for Lakes Miski and Huamanmarca. * Rejected age

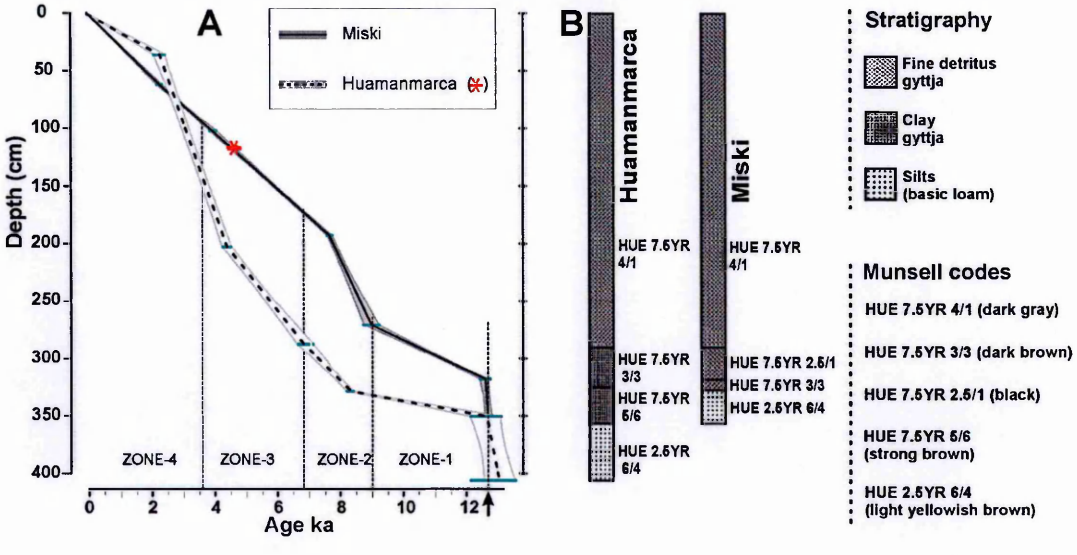

Fig. 3-12 Age model for Lakes Miski and Huamanmarca (A). The age models are accompanied by the stratigraphic description (B). The arrow depicts the age at which both cores start the overlap (c.12.6 ka).

Sample Number	Depth	^{14}C age	Mean calibrated age (cal. yr) (bold) and (minimum-maximum ranges)		Sigma range	CAMS-OS (laboratory code)
1	43cm	875 ± 25	**729**	(683 – 775)*	2σ	OS-64477
2	129cm	635 ± 25	**615.5**	(590 – 641)	2σ	OS-64479
3	187cm	1110 ± 40	**987**	(915 – 1059)	2σ	OS-64476
4	242cm	1800 ± 40	**1642**	(1543 – 1741)	2σ	CAMS-110133
5	414cm	2875 ± 40	**2953.5**	(2841 – 3066)	2σ	CAMS-110134
6	630cm	5190 ± 45	**5894.5**	(5837 – 5952)*	2σ	CAMS-110135
7	743cm	4265 ± 35	**4690**	(4614 – 4766)	2σ	CAMS-110136
8	775cm	4480 ± 40	**4972**	(4866 – 5078)	2σ	CAMS-123761
9	826cm	6025 ± 40	**6793.5**	(6675 – 6912)	2σ	CAMS-110137
10	853cm	7160 ± 35	**7926**	(7847 – 8005)	2σ	CAMS-123762
11	914cm	9430 ± 40	**10606.5**	(10493 – 10720)	2σ	CAMS-123837
12	979cm	11050 ± 45	**12916**	(12868 – 12964)	2σ	OS-64478
13	1036cm	13195 ± 50	**15366**	(12820 – 13012)	2σ	CAMS-110138
14	1124cm	18670 ± 70	**22282**	(15132 – 15600)	2σ	CAMS-123763
15	1182cm	19650 ± 110	**23477**	(22110 – 22454)**	2σ	OS-64510
16	1232cm	14275 ± 45	**16766**	(23143 – 23811)**	2σ	CAMS-123764
17	1309cm	16700 ± 50	**19830**	(16546 – 16986)	2σ	CAMS-123765
18	1427cm	20660 ± 90	**24612**	(19662 – 19998)	2σ	CAMS-123766

^{14}C-AMS dates were calibrated using Calib 5.0.2 (Stuiver *et al.*, 2005; numbers 1–11) and Fairbanks *et al.* (2005; numbers 12–18). Mean values (bold text) were used for creating the age model. Samples marked * were rejected

Table 3-6 Pacucha radiocarbon dates

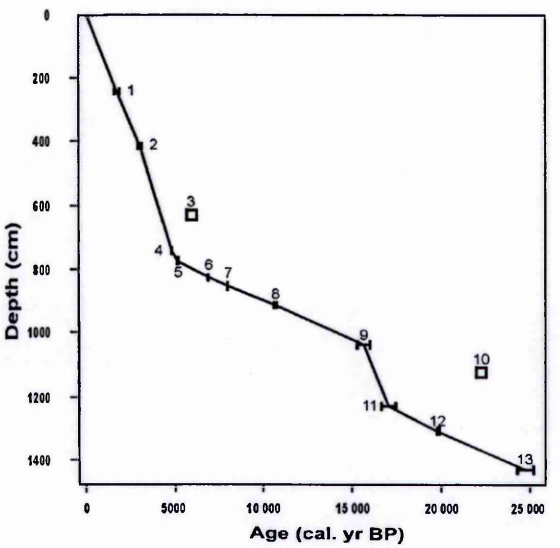

Fig. 3-13 Age model for Lake Pacucha (Hillyer et al. 2009). Squares represent rejected ages.

3.5.2) Statistical analysis

Details about statistical analysis are provided in the methodology section of chapters 4 and 5. This section provides complementary information and the rationale for the statistical techniques used in chapters 4 and 5.

3.5.2.1) *Detrended correspondence analysis (DCA)*

DCA is an indirect gradient analysis technique that is used in quantitative community ecology (McCune and Mefford 2002). As other multivariate methods, DCA is aimed to simplify the relationship between samples and species to depict them in a low-dimensional space but retaining most of the information of the original data (Gauch 1982, McCune and Mefford 2002). DCA was preferred over principal component analysis (PCA) and non-metric multidimensional scaling (NMDS) due to the following reasons: The data (vegetation assemblages based on pollen counts) do not satisfy the linearity assumptions required for PCA. Furthermore, PCA tends to produce a strong arch effect that places together samples that are located at the extremes of a gradient (i.e. convolution). On the other hand NMDS is based on ranked data that produces dimensionless results without ecological meaning. The main advantage of DCA over NMDS is that the axes are expressed in standard deviations of species turnover. Therefore, distances in the ordination space are comparable magnitudes along each axis (gradient). Although DCA generates results similar to those produced with NMDS; DCA was heavily criticized because of the arbitrary detrending and rescaling of the axes (ter Braak 1986, Minchin 1987, McCune and Mefford 2002).

Despite the arbitrary detrending and rescaling, DCA was preferred over NMDS because site comparisons (individual pollen counts from three sites) that require meaningful axis scales are required (Chapter 4). Pollen counts from multiple records could be merged into one matrix to perform a unique DCA or any other multivariate technique. This step is only possible if the same species are present in each one of the records that will be merged or if ecological equivalents are shared among records.

3.5.2.2) *Permutation techniques on ordination outputs:*

Ordination techniques are generally used to generate hypothesis but rarely to test them. Permutation techniques applied to ordination results provide the opportunity to evaluate if two or more groups in a particular ordination output are different. Hypothesis testing on ordination outputs becomes feasible as long as groups are defined prior to running any particular ordination technique (e.g. DCA). As p-values are estimated by permutations, it is possible to test the hypothesis that two or more pre-defined groups (e.g. Pleistocene vs. Holocene samples) are significantly different. The most common permutation techniques in use are ANOSIM and multiple-response permutation procedures (Biondini et al. 1988, Clarke and Green 1988, McCune and Mefford 2002).

3.5.2.3) *Species distribution modelling: MaxEnt*

MaxEnt is a method used to model the suitable habitat of a species based on presence data (individual coordinates) and multiple environmental variables (continuous or categorical data) (Phillips et al. 2006, Phillips and Dudík 2008). MaxEnt uses a subset of the presence data (training data) to create a model that predicts the preference (occurrence) of a particular species given the environmental variables included (Willems and Hill 2009, Václavík et al. 2012). A statistic AUC-training (area under the receiver operating characteristic) provides an estimate of the fit of the model to the training data. Subsequently the remaining subset of the data (testing data) is used to evaluate the actual predictive ability of the model. The AUC-testing shows the fit of the testing data to the model and is the one reported in the results. Finally, MaxEnt produces a map with a continuous logistic output where pixels take values between 0 and 1 that represent the probability of occurrence of the species (Phillips and Dudík 2008, Elith et al. 2011).

Cross-validation was preferred to evaluate the predictive ability of the model (Phillips et al. 2006). For cross-validation the presence data is split into groups of similar size (k-folds). Then, the model is run k times excluding one group (fold) in each run. After k-

runs, a mean and the standard deviation of the AUC derived from all the runs are then provided (MaxEnt manual, www.cs.princeton.edu/~schapire/maxent/). The advantage of cross-validation (k-folds) is that the entire dataset is used in training and testing. This method makes an efficient use of the data especially when dealing with small datasets.

Jackknifing was used to evaluate the contribution of each environmental variable in the model. The models are run with and without a particular environmental variable and then plotted against a run that includes all the variables. This method shows the contribution of each individual environmental variable and shows if a variable increases or reduces the performance of the model. Environmental variables that lower the predictive ability of the model can be removed.

3.6) Summary

In this chapter summarizes the rationale and scientific basis for the application of physical and palaeoenvironmental reconstruction techniques applied to the Miski, Huamanmarca and Pacucha cores that include; i) Magnetic susceptibility to infer the local deglaciation onset, ii) Loss-on-Ignition to reconstruct lake level changes and productivity, iii) fossil pollen analysis to reconstruct vegetation and trends of vegetation change and, iv) fossil diatom analysis to infer changes in the landscape influenced by vegetation changes, and v) charcoal to reconstruct fire dynamics. Chapter 3, provided a description and rationale of the statistical techniques used in chapters 4 and 5 including i) ordination techniques such as DCA and NMDS, ii) permutation techniques and, iii) species distribution modelling with MaxEnt.

The palaeoenvironmental reconstruction techniques described in the current chapter are applied in the subsequent chapters to identify ecological baselines for the Andes and use baseline concepts on the species distribution modelling

Chapter 4) Vegetation baselines for the high Andes

The following chapter is aimed to identify ecological baselines for the Andes. Pollen and diatoms records were already published for Lake Pacucha (Hillyer et al. 2009, Valencia et al. 2010b). Besides the published data, I counted additional 31 pollen samples from Lake Pacucha specifically for this thesis (appendix VIII). Anne Rockholt, Majoi de Novaes Nascimento and Robert Van (graduate and undergraduate researchers at Florida Institute of Technology) carried out the diatom counts, which are also included here. I assisted in the supervision of the undergraduate and graduate researchers, conducted all the statistical analysis and created all the diagrams.

A version of this chapter will be submitted for publication as:
Valencia, B.G., Gosling, W.D., Bush, M.B., Coe, A.L. Novaes-Nascimento M., Rockholt A., & Van R. (in preparation) Vegetation baselines for the high Andes. *Ecological Monographs*,

4.1) Abstract

The identification of "natural" ecological baselines for Andean ecosystems is fundamental to avoid having anthropogenic landscapes as goals for conservation restoration and management. Because human occupation in South America traces back to *c.*14 ka, the high Andes is considered a manufactured landscape. The vast archaeological evidence left by pre-Columbian Andean civilizations such as the Wari, Tiwanaku, and Inca over the last two millennia further reinforces the idea of an anthropogenic Andean landscape.

Although human-induced landscape transformation is undeniable, the degree of landscape transformation cannot be assumed to be spatially homogeneous. Palaeoecological reconstruction derived from Lakes Miski, Huamanmarca and Pacucha show that the impact of humans was a mosaic of "near pristine" and disturbed patches. Trajectories of past environmental change in the studied sites suggest that (i) human activities impacted substantially the Andean landscapes only after 7 ka and that (ii) the

early Holocene, i.e. 10 ka, could be used as "natural" ecological baseline for Andean ecosystems. The trajectories of vegetation change from Lakes Miski and Huamanmarca further show that ecological baselines cannot be expected to reach stability as assemblages vary constantly influenced by climate, biotic and stochastic processes.

4.2) Introduction

Andean ecosystems are among Earth's most vulnerable areas due to projected climate change and increasing human activities (Orme et al. 2005, Anderson et al. 2011, Hole et al. 2011). Conservation of these ecosystems requires an understanding of "what is natural", i.e. an ecological baseline that can provide a reference point for restoration efforts associated with carbon-offset trading and similar initiatives (Hoffmann et al. 2011). For millennia, extensive land use has produced what has been described as a "manufactured landscape" (Denevan 1992, Dillehay 2008, Sandweiss and Richardson 2008, Bauer et al. 2010). Even areas that do not show overt signs of human action may not support natural floristic communities as they could represent a perception of ecological baseline (hereafter baseline) conditions that have been previously "shifted" by past human activity. The concept of "shifting baselines" identifies a repeated intergenerational pattern of accepting a degraded environment as "natural", thereby promoting a continuous recalibration of what constitutes a high-quality habitat for restoration effects (Pauly 1995, Pauly et al. 2002).

4.2.1) Time sensitivity, species change, and shifting baselines

Though, initially, used to describe fisheries (Pauly 1995), the concept of shifting baselines is broadly applicable in ecology. Choosing what constitutes a legitimate baseline, however, is problematic. In fisheries, the limited capacity of humans to impact oceanic fish populations in pre-industrial times, allowed baselines to be set *c.*200-400 years ago (Pauly et al. 1998, Jackson 2001, Jackson et al. 2001). For example Restrepo et al (2012) identified a human impact on the flora of the Galapagos Islands around El Junco Crater Lake that occurred between settlement (1800s) and first scientific

description in 1966 (Colinvaux 1968). The acceptance of the altered habitat as a natural state constituted an example of a shifted baseline (Bush *et al.*, in review, 2014). As longer timeframes, e.g. millennial rather than centuries are considered, long-term climate change influencing community structure becomes more probable (Hooghiemstra 1989, Hanselman et al. 2011b). In terrestrial settings, where many landscapes were extensively modified by humans for millennia (Yi et al. 2003), a baseline may have to be sought from the pre-agricultural era. Furthermore, it should also be noted that humans were able to modify landscapes even in pre-agricultural times, e.g. landscape alteration through exterminating large mammals and the use of fire (Miller et al. 1999, Piperno 2007, Ugan and Byers 2007, Rule et al. 2012). Thus both, biotic and abiotic factors play a role in producing multiple potential baseline states for any given location or climate (Hobbs and Cramer 2008).

If the search for a baseline state means looking back over millennial timescales, the concept of a natural baseline becomes more problematic as it would imply community stasis or equilibrium. Indeed, long-term directional selection, i.e. natural climatic change, could be at work on communities (Pickett and Parker 1994, Choi 2004, Hobbs and Cramer 2008), or species could be essentially disequilibria due to complex climatic and migrational histories (Hutchinson 1941, 1961, Connell 1978). If a neutral view is adopted (Hubbell 2001), random drift could also cause community structure to change, while still being natural.

The current definition of baselines (sensu Pauly, 1998) still retains the implicit idea that there is a fixed assemblage that is the natural state. If such equilibrium exists, the system would revert to its former state following a pulse of disturbance. For instance, if climate or human pressure first exerts an influence, and then when the influence is ended, the landscape should return to an "equilibrium" state equivalent to the one observed prior to the disturbance (Fig. 4-1 A-C, E). Hereafter this concept will be referred to as an "equilibrium baseline". An alternative hypothesis is that baselines will not be static entities but will reflect long-term changes in an environmental gradient. The concept and identification of "dynamic baselines" (Fig. 4-1 F) should incorporate the complexity of biological and ecological processes under a changing environment. In this view,

vegetation assemblages would mirror influences such as changing insolation, differing strengths of the El Niño Southern Oscillation, and Atlantic sea-surface temperature trends, plus the individualistic responses and histories of organisms.

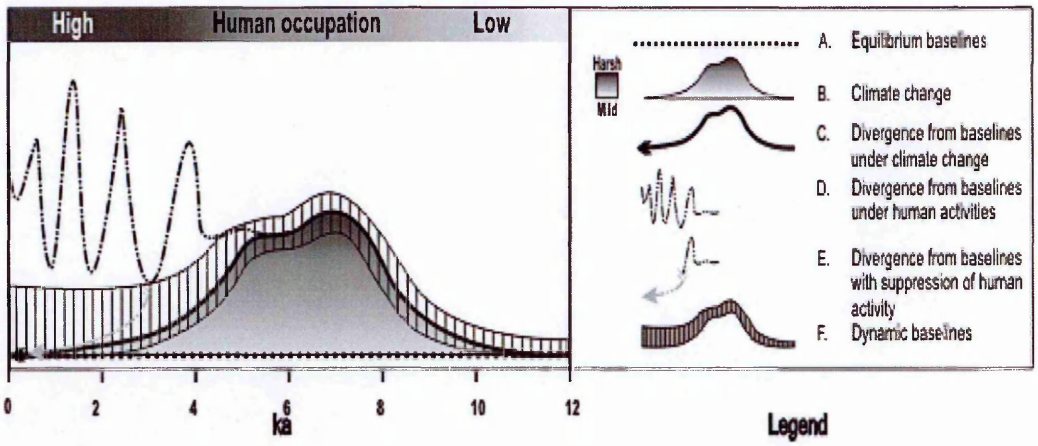

Fig. 4-1 Conceptual model of shifting baselines (left panel) and legend (right panel).

4.2.2) Climate and human-induced trajectories of change

Defining natural baselines in the Andes is particularly challenging because of the well-documented pre-Columbian occupation by societies such as the Tiwanaku, Chanka, Wari, and Inca (AD 400-1492) (Dillehay and Collins 1988, Meltzer et al. 1997, Dillehay 2008). Humans have occupied South America for at least the last *c.*14 ka (all ages are given in 000s calibrated ^{14}C years before present; ka) and have occupied the Andes for the last 11-10 ka (Pires-Ferreira et al. 1976, MacNeish et al. 1983, Lynch 1985, Lavallée 1987, Roosevelt et al. 1996b). In the high Andes, Human populations probably remained low during the late Pleistocene and early Holocene (*c.*10 ka) due to physiological and environmental limitations (Aldenderfer 2008). Prior to 10 ka humans may have visited the high Andes, but probably had few, if any, permanent settlements above 3000 meters above sea level (m asl) (Dillehay 2008). Pollen data from this period showed that vegetation typical of warm interglacial (Holocene) climates was common in the high Andes between *c.*11 ka and 10 ka, suggesting that the climate resembled modern conditions (Paduano et al. 2003). Subsequently, the climate became warmer

and drier tracking increasing summer insolation (Baker et al. 2001). The Holocene of the Central Andes was marked by falling lake levels and a series of sustained droughts known as the Mid Holocene Dry Event, MHDE (Markgraf et al. 2000, Rowe et al. 2003).

The MHDE was a time-transgressive event recorded in southern Brazil, the western Amazon and the Andes (Abbott et al. 2003, Bush et al. 2004b, Mayle and Power 2008). In the central Andes of southern Peru, the onset of drying was evident as early as 11 ka, and was commonly impacting lake levels by *c.*9 ka (Hillyer et al. 2009). Multiple indicators of moisture availability such as fossil diatoms, carbonate concentrations, and seismic profiles from high Andean lakes indicated that the MHDE was centred at *c.*5 ka (Baker et al. 2001, Rowe et al. 2002, Tapia et al. 2003, Hillyer et al. 2009, Williams et al. 2011a). Pollen records from Andean locations showed that vegetation remained largely unchanged during the Early Holocene droughts (*c.*10-8 ka) (Colinvaux et al. 1997, Valencia et al. 2010b). During the early Holocene drought conditions were composed of a series of dry and wet episodes rather than a continuous drought (Baker et al. 2009, Valencia et al. 2010b). Thus, although changes in lake level reflected a drying, vegetation changes were not apparent in fossil pollen records from the Andes (Paduano et al. 2003, Valencia et al. 2010b). In contrast, ecotonal regions experienced extreme changes such as the complete replacement of lowland forest by savanna (Absy et al. 1991, Mayle and Power 2008).

In the Andes, the MHDE coincided with a period of diminished human activity known as the "archaeological silence" (sensu Núñez et al. 2002). Although the spatiotemporal influence of this event on humans is still poorly known, extremely dry conditions were thought to have limited human activities or induced cultural collapse (Hodell et al. 1995, Binford et al. 1997, Haug et al. 2003). The late Holocene was characterized by the development of advanced Andean cultures as the MHDE weakened (Chepstow-Lusty et al. 2003, Bauer et al. 2010, Sublette et al. 2012). The widespread adoption of agricultural practices further promoted large-scale landscape transformation for nearly three millennia prior to European arrival at *c.*0.5 ka (Hastorf 2008). Crop pollen and elevated fire frequencies were common in many records from the Andes as signatures of

human occupation (Hansen and Rodbell 1995, Chepstow-Lusty et al. 1998, Valencia et al. 2010b, Sublette et al. 2012).

The detection of baselines requires the temporal identification of landscapes without human impact. Although the archaeological data provide evidence of occupation they do not necessarily provide a sensitive means to detect when landscapes were first impacted by human activities. An alternative approach to detect when landscapes were transformed is to identify trends of vegetation that are no longer primarily driven by climate change (i.e. human induced). For example, Lago Consuelo (1360 m asl), Pacucha (3090 m asl) and Titicaca (3810 m asl) experienced analogous species turnover (similar vegetation trends) due to increasing temperatures after the Last Glacial Maximum despite the differences in species composition between sites (Paduano et al. 2003, Urrego et al. 2010, Valencia et al. 2010b). When the trends of vegetation change of sites with similar climate, elevation, and species composition diverge an inference can be drawn: that climate is no longer driving the changes. Therefore, diverging trends of vegetation change can be used to provide an estimate of when landscape transformation became a product of human disturbances.

Defining a time that Andean landscapes can be considered natural could include times when humans were present but had a minimal impact on vegetation. Given that climatic shifts caused a corresponding change in vegetation, not every change was attributable to people. Contrasting vegetation responses in sites with intensive use with those that had relatively sparse human use in modern times may help to separate natural from human-induced landscape changes.

Besides the history of human occupation, the identification of baselines for Andean landscapes should consider the extent of landscape transformation. Sites that had minimal human influence should be better suited for baseline detection. It is easy to write-off all of the high Andes in southern and central Peru as being impacted by people. Every valley seems to be lined with terraces and buildings, and ancient monuments are abundant. But our perception may be biased by accessibility. Modern roads are often built on ancient tracks meaning that we tend to see the readily accessible

regions. Similarly, lakes used for paleoecological studies are often attractive locations for settlement and therefore are not necessarily representative of the entire landscape. Overall, an almost ubiquitous human influence is not challenged in this study, but we do show evidence of unchanged or minimally changed sites embedded in a matrix of human-modified landscapes

In this study we present new multi-proxy data derived from two Andean lakes (Miski and Huamanmarca) compared with previously published data (Pacucha) to answer the following research questions: (1) To what extent are the records from Miski and Huamanmarca representative of other records in the region? This question is aimed to evaluate the local and regional sensitivity of the study sites (2) Was the woodland-grassland mosaic a long-term feature of the environment? This question is aimed to define if the modern vegetation observed around the studied sites (woodland-grassland mosaic) was the product of human impacts, as mosaics are considered the product of anthropogenic activities (3) Can a period in the Holocene form a satisfactory baseline for the natural state of Andean vegetation? This question is aimed to identify if a period from the past can define what is a natural state for modern Andean ecosystems.

4.3) Site Description

At the head of the Huamanmarca Valley lie Lakes Miski (13° 1' 23"S 72° 22' 40"W; 3830 meters above sea-level (m asl)) and Huamanmarca (13° 2'1.29"S 72°22'38.48"W; 3900 m asl) (Fig. 4-2). Both lake sites lie on the Eastern cordillera of the Andes and are located 75 km northwest of Cusco, Peru. Lakes Miski and Huamanmarca were formed in near parallel valleys when a glacier retreated. Although moraines dammed both lakes, the valley where Lake Miski lies is u-shaped with slopes generally under 20%, whereas Huamanmarca lies in a V-shaped valley with slopes greater than 45%. Lake Miski has two sub-basins (200 m and 60 m wide) separated by a shallow and narrow shelf. Two small streams feed the main basin (11 m deep) from the northern and eastern shores. The lake has a single outlet with the stream flowing westward from the secondary basin (3 m deep). Multiple terminal moraines (>15) lie within 2 km of the lake

ranging between *c.*3600 and 3900 m asl with most of them located above 3800 m asl. The largest moraines occur below Lake Miski at 3770 m asl, and woodlands may hide further evidence of glacial activity below 3600 m asl. The basin of Lake Huamanmarca is 390 m x 175 m wide and 20 m deep. A single stream feeds the lake from the southeast and the outlet is located at the opposite side of the lake. Two main moraines were evident in the Huamanmarca valley. One moraine impounded a small lake at 4400 m asl, while the other, which lay at 3830 m asl has been completely in filled with organic rich material covered by *Sphagnum* moss.

Precipitation in the Huamanmarca valley region reaches *c.*2000 mm according to measurements at Huyro (1700 m asl), which is the closest meteorological station to the sites. Although Huyro lies 18 km away from the studied sites, calibrated satellite measurements indicate that Huamanmarca and Miski receive a comparable amount of rain. Approximately, 80% of the annual precipitation falls during the rainy season (November-April) coinciding with days of easterly airflow (Vuille 1999, Garreaud and Aceituno 2001, Garreaud et al. 2003). Precipitation in this area is highly influenced by El Niño Southern Oscillation (ENSO) and temperature anomalies in the tropical North Atlantic (Vuille et al. 2000a, Vuille et al. 2000b). Besides precipitation, cloud cover is an important source of moisture. Dense mats of arboreal epiphytes suggest that cloud cover is a permanent feature even during the dry season.

Mean annual temperatures at the sites are estimated to be *c.*11 °C based on measurements at 3800 m asl of elevation, allowing for a local adiabatic lapse rate of 5.5 °C per 1000 m of ascent (Bush et al. 2004b), and measurements taken at similar elevations (Zimmermann et al. 2010). While mean temperatures remain fairly constant during the year, daily fluctuations regularly exceed 20 °C (Kessler 2006, Horn and Kappelle 2009). Night frosts are usual at this elevation, especially between June and August (Lauer 1981).

Lakes Miski and Huamanmarca each have a catchment area of about 1.6 km^2. The local woodlands are dominated by the tree genus *Polylepis* (Rosaceae). Additional members of the following genera and families are also present: *Hesperomeles* (Rosaceae),

Gynoxys (Asteraceae) and Melastomataceae. Hereafter, the term 'local woodlands' describes arboreal and shrub species present in the lake catchment. Practically all the trees present in Huamanmarca valley are covered with epiphytes that, over time, form thick organic mats on the branches. Epiphytes constantly drip water as they intercept clouds that cover the site most of the day. Lake Miski has few trees growing close to the lake (i.e. within 10 m), whereas Huamanmarca is practically surrounded by woodlands. Cloud forest species are mostly present below the local timberline at 3740 m asl. Hereafter, the term "cloud forest" will be used to identify arboreal and shrub species that grow downslope of these catchments.

The land that surrounds both lakes is currently used for grazing cattle (*c.*20-30 animals) that roam freely within the main valley. Cultivation and deforestation are limited by the difficult access to the sites (rough terrain) and persistent high humidity. Earthworks, e.g. terraces, are absent in the immediate surroundings of lakes Huamanmarca and Miski. However, major Incan constructions such as Machu Picchu and Ollantaytambo are located *c.*20-30 km south of the lakes.

Burned trees provided evidence of recent fires close to both Huamanmarca and Miski sites (pers. obs. 2008). In general, most of the burned areas had moderate slopes and were located below the catchment of both lakes. The effect of fires was more evident around Lake Miski than in Huamanmarca. The few trees growing close to Lake Miski were in bare rock or craggy locations, which may have escaped fire. Wood extraction was limited in this area because of the steep slopes and wet climate. Most of the branches on dead standing trees or woody material lying on the ground were sodden, and unsuitable for burning.

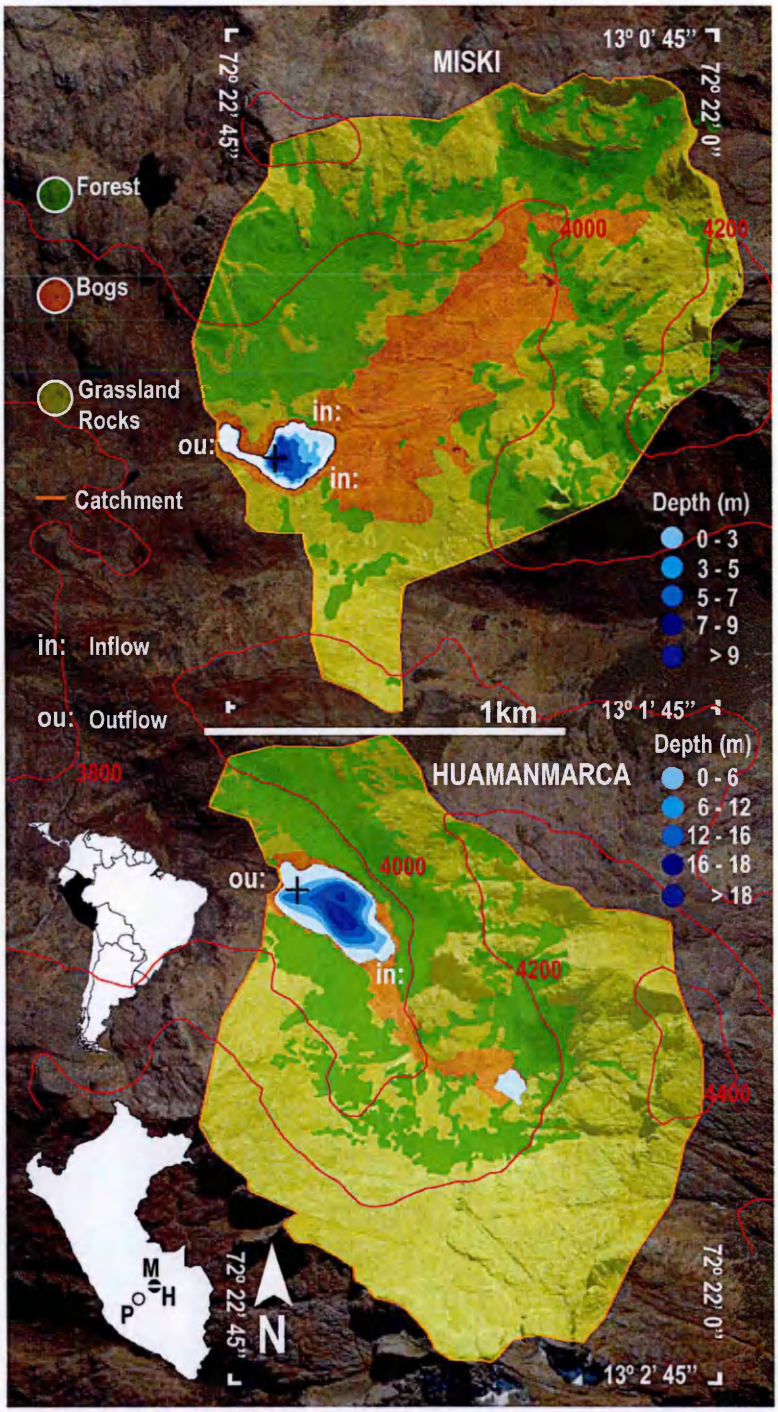

Fig. 4-2 Topographic map of the Huamanmarca valley showing Lakes Miski and Huamanmarca. The coring sites were depicted with a + in each lake. The lake catchment (orange contour) was divided in forest (green), bogs (orange) and grasslands (yellow). Elevation contours are depicted by red lines. Within the Peru map, lake initials depict the position of Miski (M), Huamanmarca (H), and Pacucha (P).

4.4) Materials and methods

In December 2008, two parallel cores were raised from Lakes Huamanmarca and Miski using a Colinvaux-Vohnout piston corer (Colinvaux et al. 1999). A total of 4.07 m (HMC-2) and 4.15 m (Miski-1) of sediment were retrieved in lexan tubes from the deepest section of Lakes Huamanmarca and Miski (Fig. 4-2). The cores were transported to Florida Institute of Technology for storage.

Core description started with the magnetic susceptibility (MS) scan at 0.5 cm using a GEOTEK core logger. The longest and most complete cores were split, described and subsampled (section 3.3). The age models were generated using AMS ^{14}C on bulk sediment (Table 4-1 age model). Sub-samples of 0.25 or 0.5 cm^3 were taken for pollen, diatoms, loss-on-ignition, and charcoal analysis, which were analysed using standard techniques (Section 3.4).

Pollen samples were mounted in glycerol and counted using a Zeiss Axioskop photomicroscope at magnifications of x400 and x1000. A minimum of 300 terrestrial pollen grains was counted per sample, per lake. Identifications were carried out using the Neotropical pollen search tool and database (Bush and Weng 2007), pollen keys and atlases (Markgraf 1978, Hooghiemstra 1984). Loss-on-ignition followed Dean (1974) with modifications made by Heiri (2001). Charcoal extraction followed the procedure by Clark and Patterson (1997b). Particles larger than 180 µm were selected and photographed with a Hitachi camera under an Olympus stereo macroscope at x25. Charcoal areas were calculated using imageJ software 1.3 (Rasband). Diatoms were processed following Battarbee (1986) and samples mounted in naphrax. Diatom counts were made using a Zeiss Axioskop photomicroscope at x1000 magnification to a total of 250 frustules per sample.

Data for all the proxies were plotted using C2 (Juggins 1991). The zonation was based on Coniss run on the combined pollen data from Lakes Miski and Huamanmarca using the R-package Rioja (Juggins 2012). Sample groups generated with Coniss were superimposed on a detrended correspondence analysis (DCA; Hill 1979) output. Differences between groups in the DCA output were estimated using Multiple-Response

Permutation Procedures (Mielke 1984, Mielke 1991, Mielke and Berry 2001, Oksanen et al. 2010). Euclidean distances were calculated based on pollen percentages with the R-package paleoMAS (Correa-Metrio et al. 2012). Comparisons between the pollen assemblages of Lakes Miski, Huamanmarca, and Pacucha were based on DCA analysis run on 44 robust taxonomic groups, i.e. identifiable and consistently represented groups (appendix V, Table A4-1). Comparisons between diatom assemblages for Lakes Miski and Pacucha were based on DCA analysis run on 11 robust taxonomic groups (appendix V, Table A4-2). The DCA axis-1 was plotted against time to depict the trends of vegetation change. Maps and bathymetric contours were elaborated using Quantum GIS 1.8, R 2.15.1 (R 2011) and ImageJ (Rasband).

4.5) Results

4.5.1) Age model:

The age model of Lakes Miski and Huamanmarca (Table 4-1 and Fig. 4-3) is based on six bulk radiocarbon dates per record. Samples for radiocarbon dating were taken from sections of the sediment cores that did not react with 10% HCl, i.e. had low carbonate concentration, to minimize hard water error. An improbably old date for the sample from 117 cm sediment depth from Lake Huamanmarca was rejected.

4.5.2) Local Pollen and Diatom Zonation

Four local zones were defined running Coniss on the combined pollen data from Miski and Huamanmarca (Fig. 4-4). The four groups were subsequently defined on a DCA output in the same combined data (Fig. 4-5). A Multiple-Response Permutation Procedures (MRPP) run on the DCA output showed that the four zones were significantly different with significance of delta < 0.0001 and a high A-statistic, i.e. 0.3423. The number of permutations used for the MRPP analysis was 10,000. The pollen zones were subsequently applied on the pollen and diatom diagram for Lake Miski (Figs. 4-6 to 4-9).

Site Name	Laboratory code	Depth (cm)	14C age	Mean calibrated age (bold) and (minimum-maximum ranges)		
Miski	OS-72741	62	2250 ± 45	2220	(2102 -	2337)
Miski	OS-79411	102	3840 ± 127	3840	(3716 -	3970)
Miski	OS-72742	193	6810 ± 55	7600	(7505 -	7693)
Miski	OS-72743	271	8080 ± 60	8840	(8644 -	9032)
Miski	OS-72744	318	10700 ± 80	12650	(12520 -	12784)
Miski	OS-79554	356	10800 ± 22	12710	(12578 -	12836)
Huamanmarca	OS-79412	35	2550 ± 70	2590	(2453 -	2735)
Huamanmarca	OS-77624	117	4060 ± 70	4490	(4405 -	4582)**
Huamanmarca	OS-77516	202	3940 ± 50	4330	(4232 -	4418)
Huamanmarca	OS-77517	287	5980 ± 80	6760	(6657 -	6862)
Huamanmarca	OS-77532	328	7540 ± 60	8330	(8275 -	8380)
Huamanmarca	OS-79431	350	10800 ± 200	12740	(12553 -	12924)
Huamanmarca	OS-86833	406	11050 ± 320	12940	(12636 -	13242)

Table 4-1 Calibrated ages for Lakes Miski and Huamanmarca. Rejected ages were marked (**)

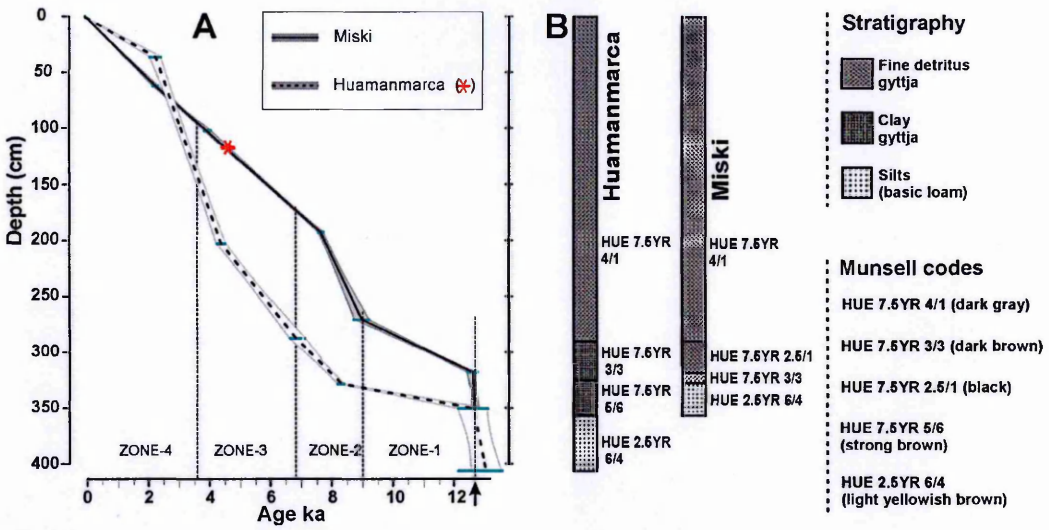

Fig. 4-3 Age model (A) and lake stratigraphy (B) for Lakes Miski and Huamanmarca. A rejected age from Huamanmarca is depicted by (*). The arrow depicts the age at which both cores start the overlap (*c.*12.6 ka) and defines the origin of zone 1.

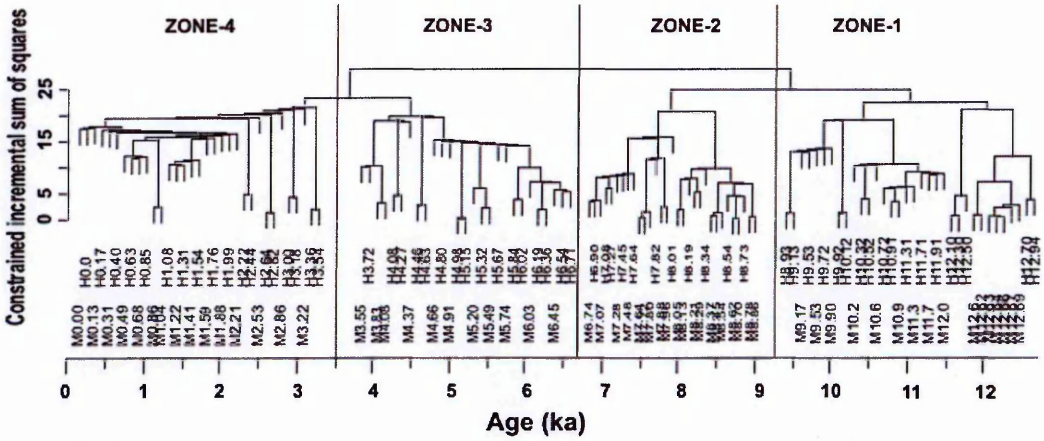

Fig. 4-4 Stratigraphically constrained cluster (Coniss) for the combined pollen data from Lakes Miski and Huamanmarca.

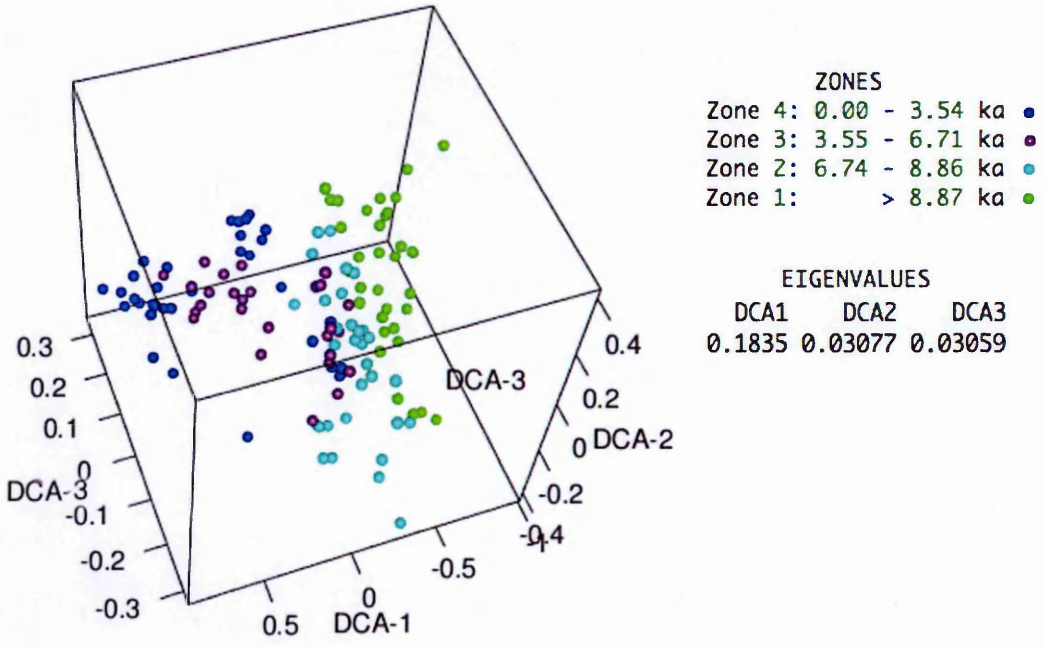

Fig. 4-5 Plot of the first three DCA-axes of the combined pollen data from Lakes Miski and Huamanmarca. The zone selection was based on the Coniss clustering.

4.5.2.1) *Zone 1: 12.6 – 9 ka*

This period corresponded to the depth interval between 350 and 260 in Lake Miski and 350 to 316 cm in Huamanmarca. The sediment in both cores was enriched with glacial silts (Fig. 4-3) and in Miski showed fine but weak laminations. MS values dropped 15 SI units at 12.6 ka in Miski coinciding with the highest values of Silica (96%) derived from LOI (Fig. 4-6). No major MS changes were observed afterwards. In this zone silica values remained > 80% while Organics and carbonates remained < 18 and 2% respectively.

Pollen influx varied substantially in both records especially prior to 12 ka. The maxima of the record (Miski) and the zone (Huamanmarca) reached 18,000 and 1700 grains cm^{-2} $year^{-1}$, respectively (Figs. 6 and 7). Pollen concentrations were more stable in Miski than in Huamanmarca. Representation of local woodlands in both records was < 5%, but showed a slight increase toward the top of the zone. The herbaceous taxa did not experience any change except for Poaceae, which increased in abundance (*c.*> 10%) between 12.6 ka and 11 ka, before stabilizing. Montane forest species such as *Hedyosmum, Podocarpus, Acalypha, Cecropia* and most of the psilate fern spores, reached their maximum values for both records in Zone-1. Low montane species remained at very low but stable percentages. The water fern *Isoëtes* fluctuated between 80 and 50% in Miski and was constantly < 60% in Huamanmarca. Charcoal particles from Lake Miski were present in 6 out of 25 samples, while charcoal was practically absent in Lake Huamanmarca (Fig. 4-6, 4-7, and 4-9).

Planktonic diatoms (centric) represented by *Aulacoseira* increased in three main pulses, at *c.*11, 10 and 9.2 ka, as benthic diatoms, especially *Achnanthidium* and *Brachysira,* responded negatively to increases in the planktonic taxon, *Aulacoseira* (Fig. 4-8 and 4-9C). Pennate, araphinid, diatoms from the genus *Fragilaria* and *Tabellaria* decreased from *c.*13 to *c.*< 3% after 11 ka.

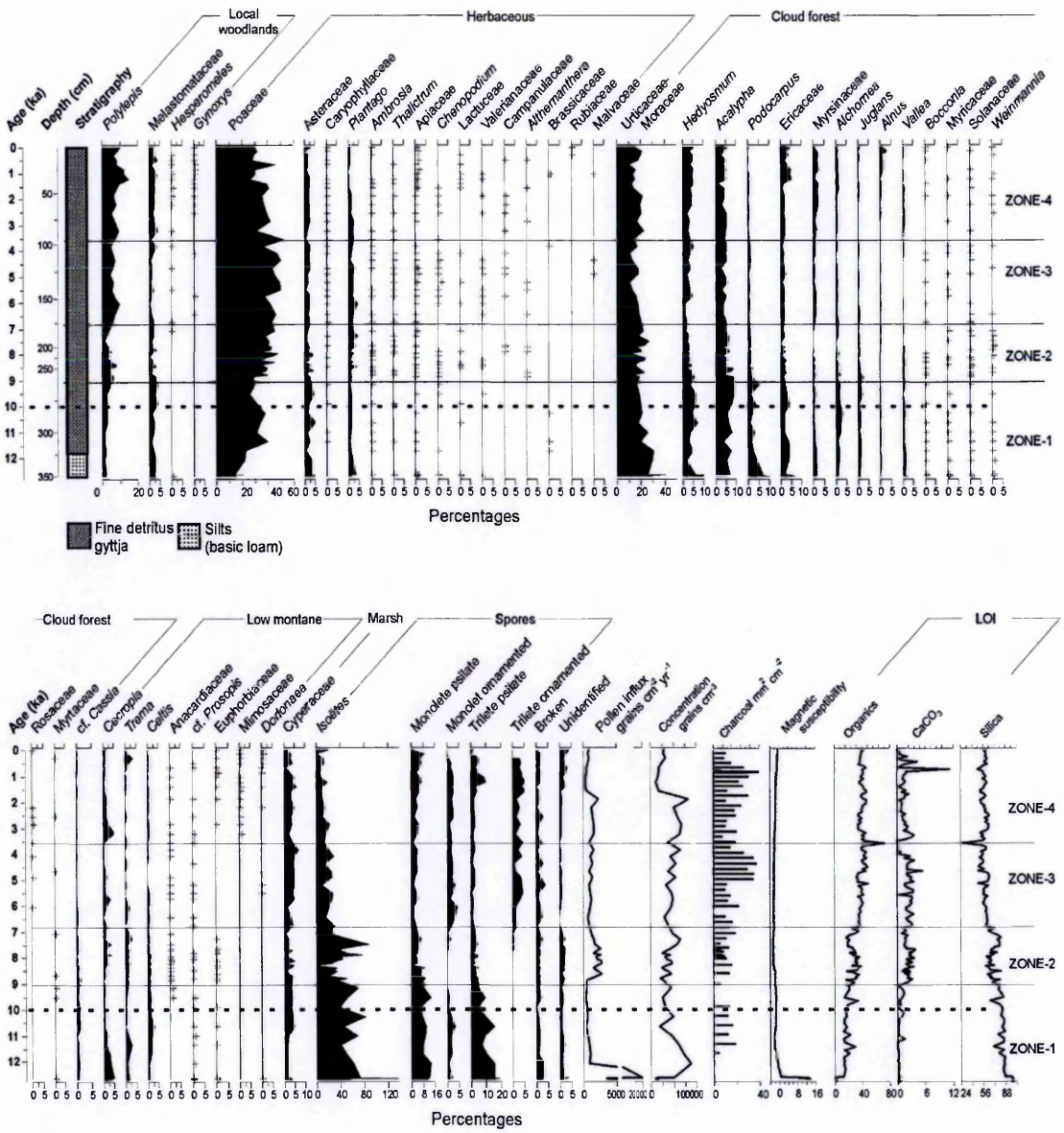

Fig. 4-6 Pollen Diagram from Lake Miski showing taxa grouped by vegetation type. Charcoal concentrations, magnetic susceptibility and Loss-on-ignition are shown at the end of the diagram. Pollen percentages under 3% were marked with +. Taxa under 3% present in less than 6 samples were excluded. A doted line at 10 ka represents the identified baseline.

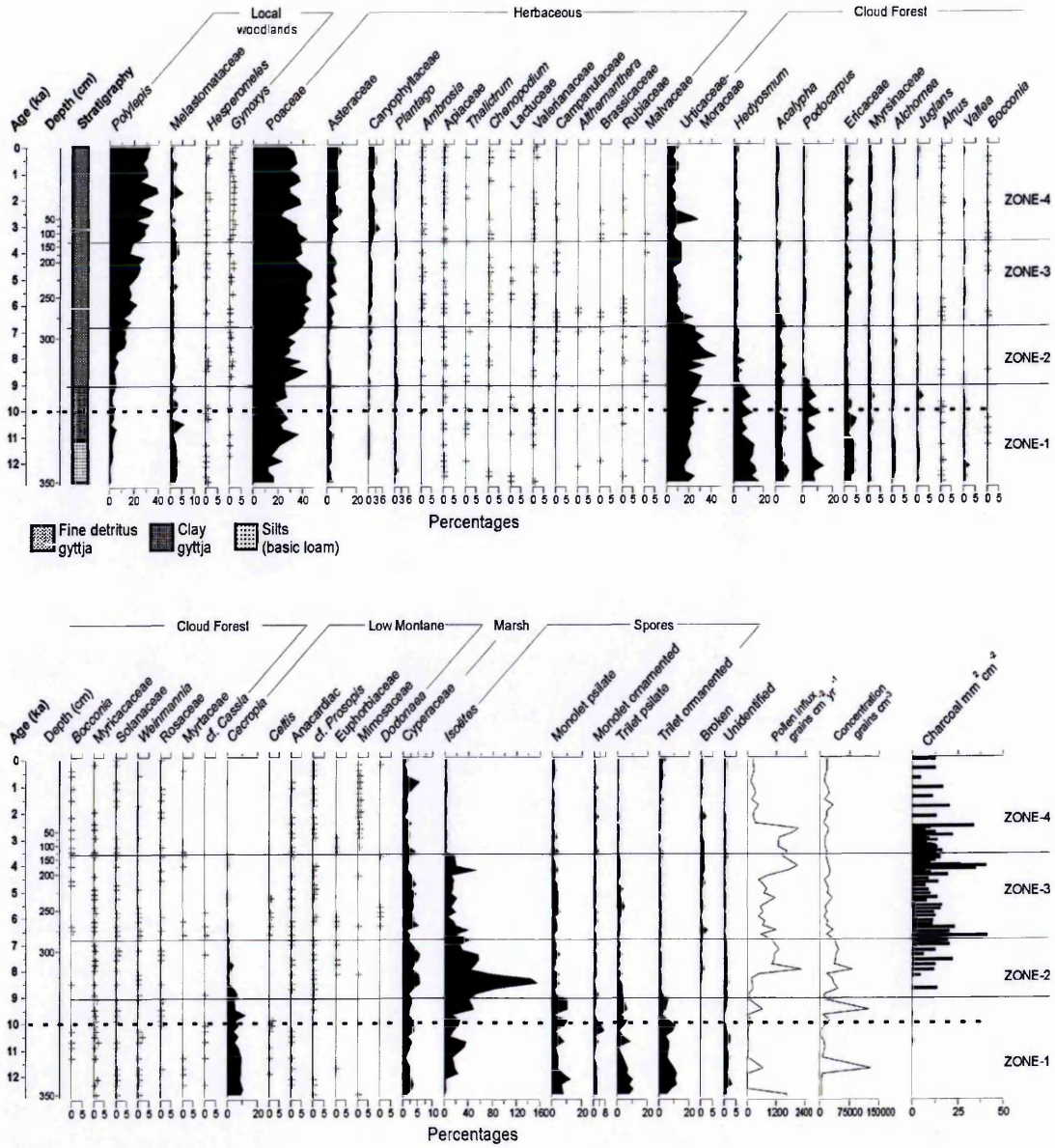

Fig. 4-7 Pollen diagram from Lake Huamanmarca. Charcoal concentrations are shown at the end of the diagram. Pollen percentages under 3% were marked with +. Taxa under 3% present in less than 6 samples were excluded. A doted line at 10 ka represents the identified baseline.

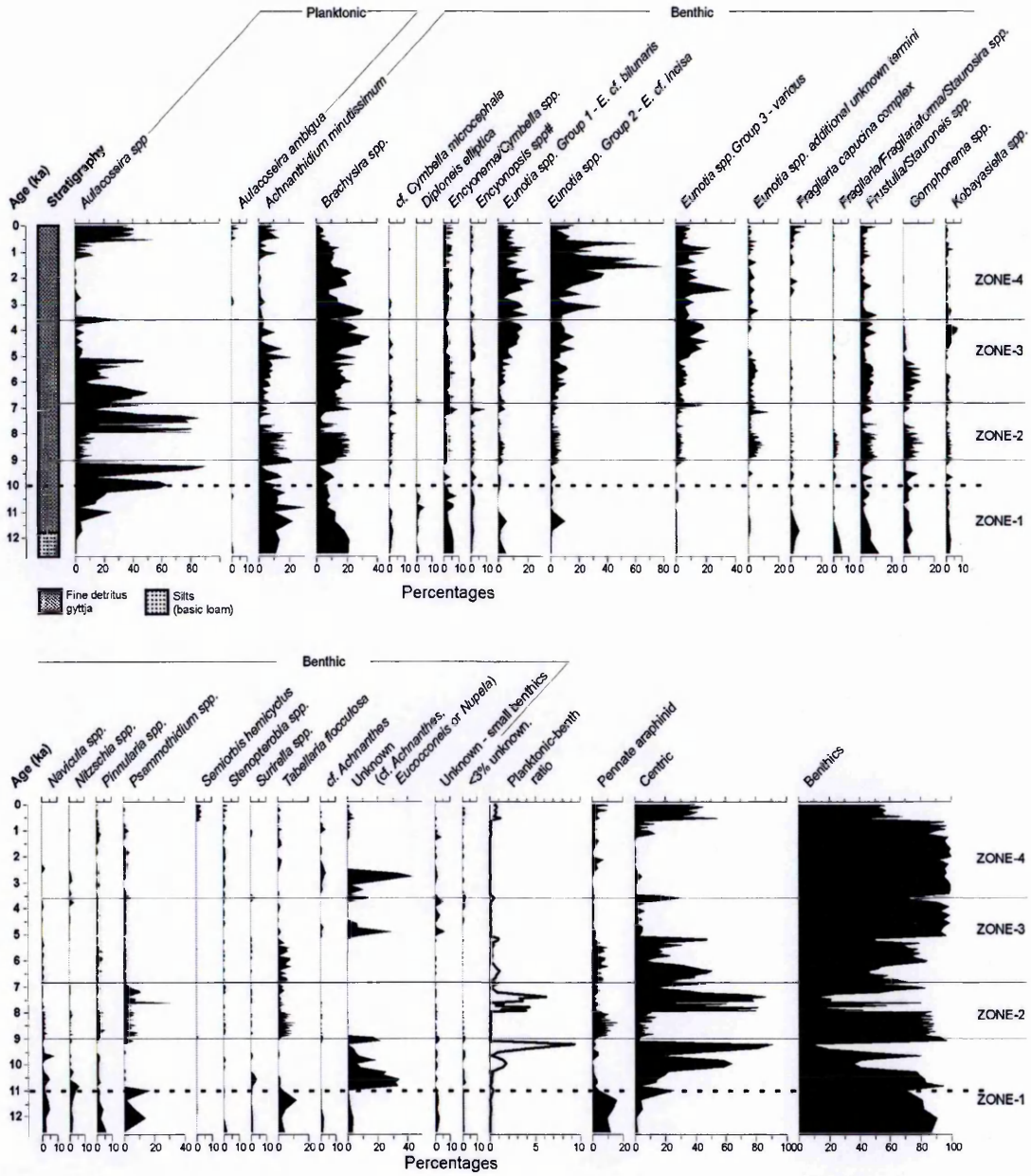

Fig. 4-8 Diatom diagram for Lake Miski. All the taxa are depicted. The counts were carried out by Anne Rockholt, Majoi de Novaes Nascimento and Robert Van. A doted line at 10 ka represents the identified baseline.

4.5.2.2) *Zone 2: 9.1 – 6.8 ka*

This period corresponded to the sediment depth interval from 260 to 175 cm in Lake Miski and from 316 to 285 cm in Huamanmarca. The sediment in Zone-2 had fewer laminations than Zone-1. The MS readings indicated a lower ratio of clastic to organic inputs in Zone-2 relative to Zone-1. In Zone-2, the organic content of the sediment was greater than 25% except for the period between 7.7 and 7 ka. The MS values remained unchanged except for a small peak centred at 8.5 ka.

Pollen data from cloud forest types consistently decreased at the onset of Zone-2 (*c.*10%) except for Urticaceae-Moraceae, which remained stable in Miski and increased in Huamanmarca (Fig. 4-9A). The local woodlands in Miski experienced a decline from 8.5 to 7.5 ka, recovering afterwards (Fig. 4-9A). In contrast, pollen from local woodlands, i.e. *Polylepis*, increased gradually in Huamanmarca. Most of the herbaceous types remained stable in both records except for Poaceae that increased in Miski and decreased slightly between 8.4 and 7 ka in Huamanmarca. *Isoëtes* spores reached their lowest values at Miski around 8.2 ka, recovering by 7.4 ka. *Isoëtes* had the opposite behaviour in Huamanmarca reaching a local maximum at 8.5 and gradually decreasing afterwards. Monolete and trilete ornamented spores in Zone-2 were practically absent. The first unmistakable charcoal peak in Huamanmarca occurred at 8.7 ka reaching 14 mm^2 cm^{-2}. After *c.*8.5 ka, the charcoal signal became a regular feature of both records. Zone-2 started with a reduction in the abundance of planktonic diatoms, i.e. *Aulacoseira,* from *c.*80 to <15%. Pennate, araphinid, and benthic taxa rose to *c.*10 and c 80 %, respectively (Fig 9C). After *c.*8 ka, *Aulacoseira* fluctuated between 20 and 80%.

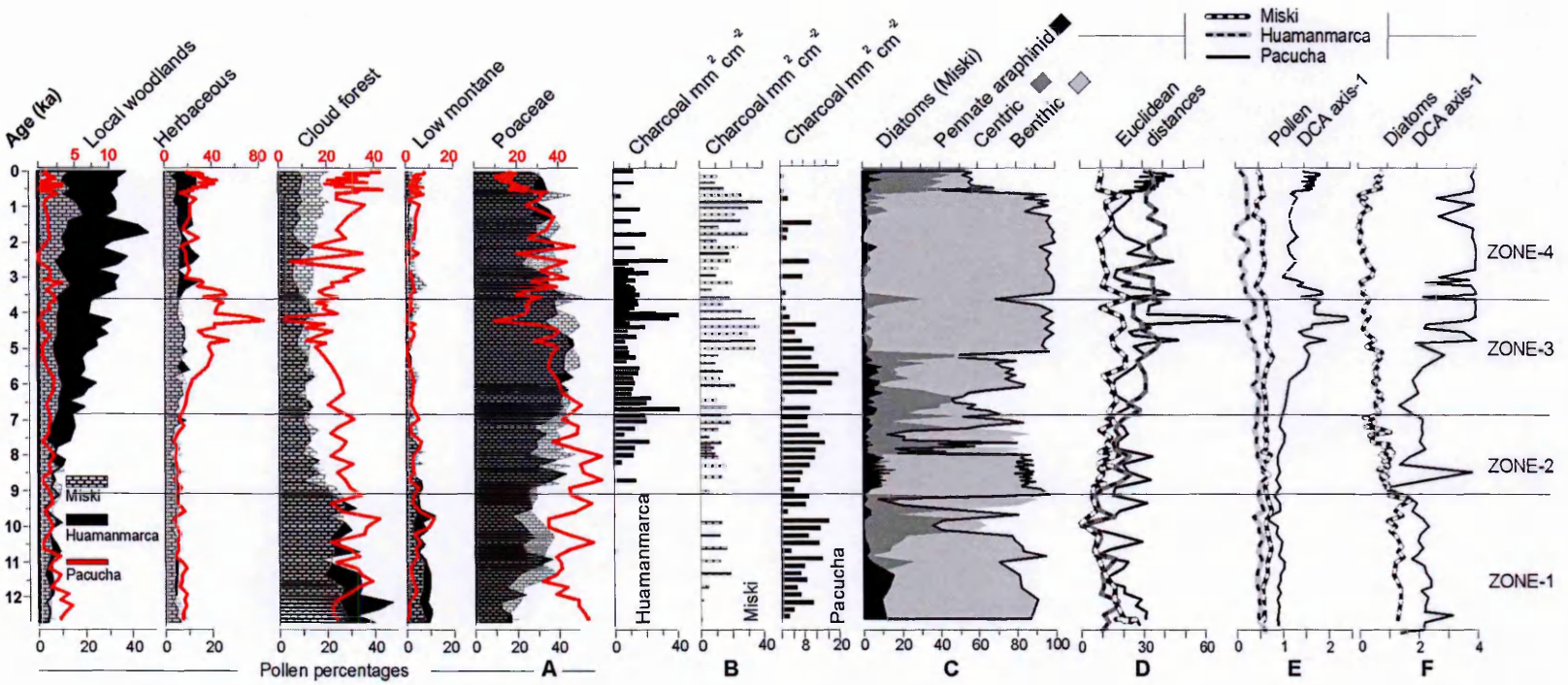

Fig. 4-9 Summary diagram for Miski, Huamanmarca and Pacucha. A) Pollen diagram depicting vegetation type abundances. B) Charcoal data for Lakes Miski and Huamanmarca. C) Diatom diagram for Lake Miski showing pennate araphinid, centric, and benthic abundances. D) Euclidean distances for Lakes Miski, Huamanmarca and Pacucha. E) Pollen DCA axis-1 scores for Lakes Miski, Huamanmarca and Pacucha. F) Diatom DCA axis-1 scores for Lakes Miski and Pacucha.

4.5.2.3) *Zone 3: 6.8 – 3.6 ka*

This period corresponded to the sediment depth interval between 175 and 97 cm in Lake Miski and 285 to 133 cm in Huamanmarca. The sediment from both lakes was very dark and rich in organic material. The MS from Lake Miski did not show any changes. Silica values gradually decreased during this zone while organic content consistently increased. Carbonates did not show any trend but were consistently higher than in any other zone.

The pollen abundances of *Polylepis* remained stable in Lake Miski and increased in Huamanmarca in Zone-3. Herbaceous species were stable during this zone, although, Poaceae pollen achieved their highest values in both records at 5 ka (Figs. 6 and 7). The peak in Poaceae coincided with a reduction of pollen grains of Urticaceae-Moraceae in Huamanmarca and in Miski. *Isoëtes* gradually declined in both records and was consistently lower than in previous zones. The majority of charcoal peaks were concentrated in Zone-3 with the highest values centred at 4.5 ka, reaching nearly 40 mm^2 cm^{-3}. The maxima of Poaceae coincided with the peak of *Brachysira* and the demise of *Aulacoseira* and *Isoëtes*. The genus *Achnanthidium* peaked with *Brachysira* and decreased by 4 ka. In contrast, pennate, araphinids became abundant at 6 ka and species of the genus *Eunotia* at the end of Zone-3.

4.5.2.4) *Zone 4: 3.6 ka – to Modern*

This period was represented by the sediment depth interval between 97 and 0 cm in Lake Miski and 133 to 0 cm in Huamanmarca. The sediment from both lakes was greyish dark with organic and silica content similar to Zone-3. Carbonate percentages were slightly lower than Zone-3 but showed the maxima for the entire record at *c.*0.9 ka reaching 12%.

Polylepis attained its maximum values in both records in Zone-4 while *Gynoxys*, *Hesperomeles,* and Melastomataceae became more evident in both records. A gradual decline in Poaceae was accompanied by increasing percentages of Asteraceae and Caryophyllaceae in Huamanmarca. All the herbaceous taxa remained stable in Miski.

The abundances of montane forest taxa stayed low and stable except for Ericaceae and *Alnus*, which rose after *c.*1.5 ka. Pollen from lower montane taxa continued to be highly variable and did not show a clear trend. Concentration of trilete spores covaried with the minor pollen increase observed in *Alnus* and Ericaceae. In contrast, *Isoëtes* concentrations steadily decreased during Zone-4 in Lake Miski and were below 10% in Huamanmarca. Charcoal peaks in Zone-4 were similar to Zone-3 in terms of their variability and concentrations. At Lake Miski, the charcoal signal coincided with the peak in carbonates and the decline of *Polylepis* pollen. Overall, changes in charcoal abundances were independent of the response of local woodland and montane forest taxa.

Planktonic diatoms of the genus *Aulacoseira* became abundant only after 1.2 ka. The abundance of *Achnanthidium* appeared to be negatively correlated with the changes observed in *Aulacoseira*. The genus *Brachysira* experienced an overall decline from 3.5 ka to modern. Multiple types of *Eunotia* reached their highest values of the record in Zone-4, between 3 and 1 ka, declining during the last millennium.

4.6) Discussion:

4.6.1) To what extent were the records from Miski and Huamanmarca representative of the broader region?

This question was answered by interpreting the paleoecological records from Miski and Huamanmarca comparing them with other regional paleoecological records. The aim was to evaluate if both records registered regional (e.g. Central Andes) climatic events such as the Mid Holocene Dry Event centred at *c.*5 ka (Abbott et al. 2003) or increasing precipitation at the end of the Holocene after *c.*3 ka (Abbott et al. 1997, Valencia et al. 2010b).

4.6.1.1) *Early Holocene environments (Zone-1, 12.6-9 ka)*

A rapid decline in sediment magnetic susceptibility and density at Lakes Miski and Huamanmarca signaled local glacier retreat about *c.*12.6 ka. Although coincident with the onset of the Younger Dryas thermal reversal (*c.*7 °C cooling) in northern Europe and the Andes (Alley 2000, Rodbell and Seltzer 2000, Bakke et al. 2009), no comparable cooling event was observed either at Miski or Huamanmarca. The absence of additional peaks in MS after the glacier began its retreat suggested that local deglaciation was unidirectional and without thermal reversals. Pollen records from Lakes Chochos, Pacucha, and Titicaca were consistent with data derived from Miski and Huamanmarca, suggesting a regional and gradual warming in the Central Andes (Paduano et al. 2003, Bush et al. 2005, Hillyer et al. 2009, Bush et al. 2011). By *c.*12 ka most of the glacial silts were trapped in moraines formed above Miski and Huamanmarca. This change was reflected in both cores as a switch from clear silty material to dark organic-rich sediments. The increase of *Isoëtes* spores at c.12 ka was consistent with the reduction of suspended silts that favoured light penetration and the spread of this aquatic species.

Falling concentrations of benthic diatoms and carbonate at Lake Miski indicated that lake level was increasing between *c.*11.5 and 9.1 ka (Figs 4-8 and 4-9). Increasing precipitation was also recorded in Lake Titicaca after *c.*10 ka (Tapia et al. 2003) and was consistent with the initial local woodland expansion observed in Lakes Miski and Huamanmarca. At this time Lake Pacucha remained as a shallow lake and its diatom flora was dominated by benthic species (Hillyer et al. 2009).

As at other Andean locations, e.g. Lakes Chochos, Baja, Junín, Surucucho, and Titicaca (Hansen et al. 1984, Hansen and Rodbell 1995, Colinvaux et al. 1997, Paduano et al. 2003, Bush et al. 2005), forest expansion took place in the catchment of Miski and Huamanmarca between *c.*12 ka and 11 ka. Vegetation histories from all these sites suggested a period of apparent forest stability between *c.*11 and 9.1 ka. Some contrasting records from southern Peru and Bolivia were characterized by grassland expansion suggesting that fire became important between *c.*11 and 9.1 ka (Urrego et al. 2011, Williams et al. 2011a).

4.6.1.2) *The mid Holocene environments (Zones 2 and 3; 9-3.5 ka)*

The first indication of the MHDE was evident in Lake Miski at *c.*9.1 ka when planktonic diatoms, e.g. *Aulacoseira sp.* and *Aulacoseira ambigua*, fell in abundance (Fig 8-9). This initial Miski dry period was sustained between *c.*9.1 and 8 ka and characterized by high concentrations of benthic diatoms such as *Brachysira, Achnanthidium, Frustulia, Gomphonema,* and *Psammothidium* sp. Concentrations of calcium carbonates were higher in this period than in Zone-1. Increasing percentages of Poaceae and reduction of cloud forest types in Lakes Miski and Huamanmarca further supported the onset of the MHDE. Lake level drops triggered the decline of *Isoëtes* in Lake Miski at *c.*8.4 ka. As the lake became shallow, *Isoëtes* individuals growing on the shore were exposed to night frost. In contrast, Lake Huamanmarca was deep enough to retain sufficient water to support an abundant *Isoëtes* population when lake levels fell below the lake outlet (3906 masl). The onset of a dry period was registered *c.*0.6 ka earlier in Miski than in Lake Titicaca, and *c.*>2 ka later than in Lake Pacucha.

The development of the drought in Lake Miski was depicted by the increased abundance of benthic diatoms and deposition of carbonates between *c.*9.1 and 8 ka. The MHDE was interrupted by a sequence of wet events between 8 and 5 ka indicated by population fluctuations of planktonic diatoms in Lake Miski. However, the main trend of increasing drought resumed after *c.*7.5 ka as Poaceae and *Brachysira* percentages gradually increased. A comparison of the DCA scores derived from Miski and Pacucha showed that diatom assemblages followed the same trend of change prior to 7 ka and diverged afterwards (Fig. 4-9F). This finding suggests that despite the expected difference in sensitivity, i.e. non-overlapping DCA scores, both lakes responded similarly to the increasing drought prior to 7 ka. The tendency of increasing drought observed after 7 ka in Miski and Huamanmarca was characterized by elevated abundances of Poaceae pollen and benthic diatoms like *Brachysira* from Lake Miski. These drought indicator taxa alternated rapidly with peaks of planktonic diatoms, suggesting that both dry and wet episodes were taking place.

Local woodland cover was constant or increased slightly after *c.*9.1 ka in both Miski and Huamanmarca. Thus, the climate probably consisted of alternating wet and dry

episodes that left a signature of drying within the sediment, but did not cause a major change in forest flammability or cover. An alternative possibility would be that although less rainy, persistent cloud cover caused the potential fuel to remain damp and thereby reduce flammability. At other Andean sites, e.g. Chorreras and Chochos (Hansen et al. 2003, Bush et al. 2005), the onset of the MHDE was marked by an expansion of Poaceae, coupled with increased charcoal deposition. Although Poaceae increased in abundance, forest was not completely lost at these sites, suggesting patchiness caused by fire, rather than a biome shift.

The period between *c.*7 and 5 ka may have been influenced by a pulsing ENSO that became more active starting at *c.*7 ka in the high Andes (Rodbell et al. 1999, Moy et al. 2002). Although ENSO is recognized as being an important source of Andean climatic variability, recent droughts were linked to Atlantic rather than the Pacific forcing. (Marengo et al. 2011, Marengo et al. 2012). Anomalous temperatures in the tropical North Atlantic were also linked to weakening trade winds and the northward displacement of the ITCZ reducing moisture in the Amazon and the Andes (Ekdahl et al. 2008, Zeng et al. 2008, Marengo et al. 2012). Although the mechanism that drove the mid-Holocene moisture fluctuations remains to be identified, reconstructions from Lakes Chochos, Pacucha, Umayo, and Pumacocha suggest that decadal to multi-decadal fluctuations were taking place in the Andes (Bush et al. 2005, Baker et al. 2009, Bird et al. 2011).

At *c.*5 ka Lake Miski reached its lowest lake level of the Holocene. High concentrations of carbonates and the benthic diatom, *Brachysira,* coincided with a peak of Poaceae pollen. The Poaceae pollen curve from Lake Huamanmarca mirrored that of Lake Miski. This drought was consistent with low stands recorded in other sites from the Altiplano and the central Andes (Seltzer et al. 1998, Baker et al. 2001, Tapia et al. 2003, Ekdahl et al. 2008, Hillyer et al. 2009, Williams et al. 2011a).

4.6.1.3) *Late Holocene environments (Zone 4, 3.5-0 ka)*

The effects of the MHDE in Miski and Huamanmarca faded between 4 and 3 ka as Poaceae percentages and the benthic diatom *Brachysira* decreased. After 3.5 ka Lake Miski became acidic as *Eunotia* percentages rose coinciding with the largest peak in organics registered in the core. *Eunotia* became the most abundant benthic diatom until *c.* 0.8 ka when it was replaced by the planktonic genus *Aulacoseira.* The shift produced at 0.8 ka coincided with a reduction of the local woodlands around Lake Miski, i.e. *Polylepis* pollen abundance declined. Fire incidence was the most likely factor that induced this shift. Increasing precipitation between 4 and 3 ka was a regional event (Abbott et al. 2003, Tapia et al. 2003). For instance, saline diatoms, carbonates and $\delta^{13}C$ organics declined as Lake Titicaca overflowed filling the Huiñaymarca basin between 3.5 and 3.3 ka (Abbott et al. 1997, Baker et al. 2001, Tapia et al. 2003).

4.6.1.4) *Trajectory of environmental change*

The trajectory of the vegetation change between records from Miski, Huamanmarca and Pacucha was similar prior to *c.*7 ka suggesting that climate change was the main driving force. Similar trajectories in the pollen DCA scores (Fig. 4-9E) implied a similar controlling mechanism was influencing these lakes. Diverging vegetation trajectories were evident after *c.*6 ka when human activity began to impact Lake Pacucha probably due to cultivation of Amaranthaceae crops (Valencia et al. 2010b). In contrast, Miski and Huamanmarca followed the same trajectories without evidence of human activity. Surprisingly, the trajectories derived from the diatom records from Miski and Pacucha matched the trends of change observed in the vegetation (Fig. 4-9E and F). DCA scores increased rapidly after 7 ka for pollen and diatoms in Pacucha suggesting eutrophication while scores declined in Miski and Huamanmarca.

The temporal continuity of forests observed in Miski and Huamanmarca, despite the regional evidence of the mid-Holocene drought, indicates that cloud cover may have been an important part of the hydrological balance. Halladay et al., (2012) identified a cloud cover band of high frequency that persisted through all seasons along the eastern

slope of the Andes in southern Peru. Our study sites lay within the elevational range of high cloud frequency that was suggested to decrease above 4000 m asl in this area. The apparent contradiction of lowered lake level, but persistent forest cover was interpreted to reflect reduced precipitation, but continued frequent cloud immersion at these sites. Despite the regional reduction of precipitation at 5 ka, cloud cover was maintained and supported the forest expansion during the MHDE maxima (Fig. 4-9A).

The MHDE was suggested to have been time-transgressive migrating from north to south tracking the peak of rainy season insolation (Abbott et al. 2003). Between latitudes 18 °S and 13 °S, maximum abundances in Poaceae pollen and lake lowstands, defined the peak of the MHDE to have occurred between 5 and 4 ka at Titicaca, Baja and Pacucha (Hansen and Rodbell 1995, Paduano et al. 2003, Valencia et al. 2010b). The peak of the MHDE clearly lagged the insolation minima corresponding to the austral rainy season by several millennia (Seltzer et al. 2000, Tapia et al. 2003, Hillyer et al. 2009, Bird et al. 2011). The Miski and Huamanmarca records mirrored the moisture trends observed in northern sites (i.e. Chochos, Baja, and Chorreras among others) and also depicted the peak of the MHDE in agreement with southern sites (i.e. Titicaca, Khomer Kocha, and Refugio). Therefore, rather than being a single time-transgressive event, MHDE appears to have been composed of at least two independent phases, with one of them being weakly expressed at our study sites. Again, the absence of major vegetation changes in Miski and Huamanmarca, suggests that cloud cover was more persisted even when precipitation dropped during the peak of the MHDE.

In the wetter portion of the Holocene post *c.*4 ka, Poaceae concentrations declined gradually as savanna was replaced by evergreen forest in the lowlands of eastern Bolivia whereas Lake Titicaca in the high Andes overflowed southwards once more as lake levels rose (Abbott et al. 1997, Mayle et al. 2000, Baker et al. 2001). The records of Vacas and Marcacocha also experienced a positive water balance (Chepstow-Lusty et al. 1998, Williams et al. 2011b). This change was also observed as a substantial reduction of *Isoëtes* in Huamanmarca and the expansion of the local vegetation, e.g. *Polylepis* (Fig. 6-7). Around Lakes Miski and Huamanmarca the local woodlands kept expanding after 3.3 ka, whereas Poaceae percentages declined. Conversely, cloud forest species and

herbaceous types remained stable and insensitive to the wetter conditions that followed the MHDE.

Lakes Miski and Huamanmarca remained without signals of anthropogenic disturbances during the Mid- and Late-Holocene. The gradual development of the local forest around Miski and Huamanmarca did not parallel the anthropogenic impacts observed elsewhere in the southern Andes (Chepstow-Lusty et al. 1998, Hastorf 2008, Isbell 2008, Bauer et al. 2010, Sublette et al. 2010, Valencia et al. 2010b). For instance, elsewhere in the Andes, the late Holocene was characterized by severe landscape transformation as cultivation became widespread, e.g. increased erosion, occurrence of crop pollen; evidence for intensification of agriculture is particularly strong in the Cuzco region (Chepstow-Lusty et al. 1996).

At about 1.3 ka the local woodlands, mostly represented by *Polylepis,* experienced a decline around Lake Miski, though not at Huamanmarca. These observations contrasted records of increasing woodland cover attributed to agroforestry practices and fire suppression in records like Huaypo and Marcacocha located at 40 and 20 km away from Miski and Huamanmarca (Chepstow-Lusty et al. 1996, Chepstow-Lusty et al. 1998, Sublette et al. 2012). Fire events were intensified between *c.*1 and 0.8 ka in Miski coinciding with the collapse of the Tiwanaku culture (Abbott et al. 1997, Binford et al. 1997). Woodlands in Miski did not recover coinciding the generalized abandonment and cessation of monumental construction in the Altiplano or afterwards (Ortloff and Kolata 1993, Abbott et al. 1997, Binford et al. 1997). The increased concentrations of *Alnus* after 0.8 ka at Miski (Fig. 4-6) may have been related to a regional (i.e. outside the valley) rather than local increase in agroforestry practices (Chepstow-Lusty and Winfield 2000). For instance, woodland development in the Miski and Huamanmarca valleys was an ongoing process that excluded *Alnus* growing locally. Furthermore, fires were not suppressed locally suggesting limited human intervention related to agroforestry practices (Chepstow-Lusty and Winfield 2000). Overall, the records from Lakes Miski and Huamanmarca were consistent with the main climate events registered regionally in other Andean sites e.g. the MHDE and the drought at 0.9 ka. However, human

influence was negligible in both sites, i.e. absence of human indicators such as landscape transformation or evidence of cultivated species.

4.6.2) Was the woodland-grassland mosaic a long-term feature of the high Andean landscape?

Modern *Polylepis* stands occur as small, disjunct, isolates in a matrix of Puna grassland. Anthropogenic fire is generally considered to be the underlying cause of this mosaic, with *Polylepis* surviving in areas that seldom or never burn (Ellenberg 1958, Kessler 1995). This section focuses on the evidence of long-term patchiness within a local landscape.

Between 12.6 and 9.1 ka (Zone-1) fire events (charcoal peaks) were absent from Huamanmarca and rare at Miski (Fig. 4-9B). From a total of 25 samples evaluated for this time interval in the Miski record, only 6 samples contained charcoal as evidence of fire. Furthermore, identification of charcoal particles using scanning electron microscope images (Fig. 6-10) showed that a minimum of 60% of the charcoal signal was derived from Poaceae in Miski. Most of the remaining percentage of charcoal fragments were covered in other organic and mineralogical debris and were therefore unidentifiable. Consequently, it is highly probable that most of the unidentified fragments also belong to Poaceae. The high representation of grassland-derived particles in the charcoal signal is supported by the paucity of change of the local woodlands indicated by the fossil pollen (Figs. 4-6, 4-7 and 4-9A). Pollen percentages from arboreal species were stable in Miski and Huamanmarca implying that fires did not affect these forests during the late glacial and early Holocene (12.6-9.1 ka). That natural fires occurred in grassland was probably a result of the higher susceptibility of grassland to desiccation by strong daily insolation, with lightning being the ignition source.

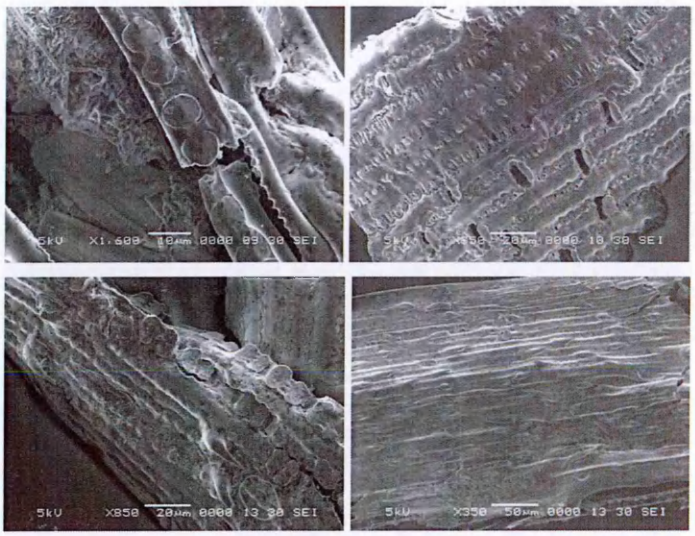

Fig. 4-10 Scanning electron microscope images from charcoal particles extracted from sediment of Lake Miski at 305 cm. The images show the epidermis of burned grasses (Poaceae) with phytoliths arranged in rows.

The difference in fire incidence between Miski (fires present) and Huamanmarca (no fires) prior to 9 ka (Zone-1, Fig. 4-9B) was probably explained by topographic features of each catchment rather than direct human influence. Huamanmarca lies in a V-shaped valley with multiple boulders that should restrict the spread of fires. In contrast, Lake Miski lies in an open U-shaped valley that has gentler, more vegetated slopes (grasses) than Huamanmarca. The lakes are separated by just 1.2 km; it is unlikely that humans would have used one site but not the other. It seems probable that climate rather than anthropogenic disturbance shaped these settings in the early Holocene.

Fire increased gradually in Miski and Huamanmarca after *c.*9 ka (Zone-2). The maxima observed in both records coincided with the two phases of the MHDE centred at *c.*7 and 5 ka in Zone-3 (Fig. 4-9B). The patterns of fire fluctuation and vegetation change observed in Miski and Huamanmarca were consistent with those of records from Chorreras, Chochos, and Pallcacocha (Hansen et al. 2003, Bush et al. 2005). All these sites probably were more dependent on cloud cover moisture than precipitation during periods of drought. Consequently, vegetation changes induced by fires were relatively minor in Chorreras, Chochos, and Pallcacocha (Hansen et al. 2003, Bush et al. 2005).

In contrast, records from Khomer Kocha and the Refugio sites were heavily influenced by fire (Urrego et al. 2011, Williams et al. 2011a). The charcoal signal suggested that fires became common in Lake Khomer Kocha and the Refugio sites after 9.1 ka and remained high until modern times. The local topography (U-shaped valleys) and/or location outside areas of high frequency cloud cover probably favoured fire propagation at both Khomer Kocha and Refugio (Urrego et al. 2011, Williams et al. 2011a). The incidence of fire coincident with the continuous woodland expansion suggests that the landscape around Miski and Huamanmarca was a mosaic of woodland and grassland patches. The difference in fire onset between both lakes further supports the idea of a patchy landscape.

Large charcoal peaks were not exclusive to the timespan of the MHDE in Zones-2 and -3. Charcoal peaks were also observed in the Late Holocene (Zone-4) with the highest peaks registered at 2.5 and 0.9 ka (Fig. 4-9B). The most recent period of intensified fire activity (elevated charcoal abundance) around Lake Miski occurred between *c.*1 and 0.7 ka (Fig. 4-6). The periods of fire intensification coincided with the lowest lake levels (largest carbonate peak; Fig. 4-6) from the record and the decrease in abundance of local woodland taxa around Lake Miski. The increased fire activity centred at *c.*2.5 and 1 ka coincided with periods of lake level decline in the Titicaca record (Abbott et al. 1997, Binford et al. 1997). Conversely at Huamanmarca no further peak in charcoal was observed, nor was there any discernible impact on the vegetation (Fig. 4-6).

The arboreal vegetation appeared to be unchanged by the increased fire incidence around Miski and Huamanmarca. Extended periods of drought were previously linked to desiccation and fire intensification in grasslands and tropical forests (Nepstad et al. 2004a, Asbjornsen et al. 2005, Román-Cuesta et al. 2011, Oliveras et al. 2013). In systems without adaptations to fire, recurrent burning led to positive feedbacks and enhanced fire susceptibility promoting shifts in species composition (Cochrane et al. 1999, Cochrane 2001, Barlow 2002, Laurance 2004). None of these changes were observed in the records of Miski and Huamanmarca. Nor was obvious fire suppression, which has been suggested to have been used in Incan agroforestry practices (Chepstow-Lusty and Winfield 2000) (Fig. 4-9B, Zone-4). The fire activity at Huamanmarca and

Miski over the last 2 ka indicated a lack of landscape management for forestry. The gradual expansion of the forest observed during the Holocene was a consequence of the slow colonization of the area above both lakes that was mainly represented by bare rocks and sparse vegetation patches (Fig. 4-2). Therefore, the vegetation should not carry fires (i.e. low fuel and fuel discontinuity) that could limit the forest expansion, especially for Huamanmarca. In summary, the woodland-grassland mosaic was a persistent feature observed during the last *c.*12 ka in lakes Miski and Huamanmarca.

4.6.3) Can a period in the Holocene form a satisfactory baseline for the natural state of Andean vegetation?

Recognizing the common influence of humans modifying Andean landscapes, there is a persistent problem in defining what is a "natural baseline" (Sarmiento and Frolich 2002) in the high Andes. One possibility to address this issue is to find a pre-human-influence baseline (*sensu* Willis et al. 2004). At many Andean sites the migrational responses to the deglaciation are strong prior to *c.*11.7 ka (e.g. Bush et al. 2005, Williams et al. 2011a). Thus, *c.*11.7 ka becomes the earliest probable time to find a baseline for a modern natural state. Thereafter, major climatic changes may have caused settings to lie outside of the modern climatic norms, e.g. the MHDE. The timing and degree of anthropogenic influence would be reflected in diverging ecological trajectories compared with an undisturbed site (Fig. 4-9E). To test this hypothesis, the trajectory of vegetation change is contrasted in undisturbed settings (Miski and Huamanmarca) with that of the heavily disturbed setting around Lake Pacucha (Hillyer et al. 2009, Valencia et al. 2010b). At Pacucha, the onset of anthropogenic landscape-transformation starts at *c.*7 ka, several thousand years after the onset of fires.

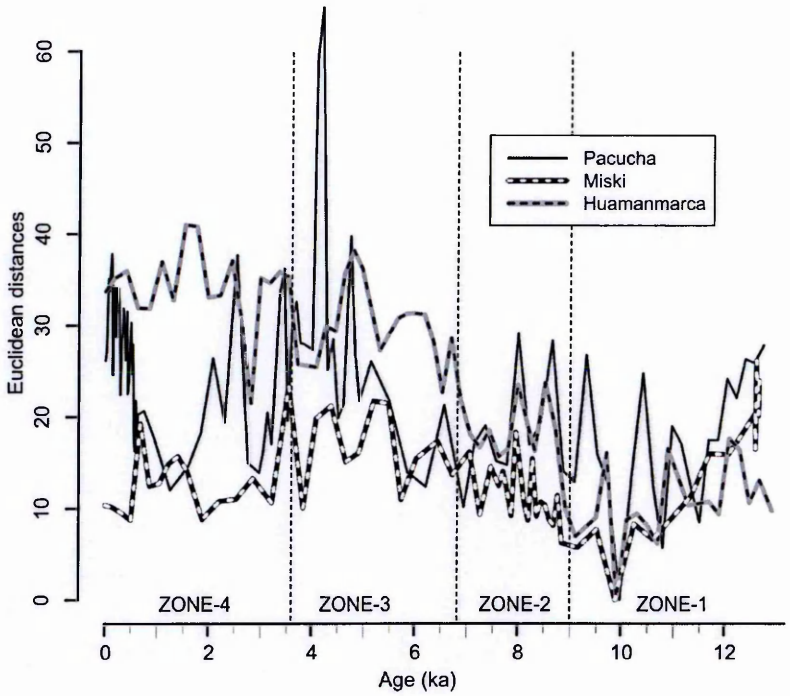

Fig. 4-11 Euclidean distances for Lakes Miski, Huamanmarca and Pacucha

Euclidean distances and DCA scores were calculated to characterize the compositional change in the fossil pollen assemblage from Miski, Huamanmarca and Pacucha through time (Fig. 4-11 and 4-12). The statistical characterizations were interpreted as a summary metric for overall compositional similarity derived from the multivariate pollen dataset. The statistical characterizations were then used to identify vegetation baselines (Fig. 4-9D and E). Changes in baseline conditions are observed by comparing the trends depicted by the statistical characterizations (Fig. 4-9D and F) with the alternate scenarios presented in our conceptual model (Fig. 4-1). If *c.*10 ka were a good baseline these relatively undisturbed sites of Lakes Miski and Huamanmarca should be similar to today whereas the heavily impacted site of Pacucha would show strong divergence.

The Euclidean coefficient provided an index of system migration away from the starting point. A limitation of using Euclidean distances is that changes depicted are relative to a fixed origin within a record. The Euclidean distance provides an index of how far a

system has come from that origin, but does not provide a proxy for the direction of that change. Thus the distance of divergence of two sites could be the same, but the ecological changes could be opposite, i.e. one becomes forested, the other a grassland. To eliminate the effect of an arbitrary origin, DCA was used on 44 pollen types that could be identified to the lowest possible taxonomic level that were commonly found in the three records (Table 4-2). A similar approach was taken to perform the DCA with diatom data derived from Lakes Miski and Pacucha. However, only 10 taxonomic groups were shared.

N°	Taxa	N°	Taxa	N°	Taxa	N°	Taxa
1	*Acalypha*	**12**	Caryophyllaceae	**23**	*Hesperomeles*	**34**	*Podocarpus*
2	*Alchornea*	**13**	*Cassia*	**24**	*Juglans*	**35**	*Polylepis*
3	*Alnus*	**14**	*Cecropia*	**25**	Lactuceae	**36**	*Prosopis*
4	Althernanthera	**15**	*Celtis*	**26**	Malvaceae	**37**	Rosaceae
5	*Ambrosia*	**16**	*Chenopodium*	**27**	Melastomataceae	**38**	Rubiaceae
6	Anacardiaceae	**17**	Cyperaceae	**28**	Mimosaceae	**39**	Solanaceae
7	Apiaceae	**18**	*Dodonaea*	**29**	Myricaceae	**40**	*Thalictrum*
8	Asteraceae	**19**	Ericaceae	**30**	Myrsinaceae	**41**	UrticMor
9	*Bocconia*	**20**	Euphorbiaceae	**31**	Myrtaceae	**42**	Valerianaceae
10	Brassicaceae	**21**	*Gynoxys*	**32**	*Plantago*	**43**	*Vallea*
11	Campanulaceae	**22**	*Hedyosmum*	**33**	Poaceae	**44**	*Weinmannia*

Table 4-2. List of pollen types shared between Miski, Huamanmarca and Pacucha.

DCA axis-scores derived from the combined matrix for the three records retained the relative score differences within each record relative to individual DCA runs. This analysis provided an index of ecosystem change through time as well as capturing the different trajectories of change between records. Overall, the DCA scores from Axis 1 resembled the results produced using Euclidean distances curves suggesting that meaningful information was not lost (Fig. 4-9D). The greatest difference lay in the relative orientation of the change through time of the Pacucha record versus the other two, clearly revealing that Pacucha was diverging from the other records. The DCA scores from Axis-1 derived from the Pacucha and Miski diatom data were consistent with the DCA result obtained with pollen. Diverging trajectories after 7 ka were evident based on these two proxies that are independent of each other.

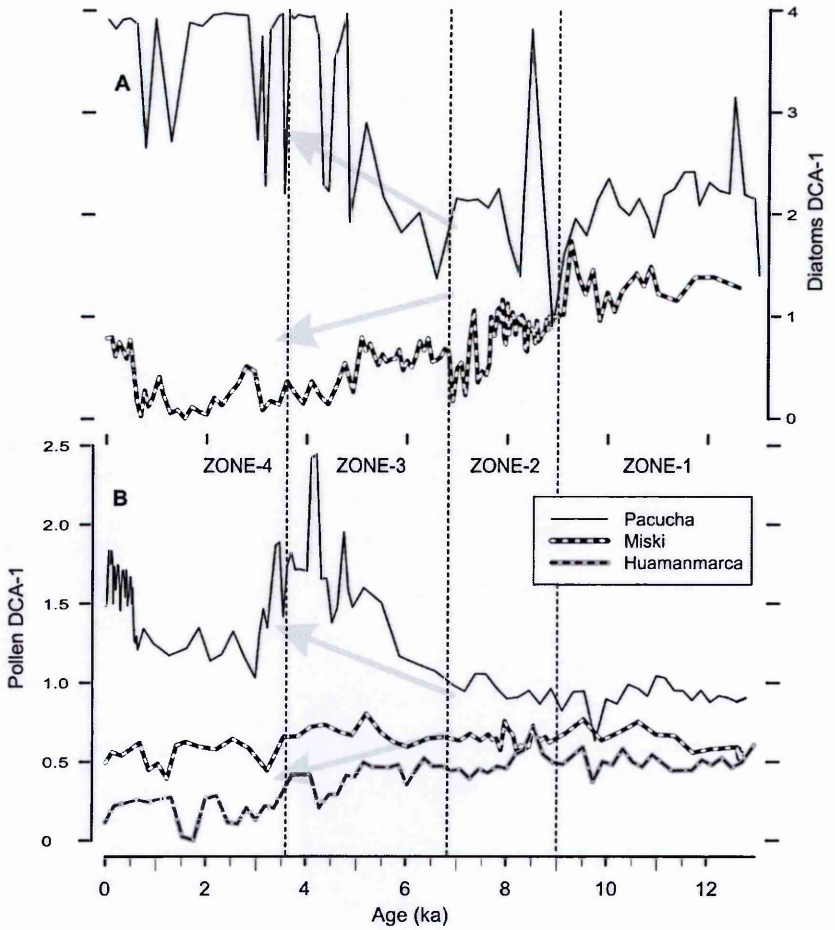

Fig. 4-12 DCA Axis-1 scores for Lakes Miski, Huamanmarca and Pacucha. The grey arrows depict the onset of divergence between records.

In the previous section (4.5.1.1, deglaciation and early Holocene) the description of the multiple proxies suggested that the period between *c.*12 and 9.1 ka was stable and had minimal influence of droughts or human intervention. The DCA scores from axis-1 derived from pollen and diatoms, supports the idea that assemblages between *c.*11 and 9.1 ka represent the most suitable baselines for modern communities. Periods after *c.*9.1 ka were discarded as suitable baselines due to extreme drought relative to modern conditions and the possibility of anthropogenic landscape modification after *c.*7 ka.

Furthermore, poor vegetation development prior to *c.*11 ka limited the use of this period as a baseline. The results were entirely consistent with the assumed baseline fixed at 10 ka.

The DCA Axis-1 portrayed the trend of vegetation development for Lakes Miski, Huamanmarca and Pacucha plus the temporal variability in each record (Fig. 4-9E). Unsurprisingly Lakes Miski and Huamanmarca plotted closer to each other than to Pacucha. In essence, the DCA plot suggested that between *c.*11 and 7.5 ka vegetation assemblages were stable and the magnitude of change among the three records was similar. Within this time interval, vegetation stability was also identified in Ecuadorian and Peruvian records such as Chorreras, Pallcacocha, Chochos, Junín, and Titicaca (Valencia et al. 2010b). This result suggested that human disturbances at regional scales were still limited and agreed with a delayed colonization of the high Andes (Hansen et al. 2003, Paduano et al. 2003, Bush et al. 2005). The onset of the MHDE determined the beginning of the divergence among Andean records. For instance, after 7.5 ka the DCA scores from Lake Pacucha drifted in the opposite direction to those from Lakes Huamanmarca and Miski. The divergence of Pacucha versus Miski and Huamanmarca was determined by the deforestation around Pacucha contrasting with the steady forest expansion around Huamanmarca. Although Miski experienced a similar trend of forest expansion observed at Huamanmarca, colonization at Miski was slowed by fire events favoured by the local topography (i.e. gentle slopes and lack of fire breaks).

The DCA scores for Axis-1 derived from the diatom assemblages from Lakes Miski and Pacucha (Fig. 4-9F) exhibited a similar pattern to those derived from pollen. Miski and Pacucha assemblages experienced a period of stability prior to *c.*7.5 ka, diverging afterwards. The similarity between DCA scores from pollen and diatom assemblages suggests that processes within the lake mirrored the vegetation and landscape transformation in the lake catchment.

The early Holocene samples at *c.*10 ka provided a satisfactory baseline for Lake Pacucha, as the Mid-Holocene was a time of both climatic change and intensified human influence at that site. The match to the modern state was not exact and this

could represent inaccuracies in the methods, or that climatic parameters though similar were not identical. The disparities, however, may have been real prompting a consideration of whether it is ecologically valid to look at baselines over millennial timescales. Rather than considering a single state to be the only 'true' natural state, it may be more appropriate to recognize historical stochasticity as being an important factor. If following a disturbance a different set of species of equivalent plant functional types invaded the area, it would be possible to have a different natural assemblage hundreds, perhaps even thousands, of years after the event. Such individualistic responses to stimuli (Gleason 1926), as opposed to a climax system (Clements 1936) underlies modern ecological thought. So rather than considering a single, defined, baseline, perhaps as a baseline-range that encompasses multiple possible outcomes should be considered (Fig. 4-1F).

The trajectory of assemblages through time at Miski and Huamanmarca are also ecologically significant in that they quite clearly refute neutral (sensu Hubbell 2001) patterns. My data for an assemblage being disrupted, but then reforming close to its original composition are strikingly similar to those shown by Clark and McLachlan 2003) for the Midwestern USA, and to the Galapagos Islands (Restrepo et al. 2012, Bush et al. 2013). Niche-based hypotheses of assemblage formation would lead to similar dominants re-emerging at a site, so long as the fundamental site conditions were similar (Clark and MacLachlan 2003). An exact replication of former conditions would not be expected as chance and individualistic migrations would play a part in forming a new assemblage. Contrastingly, neutrality would predict that following disruption a random walk would begin, with the most abundant species *at the time of the end of the disruption* having the greatest opportunity to expand its population (Hubbell 2001). The divergence through time from the original baseline seen in the record from Pacucha has the expected shape afforded by neutrality, but for very different reasons. In contrast to the Pacucha record reflecting a random process of species assembling, human intervention in the landscape actively shaped that assemblage. Thus the divergence is not a random walk but a very directed march toward a manufactured landscape (sensu Erickson 2000, 2010).

4.7) Conclusions:

The records from Lakes Miski and Huamanmarca provide a detailed reconstruction of vegetation and climate change for the high Andes with limited influence of human impact over the last 12.6 ka. Both records show a consistent response to local climate and depict similar changes over time. Trends of vegetation change in Miski and Huamanmarca were consistent with regional events and the gradual warming during the Pleistocene-Holocene transition.

Lakes Miski and Huamanmarca experienced a MHDE in two phases. An early phase that coincided with events registered in the northern Andes and a delayed phase that peaked at *c.*5 ka in phase with southern records. The MHDE maximum aridity occurred between *c.*6 and 4 ka and was probably induced increased seasonality that produced a hydrological deficit in the high Andes that was perceived as lake level drops at regional scales.

The trajectory of change derived from pollen and diatoms from lakes Miski, Huamanmarca and Pacucha suggested that vegetation changes were driven by climate change prior to *c.*7.5 ka. A first period of vegetation stability based on pollen was identified between *c.*11 and 7.5 ka in Miski Huamanmarca and Pacucha. Like the pollen data, the diatom data derived from Lakes Miski and Pacucha produced similar ordination patterns of change prior to human disturbance. After *c.*7.5 ka, human disturbances muted the climate signal in Lake Pacucha when its trajectory of vegetation change diverged with the ones observed in Miski and Huamanmarca. Our study does not deny the presence of humans in the Andes prior to *c.*7.5 ka, but shows that landscape transformation became significant only after *c.*7.5 ka. Furthermore, the high Andean landscapes were not equally transformed even during the mid or late Holocene as areas around Miski and Huamanmarca remained with negligible signs of human impacts. The continuous forest expansion observed in Miski and Huamanmarca despite the occurrence of fire (natural or anthropogenic) suggests that the landscape was a mosaic of grasslands and woodlands. Cloud cover probably limited the frequency and intensity of fires and enabled woodlands to expand in the study sites, especially during the MHDE.

The period between *c.*10.6 and 9.8 ka was considered to be the best estimate from which to derive baselines of "naturalness" in the Andes because of the paucity of climate anomalies, the consistency observed among Andean records, and near absence of human disturbances. However, the trends in vegetation change observed in Lakes Miski and Huamanmarca emphasized that assemblages were dynamic and do not converge into or return to a climax system.

Over short periods of time in simple systems, assemblages may be disturbed and rebound to a similar state (Restrepo et al. 2012). In complex systems, however, multiple possible pathways of successional recovery are possible and the actual course may reflect a combination of historical contingency, local population densities, plant functional types and biotic and abiotic pressures. Consequently multiple natural outcomes are possible that are likely to offer potentially divergent trajectories through time. Hence, over long-term scales complex systems and additional dimensions of variability need to be added so that the baseline becomes a range.

4.8) Summary

In this chapter the nature, trajectories and drivers of vegetation change in Lakes Miski Huamanmarca and Pacucha have been established. The period between *c.*10.6 and 9.8 has been identified as the most likely to give an indication of ecological baselines that might be anticipated today. However, variations identified during the past *c.*5 ka, indicates that ecological baselines should be considered dynamic rather than fixed concepts.

In the next chapter the concept of ecological baselines is applied to multiple environmental records to evaluate changes in the spatial structure of high Andean woodlands.

Chapter 5) Polylepis woodland dynamics

The following chapter is aimed to apply the concept of ecological baselines from chapter 4 to evaluate the spatiotemporal variations in woodland cover in the the Andes. A version of this chapter will be submitted for publication as:

Valencia, B.G., Gosling, W.D., Bush, M.B. & Coe, A.L. (in preparation) *Polylepis* woodland dynamics during the last 17, 000 years. *Quaternary Science Reviews.*

5.1) Abstract

The modern distribution and environmental history of *Polylepis* woodlands in the Andes was investigated to determine if the patchy spatial distribution of this tree genus can be attributed to natural causes or human influence. The modern spatial distribution of *Polylepis* was modelled for the Andes between 9°N and 32°S at elevations above 1200 m using MaxEnt. The model, based on 22 environmental variables and modern *Polylepis* presence data, suggested that *Polylepis* has a discontinuous spatial distribution. The results of the model were consistent with the pollen and charcoal data derived from 13 Andean fossil pollen records. Throughout the last 17 ka (thousand years), the spatial structure of *Polylepis* woodlands was disjoined including the period between 7 and 17 ka when landscapes were patchy despite not being heavily impacted by humans. However, the pattern of patchiness became intensified due to human impacts after 7 ka leading to hyper-fragmented[1] landscapes. The pollen data does not support the presence of a continuous woodland belt anytime over the last 17 ka.

5.2) Introduction

In the tropical Andes, one of the most biologically diverse and environmentally threatened regions on Earth, *Polylepis* is an ecologically important tree genus (Fjeldså and Kessler 1996, Myers et al. 2000, Orme et al. 2005, Malcolm et al. 2006, Chepstow-Lusty et al. 2009, Gareca et al. 2010). *Polylepis* is an endemic Neotropical genus

[1] Naturally patchy pattern further fragmented by anthropogenic activities

comprising 28 species (Schmidt-Lebuhn et al. 2006). Although occurring as low as *c.*2000 m asl. (metres above sea level), it is the almost monotypic stands of *Polylepis* between timberline and 5000 m asl that are most important ecologically (Ellenberg 1958, Fjeldså and Kessler 1996). The presence of these woodland areas above timberline provides unique high-elevation habitats for range-restricted, habitat specialist birds, mammals, and insects (Fjeldså et al. 1999, Yensen and Tarifa 2002, Chesser 2004, Witt and Lane 2009, Gareca et al. 2010). Because of their role in providing high elevation habitat diversity, *Polylepis* is identified as a key genus for Andean conservation throughout the tropical Andes (Fjeldså and Kessler 1996, Fjeldså 2002c, Servat et al. 2002, Young and León 2007, Gareca et al. 2010).

Whether humans or natural processes cause the patchy distribution of *Polylepis* woodlands seen today has been debated for more than 50 years. Ellenberg (1958) suggested that prior to human modification of the landscape, large, continuous, tracts of *Polylepis* woodland existed in the highlands. Other research has suggested that natural mechanisms such as fire and microclimate preferences caused the modern population disjunctions (Simpson 1979, Fjeldså 2002a, Hensen 2002, Kessler 2002, Purcell and Brelsford 2004, Kessler 2006). While the prehistoric extent of these woodlands remains unknown, ecological studies have shown the importance of fire as the main factor influencing the spatial distribution and the upslope expansion of *Polylepis* woodlands (Di Pasquale et al. 2008, Gosling et al. 2009, Hanselman et al. 2011b, Román-Cuesta et al. 2011).

Prior to human arrival in South America at *c.*14 ka (thousands of calibrated radiocarbon years before present, (henceforth ka) (Dillehay 1997) fossil charcoal records indicate that fire was a natural phenomenon in the high Andes (Hanselman et al. 2011b). However, human incursion in the high Andes was probably delayed until 10 ka (Aldenderfer 2008). Human activity progressively increased the probability of fire in Andean landscapes (Mayle and Power 2008, Niemann and Behling 2008, Armesto et al. 2010, Urrego et al. 2011). After *c.*7 ka anthropogenic influences on local vegetation in southern Peru was evident in paleoecological records (Hansen and Rodbell 1995, Niemann and Behling 2008, Valencia et al. 2010b). Human influence, however, was

probably spatially heterogeneous, with some regions being more attractive for settlement or some systems being more susceptible to alteration. One of the key variants in determining habitats suitable for human occupation and burning may have been cloud cover. Sites with frequent cloud cover were apparently more resilient to human impacts as very humid sites were probably less appealing to human settlement and less prone to carry fire (Valencia et al in prep, chapter 4).

Of the last 100,000 years, the post-glacial period between *c.*11 and 9 ka was climatically the most similar to modern conditions in the Andes. Between *c.*9 ka and 4.4 ka much of the tropical Andes was drought prone, with many lakes drying up, turning saline, or having marked lowstands (Cross et al. 2000a, Bush et al. 2005, Mayle and Power 2008, Hillyer et al. 2009). Overlapping the drought, human occupation began to alter landscapes after 7 ka, so that as wetter conditions returned around 4.4 ka, many areas were occupied and altered by humans (Valencia et al. 2010b, Ledru et al. 2013). Thus, the early Holocene between 11 and 7 ka offers the opportunity to observe the response of relatively natural systems undergoing climatic change and the resulting temporal and spatial population responses of *Polylepis* woodlands in the Andes.

While the fundamental niche or bioclimatic envelope of *Polylepis* would be determined by multiple environmental variables such as precipitation, seasonality, temperature, and topography, its realized niche would be modified by fire. The probability that *Polylepis* ever formed continuous woodlands above modern timberline can be assessed through bioclimatic envelope modelling (sensu Hannah et al. 2002). Maximum Entropy (MaxEnt, Phillips et al. 2004, Phillips et al. 2006) modelling coupled with empirical collection data offer a powerful way to assess the potential coverage of *Polylepis* and the relative contribution of the included environmental variables. To assess the temporal components of *Polylepis* distribution we synthesize data from 13 fossil pollen and charcoal records from the Central Andes covering the last 17 ka. By considering variation in *Polylepis* woodland distribution through space and time and modelling its distribution we can address two research questions: i) Has *Polylepis* woodland formed a natural continuous 'belt' along the Andes in the last 17 ka? And, ii) What environmental factors controlled the spatial distribution of *Polylepis* woodland?

Three scenarios that are ecologically important were tested as they lead to distinctly different population outcomes.

Polylepis existed in widespread geographically continuous populations resistant to natural levels of fire. Disjunctions occur under heightened anthropogenic fire regime after 7 ka (Fig. 5-1, scenario 1).

Polylepis existed in discontinuous populations prior to heightened anthropogenic fire regimes; populations were quickly fragmented by increased natural fire frequency. Woodlands become hyper-fragmented by human activity post 7 ka (Fig. 5-1, scenario 2).

Polylepis existed in patchy metapopulations in the past as they do today. Little change in abundance followed human occupation of the Andes (Fig. 5-1, scenario 3)

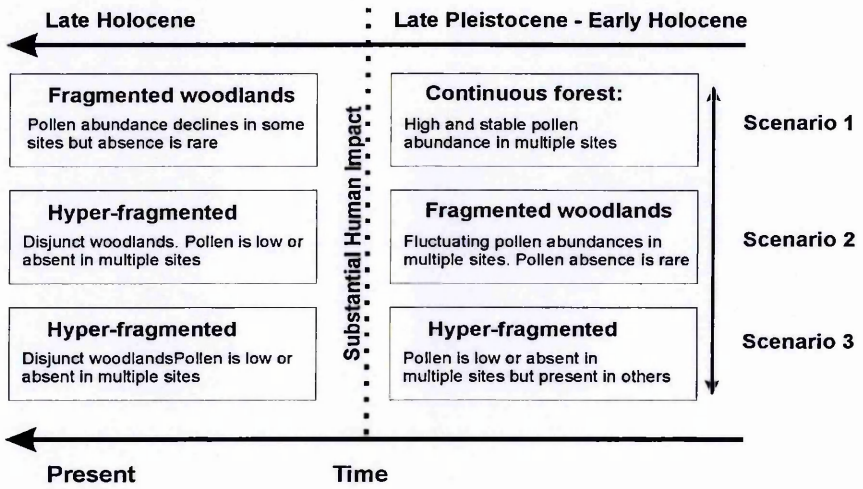

Fig. 5-1 Conceptual model of the spatial distribution of *Polylepis* over time showing three possible scenarios

5.3) Materials and methods

A total of 13 lacustrine sediment-records from which *Polylepis* pollen and charcoal data were gathered from original publications and online material (Hansen and Rodbell 1995, Colinvaux et al. 1997, Hansen et al. 2003, Mourguiart and Ledru 2003, Paduano et al. 2003, Bush et al. 2005, Weng et al. 2006, Valencia et al. 2010b, Urrego et al. 2011, Williams et al. 2011a, www.ncdc.noaa.gov/paleo/lapd.html). All the selected sites

(Figure 5-2) were located above 3000 m asl, providing a climatic and vegetation history above the elevation of modern timberline since the late Pleistocene. Pollen and charcoal data were rescaled by the maximum value observed in each record (i.e. maximum abundance accounts for 100%) and plotted against age using R (Development-Core-Team 2011) and C2 (Juggins 1991).

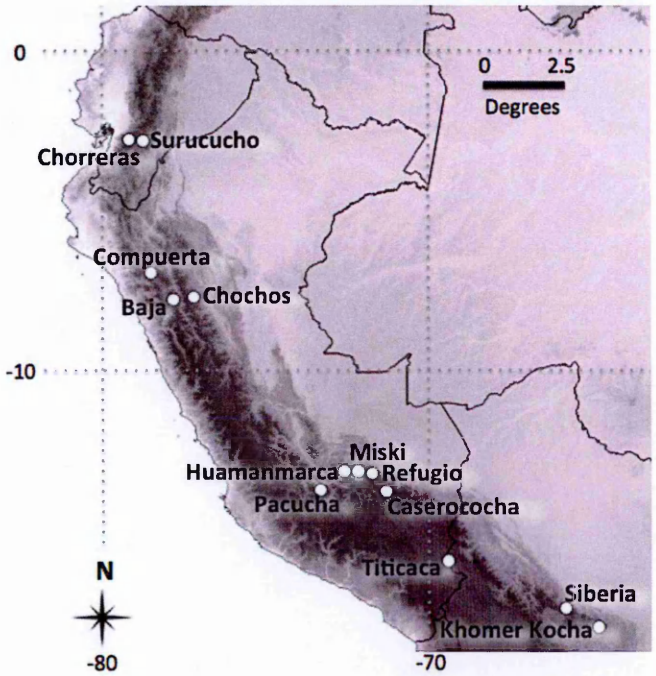

Fig. 5-2 Map depicting the location of 13 pollen records in the Andes.

Spatial digital data (layers) for 29 modern environmental variables were compiled for the Andes (9° N - 32° S, 80° W - 63° W) and resampled at a resolution of 3 km for areas above 1200 m elevation. Seven variables were excluded as they lowered the model performance (Appendix VII). Data were derived from WorldClim (Hijmans et al. 2005, www.worldclim.org), Bookhagen Bookhagen (Bookhagen and Strecker 2008, www.geog.ucsb.edu/), the Climatic Research Unit of the British Atmospheric Data Centre (BADC, badc.nerc.ac.uk) compiled at the Consortium for Spatial Information CGIAR-CSI (www.cgiar-csi.org), U.S. Geological Survey (USGS, www.usgs.gov), and the Joint Research Centre of the Global Environment Monitoring Unit of the European

Commission (JRC, bioval.jrc.ec.europa.eu). Sources and layer information are provided in appendix VI. All the spatial analyses were carried on in QGIS 1.8.0 with the GDAL libraries (QGIS, 2009), ArcGIS version 10, and R 2.14.0 (Development-Core-Team, 2011) using the packages *spatstat* (Baddeley and Turner 2005), and *sp* (Pebesma and Bivand 2005, Bivand et al. 2008).

To link modern woodland distribution with the digital environmental data, georeferenced entries (11,254) were used to determine the modern occurrence of *Polylepis* (data were derived from The Global Biodiversity Information Facility, GBIF (http://www.data.gbif.org) and Tropicos (http://www.tropicos.org). The data were filtered to eliminate duplicates. Individuals of the same species growing closer than 4 km from each other were removed to reduce the effect of sampling intensity. The threshold of 4 km was used to minimize the probability of two individuals co-occurring in the same pixel of 3 x 3 km, which is equivalent to the average valley slope-length within the Andes (Bookhagen and Strecker 2008). After the filtering, a total of 302 entries were used to model the modern distribution of *Polylepis*.

Modelling the suitable habitat for *Polylepis* was carried out using Maxent version 1.0 for Mac. Cross-validation (k-fold) was performed using 20 replicates to evaluate the predictive performance of the model as well as area under the receiver operating characteristic (AUC). The importance of the covariate contribution to the model was determined using a Jackknife test.

5.4) Results

5.4.1) Fossil pollen and charcoal records

Polylepis relative abundances fluctuated (0-100%) in all the studied records during the last *c.*17 ka (thousand calibrated ^{14}C years before present), with peaks of abundance that were time transgressive between records (Fig. 5-3). Maximum pollen abundances were attained during the late Pleistocene (>11 ka) in 8 records, and during the Holocene (11-0 ka) in 5 records. The *Polylepis* maxima generally lasted 2 to 3 millennia in the fossil

pollen records, but differed in timing and magnitude between sites. Fire events were common in all the records during the last 17 ka; however, the largest peaks were restricted to the Holocene.

Pollen abundances of *Polylepis* from Lakes Chorreras, Surucucho, Chochos, Miski, Huamanmarca and Titicaca, did not decrease when charcoal values peaked during the Pleistocene or the Holocene (Fig. 5-3). Between *c.*12.5 and 10 ka *Polylepis* abundances declined only in records from Surucucho, Compuerta, Baja, Pacucha, Caserococha, Khomer Kocha upper (hereafter Khomer Kocha) and Siberia. By c.10 ka, *Polylepis* abundances rose in Chorreras, Surucucho, Chochos, Baja, Caserococha, Miski, Huamanmarca and Titicaca. After the decline observed between *c.*12.5 and 10 ka, *Polylepis* did not recover in records from Compuerta, Pacucha, Refugio, and Siberia. Furthermore, the onset of fire produced a clear decline in *Polylepis* pollen only in Compuerta, Pacucha, Refugio, and Siberia records.

Holocene fire events were more common and had higher charcoal peaks than during the Pleistocene (Fig. 5-3). For instance, 10 of the 13 records had their highest charcoal peak during the Holocene and only 3 during the Pleistocene. Furthermore, Holocene fires did not produce a clear *Polylepis* pollen decline in 9 records, i.e. Chorreras, Surucucho, Chochos, Baja, Caserococha, Miski, Huamanmarca, Titicaca, and Khomer Kocha. *Polylepis* pollen abundances fluctuated constantly in these sites except for Miski and Huamanmarca, where *Polylepis* pollen abundance increased continuously from 20% at the Holocene onset until >60% in modern times (Fig. 5-3). *Polylepis* pollen abundances remained under 10% or below the detection limit in Compuerta, Pacucha, Refugio, and Siberia during the Holocene.

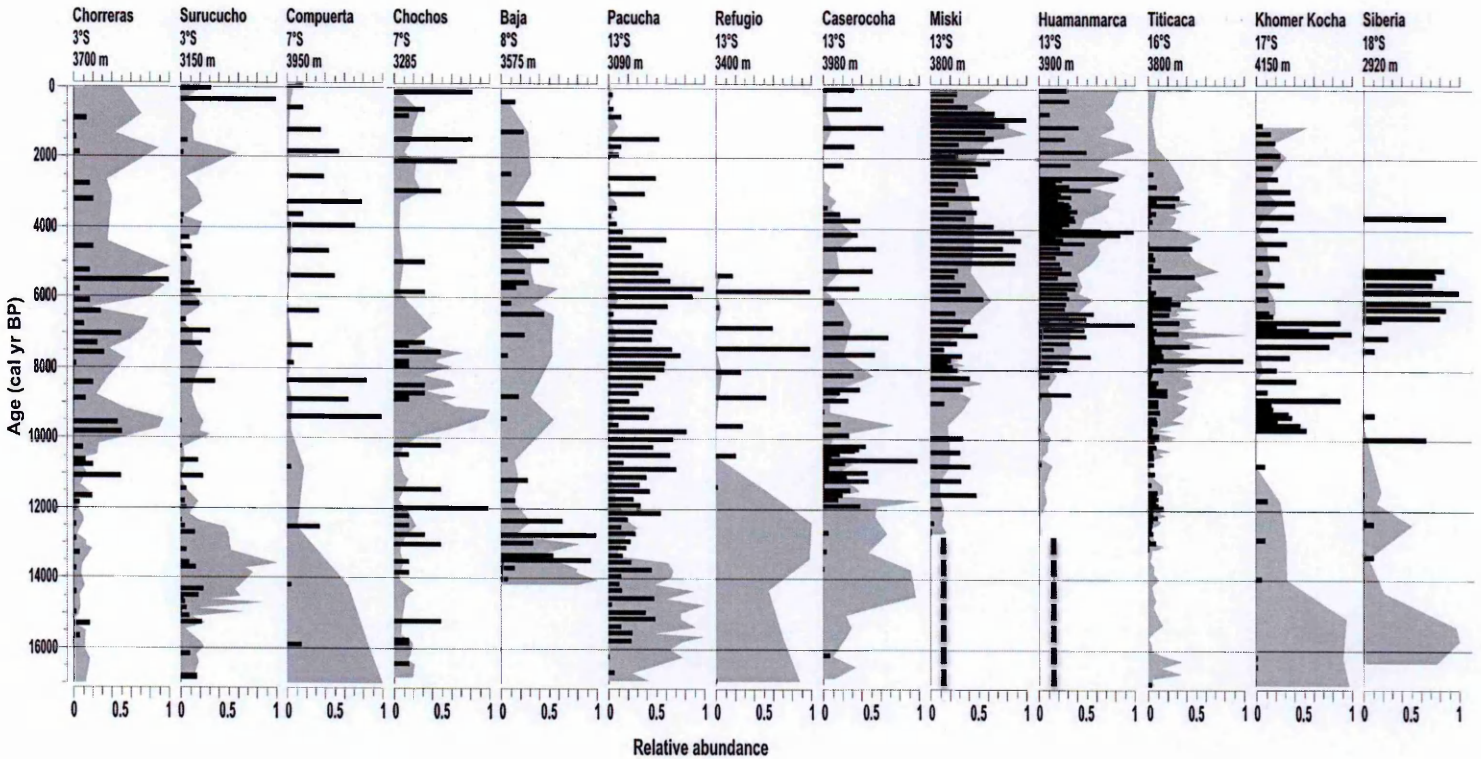

Fig. 5-3 Post-glacial *Polylepis* pollen (grey contours) and charcoal data (black bars) data from 13 sites (Hansen & Rodbell, 1995; Colinvaux *et al.*, 1997; Hansen *et al.*, 2003; Paduano *et al.*, 2003; Bush *et al.*, 2005; Weng *et al.*, 2006; Valencia *et al.*, 2010; Urrego *et al.*, 2011; Williams *et al.*, 2011) for a latitude range from 3°S to 18 °S. Pollen and charcoal data were scaled by the maximum value in each record. Vertical dashed lines represent the period when Miski and Huamanmarca were glaciated.

5.4.2) Environmental modelling

MaxEnt generated a map where each pixel represents the probability of finding suitable environmental conditions for *Polylepis* (Fig. 5-4). Cross-validation of the model produced an average AUC of 0.898 with standard deviation of 0.037 based on 20 replicate runs. The model faithfully reflected known *Polylepis* occurrence records, but also suggested possible sites for this genus where none grow today.

The results of the Jackknife test suggested that annual cloud cover (Clyr) and the ruggedness (Rugg) index were the most important environmental parameters to determine the suitable area for *Polylepis* today (Fig. 5-5). When used in isolation, cloud cover (Clyr) was the environmental parameter that contributed the most to the modelled distribution of modern *Polylepis* populations. The next three most important environmental variables when used in isolation were cloud cover from December to February (Cldjf), precipitation of the wettest quarter (Bio16), and cloud cover from June to August (Cljja). In contrast, in model runs that excluded one variable at a time, excluding ruggedness caused the largest performance loss of the model (Fig. 5-5); the second most important environmental parameter in this test was elevation. The observed decline in the model performance indicated that the information supplied by ruggedness and elevation was not included in other environmental variables.

Fires were generally considered the main factors affecting woodlands in the high Andes. However, when modelled, fires were unable to explain the modern distribution of *Polylepis* and lowered the performance of the MaxEnt model. The inability to differentiate natural from anthropogenic fires should explain this issue. Natural fires, although random should be limited by natural barriers and constrained to periods when conditions are favourable (e.g. low moisture content and biomass availability). In contrast, human induced fires may benefit of favourable conditions but are not limited to them. Modern fire data was not a suitable variable to be used in the MaxEnt model.

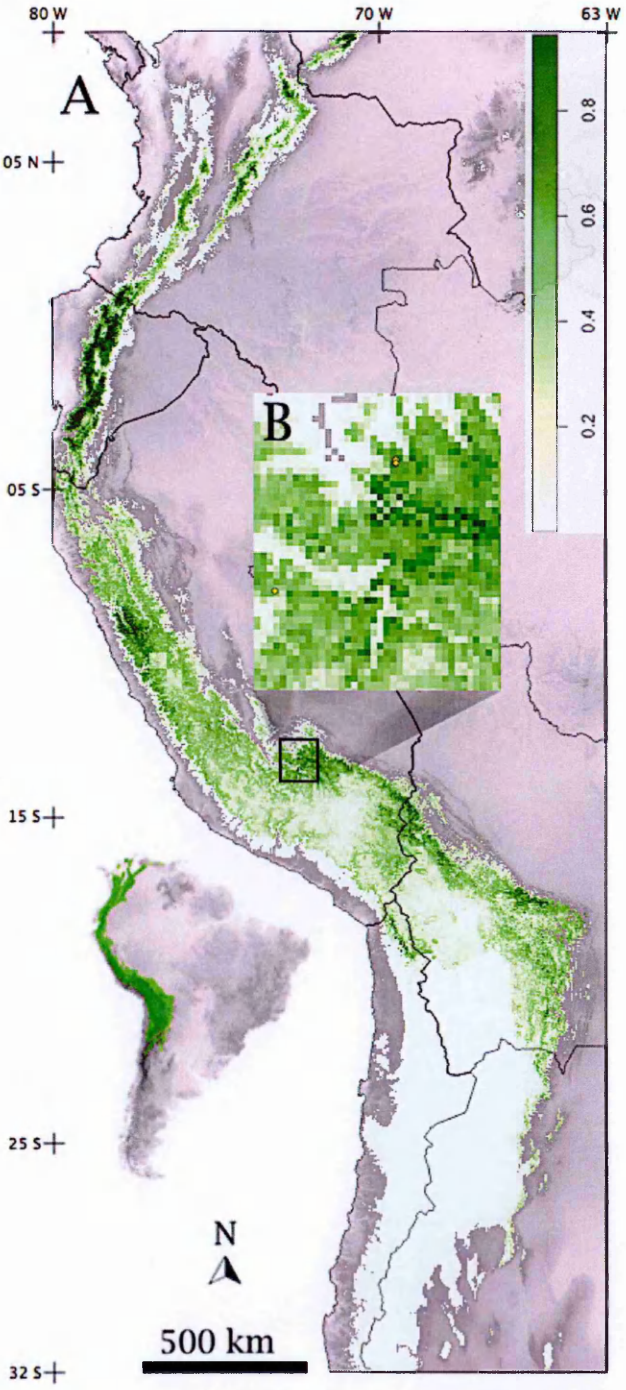

Fig. 5-4 MaxEnt output showing the modelled probabilities of suitable habitat for *Polylepis* forests (A). The zoom in the map (B) depicts the heterogeneous woodland cover.

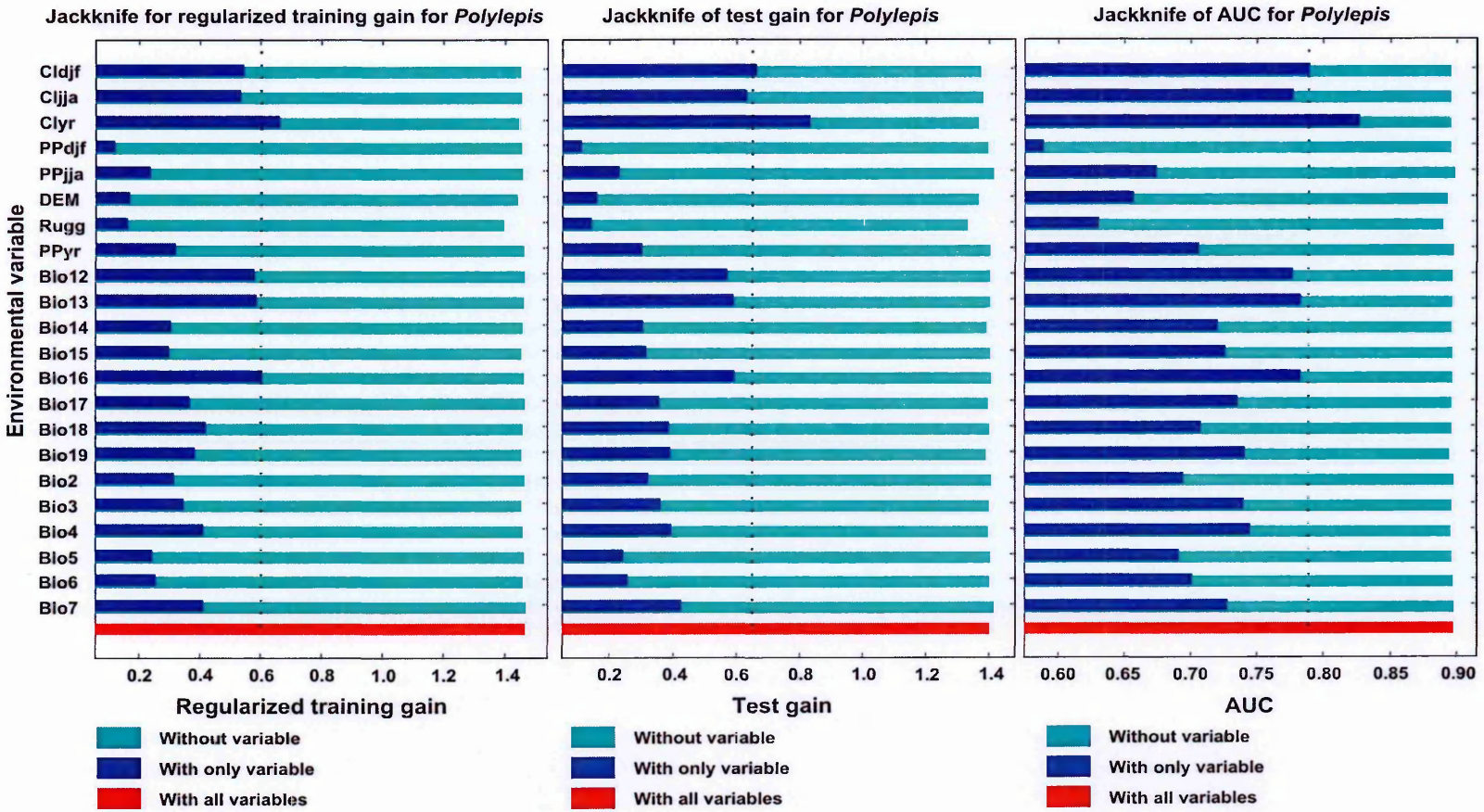

Fig. 5-5 Jackknife test for the *Polylepis* model. The Jackknife test for training gain (left), testing gain (mid) and AUC (area under the ROC curve, right) show the relative contribution of each environmental variable for the model. A dotted line was inserted in each panel for comparison purposes.

Code	Environmental variables	Jackknife of AUC for *Polylepis* (rank)	
		With only variable	Without variable
Cldjf	Average Cloud Cover for Dec, Jan, and Feb from 1998 to 2009	2	-
Cljja	Average Cloud Cover for Jun, Jul, and Aug from 1998 to 2010	5	-
Clyr	Average Cloud Cover annual, 1998 to 2009	1	-
PPdjf	Cumulative precipitation for Dec, Jan, and Feb	22	-
PPjja	Cumulative precipitation for Jun, Jul, and Aug	19	-
DEM	Digital elevation model	20	2
Rugg	Ruggedness	21	1
PPyr	Cumulative precipitation, annual	15	-
Bio12	Temperature Seasonality	6	-
Bio13	Max Temperature of Warmest Month	4	-
Bio14	Min Temperature of Coldest Month	13	-
Bio15	Temperature Annual Range	12	-
Bio16	Mean Temperature of Wettest Quarter	3	-
Bio17	Mean Temperature of Driest Quarter	10	-
Bio18	Mean Temperature of Warmest Quarter	14	-
Bio19	Mean Temperature of Coldest Quarter	8	3
Bio2	Annual Precipitation	17	-
Bio3	Precipitation of Wettest Month	9	-
Bio4	Precipitation of Driest Month	7	4
Bio5	Precipitation Seasonality	18	-
Bio6	Precipitation of Wettest Quarter	16	-
Bio7	Precipitation of Driest Quarter	11	-
Bio1	Annual Mean Temperature	*	*
Bio8	Precipitation of Warmest Quarter	*	*
Bio9	Precipitation of Coldest Quarter	*	*
Bio10	Mean Diurnal Range	*	*
Bio11	Isothermality	*	*
Shade	Average Shade for June-Dec 2005	*	*
Fire	Fires during the 2005	*	*

Table 5-1. List of environmental variables used in MaxEnt modelling. Hyphens (-) are used for AUC values that are near identical and which rank interpretation would be misleading. Asterisks (*) depict variables excluded from the analysis because they lowered or did not improve the model performance in preliminary runs.

5.5) Discussion

5.5.1) MaxEnt, environmental parameters, and spatial modelling

A total of 22 environmental variables were used to generate the MaxEnt model depicted in Fig. 5-4. Among them, annual cloud cover was the single most important environmental variable in predicting the distribution of high Andean woodlands in the model when used alone (Fig. 5-5). The next two most important environmental variables were austral summer cloud-cover (December to February) and annual precipitation. Overall, moisture supply as cloud cover and precipitation provided the moisture required for growth and limited desiccation thereby limiting flammability especially at the end of wintertime (Asbjornsen et al. 2005, Bush et al. 2008). For instance, landscapes were unlikely to burn whenever humidity was high, despite the fuel availability or ignition source (Nepstad et al. 2004a, Bush et al. 2008, Cochrane and Ryan 2009).

Fires are generally scarcer in aseasonal than in seasonal sites (Bush et al. 2008). For instance, the Amazon Basin and the Eastern Andes of Ecuador have the lowest fire probabilities in South America because the moisture supply is near continuous year round at these locations (Bush et al. 2008). Furthermore, an elevational band where ground-level cloud forms year–round is identified in the Eastern Andes (Halladay et al. 2012). The probability of this band occurring between 2000 and 3000 m asl is high, but declines substantially above *c.*4000 m (Halladay et al. 2012).

Terrain heterogeneity (ruggedness) and elevation had the greatest negative influence on model performance when they were removed (Fig. 5-5). Evidently, no other environmental layer supplied the information contributed by ruggedness and elevation, i.e. these factors were not autocorrelated strongly with other variables. Ruggedness was quantified as an index of topographic heterogeneity based on elevation differences of a central pixel relative to the surrounding ones. High topographic heterogeneity should have promoted the presence of firebreaks reducing the chance of fires from spreading into the adjacent areas, e.g. grassland fires spreading into woodlands eliminating *Polylepis* among other fire-sensitive tree species (Horn and Kappelle 2009, Román-Cuesta et al.

2011). The potential for within catchment topographic heterogeneity was especially important as charcoal and *Polylepis* pollen were registered simultaneously in lake sediments suggesting that woodlands and burned patches coexisted side by side.

The spatial distribution of *Polylepis* was modelled with MaxEnt to assess whether *Polylepis* could have formed a continuous woodland-belt along the Andes. In general, high probabilities were allocated by the model to the three countries that currently harbour most of the *Polylepis* species diversity for the Andes (Schmidt-Lebuhn et al. 2006). The probabilities showing suitable habitat for *Polylepis* were highest in the Andes of Ecuador, the central and southern Andes of Peru, and the northern and central Andes of Bolivia. Despite its widespread geographic range, *Polylepis* was projected to have a discontinuous, patchy, distribution from Venezuela to Bolivia.

The MaxEnt outputs were powerful indicators of the probable patchiness of habitat, but it is possible that the data were biased by historical factors. For example, if humans had changed the fire regime to such an extent that whole classes of *Polylepis* woodland habitat were transformed to another type, the MaxEnt model would suffer from a systematic exaggeration of fragmentation; a shifted baseline of what we perceive to be natural (sensu Pauly et al. 1998). Pollen data could be used to infer if this scenario applied in the past. If this scenario was true for modern fires, an overlap with low MaxEnt probabilities i.e. < 0.3 should be expected. However, modern fires did not follow this expectation (Fig 5).

5.5.2) *Polylepis* distributional trends from fossil pollen data

The modern *Polylepis* abundances derived from pollen records depicted a coarse landscape similar to the one generated with the MaxEnt model. Overall, the studied sites where modern pollen reached > 20 % had modelled probabilities for *Polylepis* presence greater than 0.50 (i.e. Chorreras, Surucucho, Miski and Huamanmarca). Records from Lakes Compuerta, Chochos, Baja, Pacucha, Refugio, Caserococha, and Siberia with modern pollen < 20 % had probabilities under 0.41. The modern pollen

signal for Lake Titicaca was < 10% and because of its size a range of probabilities was obtained (from 0.1 to 0.6) with most of them (95 %) under 0.4. In contrast, in Lake Khomer Kocha the modern *Polylepis* pollen was virtually absent but had a modelled probability of 0.64. In summary, the model misclassified only Lake Khomer Kocha as a false positive.

Note that the MaxEnt model probably overestimated the overall distribution for *Polylepis* because parameters taking into account human impacts such as fires or changes in land use were not included (details in following sections). For instance the inclusion of modern fire data substantially lowered the performance of the model. Fires should have been most common in sites under human influence and may have randomly overlapped with the *Polylepis* sites. Fires may have been natural or caused by humans, but was still not possible to differentiate them for modelling purposes. The model outputs suggested that autecology not contingencies of history caused modern *Polylepis* woodlands to be disjunct (Fig. 5-4 Zoom). It was not surprising to find that *Polylepis* woodlands were discontinuous given that topography was one of the principal correlates with modern distribution.

5.5.3) *Polylepis* woodlands

A review of records predating 17 ka showed a pattern of asynchronous peaks in *Polylepis* abundances in records from Lakes Titicaca (16 °S; Hanselman et al. 2011b), Huiñaymarca (16.3 °S; Gosling et al. 2008), Salar de Uyuni (20°S; Chepstow-Lusty et al. 2005), and Lake Fuquene (5.5°N; van der Hammen and Hooghiemstra 2003). The pollen data suggested that the *Polylepis* abundances rose and fell at different times in different landscapes during previous glacial, and interglacial periods (Gosling et al. 2009).

Between *c.*20 and 10 ka, snowline had risen between 300 m and 1300 m from its maximum expansion prior to 20 ka, but this process of deglaciation was not homogeneous at regional or local scales (Porter 2001, Smith et al. 2005). The presence

of glaciers and ice tongues between 17 and 12 ka were probably enough to cause some division of *Polylepis* populations as they expanded upslope in response to warming.
As conditions warmed asynchronous peaks in abundance were characteristic of the records in this study. For instance, Chorreras, Chochos, and Titicaca (Fig. 5-3) had low and stable *Polylepis* pollen abundances (mostly <20 ±10%) contrasting with high and fluctuating abundances (mostly >40 ±20%) in records from Surucucho, Compuerta, Pacucha, Refugio, Caserococha, Khomer Kocha, and Siberia. Overall population trends also appeared to differ between sites, with *Polylepis* pollen abundances declining in Compuerta, Khomer Kocha, and Siberia as they rose in Surucucho, Pacucha, and Caserococha. During this period the sites of Baja, Miski, and Huamanmarca were still glaciated.

Polylepis is a fire-susceptible genus that produces a strong pollen signal (*c.*30-40%) only when growing close to a lake. A basic expectation would be that as fuel loads increased during the deglacial climatic warming, so fire frequency and intensity would increase and *Polylepis* abundance would decline. The history of *Polylepis* and fire, though was found to be more complex than this simple model. At lakes Compuerta, Refugio, and Siberia, *Polylepis* pollen abundance declined coincident with charcoal peaks at *c.*13, 10.5 and 10 ka. In contrast, *Polylepis* abundances in Lakes Chorreras, Surucucho, Chochos, Baja, Caserococha, Miski, Huamanmarca, Titicaca, and Khomer Kocha did not decline when charcoal peaked. Overall, peaks in charcoal were rarely followed by a marked decline in *Polylepis* pollen at these sites suggesting that although fires burned within the catchment they did not burn all the *Polylepis* woodlands. Because, *Polylepis* pollen and charcoal fluctuations represented changes in the immediate landscape around the studied sites, where *Polylepis* and charcoal peaks coincided, a local history of incomplete burning is inferred. Fires in topographically complex landscapes often leave areas such as scree slopes unburned (Kessler 1995). This landscape and fire-history heterogeneity permitted the persistence of *Polylepis* woodlands despite the incidence of fire, and constitutes evidence of woodland fragmentation. For instance, a lake surrounded by rugged terrain (firebreaks) should allow the coexistence of woodlands and burned patches side by side. Contrastingly, sites that have smooth or simple topographies might be expected to show less capacity for simultaneous co-occurrence of

Polylepis woodlands and fire. Thus, in the proxy record, both charcoal and *Polylepis* pollen could co-occur as a signature of locally fragmented woodlands.

Between 12 and 10 ka *Polylepis* pollen abundances declined in all the records. During this time interval *Polylepis* woodlands virtually disappeared from Compuerta, Pacucha, Refugio and Siberia. However, starting at 10 ka *Polylepis* abundances increased in most of the records, i.e. Chorreras, Surucucho, Chochos, Baja, Caserococha, Miski, Huamanmarca and Titicaca.

If the generalized decline in *Polylepis* between 12 and 10 ka along the Andes were attributed to humans, this would imply that humans were widespread in the high Andes. If so, after 10 ka the human influence had to be suppressed to favour the observed woodland recovery or the people had to be constrained to sites where *Polylepis* remained rare. Although humans were present on the Peruvian and Chilean coast between *c.*14 and 12 ka, there was limited evidence of widespread human occupation of the high Andes prior to 10 ka (Aldenderfer 2008). Valencia et al., (in prep., chapter 4) showed that the human incursion in the high Andes had a minimal impact on the vegetation between 14 and 7 ka. During this period, trends of vegetation change were similar in sites with unfavourable (Miski and Huamanmarca) and favourable (Pacucha) conditions for human settlements. The trends in vegetation change diverged only after 7 ka as a response to the human influence (Valencia et al., in prep.). Given the weak evidence of a widespread human occupation of the Andes prior to 10 ka, it appeared most parsimonious to suggest that the oscillation in *Polylepis* abundance between 12 and 10 ka was natural and could relate to climatic events or ecological events such as the megafaunal extinction.

The discontinuous *Polylepis* woodlands depicted in the spatial MaxEnt model were also inferred from temporal responses evident in the pollen record over the last 17 ka. Prior to 7 ka, *Polylepis* abundance was highly variable in all the studied sites and was consistent with the hypothesis that *Polylepis* woodlands were naturally disjunct prior to widespread landscape transformation due to human activities, i.e. scenario 1 is rejected (Fig. 5-1).

5.5.4) Spatial and temporal distribution of *Polylepis* woodlands after 7 ka

The period after 7 ka was characterized by intensified landscape transformation. Plant and animal domestication, the development of agriculture, construction, and the widespread use of wood as fuel, had a substantial impact on the high Andean woodlands. These activities should have increased the use of *Polylepis,* promoting its decline, as wood sources in the high Andes were limited (Hastorf et al. 2005).

During the Holocene the records from Refugio, Siberia, Pacucha, and Compuerta showed deforestation taking place (Fig. 5-3). Contrastingly at the high, wet, sites of Lakes Miski and Huamanmarca a continuous woodland expansion was evident, despite the incidence of fire. The absence of *Polylepis* in Compuerta, Pacucha, Refugio and Siberia during the most of the Holocene was probably a combination of climate and human activities limiting *Polylepis* re-colonization. Additional sites like Chorreras, Surucucho, Baja and Chochos were climatically alike to Miski and Huamanmarca, but recorded *Polylepis* pollen fluctuations instead of a gradual increase (*c.*>40%) during the last 7 ka (Fig. 5-3). It is probable that accessibility of each of the sites by human populations and availability of alternative wood sources nearby was the reason for these dissimilar trajectories of vegetation change besides climate.

Fluctuations in *Polylepis* pollen abundances suggest that the landscape became a mosaic of disrupted areas, e.g. Refugio, Siberia, Pacucha, and Compuerta, contrasting with sites that were minimally impacted, e.g. Miski and Huamanmarca. This historical dichotomy continued throughout the rise of the dynastic empires such as the Wari, and Inca. Major Inca constructions such as Machupicchu and Ollantaytambo were only *c.*22 km away from Lakes Miski and Huamanmarca, emphasizing the mosaic effect of impacted and minimally transformed areas within this landscape.

Taken as a whole, the spatial and temporal variability in *Polylepis* pollen does not support the presence of a continuous woodland-belt along the Andes at any time in the last 7 ka. The substantial fluctuations in *Polylepis* pollen abundance in the palaeoecological records indicate a patchwork, or landscape mosaic, of *Polylepis* woodlands at local and regional scales that predate the onset of widespread human populations and continue over the last *c.*7 ka. As people enter the landscape, the most

heavily used sites lose their *Polylepis*, suggesting a decrease in *Polylepis* patch occupancy leading to hyper-fragmentation.

5.6) Conclusions

A distribution model for *Polylepis* was modelled with MaxEnt based on 22 environmental parameters to evaluate if this genus was able to form a continuous woodland belt along the Andes. The model showed that *Polylepis* woodlands were spatially disjunct despite the exclusion of additional layers such as agricultural sites or earthworks (human influence) that would enhance the spatial fragmentation.

Palaeoecological reconstructions supported the results of the model and showed that *Polylepis* woodlands were spatiotemporally disjunct along the Andes over the last 17,000 years. Pollen records do not support the presence of an uninterrupted woodland belt above the modern continuous timberline prior human arrival, i.e. 14 ka. Pollen and charcoal records suggested *Polylepis* woodlands and burned patches coexisted (i.e. were fragmented) at local scales and that this pattern was recurrent regionally prior 7 ka. The *Polylepis* woodlands became hyper-fragmented during the Holocene, especially after 7 ka, when human activities eradicated large patches of forest (Valencia et al., in prep). Hyper-fragmented landscapes were represented in multiple pollen record as a mosaic of sites with some showing almost no woodland loss coexisting with deforested sites that would have supported *Polylepis* woodlands in the absence of human land use.

The MaxEnt model showed that the most important environmental parameters determining suitable habitat for *Polylepis* were cloud cover, precipitation and ruggedness. Cloud cover and precipitation contributed most of the information to model *Polylepis* presence when used alone. On the other hand ruggedness was the only variable that contributed topographic heterogeneity data to the model.

Overall, The MaxEnt model and pollen data supported that *Polylepis* woodlands were naturally fragmented in contrast to modern *Polylepis* woodlands that are hyper-

fragmented due to human activities. The broader occurrence of *Polylepis* within the model compared with the actual occurrence of woodlands, suggests that enough natural *Polylepis* cover remains that the MaxEnt model can provide an accurate indication of potential *Polylepis* habitat.

Chapter 6) Conclusions

The following chapter briefly reviews and summarizes the rationale, goals and synthesises the main findings of the thesis. Furthermore, details of additional publications derived from my research work completed parallel to this part time Ph.D. are provided for academic context alongside ideas for further research.

6.1) Thesis aim

The overarching aim of this research was to characterize vegetation baselines for the high tropical Andes that could be used for conservation and restoration (chapter 4). Conservation and restoration are particularly important in mega-diverse areas like the tropical Andes because of their vulnerability due to anthropogenic activities and climate change (Orme et al. 2005, Malcolm et al. 2006). Conservation efforts are directed to restore and maintain ecosystems as means to conserve species diversity and ecosystem functionality. However, these efforts rely on identifying conditions prior to degradation (baselines) for restoration and conservation purposes; otherwise, anthropogenic modified assemblages could unwittingly be reconstructed or protected (e.g. shifted baselines).

A spatial distribution model for *Polylepis* Andean woodlands was created (chapter 5) to evaluate if the modern mosaic-distribution of these woodlands was natural or the product of human activities. The concept of ecological baselines and timing defined in chapter 4 were used to as working framework. The modelled spatial distribution of *Polylepis* was tested using 11 published paleoecological reconstructions.

6.2) Establishing ecological baselines

The concept of a shifted baselines refers to the acceptance of an anthropogenically degraded landscape as natural (Pauly 1995). Each new generation takes a landscape impacted by previous generations as natural (anthropogenic baseline) promoting a continuous baseline recalibration. The use of anthropogenic baselines for restoration or

conservation would imply that degraded landscapes are used as conservation or restoration goals.

Baselines for modern ecosystems should be derived from time periods with climate similar to modern that had negligible human influence. A major limitation when establishing vegetation baselines for Andean ecosystems is that humans transformed the Andean landscapes for several millennia. Therefore and unquestionably, ecological baselines are required to understand the "natural environment" that predate the arrival of Europeans in South America. Once natural ecological baselines are identified, a new question arises: Is it valid to reset the conditions in a given area and return it to a baseline state condition? If the answer is "yes", it is implicitly assumed that baselines are static and that communities have the tendency to reach a fixed climax assemblage. If the answer is no, or maybe, it is assumed that baselines are dynamic and that the assemblage output has countless possible states influenced by past and currents events including stochastic factors.

Multi-proxy records derived from Lakes Miski, Huamanmarca and Pacucha were used to answer the following questions:

6.2.1) To what extent are the records from Miski and Huamanmarca were representative of other records in the region?
6.2.2) Can a period in the Holocene form a satisfactory baseline for the natural state of Andean vegetation?
6.2.3) Was the woodland-grassland mosaic a long-term feature of the environment?

6.2.1) To what extent are the records from Miski and Huamanmarca representative of other records in the region?

The question is aimed to verify if Miski and Huamanmarca were in close agreement with other records at regional scales (section 4.5.1). A lack of agreement with other records would indicate that Miski and Huamanmarca had a local signal making them

unsuitable for interpretations at regional scales. However, all the study sites provided clear evidence of recording changes at regional and local scales (Fig. 6-1). For instance, periods of drought (e.g. the Mid Holocene Dry Event, Fig. 6-1) and periods of oscillating precipitation during the early and late Holocene observed regionally were also registered in Miski and Huamanmarca. The studied records were sensitive to the regional and local climatic signal; therefore were suitable to study baselines and derive inferences at regional scales.

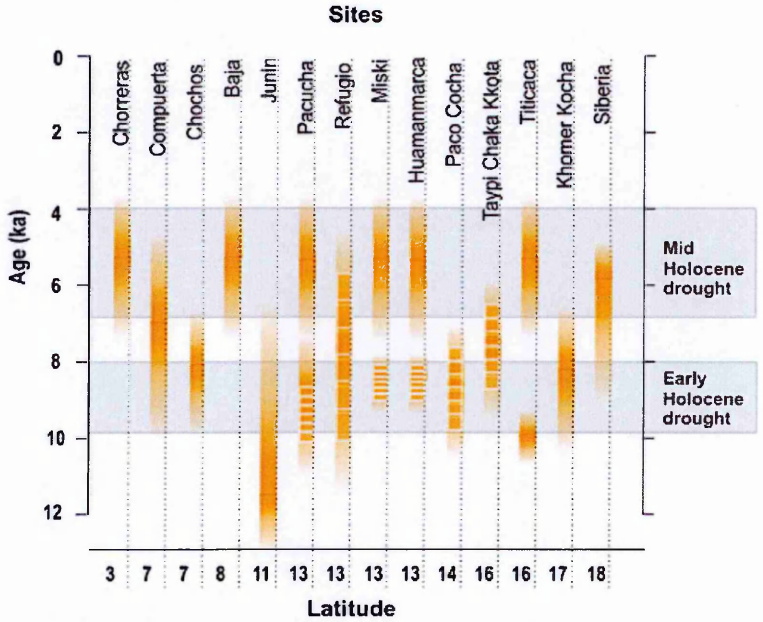

Fig. 6-1 Congruency sketch of droughts observed between 3°S and 18°S in 14 Andean records (Hansen et al. 1984, Hansen and Rodbell 1995, Seltzer et al. 2000, Abbott et al. 2003, Mourguiart and Ledru 2003, Paduano et al. 2003, Tapia et al. 2003, Bush et al. 2005, Weng et al. 2006, Hillyer et al. 2009, Valencia et al. 2010b, Williams et al. 2011a, Urrego et al. 2013). The colour intensity (orange) indicates drought. Broken colour bands indicate oscillating droughts.

6.2.2) Was the woodland-grassland mosaic a long-term feature of the environment?

This question was aimed to identify long-term trends of change in grasslands and woodlands. To answer this question, a temporal evaluation of the changes observed in

grasslands and woodlands was performed using pollen diagrams (Figs. 4-2 and 4-3). These comparisons included the analysis of charcoal to determine if vegetation changes were directly related to fire events (natural or anthropogenic).

The pollen assemblages from lakes Miski and Huamanmarca were alike especially when compared by vegetation type (Fig 4-5A). The pollen data, i.e. local woodland and Poaceae (Fig. 4-5A), supported a co-occurrence of woodlands and grasslands as a mosaic that persistent from *c.*12 ka to modern times. Woodlands expanded continuously and were minimally influenced by fires since the formation both lakes. The co-occurrence of fires (flammable grasslands) and woodlands suggest that landscape heterogeneity played a main role favouring a patchy landscape. For instance, not all the land surrounding Lakes Miski and Huamanmarca was equally susceptible to be burned. Consequently woodlands persisted despite the incidence of fires.

6.2.3) Can a period in the Holocene form a satisfactory baseline for the natural state of Andean vegetation?

The question aims to identify a period with a climate similar to modern conditions and negligible human influence. Based on paleoecological reconstructions modern-like conditions occurred once the deglaciation was over (*c.*11 ka) but predating periods of drought such as the Early- or Mid Holocene Dry Event (Fig. 6-1). The post-MHDE was also a time interval with a climate similar to modern. However, the post-MHDE was a period heavily influenced by anthropogenic activities (Fig. 1-5).

Determining when humans arrived at Miski and Huamanmarca was unfeasible. However, it was possible to determine when the influence of humans became evident in the vegetation based on comparisons of trends in vegetation change (Fig. 4-10). The occupation at any site should be closely related to all the possible benefits that the site could offer. Sites having a long history of human occupation probably had conditions that favoured an early human settlement. In contrast sites with unfavourable conditions were unlikely to be occupied. Finally, vegetation assemblages from sites with favourable

and unfavourable conditions were compared using trends of vegetation change to determine when the human influence produced a divergence between them. This comparison assumes that vegetation changes prior human influence should be under natural climate control. The assumption should be valid since, all the sites recorded consistently climatic events observed regionally. A comparison of this kind (sites with favourable and unfavourable conditions) is only valid when all the sites belong to a similar region and have similar species. For instance, highland and lowland sites may not have the same species and therefore could not be compared.

The trends of vegetation from Lakes Miski and Huamanmarca diverged from the ones observed in Pacucha at *c.*7 ka suggesting that the human influence became conspicuous after *c.*7 ka (Fig. 6-2). The diatom data from Miski and Pacucha showed a similar behaviour supporting independently to the pollen proxy that Pacucha assemblages diverged from Miski at c 7 ka (Fig. 6-2).

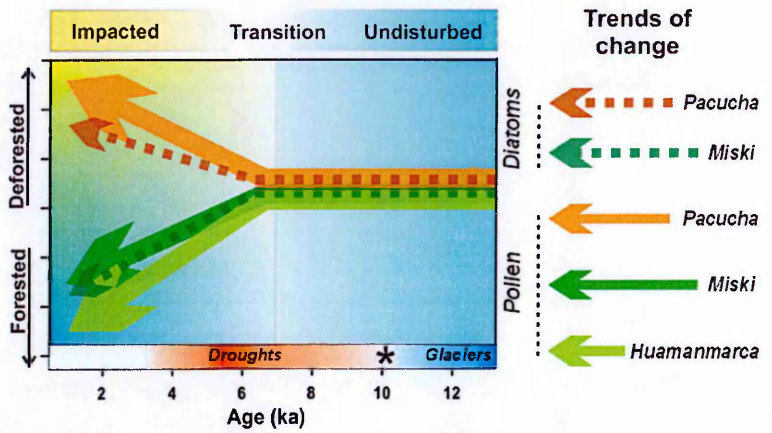

Fig. 6-2 Summary diagram showing the trends of change in pollen and diatoms in Lakes Miski, Huamanmarca, and Pacucha (coloured arrows) depicting the baseline at 10 ka (★). The background of the plot shows the degree of landscape transformation from disturbed (light blue) to impacted (yellow). Periods of glacial activity (blue) and drought (red) are depicted in the bottom of the diagram.

The period between 11 and 9 ka was the best climate analogue of modern conditions at it was free of the glacial influence and droughts. Because of the climatic similarity and

limited human influence, assemblages centred at 10 ka were identified as satisfactory baselines for the Andes for sites with uncertain anthropogenic influence.

The pollen reconstructions from Lakes Miski and Huamanmarca suggest that the human influence around these sites was insignificant. This particular result challenges the idea of a homogeneous anthropogenic landscape for the Andes especially during the late Holocene. Furthermore, the baselines for Miski and Huamanmarca drifted naturally and continuously since their formation suggesting that baselines are dynamic. Consequently, vegetation assemblages may not necessarily converge into a climax system once the influence of a given disturbance ceases, i.e. Baselines should be used as one multiple assemblage possibilities and not as a fixed objective or restoration goal. The reconstruction of baselines could be used with species distribution models to provide a modern spatiotemporal support. An example of baselines and distribution model is detailed in chapter 5 and the following section.

A seminal work by Holling (Holling 1973) that introduced a novel concept of resilience applied to ecology. Resilience theory provides a conceptual foundation and working framework to evaluate changes in ecological systems once thresholds are surpassed and beyond which the ecological system changes into an alternate state (Carpenter et al. 2005, Cumming et al. 2005). Resilience theory can be applied to past landscapes such as the studied records and is closely related to ecosystem integrity and services (Redman and Kinzig 2003, Gillson and Marchant 2014). The woodlands around Miski, Huamanmarca, and Pacucha prior *c.*7 ka experienced fluctuations but maintained a similar trend. The vegetation was resilient to local changes (including humans as surrogates) while it responded to climatic forcing (i.e. shared trend among records). After *c.*7 ka Pacucha, gradually transitioned to an alternate state due to human pressure. By *c.*6 ka Pacucha was an agricultural landscape while Miski and Huamanmarca remained forested and dominated by *Polylepis*. The agricultural landscape around Pacucha was subjected to two additional shifts corresponding to (i) the replacement of quinoa cultivation (*c.*6-3 ka) by maize at *c.* 3 ka, and (ii) a change in landscape management at the time of European arrival (*c.*0.5 ka). Climate probably facilitated the onset of maize cultivation as the drought (HMDE) ended. Consequently, through the

modulation of ecosystem services (water availability), climate became a surrogate and changed the agricultural practices at *c.*3 ka regionally (Valencia et al. 2010b, Mosblech et al. 2012). As water was no longer limiting agriculture, the cultivated areas could be expanded, probably to the detriment of Andean woodlands. If the structure and function of the Andean ecosystem were no longer maintained after *c.*3 ka, it would indicate that a new alternate state was reached. However, because these changes were not perceptible in Miski and Huamanmarca, the alteration was likely produced as a regional mosaic. The implementation of agroforestry practices (Mosblech et al. 2012) indicated that wood resources became scarce and that that management was required to overcome this and other ecosystem service issues such as water retention or erosion control (Chepstow-Lusty et al. 1998). At *c.*0.5 ka, the arrival of Spaniards and conquest of the Inca had a profound impact on the landscape (Chepstow-Lusty and Winfield 2000). The practices and management introduced by the Spaniards, e.g. the suppression of agroforestry, probably made humans the main surrogate (Chepstow-Lusty and Winfield 2000). As with the cultivation transition at *c.*3 ka, the effect of the Spaniard arrival may have induced a new alternate state. Overall, by comparing trends of change in the studied sites it was possible to identify surrogates that could be responsible of the multiple changes observed in the studied records. However, these are observations that require further testing. Moreover, it remains elusive the identification of additional surrogates and the quantification of each of them to define specific thresholds to have a comprehensive estimate of resilience. The use of empirical modern data could be employed to model surrogates and based on them, define resilience thresholds in Andean ecosystems.

6.3) *Polylepis* woodland dynamics

Polylepis is the most representative tree of the high Andes at elevations higher than 3500 m. This genus has no ecological equivalents since no other arboreal species has a similar elevational distribution. Today, *Polylepis* has a patchy spatial distribution that was debated as being natural or product of anthropogenic activities (Raimondi 1874, Simpson 1979, Fjeldså 1992, Herzog et al. 2002, Kessler 2002). In chapter 5 the spatial

distribution of *Polylepis* was evaluated based on models and pollen records to address two research questions:

6.3.1) Has *Polylepis* woodland formed a natural continuous 'belt' along the Andes in the last 17 ka? And,
6.3.2) What environmental factors controlled the spatial distribution of *Polylepis* woodland?

6.3.1) What environmental factors controlled the spatial distribution of *Polylepis* woodland?

This question was directed to identify those variables that had the largest contribution for predicting the spatial distribution of modern *Polylepis* woodlands. A total of 22 variables and georeferenced *Polylepis* occurrences were used to model the modern spatial distribution of *Polylepis* using MaxEnt (Appendix VI). From all the variables, annual cloud cover and precipitation contributed the most in the model when used alone (Fig. 5-5). In contrast, ruggedness (terrain heterogeneity) and elevation were the variables that reduced the most the model performance when removed (Fig. 5-5). In summary, moisture and landscape heterogeneity played the most important role in predicting the spatial distribution of *Polylepis*.

The results of the MaxEnt model showed a mosaic of high probabilities of *Polylepis* occurrences for the Andes embedded in a matrix of low probabilities (Fig. 5-4). The MaxEnt predictions assigned most of the highest probabilities to the countries that currently harbour most of the diversity of *Polylepis* in the Andes. Furthermore, the model correctly classified the modern counts of 12 out of 13 *Polylepis* sites into low (below 20%) and high (above 20%) concentrations based on a probability threshold of 0.2. The model did not include variables for anthropogenic impacts (past and modern) such as agricultural fields or developed areas that could bring to zero the model probabilities. Therefore, the model depicted non-anthropogenic fragmentation. A total of 13 paleoecological reconstructions were used to determine if the model was reflected

during any particular time period over the last 17 ka. Pollen reconstructions were compared with the model prior and after human disturbances became commonplace in the Andes.

6.3.2) Has *Polylepis* woodland formed a natural continuous 'belt' along the Andes in the last 17 ka?

The aim of this question was to determine if *Polylepis* could form continuous woodlands when humans were absent. If *Polylepis* formed continuous woodlands prior human impacts became evident in the Andes (i.e. *c.*7 ka, chapter 4); then, its modern patchy distribution was the product of human disturbance. However, if *Polylepis* distribution was patchy prior *c.*7 ka a second and a third possible outcomes are possible: *Polylepis* could have formed discontinuous patches prior human disturbances becoming hyper-fragmented after *c.*7 ka. Or, *Polylepis* was hyper-fragmented prior and after 7 ka.

Before the incursion (*c.*12 ka) or evident impact of humans in the Andes (*c.*7 ka), the pollen records derived from 13 Andean sites (Fig. 5-2, 6-3) showed that *Polylepis* followed the classic metapopulation dynamics sensu Levins (1969). The fragmentation was evident as some sites registered increasing pollen abundances while others declined or were near absent. Interestingly, the demise of *Polylepis* pollen was rarely coincident with charcoal peaks (Fig. 5-3). The co-occurrence of fires and *Polylepis* further suggested the woodland discontinuity where fire was a natural component. *Polylepis* pollen experienced a generalized decline around *c.*12 ka and recovered by *c.*10 ka that was considered natural (Fig. 5-3). A widespread human occupation after *c.*12 ka would have to collapse or migrate to favour the *Polylepis* recovery observed at *c.*10 ka (Fig. 5-3).

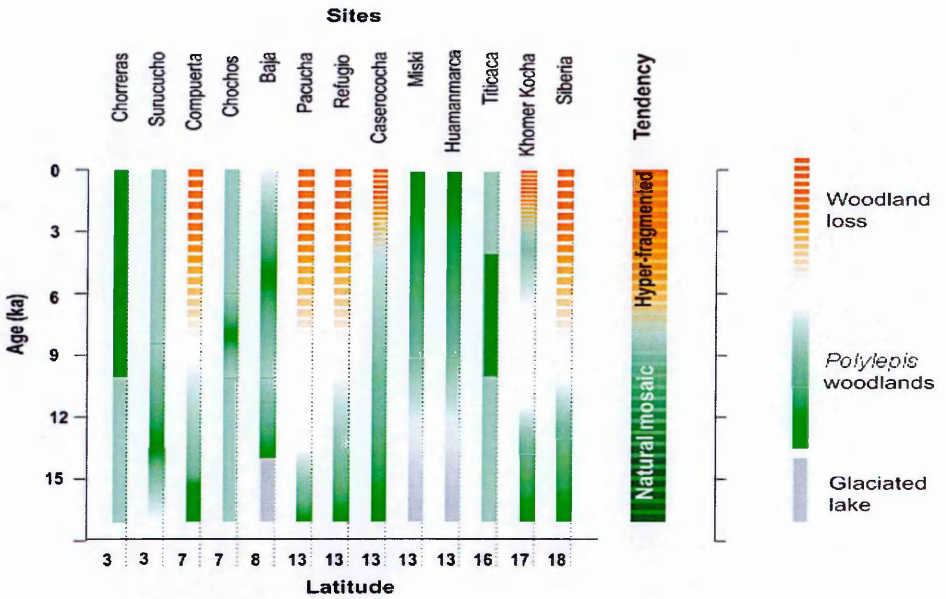

Fig. 6-3 Summary diagram of the woodland dynamics in the Andes over the last 17 ka. The intensity of the coloured bars is proportional to the woodland cover (green) or vegetation loss (orange). The three grey bars for Lakes Baja, Miski, and Huamanmarca represent periods when these sites remained glaciated.

Fragmentation became gradually enhanced during the mid-Holocene (hyper-fragmentation) especially after 7 ka. Patches of *Polylepis* woodlands were reduced or in some sites virtually eliminated. Human activities were probably responsible of the woodland decline observed (Fig 6-3). Landscape transformation and agricultural practices probably enhanced the fragmentation of *Polylepis* woodlands especially during the pinnacle of Andean civilizations (e.g. *c.*1.5 to 0.5 ka).

There is no evidence from fossil pollen to suggest that *Polylepis* woodlands formed a continuous belt prior, or after, human disturbances (Fig 6-3). The modelled distribution for *Polylepis* depicts a landscape similar to pre-human impacts and not the hyper-fragmented landscape of the late Holocene (Fig 5-4). In summary, *Polylepis* woodlands were naturally patchy prior human occupation and became hyper-fragmented once human impacts became widespread during the mid- and late-Holocene.

6.4) Thesis results and the implications for conservation and management in the Andes

Conservation and management require dynamic, adaptive, and responsive targets (i.e. adaptive management) able to accommodate variability and uncertainty in response to climate change (van Wilgen and Biggs 2011, Westgate et al. 2013, Gillson and Marchant 2014). The integration of multiple disciplines such as paleoecology, historical ecology, long-term monitoring, modelling, and remote sensing are essential in designing management plans (Thomas et al. 2004, Willis and Birks 2006, Spangenberg et al. 2012, Gillson and Marchant 2014). This thesis is aimed to provide palaeoecological insights of alternate states of the high Andean ecosystems under human intervention. The main goal of this thesis was to provide an estimate of spatiotemporal "naturalness" over the last *c.*12 ka that can be used as backbone to elaborate on an integrated adaptive management plan. The following recommendation for conservation can be drawn from the results of this thesis:

1. For conservation purposes in the Andes, vegetation assemblages from *c.*10 ka can be used as baselines in sites with a long history of human occupation or when background data about human impacts is unavailable.
2. Because ecological baselines drift continuously, they should be identified preferentially at local scales (< 20-10 km).
3. Andean cloud forests (sites like Miski and Huamanmarca) were minimally affected by human activities. These areas are a priority for conservation, as they should have close-to-pristine conditions besides being resilient to droughts. Sites like Miski and Huamanmarca may also provide further details about the community structure, diversity, and dynamics that can be used as the closest analogues of undisturbed sites.
4. The effectiveness of species distribution models should be evaluated with paleoecological reconstructions to verify and improve the model interpretations.
5. The management of *Polylepis* woodlands should be carried out taking into account the natural spatial patchiness of this genus. Reforestation in areas that can support *Polylepis* (i.e. flat areas) that are naturally devoid of woodlands (i.e. the Altiplano) have a low probability of success in the long term. Under this

scenario, the reforestation effort will be lost because the spatial woodland continuity in absence of barriers is vulnerable to fire. In puna brava landscapes (i.e. above 4500 m) that are fuel limited (low biomass) reforestation could be continuous but maintaining individuals scattered to avoid the possibility of fires spreading through the tree crowns.

6. As rising temperatures are forcing an upslope migration of species, it becomes important to protect areas that in the future will have the conditions to nurse migrating species such as *Polylepis*.
7. The degree of anthropogenic landscape transformation in the Andes was not uniform. Therefore, the observed landscape use around archaeological sites must not be extrapolated to the entire Andean region. This scenario would discourage the conservation of Andean sites as it assumes that all the Andean landscapes are anthropogenic.

Chapters 4 and 5 provide a background of past alternate states and resilience for Andean systems. Based on palaeoecological reconstructions (Chapter 4) and species distribution models (Chapter 5), conservation and restoration goals can be assessed. However, a dynamic conservation approach is required to manage, protect, or restore Andean ecosystems given the future climate scenarios and projected landscape transformation built upon palaeoecological concepts. For instance, from the palaeoecological perspective (this thesis), conservation initiatives should avoid the recreation and maintenance of historical baselines in a given site because baselines are dynamic and respond to climate and landscape changes that are dynamic too. Therefore, careful planning is required to ensure that conservation initiatives can effectively aid and facilitate biotic change influenced by climate change (Hannah and Hansen 2005). Selecting protected areas that overlap with the modern and future distribution of the biota must be done maintaining connectivity and aspects related to of biodiversity such as gene flow, species pools, species interactions and the human component (Alcorn 1993, Hannah and Hansen 2005, Moon and Cocklin 2011, Reyes-Garcia et al. 2013).

The Andean regions may experience substantial transformation under anthropogenic pressure due to increasing human population and subsequent rise in resource consumption (Satterthwaite 2009, van Wilgen and Biggs 2011, Westgate et al. 2013). Demographics and consumption have a direct input on urbanization, agricultural field expansion (market driven), resource extraction (minerals and fossil fuels), heavy metal contamination, woodland logging, and change in anthropogenic fire regimes with direct impact on biodiversity (Sala et al. 2000, Pacheco et al. 2010, Rodbell et al. 2013). Note that all these factors involve landscape transformation despite the spatiotemporal differences of influence. Land-use change is considered the main threat to biodiversity through habitat destruction and barrier formation that hinders migration processes (Pimm and Raven 2000, Sala et al. 2000, Feeley and Silman 2010). Therefore, the success of conservation initiatives and the suitability for protecting or facilitating the restoration of any particular system will have to incorporate the human component including demographic and economic processes linked to landscape transformation and future climate scenarios (Gillson and Marchant 2014). At the same time conservation and management will have to ensure the sustainable use and continuous provision of ecosystem services, especially related to water supply and carbon sequestration that have direct implications for the human component (Josse et al. 2009, Rabatel et al. 2013, Gillson and Marchant 2014).

6.5) Future and on-going research activity

To provide further insight into natural ecological baselines, and their dynamics, in the high central Andes I have identified three further areas of research interest and technical development as priorities for the future. By developing research in these three areas I hope it will be possible to obtain: i) independent climate change information (through element detection in sediments using Energy Dispersive Spectroscopy), ii) new insight into human cultivation practices (through improved identification of crop pollen using Scanning Electron Microscope imagery), and iii) improved understanding of natural and anthropogenic fire regimes (through Scanning Electron Microscope

imagery of charcoal). Progress, and research promise, of these three areas and their technical developments are outlined below.

6.5.1) Energy Dispersive Spectroscopy (EDS or EDAX) element detection

EDS is a technique analogous to X-ray fluorescence (XRF), a fairly new technique used to identify elements in sediment cores. Changes in element abundances over time can be used to identify past climatic events, infer hydrological changes, estimate diatom productivity and counting varves (Haug et al. 2001, Brown et al. 2007, Nakagawa 2007, Francus et al. 2009). EDS is an alternative and cheaper option for element detection than XRF as the equipment could be incorporated to most scanning electron microscope units. Sediment pellets derived from Loss-on-ignition (LOI) can be used for element analysis using an EDS.

LOI pellets derived from lakes Miski and Huamanmarca were analysed using EDS to determine if changes in elemental are correlated with climatic events. Preliminary results are depicted in figures 6-1 and 6-2. The EDS statistical analysis is in progress and should provide insights of climate variability but from a geochemical perspective at high resolution (e.g. < 50 years).

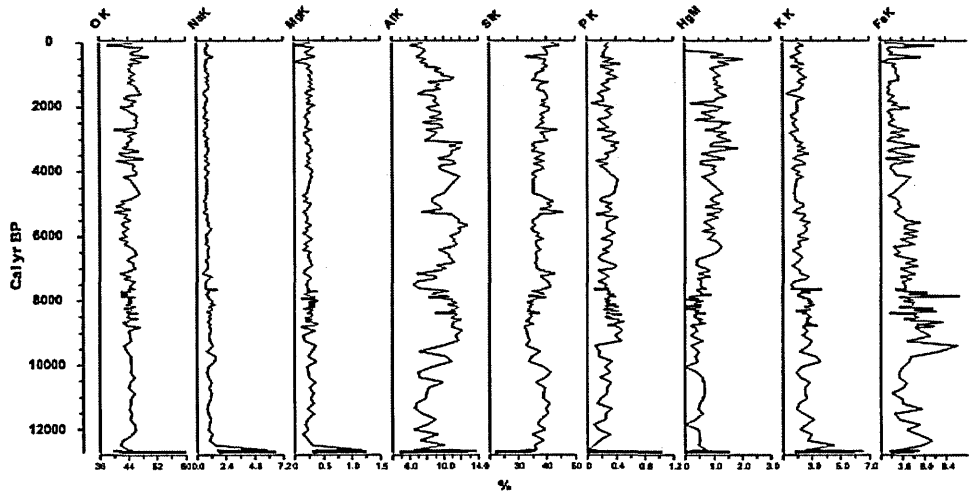

Fig. 6-4 EDX data for Lake Miski

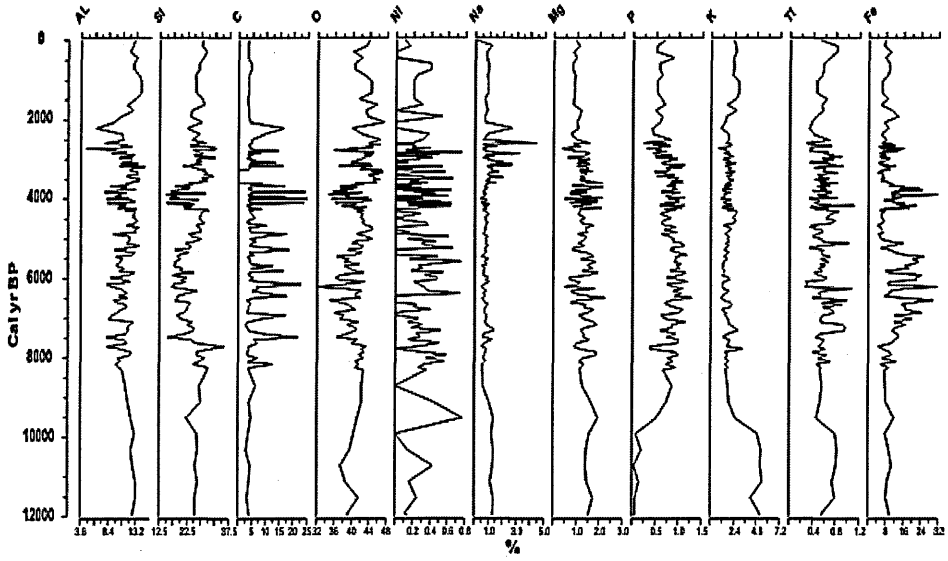

Fig. 6-5 EDX data for Lake Huamanmarca.

6.5.2) Detection of cultivated species using Scanning electron microscope (SEM) pollen images.

The SEM (scanning electron microscope) generates high-resolution images and provide the opportunity to differentiate between species of pollen grains based on morphological characteristics Modern and fossil pollen grains from the family Amaranthaceae have been prepared and imaged using Jeol jsm 6380LV SEM. Pollen grain features (Fig. 6-3) such as diameter, number of pores, number of spines and pollen roundness will be measured in images taken at magnifications between 3000 and 7000x using ImageJ (Rasband). The measurements can be used to differentiate cultivated from wild species of the family Amaranthaceae e.g. quinoa and amaranth (Fig. 6-4). Currently, a SEM reference collection is being implemented for the family Amaranthaceae. The reference material will then be compared with, pollen grains extracted from Lake Pacucha sediment.

Preliminary structure comparisons of the reference material show that *Amaranthus* and Quinoa can be differentiated by the number of spines (Fig 6-4). Additional reference material is still required to identify Amaranthaceae fossil pollen and determine if quinoa and amaranth were cultivated prior 6 ka. This SEM approach could be also used to improve the taxonomy of pollen counts to improve estimates of diversity.

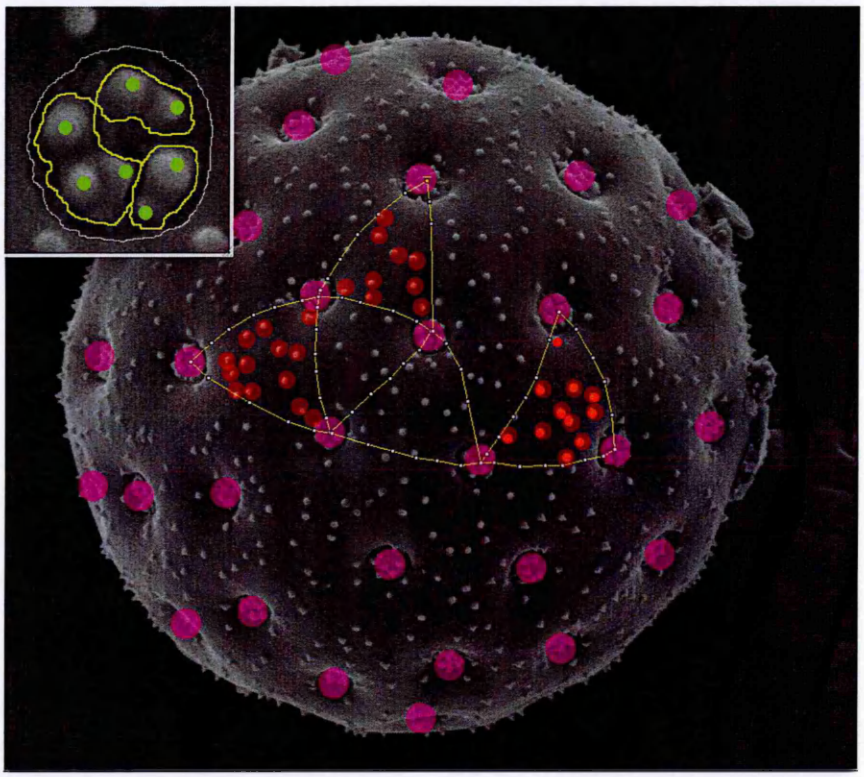

Fig. 6-6 Morphological features measured in selected pollen grain SEM images. Pore coordinates (purple), spines (red dots) inside triangular section (yellow lines), pore diameter and number of spines within each pore (green dots in the top left panel).

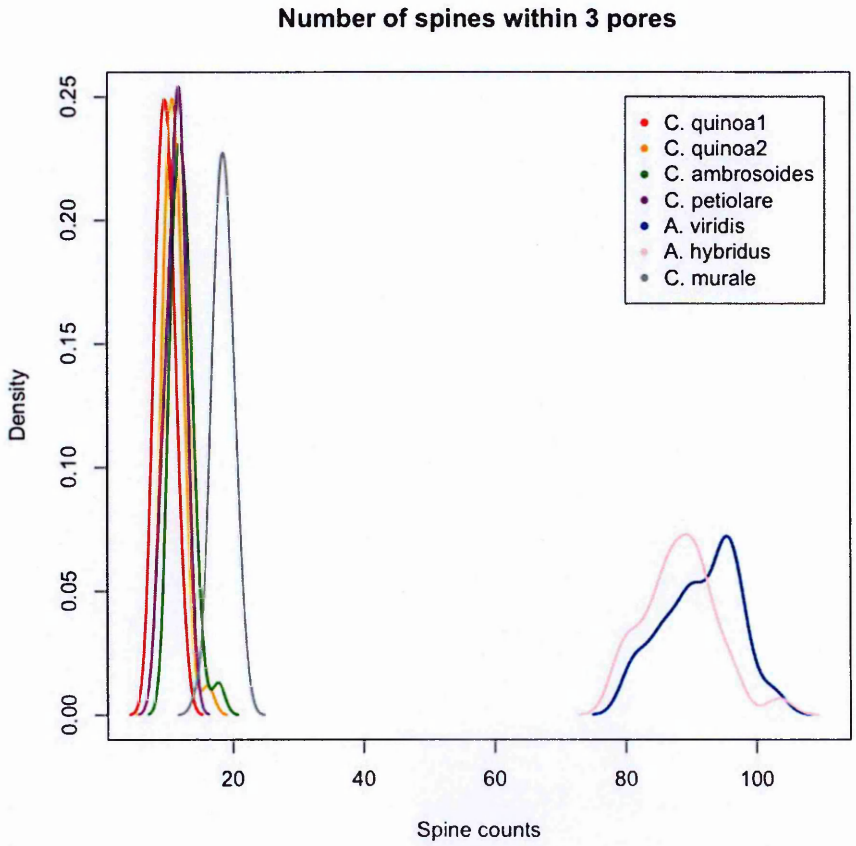

Fig. 6-7 Preliminary comparisons between species of Amaranthaceae: *Chenopodium quinoa, C. ambrosoides, C. petiolare, C. murale, Amaranthus viridis* and *A. hybridus*, depicted as probability density functions based on surface landmarks.

6.5.3) Differentiation between grassland and woodland charcoal particles using scanning electron microscope (SEM) images

Charcoal particles can be prepared and scanned with and SEM. Images can be used to differentiate charcoal particles derived from grasslands and woodlands. The preliminary results were shown in chapter 4. The differentiation of the charcoal particles should improve the interpretation of the charcoal proxy related to its ecological impact on the vegetation. For instance, charcoal derived from Miski and Huamanmarca could be use to infer the degree of fire influence over grasslands and forests.

6.6) Additional contributions

The following articles were published with my contribution during my registration as a part time Ph.D. student. Articles are listed in reverse chronological order summarizing my specific contribution. Author names underlined indicate PhD supervisors.

- M. B. Bush, A. M., Alfonso-Reynolds, D. Urrego, **B.G Valencia,** A. Correa-Metrio, M. Zimmermann, M. R. Silman (In review). Upslope expansion of degraded forest: our tropical Andean future. Journal of Biogeography.

Aim: Evaluate the treeline dynamics during the last 2000 years in the Eastern Andes

Results: Transitional areas between Puna and woodlands expanded. Sites that in the past were forested or covered in grasslands became transitional.

Main conclusion: The woodlands had the tendency to migrate upslope; however, fires and anthropogenic activities were continuously depressing the treeline.

Contribution: Laboratory techniques, data analysis, and data interpretation. I optimized the pollen processing protocol and taught pollen taxonomy to Alfonso-Reynolds whom counted most of the pollen samples. As additional samples were incorporated I re-run the procrustes rotation proposed by Alfonso-Reynolds and evaluated the performance of the test.

- Mosblech, N. A., M. B. Bush, W. D. Gosling, D. Hodell, L. Thomas, P. van Calsteren, A. Correa-Metrio, **B. G. Valencia**, J. Curtis, and R. van Woesik. 2012. North Atlantic forcing of Amazonian precipitation during the last ice age. Nature Geoscience **5**:817-820.

Aim: Determine the mechanisms forcing precipitation changes in the Amazon over the last 94 ka based on a $\delta^{18}O$ record from a speleothem.

Results: The North Atlantic Circulation influenced the precipitation changes prior 40 ka and after 17 ka. The precessional cycle was also registered in the oxygen record.

Main conclusion: The record suggests that the Amazon did not experience extreme droughts during the last 94 ka, but that moisture availability varied during this time.

Contribution: Speleothem collection, sampling, and data interpretation. I was actively involved in finding a collection site and collecting the speleothem specimens used in this study. I prepared and calibrated the equipment used for sampling (micro-drilling). I actively participated in the discussions related to data interpretation.

- Mosblech, N. A. S., A. Chepstow-Lusty, **B. G. Valencia**, and M. B. Bush. 2012. Anthropogenic control of late-Holocene landscapes in the Cuzco region, Peru. The Holocene **22**:1361-1372.

Aim: Determine if vegetation and crop cultivation shifts in the Cuzco region were the product of to climate change, human activities or both.
Results: Climate influenced the cultivation replacement of quinoa by maize. However the vegetation change observed after the cultivar shift was anthropogenic.
Main conclusion: Climate change favoured the cultivation of maize in the Cuzco region. The transition to maize cultivation was followed by the development and expansion of Andean cultures such as the Wari. Subsequently, as human population expanded the landscapes became transformed at regional scales inducing shift in the vegetation.
Contribution: I cored Lake Huaypo, prepared the core prior sampling, and helped with the pollen taxonomic identification. I provided multiproxy data derived from Lake Pacucha and helped with the ecological interpretation of the data.

References

Abbott, M. B., M. W. Binford, M. Brenner, and K. Kelts. 1997. A 3500 14C high-resolution record of water-level changes in Lake Titicaca, Bolivia/Peru. Quaternary Research **47**:169-180.

Abbott, M. B., B. B. Wolfe, A. P. Wolfe, G. O. Seltzer, R. Aravena, B. G. Mark, P. J. Polissar, D. T. Rodbell, H. D. Rowe, and M. Vuille. 2003. Holocene paleohydrology and glacial history of the central Andes using multiproxy lake sediment studies. Palaeogeography Palaeoclimatology Palaeoecology **194**:123-138.

Absy, M. L., A. Cleef, M. Fornier, M. Servant, A. Siffedine, M. F. da Silva, F. Soubies, K. Suguio, B. Turcq, and T. van der Hammen. 1991. Mise en evidence de quatre phases d'ouverture de la foret dense dans le sud-est de l'Amazonie au cours des 60 000 dernieres annees. Comptes Rendues Academie des Sciences. Paris **313**:673-678.

Aguirre, Z., L. P. Kvist, and O. Sánchez. 2006. Bosques secos en Ecuador y su diversidad. Pages 161-187 *in* M. M. R., B. Øllgaard, L. P. Kvist, F. Borchsenius, and H. Balslev, editors. Botánica Económica de los Andes Centrales. Universidad Mayor de San Andrés, La Paz.

Alcorn, J. B. 1993. Indigenous Peoples and Conservation. Conservation Biology **7**:424-426.

Aldenderfer, M. S. 2008. High Elevation Foraging Societies. Pages 131-143 *in* H. Silverman and W. H. Isbell, editors. The Handbook of South American Archaeology. Springer New York, New York.

Alley, R. B. 2000. The Younger Dryas cold interval as viewed from central Greenland. Quaternary Science Reviews **19**:213-226.

Anderson, E. P., J. Marengo, R. Villalba, S. Halloy, B. Young, D. Cordero, F. Gast, E. Jaimes, and D. Ruiz. 2011. Consequences of Climate Change for Ecosystems and Ecosystem Services in the Tropical Andes. Pages 1-18 *in* S. K. Herzog, R. Martínez, P. M. Jørgensen, and H. Tiessen, editors. Climate Change and Biodiversity in the Tropical Andes. Inter-American Institute for Global Change Research (IAI) and Scientific Committee on Problems of the Environment (SCOPE).

Armesto, J. J., D. Manuschevich, A. Mora, C. Smith-Ramirez, R. Rozzi, A. M. Abarzúa, and P. A. Marquet. 2010. From the Holocene to the Anthropocene: A historical framework for land cover change in southwestern South America in the past 15,000 years. Land Use Policy **27**:148-160.

Asbjornsen, H., N. Velázquez-Rosas, R. García-Soriano, and C. Gallardo-Hernández. 2005. Deep ground fires cause massive above- and below-ground biomass losses in tropical montane cloud forests in Oaxaca, Mexico. Journal of Tropical Ecology **21**:427-434.

Baddeley, A., and R. Turner. 2005. spatstat: An R package for analyzing spatial point patterns. Journal of Statistical Software **12**:1-42.

Bader, M. Y., I. v. Geloof, and M. Rietkerk. 2007. High solar radiation hinders tree regeneration above the alpine treeline in northern Ecuador. Plant Ecology **191**:33-45.

Bae, D.-H., I.-W. Jung, and D. P. Lettenmaier. 2011. Hydrologic uncertainties in climate change from IPCC AR4 GCM simulations of the Chungju Basin, Korea. Journal of Hydrology **401**:90-105.

Baker, P. A., S. C. Fritz, S. J. Burns, E. Ekdahl, and C. A. Rigsby. 2009. The Nature and Origin of Decadal to Millennial Scale Climate Variability in the Southern Tropics of South America: The Holocene Record of Lago Umayo, Peru. Pages 301-322 *in* F. Vimeux, F. Sylvestre, and M. Khodri, editors. Past Climate Variability in South America and Surrounding Regions. Springer Netherlands.

Baker, P. A., G. O. Seltzer, S. C. Fritz, R. B. Dunbar, M. J. Grove, P. M. Tapia, S. L. Cross, H. D. Rowe, and J. P. Broda. 2001. The history of South American tropical precipitation for the past 25,000 years. Science **291**:640-643.

Bakke, J., O. Lie, E. Heegaard, T. Dokken, G. H. Haug, H. H. Birks, P. Dulski, and T. Nilsen. 2009. Rapid oceanic and atmospheric changes during the Younger Dryas cold period. Nature Geosci **2**:1752-0894.

Barber, J., and B. Andersson. 1992. Too much of a good thing: light can be bad for photosynthesis. Trends in Biochemical Sciences **17**:61-66.

Barlow, J., et al. 2002. Effects of ground fires on understorey bird assemblages in Amazonian forests. Biological Conservation **105**:157-169.

Battarbee, R., V. Jones, R. Flower, N. Cameron, H. Bennion, L. Carvalho, and S. Juggins. 2001. Diatoms. Pages 155-202 *in* J. Smol, H. J. Birks, W. Last, R. Bradley, and K. Alverson, editors. Tracking Environmental Change Using Lake Sediments. Springer Netherlands.

Battarbee, R. W. 1986. Diatom analysis in:Handbook of Holocene Palaeoecology and Palaeohydrology. John Wiley & Sons, Chichester.

Bauer, B. S. 2004. Ancient cuzco heartland of the Inca. University of Texas Press, Austin TX.

Bauer, B. S., L. C. Kellett, M. Aráoz Silva, S. Hyland, and C. Socualaya Dávila. 2010. The Chanka : Archaeological research in Andahuaylas (Apurimac), Peru. Cotsen Institute of Archaeology Press, University of California, Los Angeles.

Bendix, J., R. Rollenbeck, and W. Palacios Cuenca. 2004. Cloud detection in the Tropics--a suitable tool for climate-ecological studies in the high mountains of Ecuador. International Journal of Remote Sensing **25**:4521-4540.

Bendix, J., R. Rollenbeck, M. Richter, P. Fabian, and P. Emck. 2008. Climate. Pages 63-73 *in* E. Beck, J. r. Bendix, I. Kottke, F. Makeschin, and R. Mosandl, editors. Gradients in a Tropical Mountain Ecosystem of Ecuador. Springer-Verlag, Berlin.

Bengtsson, L., and M. Enell. 1986. Chemical analysis. Pages 423-451 *in* B. E. Berglund, editor. Handbook of Holocene Palaeoecology and Palaeohydrology. John Wiley and Sons, Chichester.

Berger, A. 1992. Astronomical theory of paleoclimates and the last glacial-interglacial cycle. Quaternary Science Reviews **11**:571-581.

Betancourt, J. L., C. Latorre, J. A. Rech, J. Quade, and K. A. Rylander. 2000. A 22,000-year record of monsoonal precipitation from northern Chile's Atacama Desert. Science **289**:1542-1546.

Bigler, C., and R. Hall. 2002. Diatoms as indicators of climatic and limnological change in Swedish Lapland: a 100-lake calibration set and its validation for paleoecological reconstructions. Journal of Paleolimnology **27**:97-115.

Bigler, C., and R. I. Hall. 2003. Diatoms as quantitative indicators of July temperature: a validation attempt at century-scale with meteorological data from northern Sweden. Palaeogeography, Palaeoclimatology, Palaeoecology **189**:147-160.

Binford, M. W., A. L. Kolata, M. Brenner, J. Janusek, M. T. Seddon, M. B. Abbott, and J. H. Curtis. 1997. Climate variation and the rise and fall of an Andean civilization. Quaternary Research **47**: 235-248.

Biondini, M. E., P. W. M. Jr, and K. J. Berry. 1988. Data-Dependent Permutation Techniques for the Analysis of Ecological Data. Vegetatio **75**:161-168.

Bird, B. W., M. B. Abbott, D. T. Rodbell, and M. Vuille. 2011. Holocene tropical South American hydroclimate revealed from a decadally resolved lake sediment δ18O record. Earth and Planetary Science Letters **310**:192-202.

Birks, H. J. B., J. M. Line, S. Juggins, A. C. Stevenson, and C. J. F. T. Braak. 1990. Diatoms and pH Reconstruction. Philosophical Transactions of the Royal Society of London. B, Biological Sciences **327**:263-278.

Bitter, G. 1911. Revision der Gattung Polylepis. Botanische Jahrbücher für Systematik, Pflanzengeschichte und Pflanzengeographie **45**: 564-656

Bivand, R. S., E. J. Pebesma, and V. Gomez-Rubio. 2008. Applied spatial data analysis with R. Springer, NY.

Blaauw, M. 2010. Methods and code for 'classical' age-modelling of radiocarbon sequences. Quaternary Geochronology **5**:512-518.

Blandford, T. R., K. S. Humes, B. J. Harshburger, B. C. Moore, V. P. Walden, and H. Ye. 2008. Seasonal and Synoptic Variations in Near-Surface Air Temperature Lapse Rates in a Mountainous Basin. Journal of Applied Meteorology and Climatology **47**:249-261.

Bond, G., B. Kromer, J. Beer, R. Muscheler, M. N. Evans, W. Showers, S. Hoffmann, R. Lotti-Bond, I. Hajdas, and G. Bonani. 2001. Persistent Solar Influence on North Atlantic Climate During the Holocene. Science **294**:2130-2136.

Bookhagen, B. 2013. High resolution spatiotemporal distribution of rainfall seasonality and extreme events based on a 12-year TRMM time series. in review.

Bookhagen, B., and M. R. Strecker. 2008. Orographic barriers, high-resolution TRMM rainfall, and relief variations along the Eastern Andes. Geophys. Res. Lett. **35**:L06403.

Bookhagen, B., and M. R. Strecker. 2010. Modern Andean rainfall variation during ENSO cycles and its impact on the Amazon drainage basin. Pages 223-241 *in* C. Hoorn and F. Wesselingh, editors. Amazonia, Landscape and Species Evolution: A Look into the Past. Wiley-Blackwell, Chichester.

Bradley, R. S., M. Vuille, H. F. Diaz, and W. Vergara. 2006. Threats to Water Supplies in the Tropical Andes. Science **312**:1755-1756.

Brown, D. G. 1994. Predicting vegetation types at treeline using topography and biophysical disturbance variables. Journal of Vegetation Science **5**:641-656.

Brown, E. T., T. C. Johnson, C. A. Scholz, A. S. Cohen, and J. W. King. 2007. Abrupt change in tropical African climate linked to the bipolar seesaw over the past 55,000 years. Geophys. Res. Lett. **34**:L20702.

Brown, J. 1971. Mammals on Mountaintops: Nonequilibrium Insular Biogeography. The American Naturalist **105**:467-478.

Brunt, D. 1933. The adiabatic lapse-rate for dry and saturated air. Quarterly Journal of the Royal Meteorological Society **59**:351-360.

Bryan, A. L., and R. Gruhn. 2003. Some difficulties in modeling the original peopling of the Americas. Quaternary International **109-110**:175-179.

Bush, M. B., P. E. De Oliveira, P. A. Colinvaux, M. C. Miller, and E. Moreno. 2004a. Amazonian paleoecological histories: one hill, three watersheds. Palaeogeography Palaeoclimatology Palaeoecology **214**:359-393

Bush, M. B., J. A. Hanselman, and W. D. Gosling. 2010. Nonlinear climate change and Andean feedbacks: an imminent turning point? Global Change Biology **16**:3223-3232.

Bush, M. B., J. A. Hanselman, and H. Hooghiemstra. 2011. Andean montane forests and climate change. Pages 35-60 *in* M. Bush, J. Flenley, and W. Gosling, editors. Tropical Rainforest Responses to Climatic Change. Springer Berlin Heidelberg.

Bush, M. B., B. C. S. Hansen, D. T. Rodbell, G. O. Seltzer, K. R. Young, B. Leon, M. B. Abbott, M. R. Silman, and W. D. Gosling. 2005. A 17 000-year history of Andean climate and vegetation change from Laguna de Chochos, Peru. Journal of Quaternary Science **20** 703-714.

Bush, M. B., A. A. Manucci, D. H. Urrego, B. G. Valencia, A. Correa-Metrio, and M. R. Silman. *in rev.* Upslope expansion of degraded forests: Our Andean future. Journal of Biogeography.

Bush, M. B., and M. R. Silman. 2004. Observations on Late Pleistocene cooling and precipitation in the lowlands Neotropics. Journal of Quaternary Science **19**:677-684.

Bush, M. B., M. R. Silman, C. McMichael, and S. Saatchi. 2008. Fire, climate change, and biodiversity in Amazonia: A late-Holocene perspective. Philosophical Transactions of the Royal Society B **363**:1795-1802.

Bush, M. B., M. R. Silman, and D. H. Urrego. 2004b. 48,000 years of climate and forest change in a biodiversity hotspot. Science **303**:827-829.

Bush, M. B., and C. Weng. 2007. Introducing a new (freeware) tool for palynology. Journal of Biogeography **34**:377-380.

Buytaert, W., R. Célleri, B. De Bièvre, F. Cisneros, G. Wyseure, J. Deckers, and R. Hofstede. 2006. Human impact on the hydrology of the Andean páramos. Earth-Science Reviews **79**:53-72.

Carpenter, S., F. Westley, and M. Turner. 2005. Surrogates for Resilience of Social–Ecological Systems. Ecosystems **8**:941-944.

Chávez, K. L. M. 1980. The Archaeology of Marcavalle, an Early Horizon site in the Valley of Cusco. neue Folge **28**:203-239.

Chen, J., F. P. Brissette, and R. Leconte. 2011. Uncertainty of downscaling method in quantifying the impact of climate change on hydrology. Journal of Hydrology **401**:190-202.

Cheng, H., S. Ashish, F. W. Cruz, X. Wang, R. L. Edwards, F. M. d'Horta, C. C. Ribas, M. Vuille, D. S. Lowell, and A. S. Auler. 2013. Climate change patterns in Amazonia and biodiversity. Nature Communications **4**:1411-1411.

Chepstow-Lusty, A., M. R. Frogley, B. S. Bauer, M. B. Bush, and A. T. Herrera. 2003. A late Holocene record of arid events from the Cuzco region, Peru. Journal of Quaternary Science **18**:491-502.

Chepstow-Lusty, A., and M. Winfield. 2000. Inca agroforestry: Lessons from the past. Ambio **29**:322-328.

Chepstow-Lusty, A. J., K. D. Bennett, J. Fjeldsa, A. Kendall, W. Galiano, and A. Tupayachi Herrera. 1998. Tracing 4000 years of environmental history in the Cuzco area, Peru, from the pollen record. Mountain Research and Development **18**:159-172.

Chepstow-Lusty, A. J., K. D. Bennett, V. R. Switsur, and A. Kendall. 1996. 4000 years of human impact and vegetation change in the central Peruvian Andes - with events parallelling the Maya record? Antiquity **70**:824-833.

Chepstow-Lusty, A. J., M. B. Bush, M. R. Frogley, P. A. Baker, S. C. Fritz, and J. Aronson. 2005. Vegetation and climate change on the Bolivian Altiplano between 108,000 and 18,000 yr ago. Quaternary Research **63**:90-98.

Chepstow-Lusty, A. J., M. R. Frogley, B. S. Bauer, M. J. Leng, K. P. Boessenkool, C. Carcaillet, A. A. Ali, and A. Gioda. 2009. Putting the rise of the Inca Empire within a climatic and land management context. Climate of the Past Discussions **5**:771-796.

Chesser, R. T. 2004. Systematics evolution and biogeography of the South American ovenbird genus *Cinclodes*. The Auk **121**:752-766.

Choi, Y. D. 2004. Theories for ecological restoration in changing environment: Toward 'futuristic' restoration. Ecological Research **19**:75-81.

Cierjacks, A., J. E. Iglesias, K. Wesche, and I. Hensen. 2007a. Impact of sowing, canopy cover and litter on seedling dynamics of two *Polylepis* species at upper tree lines in central Ecuador. Journal of Tropical Ecology **23**:309-318.

Cierjacks, A., S. Salgado, K. Wesche, and I. Hensen. 2007b. Post-fire population dynamics of two tree species in high-altitude *Polylepis* forests of central Ecuador. Biotropica (Online early articles):1-7.

Clark, J. S. 1988. Particle motion and the theory of charcoal analysis: source area, transport, deposition, and sampling. Quaternary Research **30**:81-91.

Clark, J. S., and W. A. Patterson. 1997a. Background and Local Charcoal in Sediments: Scales of Fire Evidence in the Paleorecord. Pages 23-48 *in* J. S. Clark, H. Cachier, J. G. Goldammer, and B. Stocks, editors. Sediment Records of Biomass Burning and Global Change. Springer, Berlin.

Clark, J. S., and W. A. Patterson, III. 1997b. Background and local charcoal in sediments: Scales of fire evidence in the Paleorecord. Pages 23-48 *in* J. S. Clark, H. Cachier, J. G. Goldammer, and B. Stocks, editors. Sediment Records of Biomass Burning and Global Change. NATO ASI Series. Series 1: Global Environmental Change vol. 51. Springer, Berlin.

Clarke, K. R., and R. H. Green. 1988. Statistical design and analysis for a 'biological effects' study. Marine Ecology **46**:213-226.

Clements, F. E. 1936. Nature and structure of the climax. The Journal of Ecology **24**:252-284.

Cochrane, M. A. 2001. Synergistic Interactions between Habitat Fragmentation and Fire in Evergreen Tropical Forests.

Cochrane, M. A. 2003. Fire science for rainforests. Nature **421**:913-919.

Cochrane, M. A., A. Alencar, M. D. Schulze, C. M. Souza Jr., D. C. Nepstad, P. Lefebver, and E. A. Davidson. 1999. Positive feedbacks in the fire dynamic of closed canopy tropical forests. Science **284**:1832-1835.

Cochrane, M. A., and W. F. Laurance. 2002. Fire as a large-scale edge effect in Amazonian forests. Journal of Tropical Ecology **18**:311-325.

Cochrane, M. A., and K. C. Ryan. 2009. Fire and fire ecology: concepts and principles. Pages 25-62 *in* M. A. Cochrane, editor. Tropical Fire Ecology. Springer Berlin Heidelberg New York.

Colinvaux, P., P. E. de Olivera, and P. J. E. Moreno. 1999. Amazon Pollen Manual and Atlas. Harwood Academic Publishers, Amsterdam.

Colinvaux, P. A. 1968. Reconnaissance and Chemistry of the Lakes and Bogs of the Galapagos Islands. Nature **219**:590-594.

Colinvaux, P. A., M. B. Bush, M. Steinitz-Kannan, and M. C. Miller. 1997. Glacial and postglacial pollen records from the Ecuadorian Andes and Amazon. Quaternary Research **48**:69-78.

Condit, R., N. Pitman, E. G. Leigh, Jr., J. Chave, J. Terborgh, R. B. Foster, P. Nunez, S. Aguilar, R. Valencia, G. Villa, H. C. Muller-Landau, E. Losos, and S. P. Hubbell. 2002. Beta-Diversity in Tropical Forest Trees. Science **295**:666-669.

Connell, J. H. 1978. Diversity in Tropical Rain Forests and Coral Reefs. Science **199**:1302-1310.

Correa-Metrio, A., D. Urrego, K. Cabrera, and M. Bush. 2012. Package paleoMAS version 2.0-1. http://CRAN.R-project.org/package=paleoMAS.

Cox, P. M., R. A. Betts, C. D. Jones, S. A. Spall, and I. J. Totterdell. 2000. Acceleration of global warming due to carbon-cycling feedbacks in a coupled climate model. Nature **408**:184-187.

Cross, S. L., P. A. Baker, G. O. Seltzer, S. C. Fritz, and R. B. Dunbar. 2000a. A new estimate of the Holocene lowstand level of Lake Titicaca, central Andes, and implications for tropical palaeohydrology. The Holocene **10**:21-32.

Cross, S. L., P. A. Baker, G. O. Seltzer, S. C. Fritz, and R. B. Dunbar. 2000b. A new estimate of the Holocene lowstand level of Lake Titicaca, central Andes, and implications for tropical palaeohydrology. The Holocene **10**:21-32.

Cumming, G. S., G. Barnes, S. Perz, M. Schmink, K. E. Sieving, J. Southworth, M. Binford, R. D. Holt, C. Stickler, and T. Van Holt. 2005. An Exploratory Framework for the Empirical Measurement of Resilience. Ecosystems **8**:975-987.

Dawson, T. P., S. T. Jackson, J. I. House, I. C. Prentice, and G. M. Mace. 2011. Beyond Predictions: Biodiversity Conservation in a Changing Climate. Science **332**:53-58.

Dean, W. E. J. 1974. Determination of carbonate and organic matter in calcareous sediments and sedimentary rocks by loss on ignition: Comparison with other methods. J. Sed. Petrol. **44**:242–248.

deMenocal, P. B. 2001. Cultural Responses to Climate Change During the Late Holocene. Science **292**:667-673.

Denevan, W. M. 1992. The Pristine Myth - the Landscape of the America in 1492. Annals of the Association of American Geographers **82**:369-385.

Development-Core-Team, R. 2011. R: A Language and Environment for Statistical Computing. Vienna, Austria.

Di Pasquale, G., M. Marziano, S. Impagliazzo, C. Lubritto, A. De Natale, and M. Y. Bader. 2008. The Holocene treeline in the northern Andes (Ecuador): first evidence from soil charcoal. Palaeogeography, Palaeoclimatology, Palaeoecology **259**:17-34.

Dillehay, T. D. 1997. Monte Verde: A Late Pleistocene Settlement in Chile. Smithsonian Institution Press, Washington D.C.

Dillehay, T. D. 2008. Profiles in Pleistocene History. Pages 29-43 *in* H. Silverman and W. H. Isbell, editors. The Handbook of South American Archaeology. Springer New York, New York.

Dillehay, T. D., and M. Collins. 1988. Early cultural evidence from Monte Verde in Chile. Nature **332**:150-152.

Dillehay, T. D., H. H. Eling, and J. Rossen. 2005. Preceramic irrigation canals in the Peruvian Andes. Proceedings of the National Academy of Sciences of the United States of America **102**:17241-17244.

Dillehay, T. D., C. Ramírez, M. Pino, M. B. Collins, J. Rossen, and J. D. Pino-Navarro. 2008. Monte Verde: Seaweed, Food, Medicine, and the Peopling of South America. Science **320**:784-786.

Dillehay, T. D., J. Rossen, T. C. Andres, and D. E. Williams. 2007. Preceramic Adoption of Peanut, Squash, and Cotton in Northern Peru. Science **316**:1890-1893.

Edwards, M. E., L. B. Brubaker, A. V. Lozhkin, and P. M. Anderson. 2005. Structurally Novel Biomes: A Response to past Warming in Beringia. Ecology **86**:1696-1703.

Ekdahl, E. J., S. C. Fritz, P. A. Baker, C. A. Rigsby, and K. Coley. 2008. Holocene multidecadal- to millennial-scale hydrologic variability on the South American Altiplano. The Holocene **18**:867-876.

Elith, J., S. J. Phillips, T. Hastie, M. Dudík, Y. E. Chee, and C. J. Yates. 2011. A statistical explanation of MaxEnt for ecologists. Diversity and Distributions **17**:43-57.

Ellenberg, H. 1958. Wald oder Steppe? Die natürliche pflanzendecke der Anden Perus. Umschau **21, 22**:645-681.

Eva, H. D., A. S. Belward, E. E. De Miranda, C. M. Di Bella, V. Gond, O. Huber, S. Jones, M. Sgrenzaroli, and S. Fritz. 2004. A land cover map of South America. Global Change Biology **10**:731-744.

Faegri, K., and J. Iversen. 1989. Textbook of pollen analysis. 4th edition. Wiley, Chichester.

Fairbanks, R., R. Mortlock, T. Chiu, L. Cao, A. Kaplan, T. Guilderson, T. Fairbanks, A. Bloom, P. Grootes, and M. Nadeau. 2005. Radiocarbon calibration curve spanning 0 to 50,000 years BP based on paired 230Th/234U/238U and 14C dates on pristine corals. Quaternary Science Reviews **24**:1781-1796.

Feeley, K. J., and M. R. Silman. 2010. Land-use and climate change effects on population size and extinction risk of Andean plants. Global Change Biology **16**:3215-3222.

Feeley, K. J., M. R. Silman, M. B. Bush, W. Farfan, K. G. Cabrera, Y. Malhi, P. Meir, N. S. Revilla, M. N. R. Quisiyupanqui, and S. Saatchi. 2010. Upslope migration of Andean trees. Journal of Biogeography **38**:783-791.

Finlay, B. J., E. B. Monaghan, and S. C. Maberly. 2002. Hypothesis: The Rate and Scale of Dispersal of Freshwater Diatom Species is a Function of their Global Abundance. Protist **153**:261-273.

Fjeldså, J. 1992. Biogeographic patterns and evolution of the avifauna of relict high-altitude woodlands of the Andes. Streenstrupia **18**:9-62.

Fjeldså, J. 2002a. Key Areas for Conserving the Avifauna of Polylepis Forests. Ecotropica **8**:125-131.

Fjeldså, J. 2002b. *Polylepis* Forest – Vestiges of a Vanishing Ecosystem in the Andes. Ecotropica **8**:111-123.

Fjeldså, J., and M. Kessler. 1996. Conserving the biological diversity of Polylepis woodlands of the highland of Peru and Bolivia. A contribution to sustainable natural resource management in the Andes. NORDECO, Copenhagen, Denmark.

Fjeldså, J., E. Lambin, and B. Mertens. 1999. Correlation between endemism and local ecoclimatic stability documented by comparing andean bird distributions and remotely sensed land surface data. Ecography **22**:63-78.

Flower, R. J. 1986. The relationship between surface sediment diatom assemblages and pH in 33 Galloway lakes: Some regression models for reconstructing pH and their application to sediment cores. Hydrobiologia **143**:93-103.

Foster, P. 2001. The potential negative impacts of global climate change on tropical montane cloud forests. Earth-Science Reviews **55**:73-106.

Francus, P., H. Lamb, T. Nakagawa, M. Marshall, E. Brown, and S. P. Members. 2009. The potential of high-resolution X-ray fluorescence core scanning: Applications in paleolimnology. Pages news **17**:93-96.

Fritz, S. C., P. A. Baker, T. K. Lowenstein, G. O. Seltzer, C. A. Rigsby, G. S. Dwyer, P. M. Tapia, K. K. Arnold, T. L. Ku, and S. Luo. 2004. Hydrological variation during the last 170,000 years in the southern hemisphere tropics of South America. Quaternary Research **61**:95-104.

Fritz, S. C., P. A. Baker, G. O. Seltzer, A. Ballantyne, P. Tapia, H. Cheng, and R. L. Edwards. 2007. Quaternary glaciation and hydrologic variation in the South American tropics as reconstructed from the Lake Titicaca drilling project. Quaternary Research:410-420.

Fritz, S. C., S. Juggins, R. W. Battarbee, and D. R. Engstrom. 1991. Reconstruction of past changes in salinity and climate using a diatom-based transfer function. Nature **352**:706-708.

Gareca, E. E., M. Hermy, J. Fjeldså, and O. Honnay. 2010. *Polylepis* woodland remnants as biodiversity islands in the Bolivian high Andes. Biodiversity and Conservation **19**:3327-3346.

Garreaud, R., M. Vuille, and A. C. Clement. 2003. The climate of the Altiplano: observed current conditions and mechanisms of past changes. Palaeogeography, Palaeoclimatology, Palaeoecology **194**:5-22.

Garreaud, R. D., and P. Aceituno. 2001. Interannual rainfall variability over the South American Altiplano. Journal of Climate **14**:2779-2789.

Gauch, J. H. G. 1982. Multivariate Analysis in Community Ecology. Cambridge University Press, Cambridge.

Gentry, A. H. 1988. Changes in plant community diversity and floristic composition on environmental and geographical gradients. Annals of the Missouri Botanical Garden **75**:1-34.

Gillson, L., and R. Marchant. 2014. From myopia to clarity: sharpening the focus of ecosystem management through the lens of palaeoecology. Trends in Ecology & Evolution **29**:317-325.

Girardin, C. A. J., Y. Malhi, L. E. O. C. AragÃO, M. Mamani, W. Huaraca Huasco, L. Durand, K. J. Feeley, J. Rapp, J. E. Silva-Espejo, M. Silman, N. Salinas, and R. J. Whittaker. 2010. Net primary productivity allocation and cycling of carbon along a tropical forest elevational transect in the Peruvian Andes. Global Change Biology **16**:3176-3192.

Gleason, H. A. 1926. The Individualistic Concept of the Plant Association. Bulletin of the Torrey Botanical Club **53**:7-26.

Gosling, W. D., M. B. Bush, J. A. Hanselman, and A. Chepstow-Lusty. 2008. Glacial-interglacial changes in moisture balance and the impact on vegetation in the southern hemisphere tropical Andes (Bolivia/Peru). Palaeogeography, Palaeoclimatology, Palaeoecology **259**:35-50.

Gosling, W. D., J. A. Hanselman, C. Knox, B. G. Valencia, and M. B. Bush. 2009. Long-term drivers of change in *Polylepis* woodland distribution in the Central Andes. Journal of Vegetation Science **20**:1041-1052.

Gosling, W. D., and J. J. Williams. 2013. Ecosystem service provision sets the pace for pre-Hispanic societal development in the central Andes. The Holocene **23**:1619-1624.

Graf, K. 1981. Palynological investigations of two post-glacial peat bogs near the boundary of Bolivia and Peru. Journal of Biogeography **8**:353-368.

Groot, M. H. M., R. G. Bogotá, L. J. Lourens, H. Hooghiemstra, M. Vriend, J. C. Berrio, E. Tuenter, J. Van der Plicht, B. Van Geel, M. Ziegler, S. L. Weber, A. Betancourt, L. Contreras, S. Gaviria, C. Giraldo, N. González, J. H. F. Jansen, M. Konert, D. Ortega, O. Rangel, G. Sarmiento, J. Vandenberghe, T. Van der Hammen, M. Van der Linden, and W. Westerhoff. 2011. Ultra-high resolution pollen record from the northern Andes reveals rapid shifts in montane climates within the last two glacial cycles. Climate of the Past **7**:299-316.

Grossman, J. 1972. Early ceramic cultures of Andahuaylas, Apurimac, Perú. University of California, Berkeley.

Halladay, K., Y. Malhi, and M. New. 2012. Cloud frequency climatology at the Andes/Amazon transition: 1. Seasonal and diurnal cycles. Journal of Geophysical Research: Atmospheres **117**:D23102.

Hannah, L., G. F. Midgley, and D. Millar. 2002. Climate change-integrated conservation strategies. Global Ecology and Biogeography **11**:485-495.

Hannah, L., and L. A. Hansen. 2005. Designing Landscapes and Seascapes for Change. Pages 329-341 *in* L. Thomas and L. Hannah, editors. Climate Change and Biodiversity. Yale University Press, New Haven & London.

Hanselman, J. A., M. B. Bush, W. D. Gosling, A. Collins, C. Knox, P. A. Baker, and S. C. Fritz. 2011a. A 370,000-year record of vegetation and fire history around Lake Titicaca (Bolivia/Peru). Palaeogeography, Palaeoclimatology, Palaeoecology **In Press,**.

Hanselman, J. A., M. B. Bush, W. D. Gosling, A. Collins, C. Knox, P. A. Baker, and S. C. Fritz. 2011b. A 370,000-year record of vegetation and fire history around Lake Titicaca (Bolivia/Peru). Palaeogeography, Palaeoclimatology, Palaeoecology **305**:201-214.

Hansen, B. C., D. T. Rodbell, G. O. Seltzer, B. León, K. R. Young, and M. Abbott. 2003. Late-Glacial and Holocene vegetational history from two sites in the Western Cordillera of southwestern Ecuador. Palaeogeography, Palaeoclimatology, Paleoecology **194**:79-108.

Hansen, B. C. S., and D. T. Rodbell. 1995. A late-Glacial/Holocene pollen record from the Eastern Andes of northern Peru. Quaternary Research **44**:216-227.

Hansen, B. C. S., H. E. Wright, Jr. , and J. P. Bradbury. 1984. Pollen studies in the Junín area, Central Peruvian Andes. *Geological Society of America Bulletin*:1454-1465.

Hastorf, C. A. 2008. The Formative Period in the Titicaca Basin. Pages 545-561 *in* H. Silverman and W. H. Isbell, editors. The Handbook of South American Archaeology. Springer New York, New York.

Hastorf, C. A., W. T. Whitehead, and S. Johannessen. 2005. Late Prehistoric Wood Use in an Andean Intermontane Valley. Economic Botany **59**:337-355.

Haug, G. H., D. Gunther, L. C. Peterson, D. M. Sigman, K. A. Hughen, and B. Aeschlimann. 2003. Climate and the collapse of Maya civilization. Science **299**:1731-1735.

Haug, G. H., K. A. Hughen, D. M. Sigman, L. C. Peterson, and U. Rohl. 2001. Southward Migration of the Intertropical Convergence Zone Through the Holocene. Science **293**:1304-1308.

Haylock, M. R., T. C. Peterson, L. M. Alves, T. Ambrizzi, Y. M. T. Anunciacao, J. Baez, V. R. Barros, M. A. Berlato, M. Bidegain, G. Coronel, V. Corradi, V. J. Garcia, A. M. Grimm, D. Karoly, J. A. Marengo, M. B. Marino, D. F. Moncunill, D. Nechet, J. Quintana, E. Rebello, M. Rusticucci, J. L. Santos, I. Trebejo, and L. A. Vincent. 2006. Trends in Total and Extreme South American Rainfall in 1960-2000 and Links with Sea Surface Temperature. Journal of Climate **19**:1490-1512.

Haynes, C. V. 1997. Dating a Paleoindian Site in the Amazon in Comparison with Clovis Cuture. Science **275**:1948-1952.

Hays, J. D., J. Imbrie, and N. J. Shackleton. 1976. Variations in the Earth's Orbit: Pacemaker of the Ice Ages. Science **194**:1121-1132.

Heiri, O., A. F. Lotter, and G. Lemcke. 2001. Loss on ignition as a method for estimating organic and carbonate content in sediments: reproducibility and comparability of results. Journal of Paleolimnology **25**:101–110.

Hensen, I. 2002. Impacts of anthropogenic activity on the vegetation of *Polylepis* woodlands in the region of Cochabamba, Bolivia. Ecotropica **8**:183-203.

Herzog, S. K., J. C. M., J. Fjeldsa, M. Kessler, E. Yensen, T. Tarifa, J. Capriles, E. F. Terrazas, I. Hensen, P. L. Ibisch, Ingrid Loayza, D. Renison, E. Dellacassa, E. F. Bedregal, A. M. Cingolani, D. Lorenzo, E. Matthysen, D. Schinner, R. S. A., A. T. J., B. Stahl, and A. Vilaseca. 2002. Ecology and Conservation of High-Andean Polylepis Forest. Ecotropica **8**:93-95.

Hijmans, R. J., S. E. Cameron, J. L. Parra, P. G. Jones, and A. Jarvis. 2005. Very high resolution interpolated climate surfaces for global land areas. International Journal of Climatology **25**:1965-1978.

Hildebrandt, A., and E. A. B. Eltahir. 2008. Using a horizontal precipitation model to investigate the role of turbulent cloud deposition in survival of a seasonal cloud forest in Dhofar. Journal of Geophysical Research: Biogeosciences **113**:G04028.

Hill, M. O. 1979. DECORANA - A FORTRAN program for detrended correspondence analysis and reciprocal averaging. Ecology and Systematics. Cornell University, New York.

Hillyer, R., B. G. Valencia, M. B. Bush, M. R. Silman, and M. Steinitz-Kannan. 2009. A 24,700-yr paleolimnological history from the Peruvian Andes. Quaternary Research **71**:71-82.

Hobbs, R. J., and V. A. Cramer. 2008. Restoration Ecology: Interventionist Approaches for Restoring and Maintaining Ecosystem Function in the Face of Rapid Environmental Change. Annual Review of Environment and Resources **33**:39-61.

Hoch, G., and C. Körner. 2005. Growth, demography and carbon relations of Polylepis trees at the world's highest treeline. Functional Ecology **19**:941-951.

Hodell, D. A., F. S. Anselmetti, D. Ariztegui, M. Brenner, J. H. Curtis, A. Gilli, D. A. Grzesik, T. J. Guilderson, A. D. Müller, M. B. Bush, A. Correa-Metrio, J. Escobar, and S. Kutterolf. 2008. An 85-ka record of climate change in lowland Central America. Quaternary Science Reviews **27**:1152-1165.

Hodell , D. A., J. H. Curtis, and M. Brenner. 1995. Possible role of climate in the collapse of ancient Maya civilization. Nature **357**:391-394.

Hoffmann, D., I. Oetting, C. A. Arnillas, and R. Ulloa. 2011. Climate Change and Protected Areas in the Tropical Andes. Pages 311-325 *in* S. K. Herzog, R. Martínez, P. M. Jørgensen, and H. Tiessen, editors. Climate Change and Biodiversity in the Tropical Andes. Inter-American Institute for Global Change Research (IAI) and Scientific Committee on Problems of the Environment (SCOPE).

Hole, D. G., K. R. Young, A. Seimon, C. G. Wichtendahl, D. Hoffmann, K. S. Paez, S. Sanchez, D. Muchoney, H. R. Grau, and E. Ramirez. 2011. Adaptive Management for Biodiversity Conservation under Climate Change – a Tropical Andean Perspective.*in* S. K. Herzog, R. Martínez, P. M. Jørgensen, and H. Tiessen, editors. Climate Change and Biodiversity in the Tropical Andes. Inter-American Institute for Global Change Research (IAI) and Scientific Committee on Problems of the Environment (SCOPE).

Holling, C. S. 1973. Resilience and Stability of Ecological Systems. Annual Review of Ecology and Systematics **4**:1-23.

Holtmeier, F.-K., and G. Broll. 2005. Sensitivity and response of northern hemisphere altitudinal and polar treelines to environmental change at landscape and local scales. Global Ecology and Biogeography **14**:395-410.

Hooghiemstra, H. 1984. Vegetational and climatic history of the high plain of Bogota, Colombia: A continuous record of the last 3.5 million Years. Gantner Verlag, Vaduz.

Hooghiemstra, H. 1989. Quaternary and upper-Pliocene glaciations and forest development in the tropical Andes: Evidence from a long high-resolution pollen

record from the sedimentary basin of Bogota, Colombia. Palaeogeography, Palaeoclimatology, Palaeoecology:11-26.

Hooghiemstra, H., and T. van der Hammen. 1993. Late quaternary vegetation history and paleoecology of Laguna Pedro Palo (subandean forest belt, Eastern Cordillera, Colombia). Review of Palaeobotany and Palynology **77**:235-262.

Horn, S. P., and M. Kappelle. 2009. Fire in the páramo ecosystems of Central and South America. Pages 505-539 *in* M. A. Cochrane, editor. Tropical Fire Ecology. Springer Berlin Heidelberg.

Hubbell, S. P. 2001. The unified neutral theory of biodiversity and biogeography. Princeton University Press, Princeton.

Hughes, C., and R. Eastwood. 2006. Island radiation on a continental scale: exceptional rates of plant diversification after uplift of the Andes. PNAS **103**:10334-10339.

Hutchinson, G. E. 1941. Ecological aspects of succession in natural populations. The American Naturalist
75:406-418.

Hutchinson, G. E. 1961. The paradox of the Plankton. The American Naturalist **95**:137-145.

Imbrie, J. D., J. Hays, D. G. Martinson, A. McIntyre, A. Mix, J. J. Morley, N. G. Pisias, W. L. Prell, and N. J. Shackleton. 1984. The orbital theory of Pleistocene climate: support from a revised chronology of the marine ^{18}O record. Pages 269-305. *in* A. L. Berger, J. Imbrie, J. Hays, G. Kukla, and B. Saltzman, editors. Milankovitch and Climate. Reidel, Dordrecht, Netherlands.

INGEMMET. 2013. http://www.ingemmet.gob.pe. Accessed on December 2013.

IPCC, I. P. o. C. C. 2013. Climate Change 2013. The Physical Science Basis.

Isbell, W. H. 2008. Wari and Tiwanaku: International Identities in the Central Andean Middle Horizon. Pages 731-759 *in* H. Silverman and W. H. Isbell, editors. The Handbook of South American Archaeology. Springer New York, New York.

Jackson, J. B. C. 2001. What was natural in the coastal oceans? Proceedings of the National Academy of Sciences **98**:5411-5418.

Jackson, J. B. C., M. X. Kirby, W. H. Berger, K. A. Bjorndal, L. W. Botsford, B. J. Bourque, R. H. Bradbury, R. Cooke, J. Erlandson, J. A. Estes, T. P. Hughes, S. Kidwell, C. B. Lange, H. S. Lenihan, J. M. Pandolfi, C. H. Peterson, R. S. Steneck, M. J. Tegner, and R. R. Warner. 2001. Historical Overfishing and the Recent Collapse of Coastal Ecosystems. Science **293**:629-637.

Jones, V., and H. J. B. Birks. 2004. Lake-Sediment Records of Recent Environmental Change on Svalbard: Results of Diatom Analysis. Journal of Paleolimnology **31**:445-466.

Jordan, C. F. 1985. Soils of the Amazon rainforest. Pages 83-94 *in* G. T. Prance and T. E. L. eds., editors. Amazonia. Key Environments Series. Pergamon Press, Oxford.

Jordan, E. 1983. Die Verbreitung von Polylepis-Beständen in der Westkordillere Boliviens. Tuexenia **3**:101-112.

Josse, C., F. Cuesta, G. Navarro, V. Barrena, E. Cabrera, E. Chacón-Moreno, W. Ferreira, M. Peralvo, J. Saito, and A. Tovar. 2009. Ecosistemas de los Andes del Norte y Centro. Bolivia, Colombia, Ecuador, Perú y Venezuela. Secretaría General de la Comunidad Andina, Programa Regional ECOBONA-Intercooperation, CONDESAN-Proyecto Páramo Andino, Programa BioAndes,

EcoCiencia, NatureServe, IAvH, LTA-UNALM, ICAE-ULA, CDC-UNALM, RUMBOL SRL, Lima.

Juggins, S. 1991. C2 data analysis.

Juggins, S. 2012. rioja: Analysis of Quaternary Science Data. R package version (0.7-3).

Juggins, S. 2013. Quantitative reconstructions in palaeolimnology: new paradigm or sick science? Quaternary Science Reviews **64**:20-32.

Kerr, M. S. 2004. A phylogenetic and biogeographic analysis of Sanguisorbeae (Rosaceae), with emphasis on the Pleistocene radiation of the high Andean genus Polylepis. Dissertation. University of Maryland (College Park, Md.), Maryland

Kessler, M. 1995. Present and potential distribution of Polylepis (Rosaceae) forests in Bolivia. Pages 281-294 *in* S. P. Churchill, H. Balslev, E. Forero, and J. L. Luteyn, editors. Biodiversity and conservation of neotropical montane forests. New York Botanical Garden, New York.

Kessler, M. 2000. Elevational Gradients in Species Richness and Endemism of Selected Plant Groups in the Central Bolivian Andes. Plant Ecology **149**:181-193.

Kessler, M. 2002. The "*Polylepis* problem": Where do we stand? Ecotropica **8**:97-110.

Kessler, M. 2006. Bosques de *Polylepis*. Pages 110-120 *in* M. M. R, B. Øllgaard, L. P. Kvist, F. Borchsenius, and H. Balslev, editors. Botánica Económica de los Andes Centrales. Universidad Mayor de San Andrés, La Paz.

Kessler, M., J.-A. Grytnes, S. R. P. Halloy, J. Kluge, T. Krömer, B. León, M. J. Macía, and K. R. Young. 2011. Gradients of plant diversity: local patterns and processes. Pages 204-218 *in* S. K. Herzog, R. Martínez, P. M. Joergensen, and H. Tiessen, editors. Climate change effects on the biodiversity of the tropical Andes: an assessment of the status of scientific knowledge. Inter-American Institute of Global Change Research (IAI) and Scientific Committee on Problems of the Environment (SCOPE), São José dos Campos, Brazil, and Paris, France.

Kessler, M., S. K. Herzog, J. Fjeldsa, and K. Bach. 2001. Species richness and endemism of plant and bird communities along two gradients of elevation, humidity and land use in the Bolivian Andes. Diversity & Distributions **7**:61-77.

Kessler, M., and A. N. Schmidt-Lebuhn. 2005. Taxonomical and distributional notes on *Polylepis* (Rosaceae). Organisms Diversity & Evolution **13**:1-10.

Kilharn, S. S., E. C. Theriot, and S. C. Fritz. 1996. Linking planktonic diatoms and climate change in the large lakes of the

Yellowstone ecosystem using resource theory. Limnological Oceanography **41**:1052-1062

Killeen , T. J., M. Douglas, T. Consiglio, P. M. Jørgensen, and John Mejia. 2007. Dry spots and wet spots in the Andean hotspot. Journal of Biogeography **34**:1357-1373.

Kimura, M., and J. F. Crow. 1964. The Number of Alleles That Can Be Maintained in a Finite Population. Genetics **49**:725-738.

Kolkwitz, R. M. M. 1908. Ökologie der pflanzlichen Saprobien. Borntraeger, Berlin.

Körner, C. 2003. Alpine Plant Life: Functional Plant Ecology of High Mountain Ecosystems. Springer, Verlag.

Lange-Bertalot, H. 2000. Diatomeen der Anden / Diatoms of the Andes. y A.R.G. Gantner Verlag, Koeltz Scientific Books, Königstein, Germany.

Lange-Bertalot, H., and D. Metzeltin. 1996. Indicators of Oligotrophy. y A.R.G. Gantner Verlag, Koeltz Scientific Books, Königstein, Germany.

Lange-Bertalot, H., and D. Metzeltin. 1998. Diversity, Taxonomy and Geobotany. y A.R.G. Gantner Verlag, Koeltz Scientific Books, Königstein, Germany.

Larsen, T. H., G. Brehm, H. Navarrete, P. Franco, H. Gomez, J. L. Mena, V. Morales, J. Argollo, L. Blacutt, and V. Canhos. 2011. Range shifts and extinctions driven by climate change in the Tropical Andes: synthesis and directions. Pages 47-64 *in* S. K. Herzog, R. Martínez, P. M. Jørgensen, and H. Tiessen, editors. Climate Change and Biodiversity in the Tropical Andes. Inter-American Institute for Global Change Research (IAI) and Scientific Committee on Problems of the Environment (SCOPE).

Lauer, W. 1981. Ecoclimatological Conditions of the Paramo Belt in the Tropical High Mountains. Mountain Research and Development **1**:209-221.

Laurance, W. F. 2004. Forest-climate interactions in fragmented tropical landscapes. Philosophical Transactions of the Royal Society B **359**:345-352.

Laurance, W. F., D. Perez-Salicrup, P. Delamonica, P. M. Fearnside, S. D. D'Angelo, A. Jerozolinski, L. Pohl, and T. E. Loverjoy. 2001. Rainforest fragmentation and the structure of Amazonian liana communities. Ecology **82**:105-116.

Lavallée, D. 1987. Telarmachay: Chasseurs et Pasteurs Préhistoriques de Andes I. Institut Francais d'Etudes Andines, Paris.

Ledru, M.-P., V. Jomelli, L. Bremond, T. Ortuño, P. Cruz, I. Bentaleb, F. Sylvestre, A. Kuentz, S. Beck, C. Martin, C. Paillès, and S. Subitani. 2013. Evidence of moist niches in the Bolivian Andes during the mid-Holocene arid period. The Holocene.

Lenters, J. D., and K. H. Cook. 1997. On the Origin of the Bolivian High and Related Circulation Features of the South American Climate. Journal of the Atmospheric Sciences **54**:656-677.

Leuschner, C., A. Zach, G. Moser, J. Homeier, S. Graefe, D. Hertel, B. Wittich, N. Soethe, S. Iost, M. Röderstein, V. Horna, and K. Wolf. 2013. The Carbon Balance of Tropical Mountain Forests Along an Altitudinal Transect. Pages 117-139 *in* J. r. Bendix, E. Beck, A. B. u. F. Makeschin, R. M. S. Scheu, and W. Wilcke, editors. Ecosystem Services, Biodiversity and Environmental Change in a Tropical Mountain Ecosystem of South Ecuador, . Springer-Verlag Berlin Heidelberg

Levins, R. 1969. Some Demographic and Genetic Consequences of Environmental Heterogeneity for Biological Control. Bulletin of the ESA **15**:237-240.

Luzar, J. 2007. The Political Ecology of a "Forest Transition": Eucalyptus forestry in the Southern Peruvian Andes. Ethnobotany Research & Applications **5**:77-84.

Lynch, T. 1980. Guitarrero Cave: Early man in the high Andes. Academic Press, New York.

Lynch, T. F. 1985. Chronology of Guitarrero Cave, Peru. Science **229**:864-867.

MacNeish, R. S., R. K. Vierra, A. Nelken-Turner, R. Lurie, and A. G. Cook. 1983. Prehistory of the Ayacucho Basin, Peru. University of Michigan.

Malcolm, J. R., C. Liu, R. P. Neilson, L. Hansen, and L. E. E. Hannah. 2006. Global warming and extinctions of endemic species from biodiversity hotspots. Conservation Biology **20**:538-548.

Marengo, J., J. Tomasella, W. Soares, L. Alves, and C. Nobre. 2012. Extreme climatic events in the Amazon basin. Theoretical and Applied Climatology **107**:73-85.

Marengo, J. A., C. A. Nobre, G. Sampaio, L. F. Salazar, and L. S. Borma. 2011. Climate change in the Amazon Basin: Tipping points, changes in extremes, and impacts on natural and human systems. Pages 259-283 *in* M. Bush, J. Flenley, and W. Gosling, editors. Tropical Rainforest Responses to Climatic Change. Springer Berlin Heidelberg.

Marengo, J. A., C. A. Nobre, J. Tomasella, M. F. Cardoso, and M. D. Oyama. 2008a. Hydro-climatic and ecological behaviour of the drought of Amazonia in 2005. Philos Trans R Soc Lond B Biol Sci **363**.

Marengo, J. A., C. A. Nobre, J. Tomasella, M. D. Oyama, G. Sampaio de Oliveira, R. de Oliveira, H. Camargo, L. M. Alves, and I. F. Brown. 2008b. The Drought of Amazonia in 2005. Journal of Climate **21**:495-516.

Marengo, J. A., W. R. Soares, C. Saulo, and M. Nicolini. 2004. Climatology of the Low-Level Jet East of the Andes as Derived from the NCEP‚ÄìNCAR Reanalyses: Characteristics and Temporal Variability. Journal of Climate **17**:2261-2280.

Markgraf, V. 1978. Pollen and spores of Argentina. University of Arizona, Tucson.

Markgraf, V., T. R. Baumgartner, J. P. Bradbury, H. F. Diaz, R. B. Dunbar, B. Luckman, G. Seltzer, T. W. Swetnam, and R. Villalba. 2000. Paleoclimate Reconstruction along the Pole-Equator-Pole Transect of the Americas. Quaternary Science Reviews **19**:125-140.

Mayle, F., R. Burbridge, and T. Killeen. 2000. Millennial-scale dynamics of southern Amazonian rain forests. Science **290**:2291.

Mayle, F. E., and M. J. Power. 2008. Impact of a drier Early-Mid-Holocene climate upon Amazonian forests. Philosophical Transactions of the Royal Society B.

McCune, B., and M. J. Mefford. 2002. Analysis of Ecological Communities. MjM Software, , Gleneden Beach, OR.

Meltzer, D. J., D. K. Grayson, G. Ardila, A. B. Barker, D. F. Dincauze, C. V. Haynes, F. Mena, L. Nuñez, and D. Stanford. 1997. On the Pleistocene antiquity of Monte Verde southern Chile. American Antiquity **64**:659-663.

Mielke, P. W. 1984. Meteorological applications of permutation techniques based on distance functions, North-Holland, Amsterdam.

Mielke, P. W., and K. J. Berry. 2001. Permutation Methods: A Distance Function Approach. Springer.

Mielke, P. W., Jr. 1991. The application of multivariate permutation methods based on distance functions in the earth sciences. Earth-Science Reviews **31**:55-71.

Miller, G. H., J. W. Magee, B. J. Johnson, M. L. Fogel, N. A. Spooner, M. T. McCulloch, and L. K. Ayliffe. 1999. Pleistocene Extinction of Genyornis newtoni: Human Impact on Australian Megafauna. Science **283**:205-208.

Minchin, R. 1987. An evaluation of the relative robustness of techniques for ecological ordination. Vegetatio **69**:89-107.

Mittermeier, R. A., N. Myers, J. B. Thomsen, G. A. B. daFonseca, and S. Olivieri. 1998. Biodiversity Hotspots and Major Tropical Wilderness Areas: Approaches to Setting Conservation Priorities. Conservation Biology **12**:516–520.

Moon, K., and C. Cocklin. 2011. A Landholder-Based Approach to the Design of Private-Land Conservation Programs. Un Método Basado en Propietarios para

el Diseño de Programas de Conservación en Terrenos Privados. Conservation Biology **25**:493-503.

Moore, P. D., J. A. Webb, and M. E. Collinson. 1991. Pollen analysis. 2nd edition. Blackwell Scientific, Oxford.

Morales, M. S., R. Villalba, H. R. Grau, and L. Paolini. 2004. Rainfall-Controlled Tree Growth in High-Elevation Subtropical Treelines. Ecology **85**:3080-3089.

Mosblech, N. A. S., A. Chepstow-Lusty, B. G. Valencia, and M. B. Bush. 2012. Anthropogenic control of late-Holocene landscapes in the Cuzco region, Peru. The Holocene **22**:1361-1372.

Mourguiart, P., and M. P. Ledru. 2003. Last Glacial Maximum in an Andean cloud forest environment (Eastern Cordillera, Bolivia). Geology **31**:195-198.

Moy, C. M., G. O. Seltzer, D. T. Rodbell, and D. M. Anderson. 2002. Variability of El Nino/Southern Oscillation activity at millennial timescales during the Holocene epoch. Nature **420**:162-165.

Mueller-Dombois, D., and H. Ellenberg. 1974. Aims and Methods of Vegetation Ecology. John Wiley & sons, New York, London.

Murdock, K. J., K. Wilkie, and L. L. Brown. 2013. Rock magnetic properties, magnetic susceptibility, and òrganic geochemistry comparison in core LZ1029-7 Lake El'gygytgyn, Russia Far East. Clim. Past **9**:467-479.

Myers, N. 1988. Threatened biotas: "Hot spots" in tropical forests. The Environmentalist **8**:1-20.

Myers, N., R. A. Mittermeier, C. G. Mittermeier, G. A. B. da Fonseca, and J. Kent. 2000. Biodiversity hotspots for conservation priorities. Nature **403**:853-858.

Nakagawa, T. 2007. Double - L channel: an amazingly non - destructive method of continuous sub - sampling from sediment cores. Quaternary International **167-168**:3-486.

Navarro, G., J. A. Molina, and N. D. l. Barra. 2005. Classification of the high-Andean Polylepis forests in Bolivia. Plant Ecology **176**:113-130.

Nepstad, D., P. Lefebver, U. L. D. Silva, J. Tomasella, P. Schlesinger, L. Solorzano, P. Moutinho, D. Ray, and J. G. Benito. 2004a. Amazon drought and its implications for forest flammability and tree growth: a basin-wide analysis. Global Change Biology **10**:704-717.

Nepstad, D., P. Lefebvre, U. L. D. Silva, J. Tomasella, P. Schlesinger, L. Solórzano, P. Moutinhow, D. Ray, and J. G. Benito. 2004b. Amazon Drought and its Implications for Forest Flammability and Tree Growth: A Basin-Wide Analysis. Global Change Biology **10**:704-717.

Niemann, H., and H. Behling. 2008. Late Quaternary vegetation, climate and fire dynamics inferred from the El Tiro record in the southeastern Ecuadorian Andes. Journal of Quaternary Science **23**:203-212.

Núñez, L., M. Grosjean, and I. Cartajena. 2002. Human occupations and climate change in the Puna de Atacama, Chile. Science **298**:821-824.

Oksanen, J., F. G. Blanchet, R. Kindt, P. Legendre, R. B. O'Hara, Gavin L. Simpson, P. Solymos, M. Henry, H. Stevens, and H. Wagner. 2010. vegan: CommunityEcology Package. R package version 1.17-4.

Oliveras, I., Y. Malhi, V. H. Norma Salinas, E. Urquiaga-Flores, J. K.-. Mamani, J. A. Quintano-Loaiza, I. Cuba-Torres, N. Lizarraga-Morales, and R.-M. Román-

Cuesta. 2013. Changes in forest structure and composition after fire in tropical montane cloud forests near the Andean treeline. Plant Ecology & Diversity.

Orme, C. D. L., R. G. Davies, M. Burgess, F. Eigenbrod, N. Pickup, V. A. Olson, A. J. Webster, T.-S. Ding, P. C. Rasmussen, R. S. Ridgely, A. J. Stattersfield, P. M. Bennett, T. M. Blackburn, K. J. Gaston, and I. P. F. Owens. 2005. Global hotspots of species richness are not congruent with endemism or threat. Nature **436**:1016.

Ortloff, C. R., and A. L. Kolata. 1993. Climate and Collapse: Agro-Ecological Perspectives on the Decline of the Tiwanaku State. Journal of Archaeological Science **20**:195.

Paduano, G. 2001. Vegetation and fire history of two tropical Andean lakes, Titicaca (Peru/Bolivia), and Caserochocha (Peru) with special emphasis on the Younger Dryas chronozone. Ph.D. Florida Institute of Technology, Melbourne.

Pacheco, P., M. Aguilar-Støen, J. Börner, A. Etter, L. Putzel, and M. d. C. V. Diaz. 2010. Landscape transformation in tropical Latin America: Assessing trends and policy Implications for REDD+. Forests **2**:1-29.

Paduano, G. M., M. B. Bush, P. A. Baker, S. C. Fritz, and G. O. Seltzer. 2003. A vegetation and fire history of Lake Titicaca since the Last Glacial Maximum. Palaeogeography, Palaeoclimatology, Palaeoecology **194**:259-279.

Parmesan, C., and G. Yohe. 2003. A globally coherent fingerprint of climate change impacts across natural systems. Nature **421**:37-42.

Patrick, R., and C. W. Reimer. 1966. The diatoms of the United States. The Academy of Natural Sciences of Philadelphia.

Pauly, D. 1995. Anecdotes and the shifting baseline syndrome of fisheries. Trends in Ecology & Evolution **10**:430-430.

Pauly, D., V. Christensen, J. Dalsgaard, R. Froese, and F. J. Torres. 1998. Fishing down Marine Food Webs. Science **279**:860-863.

Pauly, D., V. Christensen, S. Guenette, T. J. Pitcher, U. R. Sumaila, C. J. Walters, R. Watson, and D. Zeller. 2002. Towards sustainability in world fisheries. Nature **418**:689-695.

Pearsall, D. M. 2008. Plant Domestication and the Shift to Agriculture in the Andes. Pages 105-120 *in* H. Silverman and W. H. Isbell, editors. The Handbook of South American Archaeology. Springer New York, New York.

Pebesma, E. J., and R. S. Bivand. 2005. Classes and methods for spatial data in R. R News **5**:9-13.

Peterson, L. C., G. H. Haug, K. A. Hughen, and U. Röhl. 2000. Rapid Changes in the Hydrologic Cycle of the Tropical Atlantic During the Last Glacial. Science **290**:1947-1951.

Phillips, O. L., P. N. Vargas, A. L. Monteagudo, A. P. Cruz, M.-E. C. Zans, W. G. Sánchez, M. Yli-Halla, and S. Rose. 2003. Habitat association among Amazonian tree species: a landscape-scale approach. Journal of Ecology **91**:757-775.

Phillips, S. J., R. P. Anderson, and R. E. Schapire. 2006. Maximum entropy modeling of species geographic distributions. Ecological Modelling **190**:231-259.

Phillips, S. J., and M. Dudík. 2008. Modeling of species distributions with Maxent: new extensions and a comprehensive evaluation. Ecography **31**:161-175.

Phillips, S. J., M. Dudík, and R. E. Schapire. 2004. A Maximum Entropy Approach to Species Distribution Modeling. Pages 655-662 Proceedings of the Twenty-First International Conference on Machine Learning, Banff Canada.

Pickett, S. T. A., and V. T. Parker. 1994. Avoiding the Old Pitfalls: Opportunities in a New Discipline. Restoration Ecology **2**:75-79.

Pimm, S. L., and P. Raven. 2000. Biodiversity: Extinction by numbers. Nature **403**:843-845.

Piper, F., L. Cavieres, M. Reyes-Díaz, and L. Corcuera. 2006. Carbon sink limitation and frost tolerance control performance of the tree Kageneckia angustifolia D. Don (Rosaceae) at the treeline in central Chile. Plant Ecology **185**:29-39.

Piperno, D. 2007. Prehistoric human occupation and impacts on Neotropical forest landscapes during the late Pleistocene and Early/Middle Holocene. Pages 193-218 *in* M. B. Bush and J. R. Flenley, editors. Tropical Rainforest Responses to Climatic Change. Springer/Praxis, Berlin; New York; Chichester.

Piperno, D. R., and K. E. Stothert. 2003. Phytolith evidence for early Holocene *Cucurbita* domestication in southwest Ecuador. Science **299**:1054-1057.

Pires-Ferreira, J. W., E. Pires-Ferreira, and P. Kaulicke. 1976. Preceramic animal utilization in the Central Peruvain Andes. Science **194**:483-490.

Pitman, N. C. A., J. W. Terborgh, M. R. Silman, P. V. Nunez, D. A. Neill, C. E. Cerón, W. E. Palacios, and M. Aulestia. 2001. Dominance and distribution of tree species in upper Amazonian terra firme forests. Ecology **82**:2101-2117.

Porter, S. C. 2001. Snowline depression in the tropics during the Last Glaciation. Quaternary Science Reviews **20**:1067-1091.

Post, L. V. 1946. The Prospect for Pollen Analysis in the Study of the Earth's Climatic History New Phytologist **45**:193-217.

Powledge, F. 2003. Island Biogeography's Lasting Impact. BioScience **53**:1032-1038.

Purcell, J., and A. Brelsford. 2004. Reassessing the causes of decline of *Polylepis*, a tropical subalpine forest. Ecotropica **10**:155-158.

Quesada, C. A., J. Lloyd, M. Schwarz, S. Patiño, T. R. Baker, C. Czimczik, N. M. Fyllas, L. Martinelli, G. B. Nardoto, J. Schmerler, A. J. B. Santos, M. G. Hodnett, R. Herrera, F. J. Luizão, A. Arneth, G. Lloyd, N. Dezzeo, I. Hilke, I. Kuhlmann, M. Raessler, W. A. Brand, H. Geilmann, J. O. Moraes Filho, F. P. Carvalho, R. N. Araujo Filho, J. E. Chaves, O. F. Cruz Junior, T. P. Pimentel, and R. Paiva. 2009. Chemical and physical properties of Amazon forest soils in relation to their genesis. Biogeosciences Discuss. **6**:3923-3992.

R, D. C. T. 2011. R: A Language and Environment for Statistical Computing. R Foundation for Statistical Computing, Vienna, Austria.

Rabatel, A., B. Francou, A. Soruco, J. Gomez, B. Cáceres, J. L. Ceballos, R. Basantes, M. Vuille, J. E. Sicart, C. Huggel, M. Scheel, Y. Lejeune, Y. Arnaud, M. Collet, T. Condom, G. Consoli, V. Favier, V. Jomelli, R. Galarraga, P. Ginot, L. Maisincho, J. Mendoza, M. Ménégoz, E. Ramirez, P. Ribstein, W. Suarez, M. Villacis, and P. Wagnon. 2013. Current state of glaciers in the tropical Andes: a multi-century perspective on glacier evolution and climate change. The Cryosphere **7**:81-102.

Racca, J. M. J., I. Gregory-Eaves, R. Pienitz, and Y. T. Prairie. 2004. Tailoring palaeolimnological diatom-based transfer functions. Canadian Journal of Fisheries and Aquatic Sciences **61**:2440-2454.

Rahbek, C. 1995. The elevational gradient of species richness: a uniform pattern? Ecography **18**:200-205.

Raimondi, A. 1874. El Perú, Lima.

Raper, S. C. B., and F. Giorgi. 2005. Climate change projections and models. . Pages 199-210 *in* T. E. Lovejoy and L. Hannah, editors. Climate Change and Biodiversity. Yale University Press, New Haven, U.S.A.

Rapp, J. M., and M. R. Silman. 2012. Diurnal, seasonal, and altitudinal trends in microclimate across a tropical montane cloud forest. Climate Research **55**:17-32.

Rasband, W. ImageJ 1.38x.

Redman, C. L., and A. P. Kinzig. 2003. Resilience of Past Landscapes: Resilience Theory, Society, and the Longue Durée. Ecology and Society **7**:1-19.

Renison, D., I. Hensen, and A. M. Cingolani. 2004. Anthropogenic soil degradation affects seed viability in Polylepis australis mountain forests of central Argentina. Forest Ecology and Management **196**:327-333.

Restrepo, A., P. Colinvaux, M. Bush, A. Correa-Metrio, J. Conroy, M. R. Gardener, P. Jaramillo, M. Steinitz-Kannan, and J. Overpeck. 2012. Impacts of climate variability and human colonization on the vegetation of the Galápagos Islands. Ecology **93**:1853-1866.

Reyes-Garcia, V., I. Ruiz-Mallen, L. Porter-Bolland, E. Garcia-Frapolli, E. A. Ellis, M.-E. Mendez, D. J. Pritchard, and M.-C. Sanchez-Gonzalez. 2013. Local Understandings of Conservation in Southeastern Mexico and Their Implications for Community-Based Conservation as an Alternative Paradigm. Conservation Biology **27**:856-865.

Rind, D., and D. Peteet. 1985. Terrestrial conditions at the Last Glacial Maximum and CLIMAP sea-surface temperature estimates: Are they consistent? Quaternary Research **24**:1-22.

Roberts, J. 2008. Core Logger Manual V 1.3 (GEOTEK). GEOTEK.

Rodbell, D. T., E. M. Delman, M. B. Abbott, M. R. Besonen, and P. M. Tapia. 2013. The heavy metal contamination of Lake Junín National Reserve, Peru: An unintended consequence of the juxtaposition of hydroelectricity and mining. GSA Today **24**:4-10.

Rodbell, D. T., and G. O. Seltzer. 2000. Rapid Ice Margin Fluctuations during the Younger Dryas in the Tropical Andes. Quaternary Research **54**:328-338.

Rodbell, D. T., G. O. Seltzer, D. M. Anderson, M. B. Abbott, D. B. Enfield, and J. H. Newman. 1999. An ~15,000-year record of El Niño-driven alluviation in southwestern Ecuador. Science **283**: 516-520.

Román-Cuesta, R. M., N. Salinas, H. Asbjornsen, I. Oliveras, V. Huaman, Y. Gutiérrez, L. Puelles, J. Kala, D. Yabar, M. Rojas, R. Astete, D. Y. Jordán, M. Silman, R. Mosandl, M. Weber, B. Stimm, S. Günter, T. Knoke, and Y. Malhi. 2011. Implications of fires on carbon budgets in Andean cloud montane forest: the importance of peat soils and tree resprouting. Forest Ecology and Management **261**:1987-1997.

Roosevelt, A. C., M. L. d. Costa, C. L. Machado, M. Michab, N. Mercier, H. Valladas, J. Feathers, W. Barnett, M. I. d. Silveira, A. Henderson, J. Sliva, B. Chernoff, D. S. Reese, J. A. Holman, N. Toth, and K. Schick. 1996a. Paleoindian Cave Dwellers in the Amazon: The Peopling of the Americas. Science **272**:373-384.

Roosevelt, A. C., M. Lima da Costa, C. Lopes Machado, M. Michab, N. Mercier, H. Valladas, J. Feathers, W. Barnett, M. Imazio da Siveira, A. Henderson, J. Sliva, B. Chernoff, D. S. Reese, J. A. Holman, N. Toth, and K. Schick. 1996b. Paleoindian Cave Dwellers in the Amazon: The Peopling of the Americas. Science **272**:373-384.

Roseacute, P. n, R. Hall, T. Korsman, and I. Renberg. 2000. Diatom transfer-functions for quantifying past air temperature, pH and total organic carbon concentration from lakes in northern Sweden. Journal of Paleolimnology **24**:109-123.

Rowe, H. D., R. B. Dunbar, D. A. Mucciarone, G. O. Seltzer, P. A. Baker, and S. Fritz. 2002. Insolation, Moisture Balance and Climate Change on the South American Altiplano since the Last Glacial Maximum. Climatic Change **52**:175-199.

Rowe, H. D., T. P. Guilderson, R. B. Dunbar, J. R. Southon, G. O. Seltzer, D. A. Mucciarone, S. C. Fritz, and P. A. Baker. 2003. Late Quaternary lake-level changes constrained by radiocarbon and stable isotope studies on sediment cores from Lake Titicaca, South America. Global and Planetary Change **38**:273–290.

Rule, S., B. W. Brook, S. G. Haberle, C. S. M. Turney, A. P. Kershaw, and C. N. Johnson. 2012. The Aftermath of Megafaunal Extinction: Ecosystem Transformation in Pleistocene Australia. Science **335**:1483-1486.

Sala, O. E., F. Stuart Chapin , III, J. J. Armesto, E. Berlow, J. Bloomfield, R. Dirzo, E. Huber-Sanwald, L. F. Huenneke, R. B. Jackson, A. Kinzig, R. Leemans, D. M. Lodge, H. A. Mooney, M. n. Oesterheld, N. L. Poff, M. T. Sykes, B. H. Walker, M. Walker, and D. H. Wall. 2000. Global Biodiversity Scenarios for the Year 2100. Science **287**:1770-1774.

Sanderson, E. W., M. Jaiteh, M. A. Levy, K. H. Redford, A. V. Wannebo, and G. Woolmer. 2002. The Human Footprint and the Last of the Wild The human footprint is a global map of human influence on the land surface, which suggests that human beings are stewards of nature, whether we like it or not. BioScience **52**:891-904.

Sandweiss, D. H., and J. B. Richardson. 2008. Central Andean Environments. Pages 93-104 *in* H. Silverman and W. H. Isbell, editors. The Handbook of South American Archaeology. Springer New York, New York.

Sarmiento, F. O., and L. M. Frolich. 2002. Andean Cloud Forest Tree Lines. Mountain Research and Development **22**:278-287.

Satterthwaite, D. 2009. The implications of population growth and urbanization for climate change. Environment and Urbanization **21**:545-567.

Schlüter, M. H., A. Kraberg, and K. H. Wiltshire. 2012. Long-term changes in the seasonality of selected diatoms related to grazers and environmental conditions. Journal of Sea Research **67**:91-97.

Schmidt-Lebuhn, A. N., M. Kessler, and M. Kumar. 2006. Promiscuity in the Andes: Species Relationships in Polylepis (Rosaceae, Sanguisorbeae) Based on AFLP and Morphology. Systematic Botany **31**:547-559.

Seltzer, G. O., S. Cross, P. Baker, R. Dunbar, and S. Fritz. 1998. High-resolution seismic reflection profiles from Lake Titicaca, Peru/Bolivia. Evidence for Holocene aridity in the tropical Andes. Geology **26**:167-170.

Seltzer, G. O., D. T. Rodbell, P. A. Baker, S. C. Fritz, P. M. Tapia, H. D. Rowe, and R. B. Dunbar. 2002a. Early deglaciation in the tropical Andes. Science **298**:1685-1686.

Seltzer, G. O., D. T. Rodbell, P. A. Baker, S. C. Fritz, P. M. Tapia, H. D. Rowe, and R. B. Dunbar. 2002b. Early warming of tropical South America at the last glacial-interglacial transition. Science **296**.

Seltzer, G. O., D. T. Rodbell, and S. Burns. 2000. Isotopic evidence for late Quaternary climatic change in tropical South America. Geology **28**:35-38.

Servat, G. P., W. M. C., and J. A. O. C. 2002. Flora y fauna de cuatro bosques de *Polylepis* (Rosaceae) en la Cordillera del Vilcanota (Cusco, Perú). Ecología Aplicada **1**:25-35.

Shackleton, N. J. 2000. The 100,000 year ice-age cycle identified and found to lag temperature, carbon dioxide and orbital eccentricity. Science **289**:1897-1902.

Shady-Solis, R., J. Haas, and W. Creamer. 2001. Dating Caral, a Preceramic Site in the Supe Valley on the Central Coast of Peru. Science **723**:723-726.

Simpson, B. B. 1979. A Revision of the Genus *Polylepis* (Rosaceae: Sanguisorbeae). Smithsonian Contributions to Botany **43**:62 pp.

Sklenar, P., E. Duskova, and H. Balslev. 2011. Tropical and Temperate: Evolutionary History of Paramo Flora. Botanical Review **77**:71-108.

Smith, J. A., G. O. Seltzer, D. L. Farber, D. T. Rodbell, and R. C. Finkel. 2005. Early Local Last Glacial Maximum in the Tropical Andes. Science **308**:678-681.

Spangenberg, J. H., A. Bondeau, T. R. Carter, S. Fronzek, J. Jaeger, K. Jylhä, I. Kühn, I. Omann, A. Paul, I. Reginster, M. Rounsevell, O. Schweiger, A. Stocker, M. T. Sykes, and J. Settele. 2012. Scenarios for investigating risks to biodiversity. Global Ecology and Biogeography **21**:5-18.

Steig, E. J., E. J. Brook, J. W. White, nbsp, C, C. M. Sucher, M. L. Bender, S. J. Lehman, D. L. Morse, E. D. Waddington, and G. D. Clow. 1998. Synchronous Climate Changes in Antarctica and the North Atlantic. Science **282**:92-95.

Stockmarr, J. 1972. Tablets with spores used in absolute pollen analysis. Pollen et Spore **XIII**:615-621.

Stothert, K. E., D. R. Piperno, and C. A. Thomas. 2003. Terminal Pleistocene/Early Holocene human adaptation in coastal Ecuador: the Las Vegas evidence. Quaternary International **109-110**:23-43.

Stueve, K. M., D. L. Cerney, R. M. Rochefort, and L. L. Kurth. 2009. Post-fire tree establishment patterns at the alpine treeline ecotone: Mount Rainier National Park, Washington, USA. Journal of Vegetation Science **20**:107-120.

Stuiver, M., P. J. Reimer, and R. Reimer. 2005. CALIB Radiocarbon Calibration 5.0.2 html.

Sublette, N. A., B. Valencia, A. Correa-Metrio, A. Chepstow-Lusty, and M. Bush. 2010. Regional-scale agricultural shifts in southern Peru (Cuzco).*in* Ecological Society of America, Pittsburgh, PA.

Sublette, N. A., B. G. Valencia, A. Chepstow-Lusty, and M. B. Bush. 2012. Anthropogenic control of Late Holocene landscapes in the Cuzco region. The Holocene **22**:1361-1372.

Sylvestre, F. 2009. Moisture Pattern During the Last Glacial Maximum in South America. Pages 3-27 *in* F. Vimeux, F. Sylvestre, and M. Khodri, editors. Past Climate Variability in South America and Surrounding Regions. Springer Netherlands.

Tapia, P. M., S. C. Fritz, P. A. Baker, G. O. Seltzer, and R. B. Dunbar. 2003. A Late Quaternary diatom record of tropical climatic history from Lake Titicaca (Peru and Bolivia). Palaeogeography Palaeoclimatology Palaeoecology **194**:139-164.

ter Braak, C. J. F. 1986. Cononical correspondence analysis: A new wigenvector technique for multivariate direct gradient analysis. Ecology **67**:1167-1179.

ter Steege, H., N. C. A. Pitman, D. Sabatier, C. Baraloto, R. P. Salomão, J. E. Guevara, O. L. Phillips, C. V. Castilho, W. E. Magnusson, J.-F. Molino, A. Monteagudo, P. Núñez Vargas, J. C. Montero, T. R. Feldpausch, E. N. H. Coronado, T. J. Killeen, B. Mostacedo, R. Vasquez, R. L. Assis, J. Terborgh, F. Wittmann, A. Andrade, W. F. Laurance, S. G. W. Laurance, B. S. Marimon, B.-H. Marimon, I. C. Guimarães Vieira, I. L. Amaral, R. Brienen, H. Castellanos, D. Cárdenas López, J. F. Duivenvoorden, H. F. Mogollón, F. D. d. A. Matos, N. Dávila, R. García-Villacorta, P. R. Stevenson Diaz, F. Costa, T. Emilio, C. Levis, J. Schietti, P. Souza, A. Alonso, F. Dallmeier, A. J. D. Montoya, M. T. Fernandez Piedade, A. Araujo-Murakami, L. Arroyo, R. Gribel, P. V. A. Fine, C. A. Peres, M. Toledo, G. A. Aymard C., T. R. Baker, C. Cerón, J. Engel, T. W. Henkel, P. Maas, P. Petronelli, J. Stropp, C. E. Zartman, D. Daly, D. Neill, M. Silveira, M. R. Paredes, J. Chave, D. d. A. Lima Filho, P. M. Jørgensen, A. Fuentes, J. Schöngart, F. Cornejo Valverde, A. Di Fiore, E. M. Jimenez, M. C. Peñuela Mora, J. F. Phillips, G. Rivas, T. R. van Andel, P. von Hildebrand, B. Hoffman, E. L. Zent, Y. Malhi, A. Prieto, A. Rudas, A. R. Ruschell, N. Silva, V. Vos, S. Zent, A. A. Oliveira, A. C. Schutz, T. Gonzales, M. Trindade Nascimento, H. Ramirez-Angulo, R. Sierra, M. Tirado, M. N. Umaña Medina, G. van der Heijden, C. I. A. Vela, E. Vilanova Torre, C. Vriesendorp, O. Wang, K. R. Young, C. Baider, H. Balslev, C. Ferreira, I. Mesones, A. Torres-Lezama, L. E. Urrego Giraldo, R. Zagt, M. N. Alexiades, L. Hernandez, I. Huamantupa-Chuquimaco, W. Milliken, W. Palacios Cuenca, D. Pauletto, E. Valderrama Sandoval, L. Valenzuela Gamarra, K. G. Dexter, K. Feeley, G. Lopez-Gonzalez, and M. R. Silman. 2013. Hyperdominance in the Amazonian Tree Flora. Science **342**.

Terborgh, J. 1977. Bird species diversity on an Andean elevational gradient. Ecology **58**:1007-1019.

Terborgh, J., and E. Andresen. 1998. The composition of Amazonian forests: patterns at local and regional sclaes. Journal of Tropical Ecology **14**:645-664.

Thekaekara, M. P., and A. J. Drummond. 1971. Standard Values for the Solar Constant and its Spectral Components. Nature:6-9.

Thomas, C. D., A. Cameron, R. E. Green, M. Bakkenes, L. J. Beaumont, Y. C. Collingham, B. F. N. Erasmus, M. F. de Siqueira, A. Grainger, L. Hannah, L. Hughes, B. Huntley, A. S. van Jaarsveld, G. F. Midgley, L. Miles, M. A. Ortega-Huerta, A. Townsend Peterson, O. L. Phillips, and S. E. Williams. 2004. Extinction risk from climate change. Nature **427**:145.

Thompson, L. G. 2000. Ice core evidence for climate change in the Tropics: implications for our future. Quaternary Science Reviews **19**:19-35.

Thompson, L. G., M. E. Davis, E. Mosley-Thompson, T. A. Sowers, K. A. Henderson, V. S. Zagorodnov, P.-N. Lin, V. N. Mikhalenko, R. K. Campen, J. F. Bolzan, J. Cole-Dai, and B. Francou. 1998. A 25,000-year tropical climate history from Bolivian ice cores. Science **282**:1858-1864.

Troll, C. 1968. The cordilleras of the tropical Americas: Aspects of climatic, phytogeographical and agrarian ecology. Pages 15-56 *in* C. Troll, editor. Proceedings of the UNESCO Symposium on Geoecology of the Mountainous Regions of the Tropical Americas. *Colloquium Geographicum.*

Tuomisto, H., K. Ruokolainen, and M. Yli-Halla. 2003. Dispersal, Environment, and Floristic Variation of Western Amazonian Forests. Science **299**:241-244.

Ugan, A., and D. Byers. 2007. Geographic and temporal trends in proboscidean and human radiocarbon histories during the late Pleistocene. Quaternary Science Reviews **26**:3058-3080.

Urrego, D. H., M. B. Bush, and M. R. Silman. 2010. A long history of cloud and forest migration from Lake Consuelo, Peru. Quaternary Research **73**:364-373.

Urrego, D. H., B. A. Niccum, C. F. La Drew, M. R. Silman, and M. B. Bush. 2011. Fire and drought as drivers of early Holocene tree line changes in the Peruvian Andes. Journal of Quaternary Science **26**:28-36.

Urrutia, R., and M. Vuille. 2009. Climate change projections for the tropical Andes using a regional climate model: Temperature and precipitation simulations for the end of the 21st century. Journal of Geophysical Research: Atmospheres **114**:D02108.

Václavík, T., J. A. Kupfer, and R. K. Meentemeyer. 2012. Accounting for multi-scale spatial autocorrelation improves performance of invasive species distribution modelling (iSDM). Journal of Biogeography **39**:42-55.

Valencia, B. 2006. Late Quaternary Vegetation and Climate Change in the Southern Andes of Peru. Ms. Florida Institute of Technology, Melbourne.

Valencia, B. G., S. N. A., and M. B. Bush. 2010a. Historia de la vegetacion, cambio climatico e influencia humana durante el holoceno tardio en los andes centrales. XV Congreso Peruano de Geologia.

Valencia, B. G., D. H. Urrego, M. R. Silman, and M. B. Bush. 2010b. From ice age to modern: a record of landscape change in an Andean cloud forest. Journal of Biogeography **37**:1637-1647.

Van der Hammen, T., and E. Gonzalez. 1965. A Late glacial and Holocene pollen diagram from Cienaga del Vistador Dep. Boyaca, Colombia. Leids Geologische Mededelingen **32**:193-201.

van der Hammen, T., and E. González. 1960. Upper Pleistocene and Holocene climate and vegetation of the Sabana de Bogotá (Colombia, South America). Leidse Geologische Mededelingen **25**: 261-315.

van der Hammen, T., and H. Hooghiemstra. 2003. Interglacial-glacial Fuquene-3 pollen record from Colombia: an Eemian to Holocene climate record. Global and Planetary Change **36**:181-199.

van Wilgen, B. W., and H. C. Biggs. 2011. A critical assessment of adaptive ecosystem management in a large savanna protected area in South Africa. Biological Conservation **144**:1179-1187.

Vuille, M. 1999. Atmospheric circulation over the Bolivian Altiplano during DRY and WET periods and extreme phases of the Southern Oscillation. International Journal of Climatology **19**:1579-1600.

Vuille, M., R. S. Bradley, and F. Keimig. 2000a. Climate variability in the Andes of Ecuador and Its relation to tropical Pacific and Atlantic sea surface temperature anomalies. Journal of Climate **13**:2520-2535.

Vuille, M., R. S. Bradley, and F. Keimig. 2000b. Interannual climate variability in the Central Andes and its relation to tropical Pacific and Atlantic forcing. Journal of Geophysical Research **105**:447-460.

Vuille, M., B. Francou, P. Wagnon, I. Juen, G. Kaser, B. G. Mark, and R. S. Bradley. 2008. Climate change and tropical Andean glaciers: Past, present and future. Earth-Science Reviews **89**:79-96.

Walker, M., S. Johnsen, S. O. Rasmussen, T. Popp, J.-P. Steffensen, P. Gibbard, W. Hoek, J. Lowe, J. Andrews, S. Björck, L. C. Cwynar, K. Hughen, P. Kershaw, B. Kromer, T. Litt, D. J. Lowe, T. Nakagawa, R. Newnham, and J. Schwander. 2009. Formal definition and dating of the GSSP (Global Stratotype Section and Point) for the base of the Holocene using the Greenland NGRIP ice core, and selected auxiliary records. Journal of Quaternary Science **24**:3-17.

Wang, H., and R. Fu. 2004. Influence of Cross-Andes Flow on the South American Low-Level Jet. Journal of Climate **17**:1247-1262.

Wang, X., A. S. Auler, R. L. Edwards, H. Cheng, P. S. Cristalli, P. L. Smart, D. A. Richards, and C.-C. Shen. 2004. Wet periods in northeastern Brazil over the past 210 kyr linked to distant climate anomalies. Nature **432**:740-743.

Warshall, P. 1995. The Madrean Sky Island Archipelago: A planetary overview. . U.S. Forest Service, Tucson, Arizona.

Webster, P. J., and N. A. Streten. 1978. Late Quaternary ice age climates of tropical Australasia: Interpretations and reconstructions. Quaternary Research **10**:279-309.

Weng, C., M. B. Bush, J. H. Curtis, A. L. Kolata, T. D. Dillehay, and M. W. Binford. 2006. Deglaciation and Holocene climate change in the western Peruvian Andes. Quaternary Research **66**:87-96.

Werner, P., and J. Smol. 2005. Diatom–environmental relationships and nutrient transfer functions from contrasting shallow and deep limestone lakes in Ontario, Canada. Hydrobiologia **533**:145-173.

Westgate, M. J., G. E. Likens, and D. B. Lindenmayer. 2013. Adaptive management of biological systems: A review. Biological Conservation **158**:128-139.

Willems, E. P., and R. A. Hill. 2009. A critical assessment of two species distribution models: a case study of the vervet monkey (Cercopithecus aethiops). Journal of Biogeography **36**:2300-2312.

Williams, J. J., W. D. Gosling, S. J. Brooks, A. L. Coe, and S. Xu. 2011a. Vegetation, climate and fire in the eastern Andes (Bolivia) during the last 18,000 years. Palaeogeography, Palaeoclimatology, Palaeoecology **312**:115-126.

Williams, J. J., W. D. Gosling, A. L. Coe, S. J. Brooks, and P. Gulliver. 2011b. Four thousand years of environmental change and human activity in the Cochabamba Basin, Bolivia. Quaternary Research **In Press,**.

Williams, J. W., and S. T. Jackson. 2007. Novel climates, no-analog communities, and ecological surprises. Frontiers in Ecology and the Environment **5**:475-482.

Willis, K. J., M. B. Araújo, K. D. Bennett, B. Figueroa-Rangel, C. A. Froyd, and N. Myers. 2007. How can a knowledge of the past help to conserve the future? Biodiversity conservation and the relevance of long-term ecological studies. Philosophical Transactions of the Royal Society B **362**:175-187.

Willis, K. J., and H. J. B. Birks. 2006. What is natural? The need for a long-term perspective in biodiversity conservation. Science **314**:1261-1265.

Willis, K. J., L. Gillson, and T. M. Brncic. 2004. How "Virgin" Is Virgin Rainforest? Science **304**:402-403.

Witt, C. C., and D. F. Lane. 2009. Range extensions for two rare high-Andean birds in central Peru. Cotinga **31**:90-94.

Wunder, S. 1996. Deforestation and ses of wood in the Ecuadorian Andes. Mountain Research and Development **16**:367-382.

Yensen, E., and T. Tarifa. 2002. Mammals of Bolivian *Polylepis* woodlands: guild structure and diversity patterns in the world's highest woodlands. Ecotropica **8**:145-162.

Yi, S., Y. Saito, H. Oshima, Y. Zhou, and H. Wei. 2003. Holocene environmental history inferred from pollen assemblages in the Huanghe (Yellow River) delta, China: climatic change and human impact. Quaternary Science Reviews **22**:609-628.

Young, K. R. 2006. Bosques húmedos. Pages 121-129 *in* M. Moraes, B. Øllgaard, L. P. Kvist, F. Borchsenius, and H. Balslev, editors. Botánica económica de los Andes centrales. Universidad Mayor de San Andrés, La Paz, Bolivia.

Young, K. R. 2009. Andean Land Use And Biodiversity: Humanized Landscapes In A Time Of Change. Annals of the Missouri Botanical Garden **96**:492-507.

Young, K. R. 2011. Introduction to Andean Geographies. Pages 128-140 *in* S. K. Herzog, R. Martínez, P. M. Jørgensen, and H. Tiessen, editors. Climate Change and Biodiversity in the Tropical Andes. Inter-American Institute for Global Change Research (IAI) and Scientific Committee on Problems of the Environment (SCOPE).

Young, K. R., and B. Leon. 1990. Catalogo de las plantas de la zona alta del Parque Nacional Rio Abieso, Peru. Publ. Mus. Hist. Nat., Ser. B. Bot. UNMSM (B) **34**:1-37.

Young, K. R., and B. León. 1999. Peru's humid eastern montane forest: An overview of their physical settings, biological diversity, human use and settlement, and conservation needs. Denmark.

Young, K. R., and B. León. 2007. Tree-line changes along the Andes: implications of spatial patterns and dynamics. Philosophical Transactions of the Royal Society B: Biological Sciences **362**:263-272.

Zeng, N., J.-H. Yoon, J. A. Marengo, A. Subramaniam, C. A. Nobre, A. Mariotti, and J. D. Neelin. 2008. Causes and impacts of the 2005 Amazon drought. Environmental Research Letters **3**:014002.

Zhou, J., and K. M. Lau. 1998. Does a monsoon climate exist over South America. Journal of Climate **11**:10120-11040.

Zimmermann, M., P. Meir, M. Silman, A. Fedders, A. Gibbon, Y. Malhi, D. Urrego, M. Bush, K. Feeley, K. Garcia, G. Dargie, W. Farfan, B. Goetz, W. Johnson, K. Kline, A. Modi, N. Q. Rurau, B. Staudt, and F. Zamora. 2010. No Differences in Soil Carbon Stocks Across the Tree Line in the Peruvian Andes. Ecosystems **13**:62-74.

Appendix I Physicochemical protocols

I.1) Magnetic susceptibility protocol:

1. Magnetic susceptible materials were moved away from the MS sensor (e.g. watches or coins or keys in the pockets).
2. The core logger was turned on and the MS meter warmed up for at least 10 minutes to minimize drift (i.e. when the same empty section measured before and after the logging yields different values)
3. Name and core dimensions were specified
4. Logging empty section to evaluate drift
5. Sensor parameters were set up.
    a. Sampling interval
    b. Sampling time (5 seconds)
    c. Zero before core (0)
    d. Units: SI
6. Cores were logged
7. Logging empty section to evaluate drift
8. Files were saved.

Further details for the core logger setup are provided by GEOTEK at http://www.geotek.co.uk.

I.2) Loss-on-ignition (LOI) protocol

Step procedure

1) Clean & label the crucibles
2) Register the volume used
3) Dry the crucibles for at least 6 hours at 105°C. Place the crucibles into a desiccator or lower the oven temperature at ~ 50°C. Register the crucibles weight when the temperature reaches 50°C.
4) Add samples into the crucibles and register the combined weight (crucibles + samples) if water content is to be determined.
5) Place crucibles into the oven at 105°C for 12 hours. Then, place the crucibles into a desiccator or lower the oven temperature at ~ 50°C. Register the crucibles weight when the temperature reaches 50°C.
6) Place crucibles into the furnace at 550°C for 4 hours (for calculating organic content). Then, place the crucibles into a desiccator or lower the oven temperature at ~ 50°C. Register the crucibles weight when the temperature reaches 50°C.
7) Place crucibles into the furnace at 950°C for 2 hours (for calculating CaCO3 content). Then place the crucibles into a desiccator or lower the oven temperature at ~ 50°C. Register the crucibles weight when the temperature reaches 50°C.

** Note: the scale for measuring the weights must have at least 4 decimal places.

Table A1-1 LOI worksheet for Lake Miski. The protocol is based on Heiri *et al.*, (Heiri et al. 2001)

Empty Crucible				Crucible + sample	CRUCIBLES + SAMPLES			
Step 1	Step 1	Step 2	Step 3	Step 4	Step 5	Step 6	Step 7	Observations
Sample ID	Crucible #	Volume (cm^3)	Weight Crucible	Weight Crucible	once dried at 105°C	once burnt at 550°C	once burnt at 950°C	Observations
Time				6 hr	12 hr	4 hr	2 hr	

Appendix II Pollen preparation protocol

Appendix II describes the pollen preparation protocol in detail. This appendix also contains the R-code to use any computer keyboard as a pollen counter and step-by-step direction to create a pollen diagram in C2.

II.1) Pollen preparation protocol

II.1.1) Pollen processing

Step procedure:

1. Measure 0.5 cm^2 of sample and transfer to centrifuge tubes
2. Spike sample with one *Lycopodium* tablet.
3. Dissolve the *Lycopodium* tablet in hot 10% HCl, for 10 minutes. This step eliminates the carbonates from the sample.
4. Centrifuge*, decant, wash with distilled water, centrifuge* and decant.
5. Mix the sample with 5 ml of 10% KOH, stir and heat the sample for 10 minutes. This step eliminates humic acids from the sample.
6. Centrifuge*, decant, wash with distilled water, centrifuge* and decant.
7. Mix the sample with 5 ml of 10% $Na_4P_2O_7$ stir and heat the sample for 30 minutes. This steps disaggregate clays.
8. Place samples in an ultrasonic bath for 30 seconds
9. Centrifuge*, decant, wash with distilled water, centrifuge* and decant.
10. Eliminate silica particles using 2-3 ml of 49% HF, heat the sample for 60 minutes.
11. Centrifuge*, decant, wash with distilled water, centrifuge* and decant. Repeat (3 times)
12. Treat the samples with 5 ml of 10% HCl, stir and heat the sample for 10 minutes. This step eliminate fluorides formed when using HF.
13. Centrifuge*, decant, wash with distilled water, centrifuge* and decant.
14. Mix the sample with 5 ml of 100% CH_3COOH, centrifuge*and decant.

This step eliminates the water from the sample. Water elimination is extremely important prior step 15 because water reacts violently with the H_2SO_4 contained in the acetolytic solution.

15. Treat the sample with 1 ml of acetolysis solution 9:1 $(CH_3CO)_2O$: H_2SO_4, heat for 3 minutes and stop the reaction adding 2 ml of 100% CH_3COOH centrifuge and decant. This step digests organic materials other than sporopollenin.
16. Wash with 100% CH_3COOH. This step inhibits the reactivity of the H2SO4 prior washing with 10% CH_3COOH that contains water.
17. Wash with 10% CH_3COOH.
18. Wash with distilled water, centrifuge* and decant. Repeat (3 times)
19. Add 1 ml of sodium metatungstate with a density equal to 2.3, mix and centrifuge. This steps is aimed to separate pollen and organic material from dense particles (e.g. sand)
20. Transfer the floating material containing pollen grains into new-labeled tubes and add 10 ml of water to lower the solution density. Adding water will reduce the density of the metatungstate solution favouring the pollen precipitation.
21. Centrifuge the samples, and decant the water containing diluted sodium metatungstate in a large beaker. The metatungstate solution can then be filtered and recycled.
22. Wash the sample with distilled water, centrifuge* and decant. Repeat (3 times).
23. Transfer the samples to vials for storage.
24. A portion of the sample that will be used for counting can be mixed with few drops of glycerol and placed in the oven for 24 hours at 70°C.

Centrifuge* for 3 minutes at 3500 RPM

Appendix II

II.2) Pollen preparation worksheet.

Table A2-1 Pollen preparation working sheet

Site: _____20 Date: / / 20

Ref. No.												
Tube No.	**1**	**2**	**3**	**4**	**5**	**6**	**7**	**8**	**9**	**10**	**11**	**12**
Hot 10% HCl ♣ + *Lycopodium*												
Wash H_2O												
Hot 10% KOH For 10 minutes												
Wash H_2O												
10% $Na_4P_2O_7$. ♣♣ for 30 min - hot												
Ultrasonic bath for 30 seconds												
Wash H_2O												
Hot HF for 1 h.												
Wash H_2O □□□												
Hot HCl for 10 min												
Wash H_2O												
Wash with 100% CH_3COOH												
Acetolysis												
Wash with 100% CH_3COOH												
Wash H_2O												
Metatungstate flotation												
Vials with glycerine												

Table remarks:

* Lycopodium tablets NO: 483216 ( )

♣ SAMPLES REACTION: LOW: + MED: ++ HIGH: +++

♣♣ REPEAT IF NESSESARY (Turbid samples)

* = 1mL sodium metatungstate s.g. 2 (i.e. 3 parts sodium metatungstate: 2 parts distilled water). Please use sodium metatungstate in brown bottle.

II.3) Pollen counter R-code

The code below should be modified and run in R. Additional help is provided in a video.

```
# To assign a specific name to any particular keyboard KEY modify the text (code
 below) that is between several *** symbols.
# when the key assignment is done, copy and run the entire code.
# record your counts using any text editor, then type: PollenCount(" ").
# Insert the text (actual counts) between the quotation marks and click enter: e.g.
 PollenCount("1 1ww33f")

PollenCount<-function(AA) {                    #this created the function named
 PollenCount
CountData<-c(AA)
nchar(CountData) # Counts character numbers
CountList<-substring(CountData,1:nchar(CountData),1:nchar(CountData)) # create
 character straction

length(which(CountList[]=="1"))->PollenType.1
length(which(CountList[]=="2"))->PollenType.2
length(which(CountList[]=="3"))->PollenType.3
length(which(CountList[]=="4"))->PollenType.4
length(which(CountList[]=="5"))->PollenType.5
length(which(CountList[]=="6"))->PollenType.6
length(which(CountList[]=="7"))->PollenType.7
length(which(CountList[]=="8"))->PollenType.8
length(which(CountList[]=="9"))->PollenType.9
length(which(CountList[]=="0"))->PollenType.0
length(which(CountList[]=="a"))->PollenType.a
length(which(CountList[]=="b"))->PollenType.b
length(which(CountList[]=="c"))->PollenType.c
length(which(CountList[]=="d"))->PollenType.d
length(which(CountList[]=="e"))->PollenType.e
length(which(CountList[]=="f"))->PollenType.f
length(which(CountList[]=="g"))->PollenType.g
length(which(CountList[]=="h"))->PollenType.h
length(which(CountList[]=="i"))->PollenType.i
length(which(CountList[]=="j"))->PollenType.j
length(which(CountList[]=="k"))->PollenType.k
length(which(CountList[]=="l"))->PollenType.l
length(which(CountList[]=="m"))->PollenType.m
length(which(CountList[]=="n"))->PollenType.n
length(which(CountList[]=="o"))->PollenType.o
length(which(CountList[]=="p"))->PollenType.p
length(which(CountList[]=="q"))->PollenType.q
```

```
length(which(CountList[]=="r"))->PollenType.r
length(which(CountList[]=="s"))->PollenType.s
length(which(CountList[]=="t"))->PollenType.t
length(which(CountList[]=="u"))->PollenType.u
length(which(CountList[]=="v"))->PollenType.v
length(which(CountList[]=="w"))->PollenType.w
length(which(CountList[]=="x"))->PollenType.x
length(which(CountList[]=="y"))->PollenType.y
length(which(CountList[]=="z"))->PollenType.z

Counts<-c( PollenType.1, PollenType.2, PollenType.3, PollenType.4, PollenType.5,
 PollenType.6, PollenType.7, PollenType.8, PollenType.9, PollenType.0,
 PollenType.a, PollenType.b, PollenType.c, PollenType.d, PollenType.e, PollenType.f,
 PollenType.g, PollenType.h, PollenType.i, PollenType.j, PollenType.k, PollenType.l,
 PollenType.m, PollenType.n, PollenType.o, PollenType.p, PollenType.q,
 PollenType.r, PollenType.s, PollenType.t, PollenType.u, PollenType.v, PollenType.w,
 PollenType.x, PollenType.y, PollenType.z )

#********** Below the code you have to modify **************************
# Modify the code below to assign names of the labels
# Example:      to asign SOLANACEAE to keybord key "W" find "PollenType.w" and
 change it to "SOLANACEAE.w"
#             to asign Poaceae to keyboard key "4" find "PollenType.4" and change it
 to "Poaceae.4"
# When done, save the file, select all the code and run it.

NAMES<-c("PollenType.1", "PollenType.2", "PollenType.3", "PollenType.4",
 "PollenType.5", "PollenType.6", "PollenType.7", "PollenType.8", "PollenType.9",
 "PollenType.0", "PollenType.a", "PollenType.b", "PollenType.c", "PollenType.d",
 "PollenType.e", "PollenType.f", "PollenType.g", "PollenType.h", "PollenType.i",
 "PollenType.j", "PollenType.k", "PollenType.l", "PollenType.m", "PollenType.n",
 "PollenType.o", "PollenType.p", "PollenType.q", "PollenType.r", "PollenType.s",
 "PollenType.t", "PollenType.u", "PollenType.v", "PollenType.w", "PollenType.x",
 "PollenType.y", "PollenType.z" )
#*****************************************************************************

A<-matrix(data=Counts, nrow=36, ncol=1, dimnames=list(NAMES,c("Counts")))
print(A)
print("The sum of grains is:")
print(sum(A))
print("Excel file named PollenCounts.csv was created in folder:")
print(getwd())
write.table(A, file="PollenCounts.csv", sep=",")
}
```

II.4) C2 Manual

1. Data entry in Excel.

Enter data in Excel having sites as rows and species as columns. The first three columns are field required by C2 (i.e. #, Code and Name). In the example the body of the table contain percentages (sheet names C2 percentages).

1. #: Sequence of the number of sites or samples and admits only integer entries
2. Code: Used for sample identification. Admits alphanumeric entries.
3. Name: Used for sample identification. Admits alphanumeric entries.

Note that the excel file should be saved with extension .xls instead of .xlsx.

The spreadsheet must be free of formulas (i.e. values only).

	A	B	C	D	E	F	G	H	I	J	K	L
1	#	Code	Name	Sp 1	Sp 2	Sp 3	Sp 4	Sp 5	Sp 6	Sp 7		
2	1	C R	Plot 1	7.692308	15.38462	19.23077	23.07692	15.38462	7.692308	11.53846		
3	2	C R	Plot 2	14.28571	22.85714	28.57143	0	5.714286	14.28571	14.28571		
4	3	C R	Plot 3	16	12	12	20	16	16	8		
5	4	C R	Plot 4	21.2766	10.6383	21.2766	10.6383	21.2766	10.6383	4.255319		
6	5	C R	Plot 5	27.58621	13.7931	6.896552	3.448276	6.896552	13.7931	27.58621		
7												
8												
9												
10												
11												

Sheet1 / Sheet2 / C2 percentages / C2 altitude

Use a new column or new sheet to incorporate additional variables. In this example the variable "Altitude" was inserted in a new sheet. Variables such as Depth or Age can be included as additional columns. In the final diagram the variable you chose will be plotted in the Y-axis.

	A	B	C	D
1	#	Code	Name	Altitude
2	1	C R	Plot 1	100
3	2	C R	Plot 2	200
4	3	C R	Plot 3	300
5	4	C R	Plot 4	400
6	5	C R	Plot 5	500
7				

The new sheet must contain the same columns, #, **Code**, and **Name** used previously.

Rename the worksheets formatted for C2 (in the example is named C2 altitude).

2 Importing data into C2

Launch C2 and go to File → Open. In the new window changes the "Files of type" and select ".xls" to view and select your data.

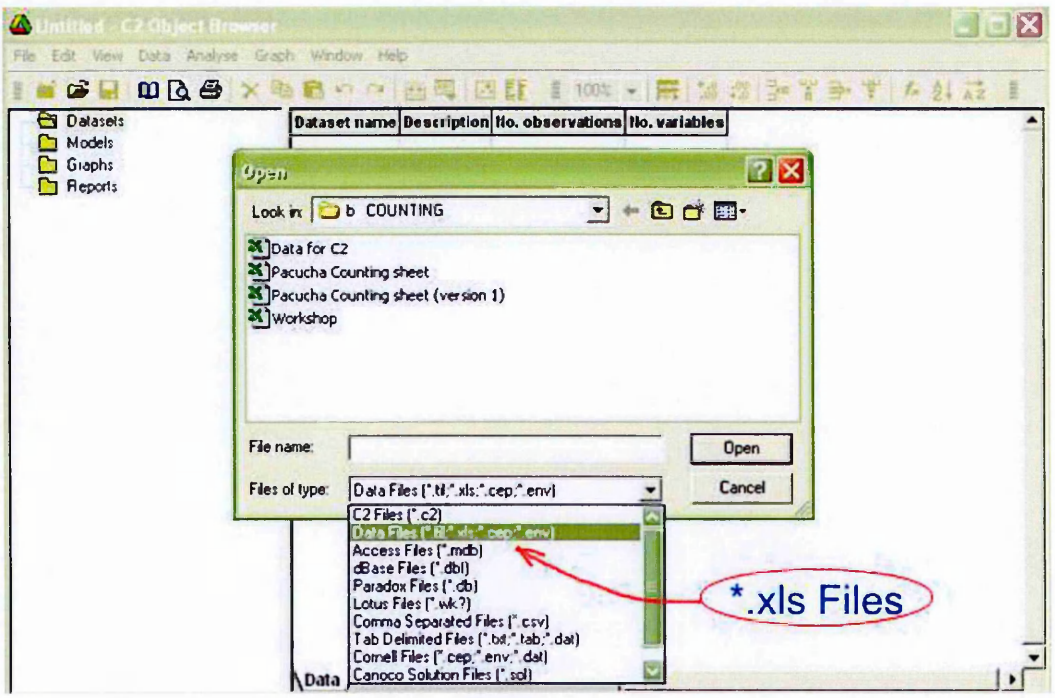

Select the work sheet containing the percentages (C2 Percentages) then click OK.

Follow the same steps to open the next worksheet (C2 Altitude)

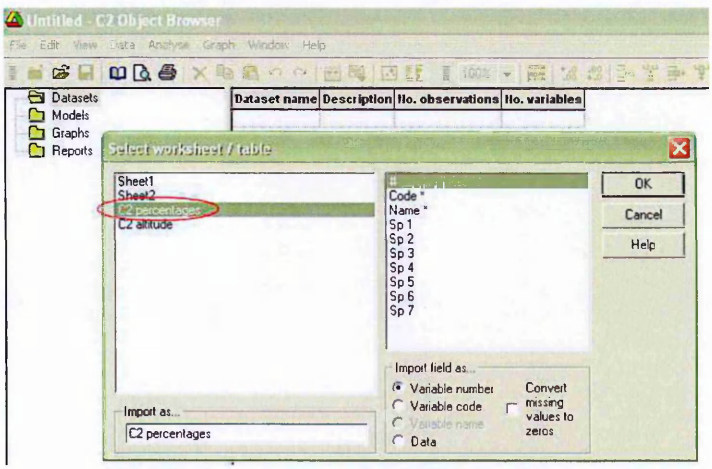

Make sure that the "number of observations" is equal in both sheets. i.e. "C2 percentages" and "C2 altitude" have 5 observations each.

Dataset name	Description	No. observations	No. variables
C2 percentages		5	7
C2 altitude		5	1

3 Generating a diagram in C2

Go to Graph and select "Stratigraphic diagram" Then, enter a name for your "graph book" and provide a "description"

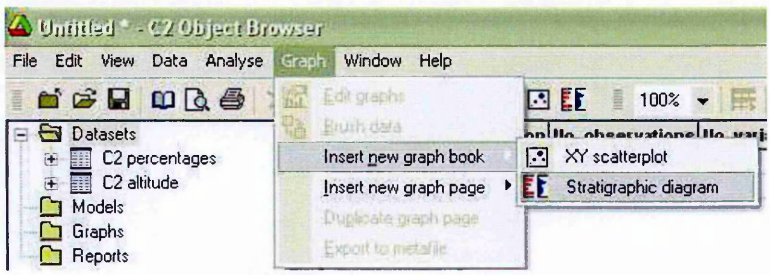

In the new window click "Add variables"

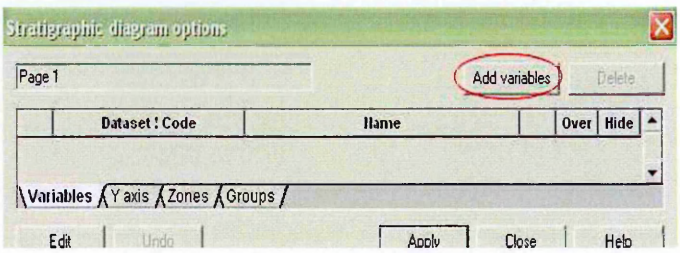

Select "C2 percentages" and the species to be plotted

Click OK

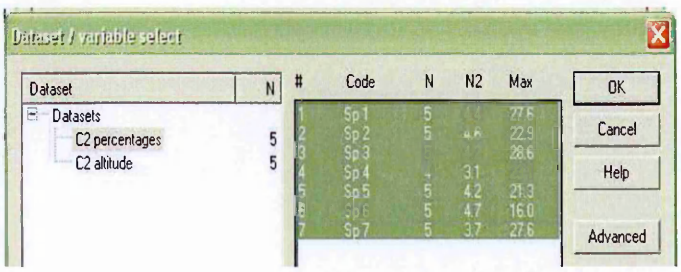

On the Stratigraphic diagram option window,
select all data again clicking and dragging (red arrow).

Then, click "Edit" →

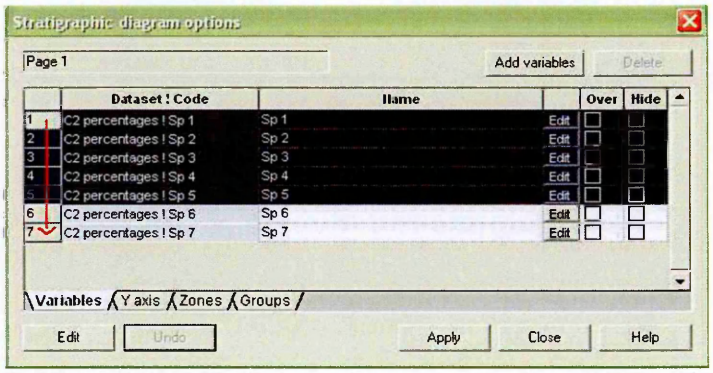

In the new window (Graph properties) select "X-axis scaling". After that, go to "Data scaling" and change "Absolute" by "Percentage", then Click "Apply all".

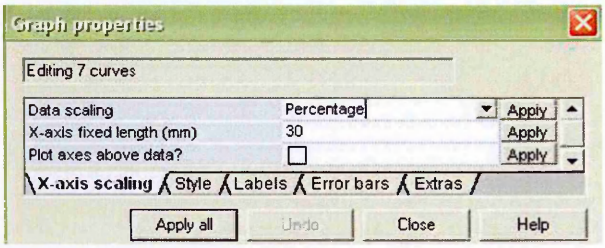

Click "Style," and select "Graph type" and select the desired diagram type.
Click "Apply all"

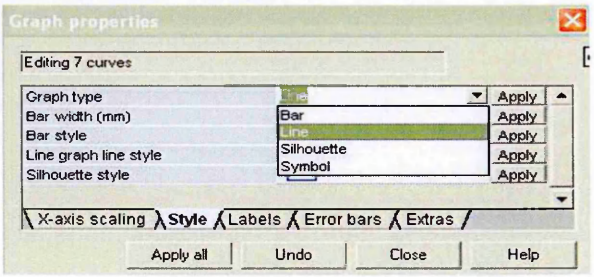

In "Labels" the font can be changed (font size, title, text orientation, and more).
Click "Apply all", then close the "Graph properties" window

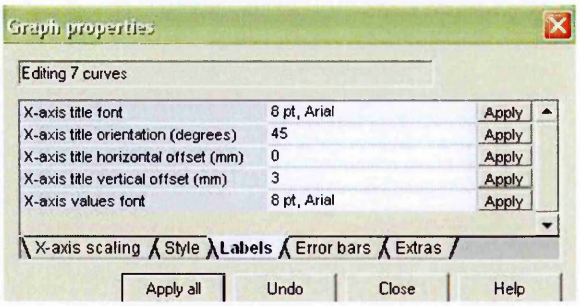

On the "Stratigraphic diagram options" window, select "Y axis" and click the arrow "Y-axis variable".

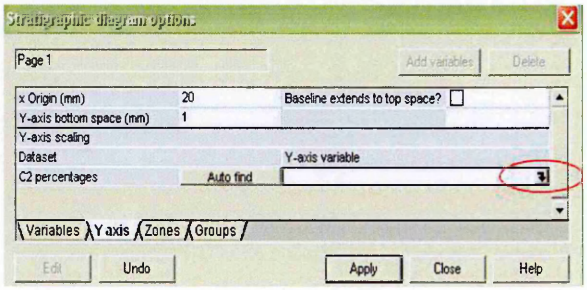

Click "C2 altitude" and select the data you want to use as Y-axis.
Then "OK" and "Apply"

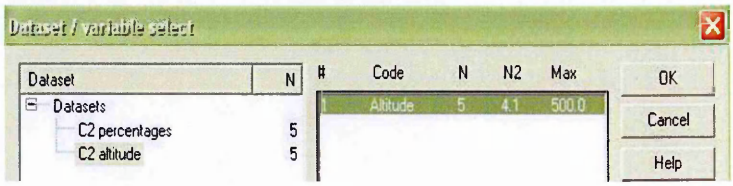

The settings of the y-axis can be modified in the displayed window.

Click apply and then close this window.

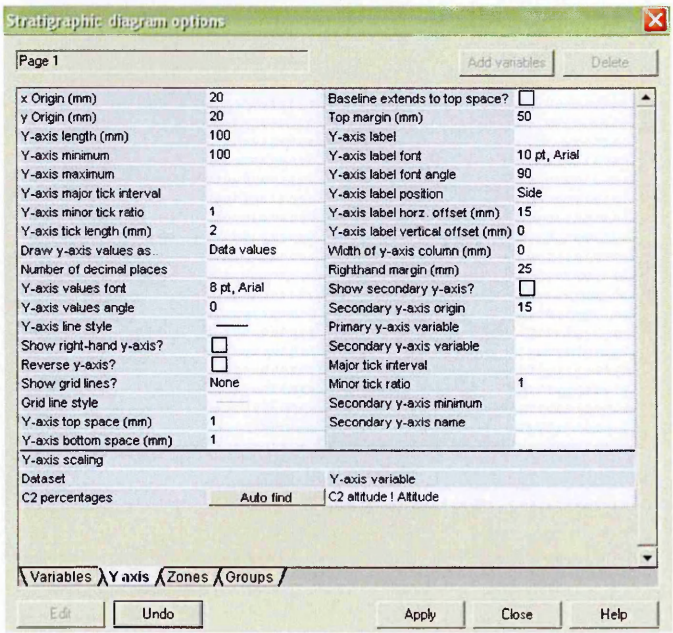

The diagram is ready.

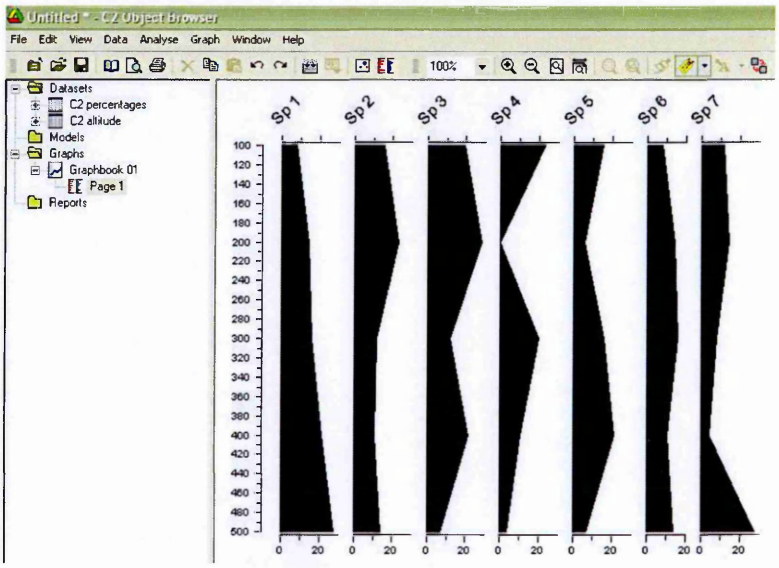

To edit the diagram go to menu → "Graph" and select "Edit graphs" The diagram can be exported as an EMF file.Menu bar → File → Export.

Appendix III Diatom preparation protocol

III.1) Diatom processing

Step procedure:

1. Measure 0.1 cm^3 of sample and transfer to centrifuge tubes
2. Add 3 ml of H_2O_2 and leave the samples overnight.
3. Carefully, centrifuge sample tubes at 1300 RPM for 8 minutes and decant.
4. If samples still contain organic material, repeat steps 2 and 3.
5. Wash the samples in water and store them in vial for mounting.

III.2) Diatom mounting

Step procedure:

1. Place a clean cover slide on a slide warmer and add enough water until a meniscus is formed.
2. Carefully homogenize the prepared diatom sample with a pipette and transfer one drop to the cover slide with water. Homogenize carefully if possible.
3. Leave the slides warming overnight until dry. Samples on the slide warmer should be covered to avoid dust and the temperature should be low enough to allow a slow evaporation (> 6 hours works best)
4. The next steps must be carried inside a fume hood
5. On a microscope slide add a drop of Naphrax® and warm it for few seconds on a heating plate.
6. Place the cover slides with the dry samples facing the warmed Naphrax® solution.
7. With a stick, push the cover slide to eliminate bubbles. Repeat this step placing and removing the microscope slide from the heating plate until no bubbles remain in the sample.

Appendix IV Charcoal preparation protocol.

Appendix III describes the protocols used to extract charcoal fragments from lacustrine sediments to be analysed with a stereoscope or a scanning electron microscope (SEM). This section includes step-by-step directions to calculate charcoal area using ImageJ.

IV.1) Standard charcoal protocol

Step Procedure

1. Retrieve 3-5 sediment samples from conspicuous stratigraphic sections of the core, e.g. organic versus inorganic sections. Place them on a petri dish and add few drops of water. Samples should be small enough to be disaggregated and disperse well in a few drops of water.
2. Place samples under a stereoscope to evaluate if the samples are rich in charcoal particles.
3. Based on this preliminary analysis decide the sample volume that will be used, i.e. 0.25, 0.5 or 1 cm^2 of sediment.
4. Retrieve all the samples required for the charcoal analysis at least at the same resolution of other proxies (i.e. pollen or diatoms). Samples should be placed in a vial with water.
5. Gently homogenize the samples to avoid breaking the fragile charcoal particles and leave them in the vials for 12 h.
6. Rinse the sample on a sieve of 180 um of aperture to eliminate small particles.
7. If the organic content of the sample is high (sticky), transfer the sample retained on the mesh into a vial and treat it with 10% KOH. Use a volume of KOH that is 5-10 times the original volume of the sample.
8. If the clay content of the sample is high, transfer the sample retained on the mesh into a vial and treat it with 0.1M $Na_4P_2O_7$. Use a volume of $Na_4P_2O_7$ that is 5-10 times the original volume of the sample.
9. Samples treated with KOH or $Na_4P_2O_7$ can be warmed up in a hot plate for 10 minutes inside a fume hood.

10. Samples treated with KOH or $Na_4P_2O_7$ should be placed on a sieve of 180 um of aperture and rinsed with water.
11. The material retained on the mesh should be transferred into a labelled petri dish for charcoal counting.

IV.2) SEM-charcoal protocol.

Charcoal preparation for scanning electron microscope (SEM) imaging.

Step Procedure

1. All the fragments selected for charcoal particle analysis (regular charcoal preparation protocol) should be transferred into an eppendorf vial containing water.
2. Samples should be gently shacked to remove the debris attached to the particles.
3. After shacking, wait until the charcoal fragments precipitate to the vial bottom and decant the water. Add more water and repeat steps 2 and 3 twice.
4. Using a stereoscope, check if the particles inside the vials are still covered with debris. If yes, add more water and repeat steps 2 and 3. Note: If a shaker is used, make sure the movement is slow enough to avoid particle breakup.
5. Once the charcoal fragments are clean, retrieve them with a pipette or decant the water with the particles onto a SEM stub that has clear double-side tape. Add enough water to be able move the particles around.
6. Arrange the fragments so they do not overlap.
7. Let the water evaporate overnight at room temperature
8. Once the sample is dry is ready for SEM imaging.
9. All the charcoal fragments should be present in the first image that is taken. Then, on the image, the fragments should be numbered.
10. Images of individual charcoal fragments should be coded using the lake name, depth, the particle number and the image number. e.g. for Lake Miski the second image of the first charcoal particle from 300 cm of depth should be labelled as MSK-300-01-02.

11. Identifications can be carried out when samples are on the SEM or based on archived images.

IV.3) Protocol for Charcoal image analysis using imageJ.

Step Procedure

1. Determine the magnification at which pictures will be taken. Calibrate the camera for the selected magnification in the stereoscope taking a picture of a micrometre.
2. Under the stereoscope, select the charcoal fragments and arrange them avoiding overlaps. Eliminate dark non-charcoal fragments before imaging.
3. Adjust the light to eliminate the shadows of the particles in the pictures. Take note of the settings used (light intensity and magnification) to use them consistently in the following samples. This step is useful when macros (automated steps) are used in imageJ software.
4. Take a picture and save the file using the sample code as the file name. If required, incorporate the depth of the sample prior the label content to facilitate the organization of the files.
5. Open the picture of the micrometre and select the straight line tool:

6. Trace a line over the scale and then set the scale (Menu bar → Analyse→Set scale)

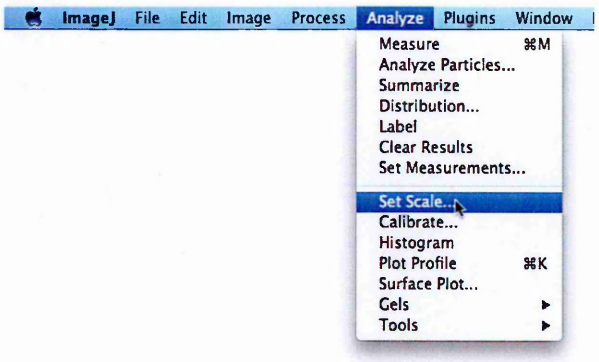

7. A new window will appear depicting the length of the traced vector in pixels.
8. In the new window, replace the values of "known distance" and "unit of length" based on the micrometre values used. Select "global" to retain these settings for subsequent analysis. Finally, take note of these calibration settings, as calibration should be performed only once to ensure the consistency of the measurements throughout the core.

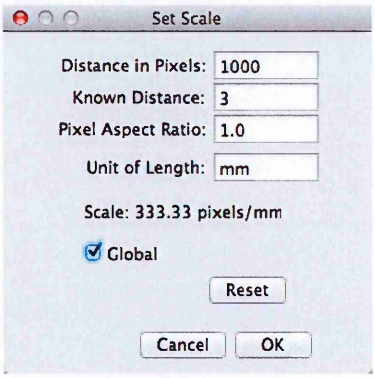

9. To analyse a charcoal image, open ImageJ and set the scale (Menu bar → Analyse→ Set scale) using all the calibration values previously obtained. The scale must be set each time imageJ is opened.
10. Select the measurements that will be taken from the "set measurements" list (Menu bar → Analyse→Set Measurements…). Make sure "area" is selected.
11. Open a charcoal image and convert its format to 8-bit (Menu bar → Image → Type → 8-bit)

12. Adjust the threshold (Menu bar → Image → Adjust → threshold…) using the slide bars until all the charcoal fragments become red and click "apply".

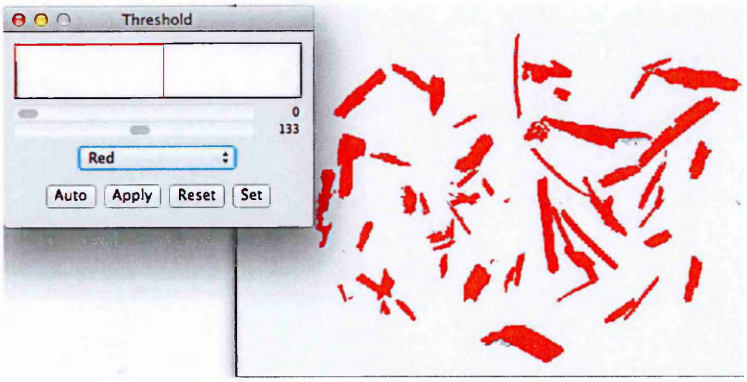

13. Calculate the area of the selected charcoal fragments (Menu bar → Analyse → Analyse particles…) making sure that "outlines" are selected and "display results" and "summarize" boxes are checked.

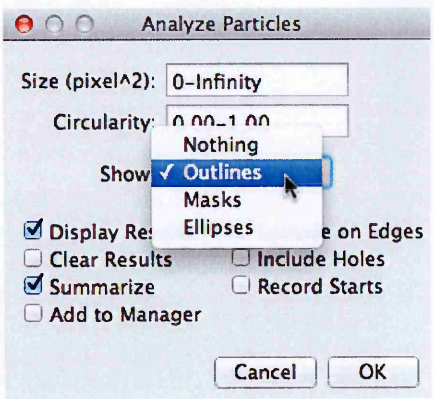

14. Three new windows will be displayed:

Outlines: Depict the particles that were included in the analysis.

Results: A list of all the measurements taken per particle.

Summary: A summary of the results

The commands used can be compiled in a macro (Menu bar → Plugins → Macros → Record…). Once the macro window appears, repeat steps 9 to 14 until results are displayed.

15. On the recording window select "create"

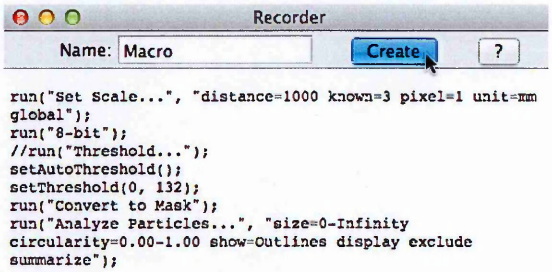

A new text-file will appear in a new window. Save this file in the same folder where the charcoal images are. Finally, open a new charcoal image and call the text file that was jus created (Menu bar → Plugins → Macros → Run…). All the used commands will be performed at once the text file is selected.

Once a sample is processed, transfer the charcoal fragment to an eppendorf vial for storage or mount for scanning electron microscope imaging.

Appendix V Supplementary material

The current appendix contains the supplementary material for Chapter 4

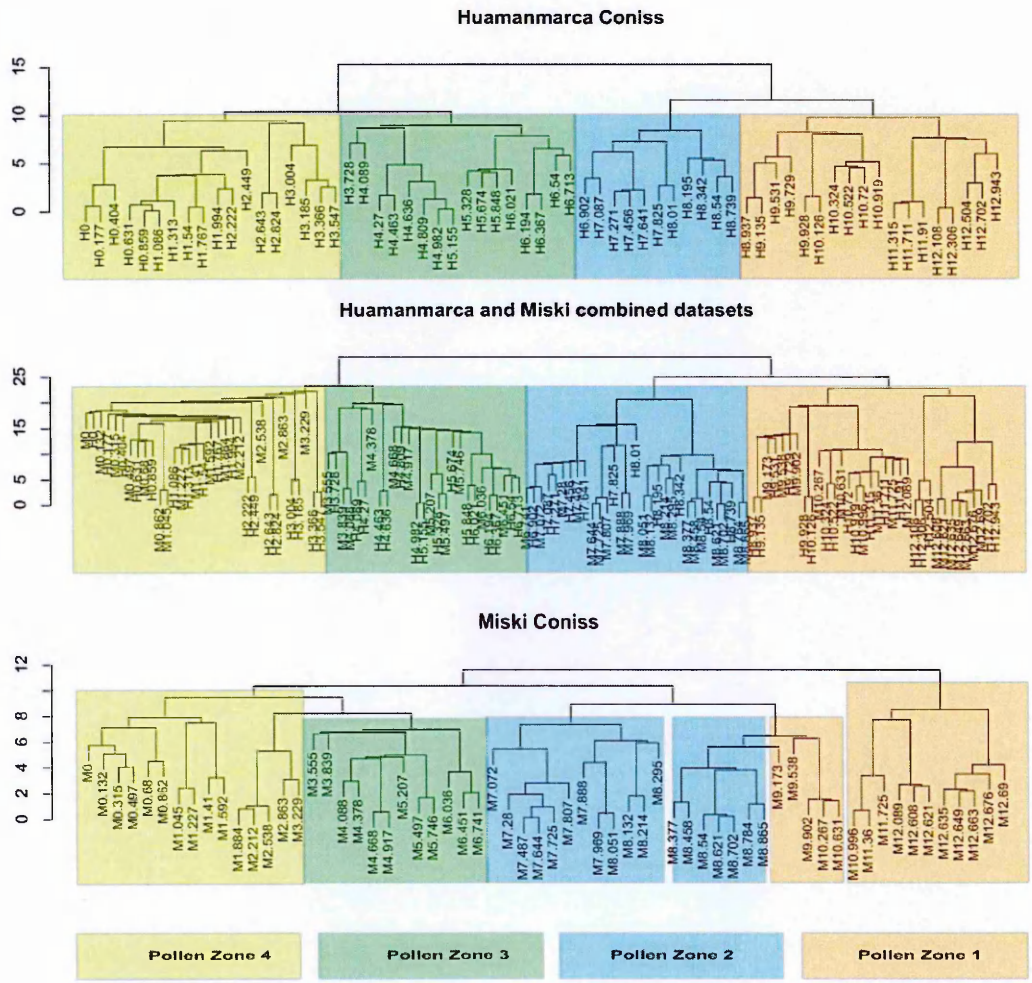

Coniss clustering performed on percentages for Lakes Huamanmarca, Miski and the combined dataset. Coloured boxes depict the pollen zones 4 (yellow), 3 (green), 2 (blue), and 1 (orange).

Appendix V

Table A5-1 List of plant taxonomic groups shared between Miski, Huamanmarca, and Pacucha. Data used for DCA zonation and Multiple-Response Permutation Procedure analyses (section 4.4).

#	Taxonomic level	#	Taxonomic level
1	Acalypha	23	Hesperomeles
2	Alchornea	24	Juglans
3	Alnus	25	Lactuceae
4	Althernanthera	26	Malvaceae
5	Ambrosia	27	Melastomataceae
6	Anacardiaceae	28	Mimosaceae
7	Apiaceae	29	Myricaceae
8	Asteraceae	30	Myrsinaceae
9	Bocconia	31	Myrtaceae
10	Brassicaceae	32	Plantago
11	Campanulaceae	33	Poaceae
12	Caryophyllaceae	34	Podocarpus
13	Cassia	35	Polylepis
14	Cecropia	36	Prosopis
15	Celtis	37	Rosaceae
16	Chenopodium	38	Rubiaceae
17	Cyperaceae	39	Solanacea
18	Dodonaea	40	Thalictrum
19	Ericaceae	41	Urticaceae Moraceae
20	Euphorbiaceae	42	Valerianaceae
21	Gynoxys	43	Vallea
22	Hedyosmum	44	Weinmannia

Table A5-2 List of diatom taxonomic groups shared between Miski and Pacucha used for DCA analysis.

#	Taxonomic level
1	Achnanthes
2	*Achnanthidium*
3	*Aulacoseira* ambigua
4	*Encyonema Cymbella*
5	*Eunotia*
6	*Fragilaria Staurosira*
7	*Gomphonema*
8	*Navicula*
9	*Nitzschia*
10	*Pinnularia*
11	*Surirella*

Appendix VI Environmental variables for MaxEnt

The current appendix contains the supplementary material for Chapter 5

Table A6-1 Environmental variables used in the *Polylepis* MaxEnt model. Variables in blue were excluded.

Details	Author/Source	Source URL	Code
Average Cloud Cover for Dec, Jan & Feb from 1998 to 2009	BADC	badc.nerc.ac.uk/home/index.html	aavgdjfcloud98to09_asc
Average Cloud Cover for Jun, Jul & Aug from 1998 to 2010	BADC	badc.nerc.ac.uk/home/index.html	aavgjjacloud98to09_asc
Average Cloud Cover annual, 1998 to 2009	BADC	badc.nerc.ac.uk/home/index.html	aavgyrcloud98to09_asc
Cumulative precipitation for Dec, Jan and Feb	UCSB Department of geography	www.geog.ucsb.edu/	acumuppbookdjf_asc
Cumulative precipitation for Jun, Jul & Aug	UCSB Department of geography	www.geog.ucsb.edu/	acumuppbookjja_asc
Digital elevation model	USGS	www.usgs.gov/	adem_asc
Ruggedness	derived from DEM	www.usgs.gov/	arugg_asc
Cumulative precipitation, annual	UCSB Department of geography	www.geog.ucsb.edu/	ayrppbookhagen_asc
Temperature Seasonality (standard deviation *100)	Hijmans et. al., 2005	www.worldclim.org	BIO4
Max Temperature of Warmest Month	Hijmans et. al., 2005	www.worldclim.org	BIO5
Min Temperature of Coldest Month	Hijmans et. al., 2005	www.worldclim.org	BIO6
Temperature Annual Range (BIO5-BIO6)	Hijmans et. al., 2005	www.worldclim.org	BIO7
Mean Temperature of Wettest Quarter	Hijmans et. al., 2005	www.worldclim.org	BIO8
Mean Temperature of Driest Quarter	Hijmans et. al., 2005	www.worldclim.org	BIO9
Mean Temperature of Warmest Quarter	Hijmans et. al., 2005	www.worldclim.org	BIO10
Mean Temperature of Coldest Quarter	Hijmans et. al., 2005	www.worldclim.org	BIO11
Annual Precipitation	Hijmans et. al., 2005	www.worldclim.org	BIO12

Appendix VI

Precipitation of Wettest Month	Hijmans et. al., 2005	www.worldclim.org	BIO13
Precipitation of Driest Month	Hijmans et. al., 2005	www.worldclim.org	BIO14
Precipitation Seasonality (Coefficient of Variation)	Hijmans et. al., 2005	www.worldclim.org	BIO15
Precipitation of Wettest Quarter	Hijmans et. al., 2005	www.worldclim.org	BIO16
Precipitation of Driest Quarter	Hijmans et. al., 2005	www.worldclim.org	BIO17
Fire 2005	JRC	bioval.jrc.ec.europa.eu/AboutUs.php	afire_asc
Average Shade for June-Dec 2005	derived from DEM	www.usgs.gov/	aavgshadesjundec2005_asc
Annual Mean Temperature	Hijmans et. al., 2005	www.worldclim.org	BIO1
Precipitation of Warmest Quarter	Hijmans et. al., 2005	www.worldclim.org	BIO18
Precipitation of Coldest Quarter	Hijmans et. al., 2005	www.worldclim.org	BIO19
Mean Diurnal Range (Mean of monthly (max temp - min temp))	Hijmans et. al., 2005	www.worldclim.org	BIO2
Isothermality (BIO2/BIO7) (* 100)	Hijmans et. al., 2005	www.worldclim.org	BIO3

Appendix VII Acronyms

The current appendix contains the supplementary material for Chapter 5

ANOSIM	Analysis of similarity
AUC	Area under the Receiver Operating Characteristic
BH	Bolivian High
DCA	Detrended Correspondence Analysis
ENSO	El Niño Southern Oscillation
GCM	General Circulation Models
ITCZ	Intertropical Convergence Zone
LGM	Last Glacial Maximum
LOI	Loss-on-ignition
masl	Metres above sea level
MaxEnt	Maximum entropy
MHDE	Mid Holocene Dry Event
MS	Magnetic Susceptibility
Negative ENSO	La Niña
NMDS	Non-metric Multidimensional Scaling
PCA	Principal Component Analysis
Positive ENSO	El Niño
SALLJ	South American Low Level Jet
SASM	South American Summer Monsoon
SST	Sea Surface Temperature
YD	Younger Dryas

Appendix VIII Palaeoecological data

Table A8-1 Lake Pacucha pollen counts, 1 of 11. New (bold text) and published data (Valencia et al. 2010) is included.

Volume CC	0.5	**0.5**	**0.5**	**0.5**	**0.5**	**0.5**	**0.5**	**0.5**	0.5	**0.5**
Age	0	**19.1**	**38.2**	**57.3**	**76.3**	**95.4**	**114.5**	**133.6**	143.1	**152.7**
Depth (cm)	0	***4***	***8***	***12***	***16***	***20***	***24***	***28***	30	***32***
Lycopodium	730	**1923**	**1033**	**1400**	**1375**	**999**	**1378**	**1394**	464	**1089**
Pollen Sum	308	**357**	**314**	**316**	**322**	**325**	**310**	**312**	371	**327**
Polylepis	0	**1**	**1**	**2**	**2**	**1**	**2**	**3**	2	**0**
Melastomataceae	3	**2**	**3**	**1**	**1**	**3**	**1**	**0**	0	**3**
Hesperomeles	0	**0**	**0**	**1**	**0**	**0**	**0**	**3**	6	**4**
Gynoxys	0	**0**	**0**	**0**	**0**	**0**	**0**	**0**	0	**0**
Poaceae	51	**72**	**48**	**47**	**43**	**47**	**33**	**45**	69	**35**
Asteraceae	20	**0**	**27**	**32**	**26**	**24**	**19**	**39**	43	**32**
Caryophyllaceae	2	**0**	**1**	**0**	**1**	**1**	**2**	**1**	0	**0**
Plantago	5	**13**	**11**	**9**	**3**	**6**	**9**	**4**	7	**5**
Ambrosia	16	**31**	**26**	**36**	**36**	**29**	**50**	**33**	42	**44**
Thalictrum	1	**2**	**2**	**3**	**4**	**3**	**5**	**3**	1	**2**
Apiaceae	3	**9**	**4**	**1**	**0**	**1**	**1**	**3**	1	**1**
Chenopodium	1	**5**	**4**	**5**	**3**	**4**	**4**	**3**	3	**2**
Lactuceae	0	**1**	**0**	**2**	**1**	**0**	**3**	**2**	1	**0**
Valerianaceae	0	**0**	**0**	**1**	**2**	**0**	**0**	**0**	1	**0**
Campanulaceae	0	**0**	**0**	**0**	**0**	**0**	**0**	**0**	0	**0**
Althernanthera	0	**1**	**1**	**0**	**0**	**1**	**0**	**1**	1	**0**
Brassicaceae	9	**9**	**18**	**12**	**13**	**10**	**5**	**14**	7	**12**
Rubiaceae	0	**0**	**0**	**0**	**0**	**0**	**0**	**0**	0	**0**
Malvaceae	1	**0**	**0**	**0**	**1**	**0**	**1**	**1**	0	**1**
Urticaceae Moraceae	38	**25**	**17**	**9**	**20**	**12**	**13**	**15**	50	**37**
Hedyosmum	7	**8**	**6**	**9**	**13**	**12**	**3**	**4**	13	**5**
Acalypha	16	**11**	**15**	**8**	**19**	**10**	**13**	**11**	20	**15**
Podocarpus	6	**20**	**5**	**8**	**3**	**14**	**11**	**13**	9	**2**
Ericaceae	0	**1**	**0**	**0**	**0**	**0**	**3**	**0**	0	**0**
Myrsinaceae	7	**3**	**2**	**4**	**2**	**3**	**0**	**6**	7	**7**
Alchornea	6	**3**	**4**	**0**	**3**	**2**	**5**	**3**	3	**1**
Juglans	3	**4**	**1**	**0**	**2**	**2**	**2**	**0**	0	**2**
Alnus	42	**41**	**34**	**48**	**51**	**62**	**47**	**39**	22	**35**
Vallea	2	**0**	**0**	**0**	**0**	**0**	**0**	**0**	0	**0**
Bocconia	0	**0**	**0**	**0**	**0**	**0**	**1**	**0**	0	**0**
Myricaceae	0	**1**	**0**	**0**	**0**	**2**	**1**	**0**	0	**0**
Solanacea	2	**0**	**4**	**2**	**2**	**2**	**2**	**1**	1	**5**
Weinmannia	0	**1**	**1**	**0**	**0**	**1**	**1**	**0**	0	**0**
Rosaceae	0	**0**	**1**	**0**	**0**	**0**	**0**	**0**	0	**0**
Myrtaceae	2	**1**	**0**	**0**	**0**	**0**	**0**	**0**	0	**1**
Cassia	0	**0**	**0**	**0**	**0**	**0**	**0**	**0**	0	**0**
Cecropia	0	**0**	**0**	**0**	**0**	**0**	**0**	**0**	0	**0**
Celtis	6	**4**	**3**	**1**	**1**	**0**	**4**	**0**	2	**4**
Anacardiaceae	2	**5**	**4**	**6**	**5**	**4**	**4**	**3**	2	**3**
Prosopis	1	**1**	**1**	**2**	**0**	**0**	**3**	**0**	1	**1**
Euphorbiaceae	0	**0**	**0**	**0**	**1**	**0**	**0**	**0**	0	**0**
Mimosaceae	0	**0**	**0**	**0**	**0**	**0**	**0**	**0**	0	**0**
Dodonaea	6	**8**	**6**	**10**	**12**	**12**	**13**	**8**	13	**9**
Cyperaceae	17	**40**	**23**	**22**	**24**	**27**	**21**	**32**	22	**36**
Other/Broken unidentified	33	**34**	**41**	**35**	**28**	**30**	**28**	**22**	22	**23**

Appendix VIII

Table A8-1 Lake Pacucha pollen counts, continued (2 of 11). New (bold text) and published data (Valencia et al. 2010) is included.

Volume CC	**0.5**	**0.5**	**0.5**	**0.5**	**0.5**	**0.5**	0.5	**0.5**	**0.5**	**0.5**
Age	**171.8**	**190.9**	**209.9**	**229**	**248.1**	**267.2**	286.3	**305.4**	**324.4**	**343.5**
Depth (cm)	***36***	***40***	***44***	***48***	***52***	***56***	60	***64***	***68***	***72***
Lycopodium	**938**	**855**	**1244**	**1301**	**1462**	**2187**	730	**1351**	**1786**	**1749**
Pollen Sum	**303**	**324**	**291**	**307**	**324**	**313**	339	**322**	**329**	**340**
Polylepis	**1**	**4**	**5**	**4**	**2**	**1**	0	**2**	**0**	**2**
Melastomataceae	**1**	**0**	**2**	**0**	**2**	**1**	2	**0**	**3**	**3**
Hesperomeles	**2**	**0**	**0**	**0**	**1**	**0**	0	**3**	**3**	**7**
Gynoxys	**0**	**0**	**0**	**0**	**0**	**0**	0	**0**	**0**	**0**
Poaceae	**37**	**40**	**39**	**56**	**49**	**43**	66	**64**	**65**	**59**
Asteraceae	**40**	**33**	**30**	**41**	**30**	**36**	24	**39**	**29**	**39**
Caryophyllaceae	**1**	**0**	**2**	**0**	**3**	**3**	0	**0**	**0**	**1**
Plantago	**3**	**10**	**5**	**8**	**12**	**2**	5	**3**	**4**	**7**
Ambrosia	**38**	**40**	**51**	**57**	**69**	**64**	48	**56**	**66**	**74**
Thalictrum	**8**	**1**	**3**	**8**	**2**	**2**	3	**5**	**3**	**3**
Apiaceae	**3**	**3**	**3**	**2**	**3**	**1**	4	**4**	**0**	**2**
Chenopodium	**5**	**9**	**1**	**4**	**6**	**4**	5	**0**	**1**	**5**
Lactuceae	**3**	**0**	**0**	**0**	**1**	**2**	0	**0**	**0**	**2**
Valerianaceae	**0**	**1**	**1**	**0**	**0**	**0**	0	**1**	**0**	**0**
Campanulaceae	**0**	**0**	**0**	**0**	**0**	**0**	0	**0**	**0**	**0**
Althernanthera	**1**	**1**	**0**	**1**	**1**	**0**	1	**0**	**0**	**0**
Brassicaceae	**8**	**13**	**0**	**14**	**9**	**19**	9	**11**	**12**	**11**
Rubiaceae	**0**	**0**	**0**	**0**	**0**	**0**	0	**0**	**0**	**0**
Malvaceae	**1**	**0**	**0**	**1**	**0**	**0**	0	**0**	**0**	**0**
Urticaceae Moraceae	**20**	**51**	**23**	**18**	**26**	**57**	62	**32**	**31**	**34**
Hedyosmum	**8**	**2**	**8**	**4**	**7**	**6**	8	**4**	**4**	**4**
Acalypha	**7**	**19**	**13**	**4**	**10**	**11**	20	**10**	**3**	**3**
Podocarpus	**12**	**6**	**5**	**7**	**5**	**0**	10	**6**	**3**	**4**
Ericaceae	**1**	**2**	**0**	**0**	**1**	**2**	0	**1**	**2**	**1**
Myrsinaceae	**4**	**6**	**3**	**3**	**4**	**1**	2	**5**	**7**	**12**
Alchornea	**1**	**4**	**3**	**2**	**1**	**3**	0	**3**	**1**	**3**
Juglans	**0**	**0**	**1**	**3**	**0**	**2**	1	**2**	**1**	**2**
Alnus	**20**	**14**	**27**	**17**	**26**	**17**	22	**13**	**21**	**10**
Vallea	**0**	**0**	**0**	**0**	**0**	**0**	0	**0**	**0**	**0**
Bocconia	**0**	**0**	**0**	**0**	**1**	**0**	0	**1**	**0**	**1**
Myricaceae	**0**	**0**	**0**	**1**	**1**	**0**	0	**1**	**1**	**0**
Solanacea	**2**	**2**	**1**	**4**	**1**	**2**	1	**0**	**1**	**0**
Weinmannia	**0**	**0**	**0**	**1**	**0**	**1**	0	**1**	**0**	**0**
Rosaceae	**0**	**0**	**1**	**0**	**0**	**0**	0	**0**	**0**	**0**
Myrtaceae	**1**	**0**	**0**	**0**	**0**	**0**	0	**0**	**0**	**0**
Cassia	**0**	**0**	**0**	**0**	**0**	**0**	0	**0**	**0**	**0**
Cecropia	**0**	**0**	**0**	**0**	**0**	**0**	0	**0**	**0**	**0**
Celtis	**6**	**5**	**1**	**2**	**3**	**3**	3	**1**	**3**	**4**
Anacardiaceae	**1**	**3**	**2**	**0**	**3**	**1**	1	**4**	**3**	**3**
Prosopis	**3**	**2**	**1**	**1**	**5**	**3**	1	**1**	**2**	**0**
Euphorbiaceae	**0**	**0**	**0**	**0**	**0**	**0**	0	**0**	**1**	**0**
Mimosaceae	**0**	**0**	**0**	**0**	**0**	**0**	0	**0**	**0**	**0**
Dodonaea	**11**	**12**	**12**	**6**	**6**	**3**	5	**9**	**13**	**12**
Cyperaceae	**39**	**25**	**18**	**14**	**9**	**8**	18	**16**	**29**	**23**
Other/Broken unidentified	**15**	**16**	**30**	**24**	**25**	**15**	18	**24**	**17**	**9**

Table A8-1 Lake Pacucha pollen counts, continued (3 of 11). New (bold text) and published data (Valencia et al. 2010) is included.

Volume CC	**0.5**	**0.5**	**0.5**	**0.5**	0.5	**0.5**	**0.5**	**0.5**	**0.5**	**0.5**
Age	**362.6**	**381.7**	**400.8**	**419.9**	429.4	**439**	**458**	**477.1**	**496.2**	**515.3**
Depth (cm)	***76***	***80***	***84***	***88***	90	***92***	***96***	***100***	***104***	***108***
Lycopodium	**2000**	**1732**	**901**	**750**	673	**801**	**1240**	**914**	**809**	**776**
Pollen Sum	**193**	**323**	**331**	**318**	332	**322**	**319**	**319**	**323**	**327**
Polylepis	**2**	**4**	**0**	**6**	1	**2**	**4**	**2**	**0**	**1**
Melastomataceae	**0**	**3**	**1**	**0**	5	**1**	**3**	**0**	**0**	**4**
Hesperomeles	**0**	**2**	**0**	**3**	5	**2**	**1**	**3**	**0**	**1**
Gynoxys	**0**	**0**	**0**	**0**	0	**0**	**0**	**0**	**0**	**0**
Poaceae	**42**	**64**	**59**	**57**	86	**75**	**80**	**65**	**54**	**72**
Asteraceae	**20**	**39**	**16**	**26**	34	**22**	**32**	**29**	**25**	**29**
Caryophyllaceae	**0**	**1**	**1**	**2**	0	**0**	**3**	**1**	**0**	**1**
Plantago	**3**	**5**	**8**	**6**	5	**5**	**3**	**5**	**9**	**5**
Ambrosia	**39**	**38**	**55**	**66**	42	**30**	**37**	**34**	**34**	**25**
Thalictrum	**3**	**4**	**7**	**2**	5	**3**	**1**	**2**	**3**	**2**
Apiaceae	**0**	**2**	**3**	**2**	1	**5**	**3**	**1**	**1**	**1**
Chenopodium	**1**	**2**	**7**	**0**	0	**3**	**2**	**4**	**1**	**1**
Lactuceae	**1**	**0**	**0**	**0**	1	**0**	**0**	**1**	**0**	**0**
Valerianaceae	**0**	**0**	**0**	**0**	1	**0**	**0**	**0**	**1**	**1**
Campanulaceae	**0**	**0**	**0**	**0**	0	**0**	**0**	**0**	**0**	**0**
Althernanthera	**0**	**2**	**0**	**0**	2	**0**	**0**	**0**	**0**	**0**
Brassicaceae	**4**	**11**	**8**	**10**	2	**9**	**7**	**5**	**6**	**3**
Rubiaceae	**0**	**0**	**0**	**0**	0	**0**	**0**	**0**	**0**	**0**
Malvaceae	**0**	**0**	**0**	**0**	0	**1**	**0**	**1**	**1**	**0**
Urticaceae Moraceae	**12**	**34**	**33**	**25**	34	**39**	**38**	**31**	**37**	**40**
Hedyosmum	**6**	**6**	**8**	**4**	2	**7**	**1**	**3**	**6**	**3**
Acalypha	**8**	**7**	**6**	**12**	13	**4**	**5**	**14**	**14**	**9**
Podocarpus	**4**	**3**	**2**	**2**	9	**3**	**1**	**1**	**6**	**8**
Ericaceae	**1**	**1**	**0**	**2**	2	**2**	**0**	**1**	**0**	**0**
Myrsinaceae	**2**	**4**	**0**	**6**	6	**4**	**3**	**12**	**5**	**2**
Alchornea	**0**	**2**	**8**	**4**	3	**8**	**0**	**1**	**3**	**4**
Juglans	**0**	**2**	**0**	**1**	0	**0**	**0**	**0**	**0**	**1**
Alnus	**11**	**26**	**31**	**20**	19	**35**	**42**	**52**	**62**	**49**
Vallea	**0**	**0**	**0**	**0**	0	**0**	**0**	**0**	**1**	**1**
Bocconia	**2**	**0**	**0**	**3**	1	**0**	**2**	**2**	**0**	**0**
Myricaceae	**1**	**1**	**0**	**0**	0	**0**	**0**	**0**	**1**	**0**
Solanacea	**1**	**0**	**0**	**0**	1	**1**	**1**	**0**	**3**	**0**
Weinmannia	**0**	**0**	**3**	**0**	0	**0**	**3**	**2**	**0**	**1**
Rosaceae	**1**	**0**	**0**	**0**	0	**0**	**0**	**0**	**0**	**0**
Myrtaceae	**0**	**0**	**0**	**0**	0	**0**	**5**	**0**	**2**	**2**
Cassia	**0**	**0**	**0**	**0**	0	**0**	**0**	**0**	**0**	**0**
Cecropia	**0**	**0**	**0**	**0**	0	**0**	**0**	**0**	**0**	**0**
Celtis	**0**	**3**	**2**	**5**	3	**0**	**0**	**3**	**1**	**4**
Anacardiaceae	**0**	**0**	**2**	**2**	1	**2**	**1**	**1**	**4**	**2**
Prosopis	**0**	**2**	**3**	**1**	1	**3**	**1**	**5**	**3**	**0**
Euphorbiaceae	**0**	**1**	**0**	**1**	0	**0**	**0**	**0**	**0**	**0**
Mimosaceae	**0**	**1**	**0**	**0**	0	**0**	**1**	**0**	**0**	**1**
Dodonaea	**8**	**6**	**12**	**4**	10	**10**	**10**	**10**	**5**	**4**
Cyperaceae	**15**	**25**	**30**	**19**	30	**32**	**15**	**12**	**18**	**31**
Other/Broken unidentified	***6***	**22**	***26***	**27**	7	**14**	**14**	***16***	**17**	**19**

Table A8-1 Lake Pacucha pollen counts, continued (4 of 11) . New (bold text) and published data (Valencia et al. 2010) is included.

Volume CC	**0.5**	**0.5**	0.5	**0.5**	**0.5**	**0.5**	0.5	0.5	0.5
Age	**534.4**	**553.5**	572.6	**591.6**	**610.7**	**634.7**	750	942.2	1260.9
Depth (cm)	***112***	***116***	120	***124***	***128***	***132***	150	180	210
Lycopodium	**1358**	**1729**	203	**1818**	**378**	**1361**	2000	2000	265
Pollen Sum	**326**	**317**	359	**314**	**301**	**311**	177	228	362
Polylepis	**3**	**1**	2	**7**	**2**	**3**	2	1	0
Melastomataceae	**2**	**1**	2	**1**	**3**	**4**	0	1	5
Hesperomeles	**0**	**0**	0	**0**	**0**	**1**	0	0	0
Gynoxys	**0**	**0**	0	**0**	**0**	**0**	0	0	0
Poaceae	**73**	**111**	102	**104**	**101**	**101**	55	57	139
Asteraceae	**36**	**19**	24	**23**	**21**	**33**	21	26	18
Caryophyllaceae	**0**	**0**	2	**2**	**1**	**3**	1	1	0
Plantago	**3**	**2**	7	**5**	**1**	**4**	2	6	9
Ambrosia	**29**	**21**	15	**13**	**14**	**5**	17	13	28
Thalictrum	**0**	**10**	7	**2**	**3**	**4**	1	0	21
Apiaceae	**0**	**3**	1	**3**	**0**	**1**	1	1	0
Chenopodium	**2**	**0**	0	**1**	**0**	**0**	3	2	1
Lactuceae	**1**	**1**	0	**2**	**1**	**2**	0	0	0
Valerianaceae	**1**	**0**	0	**1**	**0**	**0**	0	0	0
Campanulaceae	**0**	**0**	0	**0**	**0**	**0**	0	0	0
Althernanthera	**0**	**0**	0	**0**	**1**	**1**	0	0	1
Brassicaceae	**8**	**1**	2	**0**	**0**	**0**	0	0	0
Rubiaceae	**0**	**0**	0	**0**	**0**	**0**	0	0	0
Malvaceae	**0**	**0**	0	**1**	**0**	**0**	0	0	0
Urticaceae Moraceae	**21**	**38**	44	**19**	**31**	**21**	17	36	53
Hedyosmum	**10**	**6**	16	**16**	**4**	**12**	6	10	13
Acalypha	**11**	**10**	13	**4**	**14**	**11**	6	10	21
Podocarpus	**4**	**6**	3	**4**	**3**	**4**	2	1	3
Ericaceae	**0**	**0**	1	**1**	**0**	**1**	0	1	1
Myrsinaceae	**3**	**1**	11	**1**	**8**	**8**	0	3	3
Alchornea	**1**	**1**	3	**9**	**6**	**3**	4	5	1
Juglans	**3**	**0**	0	**0**	**1**	**1**	0	2	0
Alnus	**43**	**40**	24	**18**	**20**	**8**	8	12	7
Vallea	**0**	**0**	2	**0**	**0**	**2**	0	0	0
Bocconia	**2**	**0**	0	**1**	**0**	**2**	0	0	0
Myricaceae	**0**	**0**	1	**2**	**1**	**0**	0	0	0
Solanacea	**3**	**0**	2	**1**	**1**	**2**	0	2	3
Weinmannia	**1**	**1**	1	**0**	**0**	**2**	0	0	0
Rosaceae	**0**	**0**	0	**0**	**0**	**0**	0	0	0
Myrtaceae	**0**	**0**	0	**0**	**0**	**0**	0	0	0
Cassia	**0**	**0**	0	**0**	**0**	**0**	0	0	0
Cecropia	**0**	**0**	0	**0**	**0**	**1**	0	0	0
Celtis	**0**	**2**	7	**1**	**1**	**6**	1	5	3
Anacardiaceae	**2**	**1**	1	**2**	**0**	**2**	1	2	2
Prosopis	**1**	**2**	5	**2**	**5**	**6**	0	0	0
Euphorbiaceae	**0**	**0**	0	**0**	**0**	**0**	0	0	0
Mimosaceae	**0**	**1**	0	**0**	**0**	**0**	0	0	0
Dodonaea	**7**	**3**	3	**5**	**2**	**0**	0	2	0
Cyperaceae	**39**	**24**	39	**45**	**44**	**44**	6	6	13
Other/Broken unidentified	**17**	**11**	19	**18**	**12**	**13**	23	23	17

Table A8-1 Lake Pacucha pollen counts, continued (5 of 11) . New (bold text) and published data (Valencia et al. 2010) is included.

Volume CC	0.5	0.5	0.5	0.5	0.5	0.5	0.5	0.5	0.5
Age	1618.2	1855.5	2084.2	2313	2541.8	2770.5	2985.2	3064.3	3143.5
Depth (cm)	240	270	300	330	360	390	420	435	450
Lycopodium	280	1085	2000	2000	2000	1279	173	380	375
Pollen Sum	321	333	141	128	59	435	314	334	335
Polylepis	2	1	0	0	0	1	1	0	2
Melastomataceae	2	4	1	0	0	5	1	3	7
Hesperomeles	0	0	0	0	0	1	3	0	2
Gynoxys	0	0	0	0	0	0	0	0	0
Poaceae	110	86	67	26	26	139	140	92	100
Asteraceae	15	22	14	6	6	19	20	18	18
Caryophyllaceae	0	1	0	1	0	1	0	1	0
Plantago	3	12	2	2	0	3	16	5	7
Ambrosia	23	36	2	11	0	36	5	54	54
Thalictrum	6	14	0	0	1	6	11	16	15
Apiaceae	1	3	0	0	0	6	0	1	0
Chenopodium	3	4	1	1	3	12	3	6	16
Lactuceae	0	0	0	0	0	0	0	0	0
Valerianaceae	0	0	0	0	0	2	0	0	0
Campanulaceae	0	0	0	0	0	0	0	0	0
Althernanthera	0	0	1	1	0	1	0	1	0
Brassicaceae	0	2	0	2	0	3	1	0	0
Rubiaceae	0	0	0	0	0	0	0	0	0
Malvaceae	0	0	0	0	0	1	0	0	0
Urticaceae Moraceae	40	35	4	21	0	60	50	50	26
Hedyosmum	9	8	4	3	0	16	4	10	2
Acalypha	13	30	4	10	1	56	18	17	21
Podocarpus	1	3	2	0	1	4	2	6	7
Ericaceae	0	1	0	0	0	0	0	2	3
Myrsinaceae	7	6	3	1	0	7	8	5	6
Alchornea	3	3	1	2	0	3	4	2	6
Juglans	0	0	0	1	0	0	2	0	0
Alnus	0	1	1	4	1	3	0	1	2
Vallea	0	1	1	2	0	5	1	1	2
Bocconia	0	0	0	0	0	0	0	2	1
Myricaceae	1	1	0	0	0	0	1	2	0
Solanacea	2	2	1	1	0	1	0	0	0
Weinmannia	3	3	0	0	0	0	0	0	0
Rosaceae	0	0	0	0	0	0	0	0	0
Myrtaceae	0	0	0	0	0	0	0	0	0
Cassia	0	0	0	0	0	0	0	0	0
Cecropia	0	0	0	2	0	1	4	3	0
Celtis	4	5	0	0	0	0	2	2	4
Anacardiaceae	0	0	0	0	0	1	0	0	0
Prosopis	1	0	0	0	0	2	0	1	1
Euphorbiaceae	0	0	0	0	0	0	0	0	0
Mimosaceae	0	0	0	0	0	0	0	0	0
Dodonaea	3	0	0	0	0	1	1	0	2
Cyperaceae	45	23	11	3	3	4	7	11	15
Other/Broken unidentified	24	26	21	28	17	35	9	22	16

Table A8-1 Lake Pacucha pollen counts, continued (6 of 11). New (bold text) and published data (Valencia et al. 2010) is included.

Volume CC	0.5	0.5	0.5	0.5	0.5	0.5	0.5	0.5
Age	3222.7	3381	3460.2	3539.4	3618.5	3697.7	3776.9	3856.1
Depth (cm)	465	495	510	525	540	555	570	585
Lycopodium	310	1218	1150	155	600	550	1500	1200
Pollen Sum	330	315	364	327	332	334	309	351
Polylepis	3	2	2	0	2	0	2	0
Melastomataceae	3	1	5	6	5	4	2	6
Hesperomeles	0	0	1	1	1	1	0	0
Gynoxys	0	0	0	0	0	0	0	0
Poaceae	130	76	74	104	86	89	76	92
Asteraceae	14	11	15	12	18	29	22	17
Caryophyllaceae	1	0	0	0	0	2	0	0
Plantago	3	6	5	9	2	3	2	5
Ambrosia	36	48	57	63	34	43	39	45
Thalictrum	6	9	3	13	11	2	9	11
Apiaceae	1	1	2	0	0	0	3	1
Chenopodium	32	80	104	12	75	84	65	74
Lactuceae	0	0	0	0	0	0	0	0
Valerianaceae	0	0	0	0	0	1	0	0
Campanulaceae	0	0	0	0	0	0	0	0
Althernanthera	0	0	0	0	1	0	0	1
Brassicaceae	0	0	2	0	1	1	1	1
Rubiaceae	0	0	0	0	0	0	0	0
Malvaceae	0	0	0	0	0	0	0	0
Urticaceae Moraceae	41	19	37	40	18	24	34	34
Hedyosmum	5	5	6	6	6	0	4	2
Acalypha	17	17	16	17	25	16	9	16
Podocarpus	2	4	2	3	3	3	2	5
Ericaceae	1	1	1	1	2	1	2	1
Myrsinaceae	6	2	3	3	8	3	4	2
Alchornea	1	1	3	5	5	2	4	1
Juglans	0	2	0	0	0	1	0	0
Alnus	2	0	1	2	0	0	0	0
Vallea	0	0	1	2	0	0	1	0
Bocconia	0	2	1	0	0	0	1	1
Myricaceae	0	0	0	0	0	0	0	1
Solanacea	0	1	0	1	1	2	1	1
Weinmannia	0	0	0	1	1	3	1	2
Rosaceae	0	0	0	0	0	0	0	0
Myrtaceae	0	0	0	0	0	0	0	0
Cassia	0	0	0	0	0	0	0	0
Cecropia	0	0	0	0	0	0	1	0
Celtis	4	3	1	0	3	1	2	2
Anacardiaceae	1	1	0	0	0	1	1	2
Prosopis	0	0	1	0	0	0	0	0
Euphorbiaceae	0	0	0	0	0	0	0	0
Mimosaceae	0	0	0	0	0	0	0	1
Dodonaea	0	0	1	0	0	0	1	0
Cyperaceae	10	7	4	12	12	5	9	11
Other/Broken unidentified	11	16	16	14	12	13	11	16

Table A8-1 Lake Pacucha pollen counts, continued (7 of 11). New (bold text) and published data (Valencia et al. 2010) is included.

Volume CC	0.5	0.5	0.5	0.5	0.5	0.5	0.5	0.5	0.5
Age	4014.4	4093.6	4199.1	4304.7	4410.3	4515.8	4621.4	4751.7	4839.8
Depth (cm)	615	630	650	670	690	710	730	750	760
Lycopodium	1039	1280	2000	265	560	175	215	536	510
Pollen Sum	318	315	117	337	329	342	401	316	343
Polylepis	1	0	0	1	0	0	3	0	2
Melastomataceae	1	1	0	2	2	2	1	3	1
Hesperomeles	0	0	0	0	0	1	3	0	0
Gynoxys	0	0	0	0	0	0	0	0	0
Poaceae	77	58	11	97	125	138	152	90	120
Asteraceae	23	24	38	27	11	20	22	23	25
Caryophyllaceae	0	2	0	0	1	0	2	1	0
Plantago	2	1	2	1	2	5	3	3	0
Ambrosia	45	35	4	45	62	34	40	31	23
Thalictrum	4	2	0	11	10	6	8	3	8
Apiaceae	2	0	0	2	0	2	3	0	0
Chenopodium	59	160	53	54	52	29	54	107	75
Lactuceae	0	0	0	0	0	0	0	0	0
Valerianaceae	0	0	0	0	1	1	0	0	0
Campanulaceae	0	0	0	0	0	0	0	0	0
Althernanthera	1	0	0	1	0	0	1	0	2
Brassicaceae	1	1	0	1	1	1	1	1	1
Rubiaceae	0	0	0	0	0	0	0	0	0
Malvaceae	0	0	0	1	0	0	1	0	0
Urticaceae Moraceae	35	5	0	27	12	26	37	16	32
Hedyosmum	3	1	3	9	9	5	5	5	7
Acalypha	26	1	0	19	5	25	11	9	12
Podocarpus	1	0	0	2	3	3	6	0	9
Ericaceae	2	0	0	1	3	1	1	0	0
Myrsinaceae	3	0	0	5	4	11	6	1	1
Alchornea	4	1	0	0	0	3	2	5	2
Juglans	0	0	0	0	0	2	0	0	2
Alnus	1	1	0	0	0	0	0	0	0
Vallea	0	0	0	0	1	0	1	0	1
Bocconia	0	0	0	0	0	1	0	1	0
Myricaceae	0	0	0	0	0	0	0	0	0
Solanacea	1	0	0	0	0	0	0	0	0
Weinmannia	1	0	0	1	1	0	1	0	1
Rosaceae	0	0	0	0	0	0	0	0	0
Myrtaceae	0	1	0	0	0	0	0	0	0
Cassia	0	0	0	0	0	0	0	0	0
Cecropia	0	0	0	1	0	0	0	0	0
Celtis	1	0	0	3	1	2	4	2	0
Anacardiaceae	1	0	0	0	0	0	2	0	2
Prosopis	0	0	0	0	0	0	0	0	0
Euphorbiaceae	0	0	0	0	0	0	0	0	0
Mimosaceae	0	0	0	0	0	1	0	0	0
Dodonaea	0	0	0	2	0	0	1	0	0
Cyperaceae	8	3	0	10	7	5	18	5	8
Other/Broken unidentified	15	18	6	14	16	18	12	10	9

Table A8-1 Lake Pacucha pollen counts, continued (8 of 11). New (bold text) and published data (Valencia et al. 2010) is included.

Volume CC	0.5	0.5	0.5	0.5	0.5	0.5	0.5	0.5	0.5
Age	4927.9	5150.6	5507.7	5864.9	6222	6579.2	6961.3	7171	7380.7
Depth (cm)	770	780	790	800	810	820	830	835	840
Lycopodium	195	245	141	140	142	173	192	167	107
Pollen Sum	358	330	351	394	372	344	372	323	350
Polylepis	1	0	1	5	1	1	3	3	1
Melastomataceae	1	2	3	2	5	3	3	1	3
Hesperomeles	0	0	0	1	1	0	0	0	1
Gynoxys	0	0	0	0	0	0	0	0	0
Poaceae	143	120	122	156	155	176	155	160	170
Asteraceae	32	22	11	18	18	16	15	16	14
Caryophyllaceae	0	1	0	1	0	0	0	0	0
Plantago	7	4	3	9	8	12	6	10	9
Ambrosia	48	39	54	37	29	15	13	5	3
Thalictrum	4	5	9	21	8	14	9	13	7
Apiaceae	3	1	3	3	1	1	0	5	2
Chenopodium	36	60	45	1	4	1	1	2	4
Lactuceae	0	0	0	0	0	0	0	0	0
Valerianaceae	0	0	0	0	0	0	1	0	0
Campanulaceae	0	0	0	0	0	0	0	0	0
Althernanthera	1	0	1	0	1	1	0	1	0
Brassicaceae	0	0	0	1	0	1	0	0	0
Rubiaceae	0	0	0	0	0	0	0	0	0
Malvaceae	2	0	1	0	1	0	0	0	0
Urticaceae Moraceae	36	27	46	55	60	37	70	60	42
Hedyosmum	2	7	6	5	2	5	7	5	1
Acalypha	4	14	12	19	12	7	9	9	10
Podocarpus	5	5	1	11	12	12	15	6	10
Ericaceae	1	1	0	2	2	0	0	0	1
Myrsinaceae	1	2	1	4	5	4	5	0	3
Alchornea	2	2	4	2	6	2	5	2	5
Juglans	0	0	3	0	0	0	0	0	2
Alnus	2	1	3	2	2	2	2	1	1
Vallea	1	0	0	0	0	2	0	0	1
Bocconia	1	0	2	0	0	0	1	0	0
Myricaceae	0	0	0	0	0	0	0	0	0
Solanacea	0	2	1	1	0	1	0	0	1
Weinmannia	0	1	0	0	0	0	3	0	0
Rosaceae	0	0	0	0	0	0	0	0	0
Myrtaceae	0	0	0	0	0	0	0	0	0
Cassia	0	0	0	0	0	0	0	0	0
Cecropia	0	0	0	0	0	0	1	0	0
Celtis	1	2	0	3	3	4	4	2	2
Anacardiaceae	0	0	1	2	0	0	2	1	0
Prosopis	0	0	3	2	4	1	9	1	3
Euphorbiaceae	0	0	0	0	0	0	0	0	0
Mimosaceae	0	0	0	0	0	0	0	0	0
Dodonaea	0	2	0	0	0	0	1	0	1
Cyperaceae	12	7	9	19	19	14	17	4	41
Other/Broken unidentified	12	3	6	12	13	12	15	16	12

Table A8-1 Lake Pacucha pollen counts, continued (9 of 11). New (bold text) and published data (Valencia et al. 2010) is included.

Volume CC	0.5	0.5	0.5	0.5	0.5	0.5	0.5	0.5	0.5
Age	7590.4	7800.2	8013.9	8233.6	8453.3	8673	8892.7	9112.5	9332.2
Depth (cm)	845	850	855	860	865	870	875	880	885
Lycopodium	179	113	195	293	181	312	1173	292	200
Pollen Sum	325	339	353	359	365	347	338	318	315
Polylepis	1	2	1	0	2	0	0	2	2
Melastomataceae	1	3	3	2	3	1	4	3	4
Hesperomeles	0	0	4	3	1	0	0	0	0
Gynoxys	0	0	0	0	0	0	0	0	0
Poaceae	120	163	214	180	190	209	153	146	175
Asteraceae	12	15	10	11	13	13	18	7	9
Caryophyllaceae	1	0	0	1	0	0	0	1	1
Plantago	2	4	5	6	4	6	7	3	5
Ambrosia	1	3	2	3	6	1	6	5	5
Thalictrum	6	15	8	5	15	5	12	4	10
Apiaceae	1	0	3	3	1	1	0	3	2
Chenopodium	0	0	0	3	5	0	2	1	0
Lactuceae	1	0	0	0	0	0	0	0	0
Valerianaceae	0	1	1	1	0	0	0	1	0
Campanulaceae	0	0	0	0	0	0	0	0	0
Althernanthera	0	0	0	0	0	0	0	1	0
Brassicaceae	0	0	0	0	0	1	1	0	0
Rubiaceae	0	0	0	0	0	0	0	0	0
Malvaceae	0	0	0	1	0	1	0	2	1
Urticaceae Moraceae	42	64	39	62	62	50	60	66	24
Hedyosmum	4	0	8	6	7	2	9	9	9
Acalypha	10	11	6	16	12	8	9	13	5
Podocarpus	21	5	9	8	0	28	18	16	21
Ericaceae	1	0	0	2	0	0	0	2	0
Myrsinaceae	4	7	9	12	4	1	0	0	1
Alchornea	6	2	1	2	1	3	3	1	3
Juglans	1	0	0	1	1	0	0	0	0
Alnus	0	0	5	2	1	1	2	1	0
Vallea	0	0	1	1	0	0	0	1	0
Bocconia	1	0	0	0	0	0	0	0	1
Myricaceae	0	0	0	0	1	1	0	0	1
Solanacea	1	0	2	1	0	0	0	1	2
Weinmannia	1	0	0	0	1	1	0	0	1
Rosaceae	0	0	0	0	0	0	0	0	0
Myrtaceae	0	0	1	0	0	0	0	0	0
Cassia	0	0	0	0	0	0	0	0	0
Cecropia	0	0	3	3	1	0	0	1	0
Celtis	5	6	1	1	2	3	4	3	2
Anacardiaceae	0	0	1	0	2	0	0	0	0
Prosopis	7	5	2	2	3	1	8	1	4
Euphorbiaceae	0	0	0	0	0	0	0	0	0
Mimosaceae	0	0	0	0	0	0	0	0	0
Dodonaea	2	3	0	2	2	0	0	2	3
Cyperaceae	49	14	3	8	4	4	6	8	9
Other/Broken unidentified	24	16	11	11	21	6	16	14	15

Table A8-1 Lake Pacucha pollen counts, continued (10 of 11). New (bold text) and published data (Valencia et al. 2010) is included.

Volume CC	0.5	0.5	0.5	0.5	0.5	0.5	0.5	0.5	0.5
Age	9551.9	9771.6	9991.3	10211	10430.7	10642	10819.7	10997.3	11175
Depth (cm)	890	895	900	905	910	915	920	925	930
Lycopodium	128	112	101	234	166	109	338	345	232
Pollen Sum	321	344	378	310	342	327	340	330	303
Polylepis	1	0	0	1	0	0	3	1	2
Melastomataceae	2	5	7	2	1	1	6	5	2
Hesperomeles	0	0	0	1	1	1	1	0	0
Gynoxys	0	0	0	0	0	0	0	0	0
Poaceae	153	120	133	136	192	147	132	135	125
Asteraceae	9	11	11	5	5	16	11	24	25
Caryophyllaceae	1	0	0	0	0	0	1	0	0
Plantago	7	6	4	6	1	2	6	1	10
Ambrosia	4	0	5	1	4	5	2	2	7
Thalictrum	19	4	8	17	15	10	5	10	7
Apiaceae	2	4	3	4	3	1	2	6	4
Chenopodium	0	0	2	0	3	2	0	1	1
Lactuceae	0	0	0	0	0	0	1	0	0
Valerianaceae	3	0	0	0	0	0	0	0	0
Campanulaceae	0	0	0	0	0	0	0	0	0
Althernanthera	1	0	0	0	1	2	0	1	1
Brassicaceae	0	0	2	3	0	0	0	1	0
Rubiaceae	0	0	0	0	0	0	0	0	0
Malvaceae	6	0	1	4	4	0	0	1	0
Urticaceae Moraceae	59	107	84	86	39	66	70	28	33
Hedyosmum	0	5	6	4	5	1	3	9	13
Acalypha	10	13	25	7	8	8	20	11	12
Podocarpus	7	4	6	3	12	12	7	14	25
Ericaceae	1	1	2	0	0	4	0	3	1
Myrsinaceae	1	4	5	3	4	4	4	4	1
Alchornea	7	6	4	3	6	2	2	8	9
Juglans	0	0	0	1	0	0	0	0	0
Alnus	0	0	1	0	0	0	0	2	0
Vallea	0	3	2	0	0	1	2	0	1
Bocconia	0	0	0	0	0	0	3	0	0
Myricaceae	0	0	2	2	0	0	0	0	0
Solanacea	0	1	0	2	0	1	1	0	3
Weinmannia	0	1	1	0	0	0	2	0	0
Rosaceae	0	0	0	0	0	0	0	0	0
Myrtaceae	0	0	0	0	1	0	0	0	0
Cassia	0	0	0	0	0	0	0	0	0
Cecropia	2	29	10	0	0	0	1	1	0
Celtis	6	4	11	3	4	3	8	5	1
Anacardiaceae	0	0	0	0	2	0	1	0	0
Prosopis	6	3	3	0	5	2	1	0	0
Euphorbiaceae	0	0	0	0	0	0	0	0	0
Mimosaceae	0	0	0	0	0	0	0	0	0
Dodonaea	2	0	0	1	0	1	1	2	1
Cyperaceae	0	3	22	4	11	20	24	14	12
Other/Broken unidentified	12	10	18	11	15	15	20	41	7

Appendix VIII

Table A8-1 Lake Pacucha pollen counts, continued (11 of 11). New (bold text) and published data (Valencia et al. 2010) is included.

Volume CC	0.5	0.5	0.5	0.5	0.5	0.5	0.5	0.5	0.5
Age	11352.6	11530.3	11708	11885.6	12063.3	12240.9	12418.6	12596.2	12773.9
Depth (cm)	935	940	945	950	955	960	965	970	975
Lycopodium	188	230	173	202	188	206	245	264	208
Pollen Sum	331	321	319	357	323	313	308	306	367
Polylepis	3	2	4	7	7	11	7	5	4
Melastomataceae	5	6	1	5	3	3	4	3	5
Hesperomeles	2	0	0	2	0	0	0	1	0
Gynoxys	0	0	0	0	0	0	0	0	0
Poaceae	127	103	140	139	159	155	160	164	204
Asteraceae	23	20	22	34	23	24	28	14	15
Caryophyllaceae	1	0	0	2	3	1	0	2	5
Plantago	5	3	7	6	11	16	11	14	7
Ambrosia	4	2	1	0	1	4	0	3	5
Thalictrum	5	6	3	3	2	5	2	6	4
Apiaceae	4	3	6	7	9	5	4	4	6
Chenopodium	2	11	0	9	2	0	1	0	0
Lactuceae	0	0	0	0	0	0	0	0	0
Valerianaceae	0	0	0	0	1	0	0	0	0
Campanulaceae	0	0	0	0	0	0	1	0	0
Althernanthera	0	0	0	1	0	0	0	1	2
Brassicaceae	1	0	0	2	0	0	0	0	4
Rubiaceae	0	0	0	0	0	0	0	0	0
Malvaceae	0	0	0	0	0	0	0	0	0
Urticaceae Moraceae	47	68	36	33	22	29	17	21	19
Hedyosmum	20	11	15	13	12	10	16	16	14
Acalypha	9	8	13	17	8	10	12	11	22
Podocarpus	13	10	23	21	24	9	10	11	16
Ericaceae	1	4	2	6	1	2	3	5	1
Myrsinaceae	8	7	0	3	0	2	2	3	0
Alchornea	13	8	5	9	5	5	5	5	0
Juglans	0	0	1	0	1	0	0	0	0
Alnus	0	1	2	0	0	1	0	0	1
Vallea	2	2	3	1	1	1	2	1	3
Bocconia	0	0	1	0	2	0	1	0	0
Myricaceae	3	3	2	0	0	0	0	1	2
Solanacea	0	2	0	0	0	0	1	0	1
Weinmannia	0	1	2	2	3	0	0	0	1
Rosaceae	0	0	0	0	0	0	0	0	0
Myrtaceae	0	0	0	0	0	0	0	0	0
Cassia	0	0	0	0	0	0	0	0	0
Cecropia	1	2	0	4	2	0	0	0	0
Celtis	1	2	2	1	1	0	1	0	4
Anacardiaceae	0	0	0	0	0	0	0	0	0
Prosopis	0	0	2	0	0	0	0	0	0
Euphorbiaceae	0	0	0	0	0	0	0	0	0
Mimosaceae	0	0	0	0	0	0	0	0	0
Dodonaea	2	0	1	0	0	0	1	0	0
Cyperaceae	17	17	5	5	2	7	2	5	5
Other/Broken unidentified	12	19	20	25	18	13	17	10	17

Appendix VIII

Table A8-2 Lake Miski pollen counts. (1 of 8)

Volume CC	0.25	0.25	0.25	0.25	0.25	0.25	0.25	0.25
Age	0.2	132.476	314.912	497.347	679.783	862.219	1044.65	1227.09
Depth (cm)	0	5	10	15	20	25	30	35
Lycopodium	249	225	192	289	345	321	403	588
Pollen Sum	386	346	339	367	337	308	338	374
Polylepis	39	30	22	31	28	38	42	56
Melastomataceae	11	9	9	16	4	8	13	13
Hesperomeles	0	0	2	1	1	0	2	1
Gynoxys	2	0	1	2	2	2	2	1
Poaceae	117	111	99	104	154	94	103	99
Asteraceae	12	0	8	6	8	4	7	11
Caryophyllaceae	1	1	0	1	1	0	0	1
Plantago	4	2	3	4	2	0	0	1
Ambrosia	2	0	1	0	0	0	0	1
Thalictrum	0	0	0	0	1	0	0	1
Apiaceae	4	6	3	6	3	7	5	5
Chenopodium	0	0	0	0	0	0	0	0
Lactuceae	0	0	1	0	1	0	2	1
Valerianaceae	0	0	0	0	0	0	1	1
Campanulaceae	0	0	0	1	0	0	0	0
Althernanthera	0	0	0	1	0	0	0	0
Brassicaceae	0	0	0	0	0	0	4	0
Rubiaceae	2	0	1	0	0	0	0	0
Malvaceae	0	0	0	0	0	0	1	0
Urticaceae Moraceae	60	78	80	71	38	49	49	58
Hedyosmum	22	12	17	18	13	16	16	18
Acalypha	22	15	9	20	13	17	15	20
Podocarpus	2	0	0	3	0	0	2	2
Ericaceae	18	11	13	7	11	15	15	20
Myrsinaceae	1	6	9	7	7	9	4	3
Alchornea	2	2	1	3	4	2	4	4
Juglans	4	0	1	1	0	0	0	0
Alnus	7	11	3	7	6	5	2	0
Vallea	3	2	1	0	0	0	3	1
Bocconia	1	1	0	1	0	0	0	0
Myricaceae	1	0	0	0	0	0	0	1
Solanacea	0	1	0	0	0	1	0	2
Weinmannia	2	0	3	0	0	0	2	1
Rosaceae	1	0	0	0	0	0	0	0
Myrtaceae	0	0	1	0	0	0	0	0
Cassia	0	1	0	2	2	1	0	0
Cecropia	5	5	5	3	2	4	3	1
Celtis	0	0	2	3	3	0	1	0
Anacardiaceae	0	0	0	0	1	0	1	0
Prosopis	0	0	0	1	2	0	0	0
Euphorbiaceae	1	0	1	0	1	3	1	0
Mimosaceae	1	1	3	2	0	0	1	2
Dodonaea	3	5	2	2	1	1	0	0
Cyperaceae	8	12	10	16	3	10	17	16
Other/Broken unidentified	28	24	28	27	25	22	20	33

Table A8-2 Lake Miski pollen counts, continued (2 of 8)

Volume CC	0.25	0.25	0.5	0.5	0.25	0.5	0.5	0.25
Age	1409.53	1591.96	1883.86	2212.24	2537.69	2863.13	3229.25	3554.69
Depth (cm)	40	45	53	62	70	78	87	95
Lycopodium	389	334	100	152	101	98	106	158
Pollen Sum	306	319	445	409	317	353	363	315
Polylepis	30	27	29	33	17	25	34	22
Melastomataceae	8	10	12	11	6	10	15	3
Hesperomeles	0	3	3	2	0	0	1	0
Gynoxys	1	1	1	1	1	0	0	0
Poaceae	121	130	158	152	125	148	114	166
Asteraceae	8	7	10	10	7	9	6	3
Caryophyllaceae	1	1	1	1	1	1	2	2
Plantago	0	1	9	6	4	9	9	8
Ambrosia	3	2	3	2	1	0	2	1
Thalictrum	1	0	3	0	1	0	1	1
Apiaceae	2	4	1	3	1	2	0	0
Chenopodium	0	1	1	1	3	0	0	1
Lactuceae	1	1	0	0	0	0	0	0
Valerianaceae	0	0	2	0	1	0	0	0
Campanulaceae	0	0	3	3	1	0	1	0
Althernanthera	0	2	1	1	3	1	0	1
Brassicaceae	0	0	0	0	0	0	0	0
Rubiaceae	0	0	0	0	0	0	0	0
Malvaceae	0	0	0	0	0	0	0	0
Urticaceae Moraceae	40	46	95	80	67	59	82	47
Hedyosmum	18	12	20	19	7	12	10	12
Acalypha	4	14	20	12	17	20	18	14
Podocarpus	2	3	1	2	3	1	2	2
Ericaceae	5	3	8	9	5	8	9	5
Myrsinaceae	8	7	10	10	5	2	7	2
Alchornea	3	5	1	2	1	3	1	0
Juglans	1	2	1	0	0	0	0	0
Alnus	2	2	1	0	1	0	0	0
Vallea	0	2	1	2	3	3	2	0
Bocconia	2	0	1	0	0	0	0	0
Myricaceae	0	0	1	0	0	1	0	0
Solanacea	0	2	0	2	0	0	1	0
Weinmannia	0	0	2	1	3	0	0	0
Rosaceae	0	0	0	2	1	2	0	1
Myrtaceae	0	0	0	0	1	0	0	0
Cassia	1	2	0	0	0	0	1	0
Cecropia	2	3	9	7	5	9	19	1
Celtis	1	2	1	3	0	3	4	0
Anacardiaceae	1	0	1	0	0	1	1	1
Prosopis	0	0	1	0	1	0	2	2
Euphorbiaceae	1	0	3	0	0	1	0	0
Mimosaceae	3	3	2	1	2	1	4	0
Dodonaea	1	0	0	1	0	0	0	0
Cyperaceae	19	11	16	21	11	13	8	13
Other/Broken unidentified	16	10	13	9	12	9	7	7

Table A8-2 Lake Miski pollen counts, continued (3 of 8)

Volume CC	0.5	0.5	0.25	0.5	0.5	0.25	0.5	0.5
Age	3839.45	4088.13	4378.26	4668.39	4917.07	5207.19	5497.32	5746
Depth (cm)	102	108	115	122	128	135	142	148
Lycopodium	109	160	107	192	125	185	163	142
Pollen Sum	379	375	315	389	371	333	401	372
Polylepis	19	22	22	24	17	21	23	25
Melastomataceae	14	7	3	6	6	2	9	4
Hesperomeles	1	0	0	1	0	0	1	0
Gynoxys	0	1	0	0	0	0	0	3
Poaceae	139	178	158	170	168	164	201	141
Asteraceae	12	9	7	12	5	6	3	11
Caryophyllaceae	1	2	0	1	1	1	1	1
Plantago	8	6	3	13	8	8	9	7
Ambrosia	2	3	1	1	0	0	1	1
Thalictrum	0	3	2	1	2	1	2	2
Apiaceae	1	3	2	5	6	3	3	2
Chenopodium	0	2	4	1	1	6	1	2
Lactuceae	0	1	0	0	0	2	0	0
Valerianaceae	0	0	1	1	2	0	1	1
Campanulaceae	0	1	0	1	1	0	0	2
Althernanthera	0	2	4	1	1	7	2	2
Brassicaceae	1	0	0	0	0	0	0	0
Rubiaceae	0	0	0	0	0	0	0	0
Malvaceae	0	0	1	0	1	0	0	0
Urticaceae Moraceae	66	41	45	69	66	37	52	62
Hedyosmum	21	15	9	17	9	10	16	18
Acalypha	22	19	18	11	16	21	13	20
Podocarpus	4	4	5	4	2	2	5	1
Ericaceae	3	6	4	7	10	3	7	9
Myrsinaceae	3	4	0	4	3	1	5	5
Alchornea	4	0	0	3	2	2	1	3
Juglans	1	1	0	0	1	2	0	0
Alnus	0	0	0	2	0	0	2	0
Vallea	2	1	0	0	0	0	0	0
Bocconia	0	1	1	0	0	1	0	0
Myricaceae	1	2	0	0	1	0	2	3
Solanacea	1	2	3	0	2	0	0	0
Weinmannia	1	0	0	1	0	0	0	0
Rosaceae	0	1	0	0	2	0	0	0
Myrtaceae	0	0	0	1	0	0	0	0
Cassia	0	1	0	0	0	0	0	0
Cecropia	19	5	1	5	7	2	5	13
Celtis	1	2	0	0	0	0	3	4
Anacardiaceae	2	1	0	0	1	1	1	2
Prosopis	0	0	1	0	0	1	1	1
Euphorbiaceae	0	0	0	0	0	0	0	0
Mimosaceae	0	0	0	0	0	0	0	0
Dodonaea	0	0	0	0	0	1	1	0
Cyperaceae	26	19	14	19	19	17	17	18
Other/Broken unidentified	4	10	6	8	11	11	13	9

Table A8-2 Lake Miski pollen counts, continued (4 of 8)

Volume CC	0.25	0.25	0.5	0.5	0.5	0.5	0.5	0.5
Age	6036.13	6450.59	6740.72	7072.29	7279.53	7486.76	7643.68	7725.12
Depth (cm)	155	165	172	180	185	190	195	200
Lycopodium	144	189	166	155	95	123	149	172
Pollen Sum	351	310	339	409	328	379	346	325
Polylepis	34	22	20	16	7	6	10	14
Melastomataceae	2	3	8	9	7	5	5	4
Hesperomeles	0	0	1	1	0	0	0	0
Gynoxys	0	1	0	0	0	0	0	0
Poaceae	147	143	146	184	125	155	140	140
Asteraceae	10	6	11	6	4	5	7	7
Caryophyllaceae	2	1	2	0	1	0	1	0
Plantago	16	7	6	9	15	8	12	10
Ambrosia	0	1	1	1	0	0	1	0
Thalictrum	0	2	1	0	1	1	1	1
Apiaceae	3	1	1	4	1	0	1	1
Chenopodium	1	0	0	0	0	0	0	0
Lactuceae	1	0	0	1	0	0	0	0
Valerianaceae	1	1	0	0	0	0	0	0
Campanulaceae	0	0	0	0	0	0	1	1
Althernanthera	1	1	0	0	0	0	0	1
Brassicaceae	0	0	0	0	0	0	0	0
Rubiaceae	0	0	0	0	0	0	0	0
Malvaceae	0	0	0	0	0	0	0	0
Urticaceae Moraceae	70	61	69	100	72	106	85	63
Hedyosmum	4	4	8	7	11	9	10	10
Acalypha	14	12	18	21	21	25	21	11
Podocarpus	5	1	3	4	4	5	6	4
Ericaceae	5	7	5	5	8	2	0	6
Myrsinaceae	4	3	3	0	0	0	0	0
Alchornea	1	1	4	3	2	0	0	0
Juglans	0	4	1	0	1	2	1	1
Alnus	1	0	0	1	0	1	0	0
Vallea	1	0	0	1	0	0	0	2
Bocconia	1	0	1	0	0	0	0	0
Myricaceae	0	0	0	4	0	1	0	0
Solanacea	1	2	1	1	3	0	0	0
Weinmannia	0	1	0	1	2	2	4	3
Rosaceae	1	0	0	0	0	0	0	0
Myrtaceae	0	0	0	1	0	0	0	0
Cassia	1	1	1	0	3	3	2	3
Cecropia	5	0	7	5	3	14	4	5
Celtis	1	2	1	2	2	1	2	1
Anacardiaceae	0	1	0	1	0	1	1	1
Prosopis	0	1	1	0	0	0	0	0
Euphorbiaceae	0	0	0	0	1	0	2	1
Mimosaceae	0	0	0	0	0	0	0	0
Dodonaea	0	0	0	0	0	0	0	0
Cyperaceae	6	11	14	3	8	10	6	13
Other/Broken unidentified	12	9	5	18	26	17	23	22

Table A8-2 Lake Miski pollen counts, continued (5 of 8)

Volume CC	0.5	0.5	0.5	0.5	0.5	0.5	0.5	0.5
Age	7806.57	7888.01	7969.46	8050.9	8132.35	8213.79	8295.24	8376.68
Depth (cm)	205	210	215	220	225	230	235	240
Lycopodium	247	146	214	196	172	169	198	298
Pollen Sum	346	337	355	376	414	426	375	395
Polylepis	12	18	11	17	11	21	20	32
Melastomataceae	12	6	5	1	3	8	6	10
Hesperomeles	0	0	0	0	0	0	0	0
Gynoxys	0	0	0	0	0	0	0	0
Poaceae	145	122	169	164	160	147	169	142
Asteraceae	7	7	13	14	10	10	0	12
Caryophyllaceae	0	0	0	0	2	0	0	0
Plantago	4	2	9	6	6	4	8	3
Ambrosia	2	1	2	2	0	1	0	0
Thalictrum	0	1	1	0	0	0	0	0
Apiaceae	0	0	1	0	1	0	0	1
Chenopodium	0	1	0	1	0	0	1	1
Lactuceae	0	1	0	0	0	0	0	1
Valerianaceae	0	0	0	0	0	2	0	1
Campanulaceae	0	1	0	0	0	0	0	0
Althernanthera	0	2	0	1	0	0	1	1
Brassicaceae	0	0	0	0	0	0	0	0
Rubiaceae	0	0	0	0	0	0	0	0
Malvaceae	0	0	0	0	0	0	0	0
Urticaceae Moraceae	72	77	50	73	102	109	76	71
Hedyosmum	12	8	14	10	15	17	8	16
Acalypha	23	23	19	15	23	27	18	21
Podocarpus	3	5	6	7	6	7	6	4
Ericaceae	3	8	6	3	6	11	9	6
Myrsinaceae	0	2	0	0	1	4	0	2
Alchornea	2	2	5	4	1	0	4	6
Juglans	3	4	4	4	0	1	1	5
Alnus	0	0	0	0	0	0	0	0
Vallea	2	1	1	2	1	3	4	6
Bocconia	0	0	1	0	1	0	1	0
Myricaceae	0	0	0	0	2	2	0	1
Solanacea	1	0	0	0	1	3	0	3
Weinmannia	1	0	0	3	0	0	0	0
Rosaceae	0	0	0	0	0	0	0	0
Myrtaceae	0	0	0	0	0	0	0	0
Cassia	1	0	0	2	2	0	2	5
Cecropia	4	13	4	8	7	11	5	3
Celtis	2	6	5	3	3	8	2	5
Anacardiaceae	0	0	1	2	3	1	0	1
Prosopis	1	0	1	1	0	0	0	0
Euphorbiaceae	1	0	0	0	2	0	1	1
Mimosaceae	0	0	0	0	0	0	0	0
Dodonaea	0	0	0	0	0	0	0	0
Cyperaceae	8	5	7	14	21	7	17	13
Other/Broken unidentified	25	21	20	19	24	22	16	22

Table A8-2 Lake Miski pollen counts, continued (6 of 8)

Volume CC	0.5	0.5	0.5	0.5	0.5	0.5	0.5	0.5
Age	8458.13	8539.57	8621.02	8702.46	8783.91	8865.35	9173.24	9537.74
Depth (cm)	245	250	255	260	265	270	275	280
Lycopodium	231	193	169	264	312	263	140	263
Pollen Sum	364	399	409	469	356	388	334	365
Polylepis	28	17	19	22	20	25	17	10
Melastomataceae	12	6	6	3	8	14	14	11
Hesperomeles	0	0	0	0	0	0	0	0
Gynoxys	0	0	0	0	0	0	0	0
Poaceae	138	158	156	163	142	112	100	95
Asteraceae	8	11	17	6	7	11	12	17
Caryophyllaceae	2	0	0	0	0	0	1	0
Plantago	16	8	5	6	4	6	3	6
Ambrosia	1	1	2	4	1	0	1	0
Thalictrum	0	0	1	1	2	0	0	0
Apiaceae	0	2	0	1	0	1	0	2
Chenopodium	0	2	0	1	0	1	1	1
Lactuceae	2	1	0	0	0	0	0	0
Valerianaceae	1	0	0	0	0	0	0	2
Campanulaceae	0	0	0	0	0	0	0	0
Althernanthera	0	2	0	2	0	2	1	1
Brassicaceae	0	0	0	0	0	0	0	0
Rubiaceae	0	0	0	0	0	0	0	0
Malvaceae	0	0	0	0	0	0	0	0
Urticaceae Moraceae	64	79	90	117	56	79	60	70
Hedyosmum	15	7	17	19	18	22	13	24
Acalypha	16	35	33	27	16	34	32	33
Podocarpus	3	10	5	10	5	8	18	5
Ericaceae	8	8	9	13	7	6	8	11
Myrsinaceae	2	3	2	2	5	3	0	5
Alchornea	4	4	5	7	8	2	6	5
Juglans	2	6	5	3	7	10	4	8
Alnus	0	0	0	0	0	0	0	1
Vallea	1	2	2	3	1	1	4	0
Bocconia	0	1	0	1	1	0	1	0
Myricaceae	0	0	0	0	0	0	0	4
Solanacea	4	1	0	1	1	1	1	0
Weinmannia	0	1	0	1	0	0	0	1
Rosaceae	0	0	0	0	0	0	0	0
Myrtaceae	0	0	0	1	0	0	2	1
Cassia	1	1	2	1	5	5	3	1
Cecropia	2	3	5	7	1	0	3	1
Celtis	4	8	4	3	3	4	3	6
Anacardiaceae	0	1	0	2	1	2	5	5
Prosopis	1	1	0	0	1	0	0	4
Euphorbiaceae	0	0	2	0	1	1	0	0
Mimosaceae	0	0	0	0	0	0	0	0
Dodonaea	0	0	0	0	0	0	0	0
Cyperaceae	6	6	9	19	15	15	12	16
Other/Broken unidentified	23	14	13	23	20	23	9	19

Table A8-2 Lake Miski pollen counts, continued (7 of 8)

Volume CC	0.5	0.5	0.5	0.5	0.5	0.5	0.5
Age	9902.25	10266.7	10631.2	10995.8	11360.3	11724.8	12089.3
Depth (cm)	285	290	295	300	305	310	315
Lycopodium	240	166	379	164	147	95	75
Pollen Sum	417	439	401	404	485	368	355
Polylepis	13	14	12	6	7	8	6
Melastomataceae	18	7	11	10	5	9	12
Hesperomeles	0	0	0	0	0	0	0
Gynoxys	0	0	0	0	0	0	0
Poaceae	132	166	136	126	193	84	77
Asteraceae	10	9	21	6	13	3	13
Caryophyllaceae	3	0	0	1	2	0	0
Plantago	6	6	6	4	3	4	8
Ambrosia	1	0	1	2	1	1	0
Thalictrum	2	0	0	0	1	0	0
Apiaceae	0	2	0	1	1	1	0
Chenopodium	0	0	0	0	0	1	0
Lactuceae	1	0	1	0	0	0	0
Valerianaceae	0	0	0	0	0	0	0
Campanulaceae	0	0	0	0	0	0	0
Althernanthera	0	0	0	0	0	1	0
Brassicaceae	0	1	0	0	1	1	0
Rubiaceae	0	0	0	0	0	0	0
Malvaceae	0	0	0	0	0	0	0
Urticaceae Moraceae	85	97	72	111	110	120	108
Hedyosmum	25	21	29	16	14	18	7
Acalypha	34	25	26	32	19	28	19
Podocarpus	15	9	5	13	9	9	16
Ericaceae	18	9	8	7	18	15	13
Myrsinaceae	2	1	1	3	4	5	5
Alchornea	8	15	10	10	4	7	5
Juglans	2	5	4	3	8	5	4
Alnus	0	1	0	1	1	0	2
Vallea	3	3	1	1	2	4	5
Bocconia	1	0	2	1	2	1	1
Myricaceae	0	1	1	1	3	0	4
Solanacea	0	2	0	1	4	3	1
Weinmannia	0	0	1	1	2	2	4
Rosaceae	0	0	0	0	0	0	0
Myrtaceae	0	0	0	0	0	0	0
Cassia	4	3	5	0	3	2	3
Cecropia	1	4	1	9	6	11	12
Celtis	5	6	12	7	9	6	2
Anacardiaceae	0	1	0	0	0	0	0
Prosopis	1	0	1	5	2	0	2
Euphorbiaceae	1	0	2	0	1	0	0
Mimosaceae	0	0	0	0	0	0	0
Dodonaea	0	0	0	0	0	0	0
Cyperaceae	15	18	20	7	7	5	5
Other/Broken unidentified	11	13	12	19	30	14	21

Table A8-2 Lake Miski pollen counts, continued (8 of 8)

Volume CC	0.5	0.5	0.5	0.5	0.5	0.5	0.5
Age	12607.5	12621.2	12635	12648.7	12662.5	12676.2	12690
Depth (cm)	320	325	330	335	340	345	350
Lycopodium	122	280	405	607	725	424	530
Pollen Sum	331	371	402	322	384	334	317
Polylepis	8	7	2	4	7	7	3
Melastomataceae	9	19	10	7	11	9	8
Hesperomeles	0	0	0	0	0	0	3
Gynoxys	0	0	0	0	0	0	0
Poaceae	47	77	69	42	53	51	40
Asteraceae	12	16	15	18	15	17	21
Caryophyllaceae	0	0	0	0	0	0	0
Plantago	12	5	5	4	5	3	1
Ambrosia	1	0	0	0	0	0	0
Thalictrum	0	0	1	0	1	0	0
Apiaceae	5	2	1	2	1	2	0
Chenopodium	0	1	0	0	1	0	0
Lactuceae	1	2	0	1	0	1	0
Valerianaceae	0	0	0	0	0	0	1
Campanulaceae	0	0	0	0	0	0	0
Althernanthera	0	1	0	0	1	0	0
Brassicaceae	0	0	0	0	0	0	0
Rubiaceae	0	0	0	0	0	0	0
Malvaceae	0	0	0	0	0	0	0
Urticaceae Moraceae	90	112	164	102	123	78	93
Hedyosmum	21	13	30	23	42	36	45
Acalypha	23	14	14	12	12	10	16
Podocarpus	23	9	14	21	26	33	22
Ericaceae	7	13	12	19	13	23	16
Myrsinaceae	5	3	2	5	5	1	3
Alchornea	3	5	6	3	1	2	4
Juglans	2	3	0	2	2	4	3
Alnus	0	0	0	0	0	0	1
Vallea	2	4	4	1	2	6	7
Bocconia	3	1	0	2	0	0	0
Myricaceae	3	1	3	2	0	3	0
Solanacea	0	0	2	0	0	2	0
Weinmannia	2	2	2	3	1	0	2
Rosaceae	0	0	0	0	0	0	0
Myrtaceae	0	0	0	0	1	0	0
Cassia	2	1	1	0	2	0	1
Cecropia	16	16	15	8	18	12	8
Celtis	3	5	2	1	2	1	2
Anacardiaceae	0	0	0	0	0	0	0
Prosopis	1	1	0	1	0	0	1
Euphorbiaceae	1	0	0	0	1	0	1
Mimosaceae	0	0	0	0	0	0	0
Dodonaea	0	0	0	1	0	0	0
Cyperaceae	5	7	11	10	14	12	8
Other/Broken unidentified	24	31	17	28	24	21	7

Appendix VIII

Table A8-3 Lake Huamanmarca pollen counts. (1 of 8)

Volume CC	0.25	0.25	0.25	0.25	0.25	0.25	0.25	0.25
Age	0.3	177.14	404.3	631.45	858.61	1085.77	1312.93	1540.09
Depth (cm)	0	3	6	9	12	15	18	21
Lycopodium	1588	1588	1212	1876	1996	1316	1280	1856
Pollen Sum	371	379	309	348	296	344	409	306
Polylepis	123	119	94	95	90	107	104	116
Melastomataceae	6	3	1	9	6	2	4	8
Hesperomeles	1	0	3	1	0	0	0	0
Gynoxys	9	4	5	2	2	5	7	6
Poaceae	100	122	106	123	86	125	155	90
Asteraceae	29	36	21	22	20	27	29	25
Caryophyllaceae	8	7	10	12	6	6	9	8
Plantago	1	0	0	2	2	4	3	1
Ambrosia	3	2	1	0	1	1	2	0
Thalictrum	0	0	1	0	0	0	0	1
Apiaceae	3	2	1	1	0	1	2	1
Chenopodium	0	1	2	1	0	0	3	0
Lactuceae	0	2	1	0	0	0	0	1
Valerianaceae	5	1	5	0	0	0	0	0
Campanulaceae	0	0	0	0	0	0	0	0
Althernanthera	0	0	0	0	0	0	0	0
Brassicaceae	0	0	0	0	0	0	0	0
Rubiaceae	0	0	0	0	0	0	0	0
Malvaceae	0	0	0	0	0	1	0	0
Urticaceae Moraceae	40	28	17	34	30	21	33	13
Hedyosmum	9	12	1	7	7	5	7	8
Acalypha	4	5	6	7	6	4	4	3
Podocarpus	3	4	6	2	2	3	4	1
Ericaceae	6	4	5	2	6	1	14	5
Myrsinaceae	3	1	5	4	4	5	6	1
Alchornea	0	3	2	3	2	1	0	0
Juglans	3	4	1	0	1	1	0	0
Alnus	1	0	1	2	1	0	0	1
Vallea	0	1	0	0	0	0	0	0
Bocconia	0	0	1	1	0	2	0	1
Myricaceae	0	2	0	0	0	0	0	0
Solanacea	1	1	0	0	1	1	0	1
Weinmannia	0	0	0	2	0	0	0	0
Rosaceae	1	0	0	0	0	2	3	1
Myrtaceae	0	0	1	0	0	0	0	0
Cassia	0	0	0	0	0	0	0	0
Cecropia	0	0	0	0	0	0	0	0
Celtis	0	0	0	0	0	0	0	0
Anacardiaceae	0	0	0	0	2	1	0	0
Prosopis	0	1	1	1	0	1	1	1
Euphorbiaceae	0	0	0	0	0	0	0	0
Mimosaceae	0	1	1	4	3	3	2	5
Dodonaea	0	1	0	0	0	0	0	0
Cyperaceae	7	2	4	5	16	12	7	4
Other/Broken unidentified	5	10	6	6	2	2	10	4

Table A8-3 Lake Huamanmarca pollen counts, continued (2 of 8)

Volume CC	0.25	0.25	0.25	0.25	0.25	0.25	0.25	0.25
Age	1767.24	1994.4	2221.56	2448.72	2642.7	2823.5	3004.3	3185.11
Depth (cm)	24	27	30	33	39	56	73	90
Lycopodium	664	1296	1284	2188	1236	1572	1640	1676
Pollen Sum	309	327	315	312	372	412	307	310
Polylepis	122	89	77	111	120	88	98	89
Melastomataceae	16	3	4	0	2	8	0	5
Hesperomeles	2	5	0	1	0	1	0	2
Gynoxys	5	5	5	5	5	6	7	4
Poaceae	92	122	121	78	83	120	107	109
Asteraceae	15	19	19	32	30	12	13	23
Caryophyllaceae	3	5	7	10	9	9	10	14
Plantago	2	1	2	0	0	0	1	1
Ambrosia	0	1	2	0	1	0	2	4
Thalictrum	0	2	0	0	0	0	0	0
Apiaceae	1	3	1	1	1	0	0	2
Chenopodium	0	0	0	0	2	1	0	0
Lactuceae	0	0	0	0	0	0	0	0
Valerianaceae	1	1	3	1	1	1	0	1
Campanulaceae	0	0	1	0	0	1	0	0
Althernanthera	0	0	0	0	0	0	0	0
Brassicaceae	0	0	0	1	0	0	2	0
Rubiaceae	0	1	0	1	0	0	0	0
Malvaceae	0	0	0	0	0	0	0	0
Urticaceae Moraceae	23	30	17	25	76	116	30	21
Hedyosmum	2	4	13	8	12	10	4	8
Acalypha	5	7	7	4	3	4	1	0
Podocarpus	1	1	2	4	1	1	5	1
Ericaceae	4	3	7	9	3	5	1	4
Myrsinaceae	3	4	3	3	2	3	0	4
Alchornea	1	2	2	0	2	0	0	0
Juglans	0	0	0	0	0	0	0	0
Alnus	0	2	2	0	0	1	1	0
Vallea	0	0	2	0	1	0	0	0
Bocconia	0	0	1	0	1	0	1	0
Myricaceae	0	1	0	1	1	0	2	0
Solanacea	1	0	0	0	0	0	1	1
Weinmannia	1	0	0	0	0	0	1	0
Rosaceae	0	1	1	0	0	0	0	0
Myrtaceae	0	0	0	0	0	0	0	1
Cassia	0	0	0	0	0	0	0	0
Cecropia	0	0	0	0	0	1	0	0
Celtis	0	0	0	0	0	0	0	0
Anacardiaceae	0	0	2	1	0	2	2	0
Prosopis	2	0	1	2	1	1	3	0
Euphorbiaceae	0	0	0	0	0	0	1	1
Mimosaceae	1	5	1	2	4	1	3	3
Dodonaea	0	0	0	0	0	0	0	0
Cyperaceae	6	5	2	9	6	10	7	5
Other/Broken unidentified	0	5	10	3	5	10	4	7

Table A8-3 Lake Huamanmarca pollen counts, continued (3 of 8)

Volume CC	0.25	0.25	0.25	0.25	0.25	0.25	0.25	0.25
Age	3365.91	3546.71	3727.52	4089.13	4269.93	4462.83	4635.92	4809.02
Depth (cm)	107	124	141	175	192	205	211	217
Lycopodium	1764	1404	1548	1228	896	984	1812	1252
Pollen Sum	323	331	316	364	305	327	316	313
Polylepis	94	83	60	61	87	79	80	75
Melastomataceae	7	6	9	13	7	1	5	1
Hesperomeles	1	0	1	3	0	1	2	0
Gynoxys	4	1	0	1	0	5	5	0
Poaceae	121	143	119	143	103	122	132	147
Asteraceae	12	10	8	8	14	20	13	14
Caryophyllaceae	6	6	3	1	2	5	5	4
Plantago	1	2	3	6	1	0	1	1
Ambrosia	2	0	0	1	0	0	1	4
Thalictrum	0	0	2	0	0	0	0	0
Apiaceae	0	1	1	0	0	1	1	0
Chenopodium	3	3	0	0	1	0	2	2
Lactuceae	0	0	0	0	0	0	1	0
Valerianaceae	1	1	0	0	0	0	3	1
Campanulaceae	0	0	2	1	0	1	0	1
Althernanthera	0	0	0	0	0	0	0	0
Brassicaceae	1	1	0	0	0	0	0	0
Rubiaceae	1	0	0	0	0	0	0	0
Malvaceae	2	0	0	3	0	0	0	0
Urticaceae Moraceae	17	22	40	47	42	39	18	16
Hedyosmum	7	16	8	8	16	10	3	9
Acalypha	3	0	11	6	2	6	4	2
Podocarpus	3	4	5	10	2	4	3	3
Ericaceae	6	3	0	8	3	6	10	4
Myrsinaceae	2	1	0	7	3	3	6	2
Alchornea	2	0	4	3	4	1	0	1
Juglans	0	0	0	1	0	0	0	1
Alnus	1	0	0	0	1	0	0	0
Vallea	0	0	1	3	1	1	0	0
Bocconia	1	1	1	1	0	0	1	1
Myricaceae	0	1	1	0	0	1	0	0
Solanacea	1	1	3	1	0	0	0	1
Weinmannia	0	0	0	0	0	0	0	0
Rosaceae	2	0	2	0	1	0	1	0
Myrtaceae	0	1	3	1	0	0	0	0
Cassia	0	0	0	0	0	0	0	0
Cecropia	0	0	2	3	0	0	0	0
Celtis	0	0	0	0	0	0	0	0
Anacardiaceae	2	1	4	0	0	1	0	0
Prosopis	0	0	0	5	1	1	0	2
Euphorbiaceae	1	1	0	0	0	0	0	0
Mimosaceae	3	0	0	0	0	1	0	0
Dodonaea	0	0	1	0	0	0	0	0
Cyperaceae	7	14	8	7	6	10	11	14
Other/Broken unidentified	9	8	14	12	8	8	8	7

Table A8-3 Lake Huamanmarca pollen counts, continued (4 of 8)

Volume CC	0.25	0.25	0.25	0.25	0.25	0.25	0.25	0.25
Age	4982.11	5155.21	5328.3	5674.49	5847.58	6020.67	6193.77	6366.86
Depth (cm)	223	229	235	247	253	259	265	271
Lycopodium	1024	1172	736	1628	1200	1780	1168	1348
Pollen Sum	310	313	326	325	305	308	329	322
Polylepis	69	60	51	58	49	70	63	54
Melastomataceae	5	3	10	2	4	5	4	6
Hesperomeles	1	0	0	0	1	0	0	1
Gynoxys	2	2	0	4	0	0	1	1
Poaceae	146	137	139	139	143	124	147	135
Asteraceae	17	19	7	20	4	8	12	15
Caryophyllaceae	4	3	6	5	3	5	2	0
Plantago	1	3	2	0	0	2	4	3
Ambrosia	1	1	0	3	1	3	1	0
Thalictrum	0	0	0	0	0	1	0	2
Apiaceae	0	1	2	2	0	1	1	1
Chenopodium	0	1	2	2	1	0	0	1
Lactuceae	0	2	0	1	1	0	0	0
Valerianaceae	0	0	1	2	1	2	1	0
Campanulaceae	0	0	0	0	0	0	0	1
Althernanthera	0	0	0	0	0	0	1	1
Brassicaceae	0	0	0	0	0	0	0	1
Rubiaceae	0	0	0	0	1	1	1	1
Malvaceae	0	0	0	0	0	0	0	0
Urticaceae Moraceae	25	27	42	29	36	26	37	40
Hedyosmum	7	8	10	7	6	11	7	5
Acalypha	6	7	8	4	11	3	7	6
Podocarpus	1	9	5	6	7	5	7	3
Ericaceae	3	2	5	9	4	4	4	2
Myrsinaceae	2	3	6	1	4	3	1	1
Alchornea	2	1	0	1	2	1	1	0
Juglans	0	0	0	0	1	0	2	2
Alnus	0	0	1	0	2	0	2	1
Vallea	0	1	1	3	1	1	0	1
Bocconia	0	0	0	0	0	0	0	1
Myricaceae	1	1	1	1	3	0	1	1
Solanacea	1	0	2	0	2	1	0	1
Weinmannia	1	0	0	1	1	2	1	0
Rosaceae	0	0	0	0	0	2	0	0
Myrtaceae	0	0	0	0	0	0	1	0
Cassia	0	0	0	0	1	0	0	1
Cecropia	0	1	2	0	0	0	1	1
Celtis	0	0	4	0	2	3	0	2
Anacardiaceae	1	0	1	1	0	0	2	1
Prosopis	4	2	1	0	0	4	1	0
Euphorbiaceae	0	0	0	0	0	1	1	1
Mimosaceae	0	0	0	0	0	0	0	1
Dodonaea	0	0	0	1	1	1	0	1
Cyperaceae	8	14	11	12	9	11	12	17
Other/Broken unidentified	2	5	6	11	3	7	3	10

Table A8-3 Lake Huamanmarca pollen counts, continued (5 of 8)

Volume CC	0.25	0.25	0.5	0.5	0.5	0.5	0.5	0.5
Age	6539.95	6713.05	6902.29	7086.89	7271.5	7456.1	7640.71	7825.31
Depth (cm)	277	283	289	294	299	304	309	314
Lycopodium	692	1388	364	304	248	284	296	336
Pollen Sum	314	335	368	344	326	315	326	338
Polylepis	37	59	47	45	41	43	39	21
Melastomataceae	3	6	5	5	7	3	3	4
Hesperomeles	0	0	0	0	0	0	1	0
Gynoxys	0	1	1	1	2	0	1	2
Poaceae	127	141	143	119	90	108	96	100
Asteraceae	8	12	9	6	4	5	1	7
Caryophyllaceae	4	3	0	6	0	2	4	0
Plantago	2	1	2	5	4	2	2	4
Ambrosia	0	1	0	0	0	0	0	0
Thalictrum	0	0	0	6	0	0	0	0
Apiaceae	0	0	0	1	1	0	1	0
Chenopodium	0	1	0	0	0	0	1	0
Lactuceae	0	0	0	0	0	0	0	0
Valerianaceae	1	0	0	1	2	1	0	1
Campanulaceae	1	1	2	2	0	1	0	1
Althernanthera	0	0	0	1	0	0	0	0
Brassicaceae	1	0	0	2	0	0	0	1
Rubiaceae	0	1	0	0	1	0	0	0
Malvaceae	0	0	0	1	0	1	0	0
Urticaceae Moraceae	72	41	97	86	109	84	99	120
Hedyosmum	5	4	6	14	9	11	8	13
Acalypha	15	18	26	12	9	12	18	13
Podocarpus	1	5	0	1	3	0	4	2
Ericaceae	4	4	5	4	3	3	4	2
Myrsinaceae	0	1	0	1	3	0	1	3
Alchornea	0	3	1	0	2	6	4	0
Juglans	1	0	0	2	0	1	0	0
Alnus	1	2	0	0	0	0	0	0
Vallea	2	0	0	0	0	0	0	0
Bocconia	2	0	0	0	0	0	0	0
Myricaceae	1	0	0	1	2	0	2	2
Solanacea	3	2	0	0	5	4	1	0
Weinmannia	3	4	0	0	1	0	0	0
Rosaceae	1	0	0	0	1	1	1	0
Myrtaceae	0	3	0	0	0	0	0	0
Cassia	0	2	0	0	0	1	0	0
Cecropia	2	0	5	1	4	3	5	14
Celtis	0	1	0	0	0	0	0	0
Anacardiaceae	0	1	1	1	0	0	2	2
Prosopis	0	0	1	1	0	1	1	0
Euphorbiaceae	0	0	0	1	0	0	3	3
Mimosaceae	0	0	0	0	0	0	0	0
Dodonaea	0	0	0	0	0	0	0	0
Cyperaceae	4	8	8	11	15	18	17	13
Other/Broken unidentified	13	9	9	7	8	4	7	10

Table A8-3 Lake Huamanmarca pollen counts, continued (6 of 8)

Volume CC	0.5	0.5	0.5	0.5	0.5	0.5	0.5	0.5
Age	8009.92	8194.53	8342.21	8540.39	8738.58	8936.76	9134.94	9531.31
Depth (cm)	319	324	328	329	330	331	332	334
Lycopodium	172	656	372	316	268	1084	1008	100
Pollen Sum	382	330	315	311	338	333	327	335
Polylepis	19	25	18	12	16	17	17	7
Melastomataceae	8	5	8	5	5	1	9	2
Hesperomeles	0	3	3	1	0	0	0	0
Gynoxys	0	4	3	0	2	0	1	0
Poaceae	96	127	92	135	123	87	84	91
Asteraceae	2	4	5	9	9	9	9	10
Caryophyllaceae	2	1	1	0	0	2	1	1
Plantago	1	3	2	1	3	5	7	4
Ambrosia	0	1	0	0	2	0	0	1
Thalictrum	1	0	1	0	1	1	0	0
Apiaceae	0	1	2	0	0	1	1	2
Chenopodium	0	1	1	0	0	0	1	0
Lactuceae	0	0	0	0	0	0	0	1
Valerianaceae	0	0	0	1	1	0	0	0
Campanulaceae	0	0	0	0	1	0	0	0
Althernanthera	0	0	0	0	0	0	0	0
Brassicaceae	0	0	0	1	0	0	0	0
Rubiaceae	0	2	0	0	0	0	0	0
Malvaceae	0	1	0	0	1	1	0	1
Urticaceae Moraceae	171	69	106	59	107	99	89	72
Hedyosmum	8	25	5	16	9	13	20	37
Acalypha	17	13	23	15	11	19	14	14
Podocarpus	1	2	2	4	3	16	14	30
Ericaceae	2	6	6	3	3	5	7	4
Myrsinaceae	2	1	4	4	2	3	2	9
Alchornea	5	2	1	2	1	3	2	2
Juglans	1	3	0	3	1	1	0	9
Alnus	0	2	0	1	1	0	0	0
Vallea	0	1	0	0	1	2	0	1
Bocconia	0	0	0	1	0	0	0	0
Myricaceae	1	0	0	1	0	1	5	1
Solanacea	1	0	0	1	0	0	2	2
Weinmannia	0	1	1	1	0	2	1	0
Rosaceae	0	0	0	1	0	0	4	1
Myrtaceae	0	0	0	0	0	0	0	0
Cassia	0	0	0	0	0	1	0	0
Cecropia	11	1	5	3	16	22	16	18
Celtis	0	0	0	0	0	0	0	0
Anacardiaceae	0	1	0	2	1	0	0	0
Prosopis	1	1	1	1	2	1	1	1
Euphorbiaceae	0	2	0	0	0	0	0	0
Mimosaceae	0	1	0	0	0	0	0	0
Dodonaea	0	0	0	0	0	0	0	0
Cyperaceae	12	17	17	18	12	7	11	8
Other/Broken unidentified	20	4	8	10	4	14	9	6

Table A8-3 Lake Huamanmarca pollen counts, continued (7 of 8)

Volume CC	0.5	0.5	0.5	0.5	0.5	0.5	0.5
Age	9729.49	9927.68	10125.86	10324.04	10522.23	10720.41	10918.59
Depth (cm)	335	336	337	338	339	340	341
Lycopodium	1688	544	952	3292	2720	1044	1072
Pollen Sum	335	382	309	300	310	315	411
Polylepis	7	20	11	11	4	18	18
Melastomataceae	10	11	3	2	19	10	5
Hesperomeles	0	4	1	3	0	0	0
Gynoxys	0	1	0	0	0	0	1
Poaceae	58	84	77	85	69	75	151
Asteraceae	12	8	6	11	10	3	19
Caryophyllaceae	0	2	0	0	0	1	1
Plantago	1	2	1	2	3	2	2
Ambrosia	0	0	1	0	0	0	0
Thalictrum	0	1	0	0	2	1	1
Apiaceae	1	0	0	0	1	1	0
Chenopodium	0	0	0	0	0	0	0
Lactuceae	0	3	0	0	0	0	1
Valerianaceae	0	2	1	1	1	0	1
Campanulaceae	0	0	0	0	0	0	0
Althernanthera	0	1	0	0	0	0	0
Brassicaceae	0	0	0	0	0	0	0
Rubiaceae	0	1	0	0	1	0	0
Malvaceae	0	0	0	0	0	0	0
Urticaceae Moraceae	120	91	74	70	76	64	91
Hedyosmum	18	30	39	15	20	29	21
Acalypha	12	17	7	21	13	23	20
Podocarpus	12	27	37	11	11	26	11
Ericaceae	10	10	3	15	13	8	7
Myrsinaceae	3	5	2	5	6	4	1
Alchornea	3	1	0	0	1	2	2
Juglans	1	2	1	1	2	0	1
Alnus	1	4	1	0	2	0	0
Vallea	4	2	1	2	3	2	1
Bocconia	0	0	0	1	0	1	1
Myricaceae	2	5	1	3	1	7	2
Solanacea	1	1	0	0	0	1	2
Weinmannia	0	0	0	2	7	2	0
Rosaceae	1	2	1	0	0	0	0
Myrtaceae	0	0	0	0	0	0	0
Cassia	0	0	1	1	0	1	0
Cecropia	41	20	22	13	23	15	31
Celtis	0	7	5	2	0	0	2
Anacardiaceae	0	0	0	1	1	1	0
Prosopis	0	0	0	0	0	0	0
Euphorbiaceae	0	0	0	0	0	0	0
Mimosaceae	0	0	0	0	0	0	0
Dodonaea	0	0	0	0	0	0	0
Cyperaceae	7	14	11	12	6	10	11
Other/Broken unidentified	10	4	2	10	15	8	7

Table A8-3 Lake Huamanmarca pollen counts, continued (8 of 8)

Volume CC	0.5	0.5	0.5	0.5	0.5	0.5	0.5	0.5
Age	11314.96	11711.33	11909.51	12107.7	12305.88	12504.06	12702.25	12942.58
Depth (cm)	343	345	346	347	348	349	350	407
Lycopodium	1808	88	1604	1964	2756	1988	1636	3596
Pollen Sum	351	308	311	307	316	348	308	324
Polylepis	7	10	7	1	2	4	3	1
Melastomataceae	9	8	11	8	11	9	6	15
Hesperomeles	1	1	1	1	0	1	3	1
Gynoxys	1	1	0	0	0	0	0	0
Poaceae	76	46	74	38	40	59	53	76
Asteraceae	12	12	10	3	8	10	13	25
Caryophyllaceae	1	1	0	0	0	0	0	1
Plantago	3	1	1	4	5	0	2	6
Ambrosia	0	0	0	0	0	0	0	0
Thalictrum	0	0	1	0	0	0	0	0
Apiaceae	2	1	1	1	3	3	0	0
Chenopodium	0	0	0	0	1	1	0	0
Lactuceae	0	0	0	0	0	2	1	0
Valerianaceae	1	0	0	0	0	0	3	0
Campanulaceae	0	0	0	0	0	0	0	0
Althernanthera	0	0	0	1	0	0	0	1
Brassicaceae	0	0	1	0	0	0	0	0
Rubiaceae	0	0	0	0	0	1	0	0
Malvaceae	0	0	1	0	0	0	0	0
Urticaceae Moraceae	67	68	56	48	54	88	61	68
Hedyosmum	48	39	32	43	49	43	52	31
Acalypha	13	20	12	22	28	25	17	17
Podocarpus	19	19	29	44	25	26	26	15
Ericaceae	16	11	14	12	15	9	8	15
Myrsinaceae	5	3	3	2	3	2	5	3
Alchornea	6	3	5	4	4	2	0	3
Juglans	2	4	3	2	1	1	3	4
Alnus	1	0	3	0	1	1	2	1
Vallea	2	1	0	8	1	6	3	2
Bocconia	1	0	0	0	0	0	0	0
Myricaceae	3	0	0	6	1	0	3	2
Solanacea	0	2	1	2	1	0	2	0
Weinmannia	1	2	1	2	1	0	2	1
Rosaceae	0	2	0	0	0	0	0	0
Myrtaceae	1	1	1	0	2	0	0	0
Cassia	1	0	0	0	1	0	0	0
Cecropia	33	28	28	26	30	37	27	21
Celtis	2	0	1	0	0	0	0	4
Anacardiaceae	1	2	0	1	1	0	0	0
Prosopis	0	0	0	1	2	0	1	0
Euphorbiaceae	0	1	0	0	0	0	0	0
Mimosaceae	0	0	0	0	0	0	1	0
Dodonaea	0	0	0	0	0	0	0	0
Cyperaceae	4	9	7	10	12	11	5	5
Other/Broken unidentified	12	12	7	17	14	7	6	6

Table A8-4 DCA axis scores for lakes Pacucha, Miski and Huamanmarca, 1 of 5

Site	Age	DCA1	DCA2	DCA3	DCA4
Pacucha	0	1.4826	0.1644	0.5876	0.6201
Pacucha	19.1	1.525	0.2599	0.5881	0.4817
Pacucha	38.2	1.6959	0.182	0.4864	0.5712
Pacucha	57.3	1.8352	0.0874	0.3693	0.4678
Pacucha	76.3	1.7458	0.0867	0.4241	0.5673
Pacucha	95.4	1.7503	0	0.409	0.4048
Pacucha	114.5	1.8314	0.125	0.475	0.5507
Pacucha	133.6	1.7664	0.121	0.4137	0.4248
Pacucha	143.1	1.4991	0.3879	0.6711	0.6358
Pacucha	152.7	1.7357	0.1429	0.5177	0.7028
Pacucha	171.8	1.7308	0.2469	0.5579	0.47
Pacucha	190.9	1.5843	0.3719	0.6982	0.7578
Pacucha	209.9	1.6528	0.3278	0.5662	0.6078
Pacucha	229	1.7456	0.4617	0.6137	0.6716
Pacucha	248.1	1.7371	0.4214	0.6359	0.7286
Pacucha	267.2	1.6131	0.424	0.7271	0.8985
Pacucha	286.3	1.4549	0.5037	0.8175	0.819
Pacucha	305.4	1.6193	0.4689	0.6241	0.6977
Pacucha	324.4	1.7047	0.3797	0.5155	0.7615
Pacucha	343.5	1.7108	0.4644	0.6094	0.714
Pacucha	362.6	1.6529	0.4907	0.5815	0.6221
Pacucha	381.7	1.5395	0.3793	0.5363	0.639
Pacucha	400.8	1.7113	0.3921	0.5812	0.762
Pacucha	419.9	1.6452	0.4701	0.5609	0.7327
Pacucha	429.4	1.4864	0.5167	0.6028	0.6339
Pacucha	439	1.5279	0.3147	0.4899	0.6519
Pacucha	458	1.5442	0.3528	0.4181	0.6586
Pacucha	477.1	1.667	0.2564	0.4297	0.6886
Pacucha	496.2	1.6665	0.1124	0.4954	0.6686
Pacucha	515.3	1.4969	0.2582	0.5092	0.5835
Pacucha	534.4	1.5992	0.2384	0.402	0.4679
Pacucha	553.5	1.3646	0.5536	0.5533	0.6736
Pacucha	572.6	1.2615	0.5138	0.6502	0.6368
Pacucha	591.6	1.2496	0.5323	0.4938	0.3739
Pacucha	610.7	1.2934	0.5778	0.5399	0.587
Pacucha	634.7	1.2074	0.6002	0.5962	0.4294
Pacucha	750	1.3403	0.7504	0.7241	0.5857
Pacucha	942.2	1.2484	0.5556	0.8007	0.6595
Pacucha	1260.9	1.1705	0.9541	0.8955	0.8737
Pacucha	1618.2	1.217	0.807	0.7295	0.7194
Pacucha	1855.5	1.345	0.8309	0.9225	0.8006
Pacucha	2084.2	1.1371	0.9563	0.6144	0.4325
Pacucha	2313	1.178	0.6742	0.9867	0.8961
Pacucha	2541.8	1.3231	1.184	0.6149	0.4199
Pacucha	2770.5	1.1579	0.9543	1.0237	0.8112

Table A8-4 DCA axis scores for lakes Pacucha, Miski and Huamanmarca. Continued (2 of 5)

Site	Age	DCA1	DCA2	DCA3	DCA4
Pacucha	2985.2	1.0281	0.9769	0.8938	0.8478
Pacucha	3064.3	1.3051	0.9293	1.0283	0.9068
Pacucha	3143.5	1.466	1.0005	0.9354	0.7959
Pacucha	3222.7	1.3451	1.1858	0.9659	0.8062
Pacucha	3381	1.8659	1.4412	1.3037	0.7196
Pacucha	3460.2	1.8857	1.4246	1.3641	0.7578
Pacucha	3539.4	1.4158	1.0262	0.9777	0.9243
Pacucha	3618.5	1.7423	1.3604	1.2385	0.6682
Pacucha	3697.7	1.8214	1.3864	1.2318	0.674
Pacucha	3776.9	1.7125	1.2758	1.2103	0.7399
Pacucha	3856.1	1.7162	1.3394	1.2328	0.7704
Pacucha	4014.4	1.7048	1.2423	1.1935	0.7727
Pacucha	4093.6	2.4165	1.9016	1.6083	0.5215
Pacucha	4199.1	2.445	1.4764	1.4602	0.1728
Pacucha	4304.7	1.6549	1.2301	1.1188	0.7358
Pacucha	4410.3	1.6565	1.3807	1.0592	0.7375
Pacucha	4515.8	1.3772	1.1812	0.9517	0.7231
Pacucha	4621.4	1.4709	1.2113	0.9738	0.6925
Pacucha	4751.7	1.9503	1.5945	1.3431	0.6049
Pacucha	4839.8	1.5809	1.3817	1.1968	0.6086
Pacucha	4927.9	1.4759	1.1505	0.9111	0.7267
Pacucha	5150.6	1.5975	1.2978	1.1037	0.6834
Pacucha	5507.7	1.5023	1.2127	1.048	0.8546
Pacucha	5864.9	1.1656	0.9706	0.8442	0.8282
Pacucha	6222	1.1156	0.9461	0.849	0.808
Pacucha	6579.2	1.0714	1.0443	0.7886	0.7275
Pacucha	6961.3	0.979	0.8917	0.853	0.7984
Pacucha	7171	0.9444	1.078	0.8521	0.8423
Pacucha	7380.7	1.0552	0.9354	0.7075	0.649
Pacucha	7590.4	1.0531	0.7229	0.7376	0.5342
Pacucha	7800.2	0.9669	1.0257	0.7834	0.9074
Pacucha	8013.9	0.8973	1.0979	0.7448	0.7005
Pacucha	8233.6	0.9057	0.9994	0.8562	0.7946
Pacucha	8453.3	0.9491	1.141	0.8298	0.8965
Pacucha	8673	0.8639	1.083	0.8491	0.6474
Pacucha	8892.7	0.9601	0.9596	0.9133	0.77
Pacucha	9112.5	0.8213	0.9586	0.9439	0.7692
Pacucha	9332.2	0.9403	1.0573	0.7807	0.5645
Pacucha	9551.9	0.9451	1.0572	0.8941	0.9835
Pacucha	9771.6	0.6326	0.7984	1.2773	1.1158
Pacucha	9991.3	0.895	0.8337	1.0351	0.9314
Pacucha	10211	0.8649	0.9931	0.9656	1.0767
Pacucha	10430.7	0.9879	1.1348	0.7998	0.759
Pacucha	10642	0.9599	0.9658	0.8583	0.7995
Pacucha	10819.7	0.9133	0.8737	0.8583	0.8145

Appendix VIII

Table A8-4 DCA axis scores for lakes Pacucha, Miski and Huamanmarca. Continued (3 of 5)

Site	Age	DCA1	DCA2	DCA3	DCA4
Pacucha	10997.3	1.0419	0.9031	0.8267	0.5273
Pacucha	11175	1.0287	0.8401	0.9314	0.4521
Pacucha	11352.6	0.9498	0.7951	0.9086	0.5227
Pacucha	11530.3	0.9477	0.8348	1.0483	0.7009
Pacucha	11708	0.8878	0.8693	0.915	0.4404
Pacucha	11885.6	0.9508	0.8951	0.9442	0.4079
Pacucha	12063.3	0.8753	0.9682	0.8403	0.3592
Pacucha	12240.9	0.9156	0.9914	0.7336	0.5345
Pacucha	12418.6	0.9042	1.0112	0.7579	0.4228
Pacucha	12596.2	0.8791	1.0407	0.8039	0.4973
Pacucha	12773.9	0.9022	1.069	0.7702	0.4997
Miski	0	0.4918	0.8155	0.797	0.4985
Miski	132.476	0.5596	0.7873	0.7759	0.7147
Miski	314.912	0.5372	0.7738	0.881	0.7042
Miski	497.347	0.5762	0.7761	0.7862	0.6136
Miski	679.783	0.6183	1.0003	0.6293	0.545
Miski	862.219	0.4487	0.8423	0.7238	0.5177
Miski	1044.65	0.4861	0.8196	0.6966	0.4596
Miski	1227.09	0.3924	0.8602	0.7018	0.4241
Miski	1409.53	0.6013	0.9019	0.6145	0.4622
Miski	1591.96	0.6236	0.9423	0.7178	0.5447
Miski	1883.86	0.5922	0.8845	0.8604	0.7615
Miski	2212.24	0.5771	0.8822	0.7922	0.6692
Miski	2537.69	0.6422	0.9647	0.8707	0.7658
Miski	2863.13	0.5843	0.9444	0.842	0.6841
Miski	3229.25	0.4419	0.8477	0.9544	0.8084
Miski	3554.69	0.6551	1.0881	0.6878	0.6624
Miski	3839.45	0.6576	0.8044	0.975	0.6928
Miski	4088.13	0.7168	1.019	0.7407	0.5713
Miski	4378.26	0.7317	1.0971	0.7231	0.6299
Miski	4668.39	0.6867	0.9235	0.7786	0.6448
Miski	4917.07	0.6643	0.9683	0.8243	0.7277
Miski	5207.19	0.8015	1.0876	0.6876	0.5628
Miski	5497.32	0.6831	1.0216	0.7413	0.6255
Miski	5746	0.6228	0.8966	0.8661	0.6751
Miski	6036.13	0.5916	0.9714	0.7405	0.7007
Miski	6450.59	0.6459	1.0175	0.7188	0.7354
Miski	6740.72	0.6542	0.9474	0.8342	0.7468
Miski	7072.29	0.6325	0.9878	0.9217	0.8597
Miski	7279.53	0.6744	0.9069	0.9859	0.831
Miski	7486.76	0.6321	0.9178	1.0786	0.9799
Miski	7643.68	0.6715	0.9486	0.9553	0.8897
Miski	7725.12	0.6374	0.9611	0.8598	0.7483
Miski	7806.57	0.6452	0.9765	0.9391	0.8055
Miski	7888.01	0.5718	0.9222	1.0308	0.8281

Table A8-4 DCA axis scores for lakes Pacucha, Miski and Huamanmarca. Continued (4 of 5)

Site	Age	DCA1	DCA2	DCA3	DCA4
Miski	7969.46	0.7548	0.9936	0.8614	0.654
Miski	8050.9	0.7014	0.9441	0.8753	0.726
Miski	8132.35	0.6713	0.8678	0.9462	0.8185
Miski	8213.79	0.5628	0.8588	1.0498	0.8341
Miski	8295.24	0.6013	0.9985	0.8631	0.7477
Miski	8376.68	0.5778	0.8951	0.8405	0.598
Miski	8458.13	0.5956	0.9142	0.8137	0.6504
Miski	8539.57	0.7252	0.9376	0.9404	0.7231
Miski	8621.02	0.6557	0.9046	0.9597	0.743
Miski	8702.46	0.6359	0.8603	0.9985	0.7667
Miski	8783.91	0.655	0.9129	0.8302	0.5808
Miski	8865.35	0.6214	0.8093	0.9554	0.6067
Miski	9173.24	0.6756	0.7809	1.0244	0.5299
Miski	9537.74	0.7654	0.6839	1.0206	0.6071
Miski	9902.25	0.6334	0.8041	1.0472	0.6078
Miski	10266.7	0.6868	0.8359	0.9769	0.6974
Miski	10631.2	0.7513	0.7818	0.9328	0.5875
Miski	10995.8	0.6696	0.7846	1.1536	0.8701
Miski	11360.3	0.6638	0.8808	0.9964	0.7797
Miski	11724.8	0.5568	0.7027	1.2969	0.904
Miski	12089.3	0.5785	0.642	1.284	0.8567
Miski	12607.5	0.5911	0.524	1.3872	0.6999
Miski	12621.2	0.5546	0.6529	1.2813	0.8642
Miski	12635	0.5247	0.5627	1.4225	0.9678
Miski	12648.7	0.5838	0.4813	1.361	0.6719
Miski	12662.5	0.5032	0.4911	1.4473	0.6886
Miski	12676.2	0.4993	0.4587	1.4335	0.3848
Miski	12690	0.5575	0.4398	1.4392	0.5237
Huamanmarca	0	0.1146	0.9631	0.169	0.149
Huamanmarca	177.1	0.2177	1.003	0.1919	0.0891
Huamanmarca	404.3	0.235	1.0447	0.1216	0.1052
Huamanmarca	631.5	0.255	1.036	0.2337	0.2497
Huamanmarca	858.6	0.2408	0.9351	0.2088	0.187
Huamanmarca	1085.8	0.2615	1.0371	0.1029	0.1574
Huamanmarca	1312.9	0.2742	1.0633	0.2641	0.2235
Huamanmarca	1540.1	0.0224	1.0434	0	0
Huamanmarca	1767.2	0	1.0724	0.061	0.1417
Huamanmarca	1994.4	0.2633	1.0555	0.1958	0.2612
Huamanmarca	2221.6	0.2832	1.0431	0.2696	0.1881
Huamanmarca	2448.7	0.1128	0.9249	0.0792	0.0283
Huamanmarca	2642.7	0.1031	0.9241	0.2867	0.3071
Huamanmarca	2823.5	0.2054	0.9371	0.525	0.6296
Huamanmarca	3004.3	0.1302	1.0391	0.0912	0.2086
Huamanmarca	3185.1	0.2141	1.0317	0.1297	0.1473
Huamanmarca	3365.9	0.2047	1.0881	0.1717	0.1785

Table A8-4 DCA axis scores for lakes Pacucha, Miski and Huamanmarca. Continued (5 of 5)

Site	Age	DCA1	DCA2	DCA3	DCA4
Huamanmarca	3546.7	0.307	1.0867	0.2786	0.2066
Huamanmarca	3727.5	0.4152	0.9958	0.4924	0.438
Huamanmarca	4089.1	0.4187	0.9786	0.583	0.4799
Huamanmarca	4269.9	0.2033	1.0101	0.3572	0.2899
Huamanmarca	4462.8	0.2885	1.0182	0.3231	0.2926
Huamanmarca	4635.9	0.29	1.1054	0.2177	0.2135
Huamanmarca	4809	0.4101	1.1311	0.2389	0.2523
Huamanmarca	4982.1	0.4034	1.1071	0.298	0.3477
Huamanmarca	5155.2	0.4931	1.0213	0.405	0.2928
Huamanmarca	5328.3	0.4646	1.0136	0.5565	0.4684
Huamanmarca	5674.5	0.462	1.0362	0.4119	0.2942
Huamanmarca	5847.6	0.479	1.0568	0.5111	0.4372
Huamanmarca	6020.7	0.3532	1.0255	0.3389	0.3144
Huamanmarca	6193.8	0.4418	1.0316	0.4283	0.3799
Huamanmarca	6366.9	0.52	1.0084	0.4392	0.458
Huamanmarca	6540	0.4693	1.0103	0.7033	0.7377
Huamanmarca	6713	0.4712	1.0571	0.4861	0.4471
Huamanmarca	6902.3	0.4422	1.0134	0.7534	0.8169
Huamanmarca	7086.9	0.4502	0.9416	0.7038	0.7317
Huamanmarca	7271.5	0.3922	0.8164	0.8416	0.8368
Huamanmarca	7456.1	0.4504	0.8931	0.7147	0.7333
Huamanmarca	7640.7	0.4295	0.8422	0.8254	0.8044
Huamanmarca	7825.3	0.4684	0.7796	1.0419	1.0009
Huamanmarca	8009.9	0.4566	0.7758	1.1574	1.1883
Huamanmarca	8194.5	0.5455	0.8793	0.7822	0.6092
Huamanmarca	8342.2	0.5684	0.8281	0.9785	0.9549
Huamanmarca	8540.4	0.7147	0.8935	0.8335	0.6717
Huamanmarca	8738.6	0.5457	0.8474	1.0251	0.9818
Huamanmarca	8936.8	0.4941	0.7159	1.2505	0.8624
Huamanmarca	9134.9	0.4827	0.6881	1.1903	0.7494
Huamanmarca	9531.3	0.5911	0.5995	1.322	0.5063
Huamanmarca	9729.5	0.3725	0.5382	1.5696	1.0105
Huamanmarca	9927.7	0.4991	0.5814	1.2043	0.5656
Huamanmarca	10125.9	0.4794	0.5595	1.3969	0.4948
Huamanmarca	10324	0.5799	0.7146	1.1559	0.6958
Huamanmarca	10522.2	0.4965	0.6345	1.3933	0.7847
Huamanmarca	10720.4	0.4667	0.6615	1.289	0.5107
Huamanmarca	10918.6	0.5432	0.8134	1.1295	0.762
Huamanmarca	11315	0.4427	0.5422	1.4707	0.5235
Huamanmarca	11711.3	0.4455	0.4803	1.481	0.556
Huamanmarca	11909.5	0.5095	0.5488	1.4346	0.4927
Huamanmarca	12107.7	0.4786	0.3788	1.7263	0.2996
Huamanmarca	12305.9	0.523	0.4139	1.6176	0.4437
Huamanmarca	12504.1	0.4617	0.4938	1.5966	0.6286
Huamanmarca	12702.2	0.4967	0.4366	1.5489	0.4432
Huamanmarca	12942.6	0.6053	0.5823	1.3706	0.6049

Appendix VIII

Table A8-5 Diatom Counts for Lake Miski,1 of 12.

Code	Sample Age (ka)	1 0	2 0.02	3 0.1	4 0.17	5 0.24
Sp1	*Aulacoseira spp*	36.29	33.02	40.37	40.67	33.08
Sp2	*Aulacoseira ambigua*	3.39	0	4.49	0	0.85
Sp3	*Achnanthidium minutissimum*	7.74	8.84	4.49	11.96	6.79
Sp4	*Brachysira* spp	1.94	2.33	3.99	4.78	4.67
Sp5	cf. *Cymbella microcephala*	0	0	0	0	0
Sp6	*Diploneis elliptica*	0	0	0	0	0
Sp7	*Encyonema Cymbella* spp	5.32	0.93	6.48	0.96	6.36
Sp8	*Encyonema* spp	0	0.93	0.5	0.96	0
Sp9	*Eunotia* spp G1 cf. *Bilunaris*	3.87	6.98	4.49	11.48	8.91
Sp10	*Eunotia* spp G2 cf. *incisa*	16.93	12.56	12.96	4.31	8.06
Sp11	*Eunotia* spp G3	9.19	6.05	9.97	8.61	5.09
Sp12	*Eunotia* spp	0.97	1.4	0	2.39	2.12
Sp13	*Fragilaria capucina* complex	6.29	10.23	2.99	2.87	6.79
Sp14	*Fragilaria Staurosira* spp	0.33	0	0.32	0	0.33
Sp15	*Frustulia Stauroneis* spp	1.94	9.77	4.49	4.78	4.67
Sp16	*Gomphonema* spp	0	0	0	0	0
Sp17	*Kobayashiela* spp	0.97	0	1	1.44	0.85
Sp18	*Navicula* spp	0	0	0	0	0
Sp19	*Nitzschia* spp	0	0	0	0	0
Sp20	*Pinnularia* spp	0.97	0	0	0	1.27
Sp21	*Psammothidium* spp	0	0	0	0.96	1.27
Sp22	*Semiorbis hemicyclus*	1.94	3.26	2.49	1.44	3.39
Sp23	*Stenopt.*spp	0.48	2.79	0	0	2.54
Sp24	*Surirella* spp	0	0	0	0	0
Sp25	*Tabellaria flocculosa*	0.97	0	0	0.96	2.12
Sp26	Unknown cf. *Achnantes*	0	0	0	0	0
Sp27	Unknown cf. *Achnantes* Eucoc *Nupela*	0	0.93	1	0	0.85
Sp28	Unknown.benthic	0.48	0	0	0	0
Sp29	X3 Unknown	0	0	0	1.44	0

Table A8-5 Diatom Counts for Lake Miski. Continued (2 of 12).

Sample	6	7	8	9	10	11	12	13	14	15	16	17
Age (ka)	0.31	0.39	0.46	0.53	0.61	0.68	0.75	0.83	0.9	0.97	1.04	1.12
Sp1	40.49	37.78	25.60	53.47	24.88	3.67	12.32	1.42	8.42	0.97	10.20	13.13
Sp2	0.89	0	3.38	0.49	0	0	0.47	0	0	0	0	0
Sp3	8.9	11.48	13.53	5.4	2.3	0.92	5.21	0.95	2.34	4.37	12.05	5.35
Sp4	2.22	6.7	3.38	3.92	7.83	9.17	8.53	15.17	11.7	10.68	12.05	11.19
Sp5	0	0	0	0	0	0	0	0	0.94	0	0	0
Sp6	0	0	0	0	0	0	0	0	0	0	0	0
Sp7	5.78	0.48	4.83	0.49	1.84	1.38	5.69	5.21	5.15	4.85	3.25	6.32
Sp8	0.44	1.43	1.45	0	1.38	0.46	0.47	0.47	1.4	1.46	0.46	0
Sp9	8.9	7.17	10.14	5.4	8.76	11.47	7.58	18.96	12.17	16.02	10.66	14.59
Sp10	9.34	14.35	12.08	10.79	29.95	60.55	30.81	24.17	19.19	29.13	15.76	22.37
Sp11	7.56	6.22	8.7	5.4	4.61	4.59	10.9	23.22	19.19	11.65	19.01	9.24
Sp12	1.78	0	1.45	0	5.99	0	4.27	0	3.74	0.97	1.85	0
Sp13	3.56	1.91	1.93	2.45	2.3	0	2.37	1.42	0	0	0	0.97
Sp14	0.33	1	0	0.92	0	0	0	0	0.33	0	0.32	0.3
Sp15	2.22	0.96	4.35	2.45	2.3	3.67	2.37	3.32	1.87	5.34	1.39	6.81
Sp16	0	0	0	0	0	0	0	0	0	0	0	0
Sp17	0.44	0.96	0.48	0	0	2.29	1.42	0.47	5.15	1.46	1.39	1.46
Sp18	0	0	0	0	0	0	0	0	0	0	0	0
Sp19	0	0	0	0	0	0	0	0	0	0.97	0.46	0
Sp20	0.44	0.48	0.48	0	0.92	0.92	1.9	0.47	1.87	1.46	1.39	3.4
Sp21	0	0.48	0	0	0	0	0.95	1.42	0.47	2.43	3.71	0.97
Sp22	3.11	1.91	3.86	1.47	2.76	0	0	0	0	0	0	0
Sp23	0	0.48	0.97	0	0.46	0	0	0.95	1.87	1.46	0.46	0.49
Sp24	0	0	0	0	0	0	0	0	0	0	0.93	0.97
Sp25	0	0.48	0.97	1.47	0.46	0.92	0	0.47	0	2.91	0.46	0.97
Sp26	0.89	0	0.97	0	0	0	1.42	1.42	1.87	3.88	1.85	0
Sp27	0.89	3.83	1.45	4.91	1.84	0	2.37	0	2.34	0	0.93	0.97
Sp28	0	0	0	0.98	0.46	0	0	0.47	0	0	1.39	0.49
Sp29	1.78	1.91	0	0	0.92	0	0.95	0	0	0	0	0

Table A8-5 Diatom Counts for Lake Miski. Continued (3 of 12).

Sample	18	19	20	21	22	23	24	25	26	27	28	29
Age (ka)	1.26	1.41	1.56	1.7	1.85	1.99	2.14	2.29	2.46	2.62	2.78	2.94
Sp1	0.93	0.00	0.00	0.46	0.89	0.00	0.85	0.00	0.40	2.34	4.33	0.44
Sp2	0	0	0	0	0	0	0	0	0	0	0.48	1.75
Sp3	0.93	0	0.48	0.46	0	1.35	0.85	0	0.8	0.94	1.44	4.39
Sp4	11.22	9.52	11.13	20.45	23.21	16.24	19.66	20.02	8.4	8.42	13.94	14.04
Sp5	0	0	0	0	0	0	0	0	0	0	0	1.32
Sp6	0	0	0	0	0	0	0	0	0	0	0	0
Sp7	0.47	4.29	0.97	5.58	3.13	3.16	4.27	6.23	4	1.87	5.29	4.39
Sp8	0	0	0	1.86	0.89	0.45	0	0.44	0	0	0.96	0.88
Sp9	5.61	12.86	5.81	19.52	12.95	12.18	24.79	14.24	16.4	7.02	4.33	14.04
Sp10	60.28	44.76	78.38	25.57	38.39	35.63	28.21	16.02	10.4	21.53	5.77	10.53
Sp11	8.41	13.33	0	14.41	9.38	14.43	8.12	23.58	37.2	11.23	5.77	12.28
Sp12	0	5.24	0	1.86	2.23	4.06	0.85	1.33	4.4	1.4	1.44	3.51
Sp13	0.93	2.38	0	0	0	0	4.7	0	2.4	0.94	0	0
Sp14	0	0	0.33	0.98	0	0.33	0	0.32	0	0.32	0	0
Sp15	1.87	2.38	0	1.86	0.45	3.16	1.71	7.12	2.4	1.87	2.4	1.32
Sp16	0	0	0	0	0	0.45	0.43	0	0	0	0	0
Sp17	0	0.95	0	2.32	1.79	2.71	0.43	3.11	1.6	0	1.44	0
Sp18	0	0	0	0	0	0	0	0	2	0	0	0
Sp19	0	0	0	0	0	0	0.43	0	0	0.94	1.44	2.19
Sp20	1.87	1.9	0	0.46	0.89	0	0	0.44	0.8	1.87	0	0.88
Sp21	1.4	0	0	1.39	4.02	2.26	1.28	3.11	2.4	0.94	1.92	0
Sp22	0	0	0	0	0	0	0	0	0	0	0	0
Sp23	0	0.48	0	0.93	0.89	1.8	0.85	0	1.2	0	0.48	0.88
Sp24	0	0	0	0	0	0	0	0	0	0	0	0
Sp25	0.47	1.9	2.42	0	0	0	2.56	2.22	1.2	0	0	0
Sp26	0	0	0	0.93	0.89	0	0	1.78	2.4	3.74	2.88	1.75
Sp27	0.93	0	0	0	0	0	0	0	0	33.7	43.75	23.68
Sp28	4.21	0	0	0.46	0	0.9	0	0	0.8	0.94	1.92	0.44
Sp29	0.47	0	0.48	0.46	0	0.9	0	0	0.8	0	0	1.32

Table A8-5 Diatom Counts for Lake Miski. Continued (4 of 12).

Sample	30	31	32	33	34	35	36	37	38	39	40	41
Age (ka)	3.11	3.27	3.43	3.6	3.76	3.92	4.09	4.25	4.42	4.59	4.75	4.92
Sp1	0.49	0.45	0.47	30.24	7.80	0.00	6.13	0.51	4.92	0.88	5.04	4.58
Sp2	0	0	0	0	0	0	0	0	0	0	0	0
Sp3	0.49	1.35	1.87	3.41	3.41	2.4	10.38	2.02	1.34	5.7	15.11	4.58
Sp4	23.9	31.12	28.97	10.24	22.93	27.32	21.23	34.87	29.55	29.39	16.94	13.33
Sp5	0.98	0	0.93	0	0	0	0.47	0	0.9	2.63	0.46	0
Sp6	0	0	0	0	0	0	0	0	0	0	0	0
Sp7	3.41	3.16	2.34	1.46	4.39	1.44	2.36	3.03	4.03	3.95	2.29	1.67
Sp8	0	0	2.8	0.98	0	0.48	0.94	1.01	1.34	3.07	0.92	3.33
Sp9	16.59	9.92	20.56	2.44	14.15	16.77	12.74	14.15	12.53	12.72	6.87	7.08
Sp10	35.61	18.49	8.41	7.8	7.8	10.06	9.91	16.68	9.85	7.02	16.94	7.08
Sp11	6.34	7.22	8.88	6.83	17.56	19.17	14.15	9.1	21.49	13.16	16.94	10.83
Sp12	0.49	6.31	1.87	1.95	0	1.92	0	0	0	0	0	2.92
Sp13	0	0	0	0.98	0	0	0.47	0	0	0	0	0
Sp14	0	0.34	0	0	0	0.32	0	0.95	0.62	0	0.65	0
Sp15	1.95	3.61	11.22	2.93	8.29	3.83	10.38	3.54	3.13	6.58	1.83	2.92
Sp16	0	0.45	0	0.98	0	0.96	0.94	1.52	0.9	1.75	2.29	0
Sp17	1.95	3.61	2.8	0.98	0.98	7.67	6.6	3.03	4.03	3.07	1.37	0
Sp18	0	0	0	0	0.49	0.96	0	0	0.45	0	0	0
Sp19	0	0.45	1.4	0	2.93	0	0	0.51	0.45	0.44	0	0
Sp20	2.44	0	0.47	0.98	0.98	0.96	0.47	2.53	0	0.88	0.92	0.83
Sp21	0	0.9	1.87	4.88	0.98	2.4	0.94	2.02	1.34	0.88	1.83	2.5
Sp22	0	0	0	0	0	0	0	0	0	0	0	0
Sp23	0.98	0	0.93	0.49	0.49	0	0.47	0.51	0	0.88	0	0
Sp24	0	0	0	2.44	0	0	0	0	0	0	0	0
Sp25	0	0	0.93	0	0	1.44	0.47	0	0.45	0	0	2.08
Sp26	0.98	1.8	0	0	0	0	0	0	0	0	2.29	0.42
Sp27	3.41	10.82	2.34	15.61	0	0.48	0	0.51	0	6.58	6.87	29.17
Sp28	0	0	0	1.95	5.85	0	0.94	3.54	1.79	0	0.46	6.67
Sp29	0	0	0.93	2.44	0.98	1.44	0	0	0.9	0.44	0	0

Table A8-5 Diatom Counts for Lake Miski. Continued (5 of 12).

Sample	42	43	44	45	46	47	48	49	50	51	52	53
Age (ka)	5.08	5.17	5.25	5.33	5.41	5.5	5.58	5.66	5.75	5.83	5.91	5.99
Sp1	2.91	48.17	47.10	15.03	31.13	18.87	15.13	18.06	16.18	23.15	14.38	7.72
Sp2	0	0	0	0	0	0	0	0	0	0	0	0
Sp3	20.38	6.31	7.74	8.82	8.94	6.62	9.54	7.1	7.12	8.02	3.27	6.43
Sp4	25.37	15.28	10.32	24.84	16.56	13.91	18.09	15.81	16.5	19.14	18.95	23.15
Sp5	2.5	0	0	0	0	0	0	0	0.32	1.54	0.65	2.57
Sp6	0	0.33	0	0	0	0	0	0	0	0	0	0
Sp7	4.99	2.99	5.81	5.56	3.97	3.64	3.62	8.06	4.85	5.25	4.58	3.86
Sp8	3.33	1.33	0	0	0	0	0	0.32	0.32	0.31	2.94	1.93
Sp9	9.56	2.99	3.23	8.17	3.31	3.31	5.26	2.26	4.85	4.01	3.27	4.82
Sp10	6.65	1.99	5.48	7.52	10.93	12.25	11.18	7.74	4.85	5.86	10.13	4.82
Sp11	8.32	3.65	2.26	3.27	6.29	3.64	6.25	6.77	8.09	4.63	7.52	5.14
Sp12	0	5.32	2.9	4.58	4.97	4.64	6.25	4.19	4.53	4.32	2.61	2.25
Sp13	0	0.33	0.65	0.33	0.33	1.66	0.33	0.65	0.32	0.93	0.65	0
Sp14	2.27	0.33	0	0.33	0	0.33	0.33	0.97	0	0.93	0	0
Sp15	3.33	3.99	2.9	6.86	7.95	8.28	8.22	6.77	9.06	6.17	5.88	8.68
Sp16	1.25	1.66	4.84	7.52	1.99	11.59	5.26	8.06	11.33	4.94	8.17	11.58
Sp17	0.83	0	0	0	0	0	0	0	2.27	3.09	1.63	1.93
Sp18	0	0.66	0.65	0.98	1.32	0.66	0.66	0	0.97	0.93	0.65	0.32
Sp19	0	0.33	0	0	0	0	0	0	0.32	0	0	0
Sp20	0	2.33	1.29	1.31	0	2.32	1.32	4.19	1.29	1.85	4.25	3.54
Sp21	0	1.33	1.29	0.33	1.99	0.66	2.63	1.29	1.94	2.78	1.31	2.89
Sp22	0	0	0	0	0	0	0.33	0	0	0	0	0
Sp23	0	0	0.32	0.33	0	0	0	0.32	0	1.23	0	0.32
Sp24	0	0.33	0.32	0	0.33	0.33	0	0.97	0	0	0.33	0
Sp25	0	0.33	2.26	4.25	0	7.28	5.59	6.13	4.21	0.93	7.84	7.72
Sp26	1.25	0	0	0	0	0	0	0	0	0	0	0
Sp27	7.07	0	0	0	0	0	0	0.32	0	0	0	0
Sp28	0	0	0.32	0	0	0	0	0	0	0	0.65	0.32
Sp29	0	0	0.32	0	0	0	0	0	0.65	0	0.33	0

Table A8-5 Diatom Counts for Lake Miski. Continued (6 of 12).

Sample	54	55	56	57	58	59	60	61	62	63	64	65
Age (ka)	6.08	6.16	6.24	6.33	6.41	6.49	6.57	6.66	6.74	6.82	6.91	6.99
Sp1	11.22	30.62	35.53	43.77	51.14	46.88	40.00	39.07	28.20	23.51	47.25	20.00
Sp2	0	0	0	0	0	0	0	0	0	0	0	0
Sp3	6.6	7.82	2.63	3.83	6.51	2.97	3.55	3.31	6.56	7.62	0.97	5.25
Sp4	18.15	15.64	16.12	12.46	12.38	13.95	12.58	17.22	12.46	17.55	11.97	18.36
Sp5	1.32	0.65	1.32	1.92	0.65	0.3	0.97	0.99	0.33	1.32	1.62	1.64
Sp6	0	0	0	0	0	0	0.32	0	3.93	0	0	0
Sp7	4.62	4.23	3.62	2.24	3.26	2.97	7.1	4.64	5.25	3.97	3.88	5.9
Sp8	1.98	1.63	0	1.28	1.3	0.59	1.61	0.66	1.31	0.99	0.97	1.64
Sp9	4.29	1.63	0.66	1.6	0.98	1.78	2.26	1.99	4.26	4.64	1.94	3.93
Sp10	11.55	8.47	5.59	5.75	3.58	3.26	5.16	5.3	1.31	5.3	1.94	5.9
Sp11	7.59	4.89	2.3	2.56	2.93	4.75	2.9	4.64	5.9	3.97	18.12	8.52
Sp12	3.96	2.28	1.32	3.19	0.98	2.37	4.19	0.99	3.28	4.64	2.59	5.57
Sp13	0	0.65	1.32	0.64	0.65	0.3	0	0.99	0.33	0	0.32	0.66
Sp14	0	0	0.33	0	0.33	0.3	0	0	0.33	0.99	0	0.33
Sp15	8.58	6.19	6.91	6.07	5.21	4.15	7.1	5.3	7.87	7.95	3.24	6.89
Sp16	8.25	4.23	7.24	5.75	0.98	5.93	5.48	3.64	4.59	5.63	0.65	4.26
Sp17	1.32	0.98	0.99	1.92	1.63	0.3	1.61	1.32	3.28	2.98	0.97	0.98
Sp18	0.66	0	0.99	0.96	0.65	0.3	1.29	0.99	0.66	0.99	0	0.66
Sp19	0	0	0	0	0	0	0	0	0	0.33	0.32	0.33
Sp20	2.64	2.28	1.32	0.32	3.58	1.19	0.65	1.32	1.97	0.99	0.32	0.98
Sp21	1.32	2.28	2.63	1.6	0.33	2.08	1.61	1.66	1.64	2.32	1.62	4.26
Sp22	0	0	0	0	0	0	0	0	0	0	0	0
Sp23	0	0	0	0.64	0.65	0	0	0	0.33	0	0	0.98
Sp24	0	0	0	0	0.65	0	0	0	0	0	0.32	0
Sp25	5.94	5.21	8.55	3.51	1.63	5.34	1.61	5.96	6.23	4.3	0.65	2.95
Sp26	0	0	0	0	0	0	0	0	0	0	0	0
Sp27	0	0	0	0	0	0	0	0	0	0	0	0
Sp28	0	0	0.66	0	0	0.3	0	0	0	0	0.32	0
Sp29	0	0.33	0	0	0	0	0	0	0	0	0	0

Table A8-5 Diatom Counts for Lake Miski. Continued (7 of 12).

Sample	66	67	68	69	70	71	72	73	74	75	76	77
Age (ka)	7.07	7.16	7.24	7.32	7.4	7.49	7.57	7.63	7.66	7.69	7.73	7.76
Sp1	14.43	34.74	43.56	74.05	86.02	76.47	78.29	16.61	60.33	51.47	39.87	52.88
Sp2	0	0	0	0	0	0	0	0	0	0	0	0
Sp3	5.25	1.3	8.59	3.16	0.62	0.33	0.66	0.34	10.67	7.17	9.48	6.41
Sp4	22.95	6.49	4.91	3.48	2.48	3.27	4.28	13.9	7.33	11.08	8.82	6.09
Sp5	0.66	3.9	4.91	0.95	0	0	0	3.39	0.33	1.3	0.98	0.32
Sp6	0	0	0	0	0	0	0	0	0	0	0	0
Sp7	9.18	6.49	5.21	1.58	0	1.63	0.66	3.73	2.33	2.28	2.61	2.24
Sp8	9.51	2.6	1.53	0	0	0	1.32	1.36	1.67	2.93	0.98	0.96
Sp9	4.59	1.3	0	0.63	0	0.98	1.32	2.03	0.33	0.33	0.33	0.96
Sp10	3.93	1.95	3.68	0.95	1.55	1.63	0.33	2.71	2.33	0	6.54	3.21
Sp11	1.97	4.22	1.53	0.95	1.55	0.65	0.66	1.36	2	4.89	3.27	1.28
Sp12	2.62	13.31	4.29	0.95	1.55	1.63	0.33	2.37	1.33	1.3	2.29	1.92
Sp13	0	0	0.31	0.32	0.31	0.65	0	0.34	0.33	0.33	0.65	0
Sp14	0	0.32	0	0.32	0	0	0	0.34	0	0	0	0.32
Sp15	7.54	4.55	1.84	1.27	1.24	0.98	1.97	10.51	2.67	2.93	4.58	3.21
Sp16	2.95	0.32	0.61	0.63	0.62	0.65	0.33	1.02	3.67	2.93	6.54	7.37
Sp17	1.64	0	1.23	0.32	0	0	0.99	2.71	0	0.98	2.29	2.24
Sp18	0.33	0.32	0.61	0.63	0.31	0	0	0.34	0.67	0.65	0.65	1.6
Sp19	0.66	0.32	0.31	0.32	0	0	0	0	0	0	0.33	0
Sp20	2.62	1.62	0.92	0.32	0	0.98	0.33	1.36	2.33	0.65	2.29	1.6
Sp21	5.25	10.71	11.04	7.28	2.48	7.84	7.24	30.51	1.33	2.61	5.23	3.53
Sp22	0	0	0	0	0	0	0	0	0	0	0	0
Sp23	1.31	0.32	1.23	0	0	0	0	0	0	0.65	0	0.64
Sp24	0	0.32	0.61	0.32	0	0.33	0.33	0.68	0	0	0	0
Sp25	2.62	4.22	2.76	1.27	0.93	1.96	0.99	3.05	0.33	4.23	1.63	2.24
Sp26	0	0	0	0	0	0	0	1.02	0	0.65	0	0.32
Sp27	0	0	0	0	0	0	0	0	0	0	0	0
Sp28	0	0.65	0.31	0.32	0.31	0	0	0	0	0.65	0.65	0.32
Sp29	0	0	0	0	0	0	0	0.34	0	0	0	0.32

Table A8-5 Diatom Counts for Lake Miski. Continued (8 of 12).

Sample	78	79	80	81	82	83	84	85	86	87	88	89
Age (ka)	7.79	7.82	7.86	7.89	7.92	7.95	7.99	8.02	8.05	8.08	8.12	8.15
Sp1	81.39	79.30	70.00	76.18	55.52	79.87	7.64	10.78	9.06	7.59	7.89	3.67
Sp2	0	0	0	0	0	0	0	0	0	0	0	0
Sp3	2.84	4.46	5.31	5.96	8.44	1.92	21.93	11.76	14.89	16.17	16.12	15.33
Sp4	3.15	1.91	5.94	4.39	5.52	3.19	19.27	16.34	19.09	19.8	16.12	19
Sp5	0.32	0.32	0.94	0.63	1.62	0	1.33	4.9	1.94	2.64	2.3	1.67
Sp6	0	0	0	0	0	0	0	0	0	0	0	0
Sp7	0.95	0.96	2.19	0.63	0.65	1.6	1.66	1.96	2.27	1.98	4.61	3.67
Sp8	0.32	0	0.63	0	0.65	1.28	0.33	1.96	0.97	0.99	0.99	0
Sp9	0	0.32	0.31	0	0	0	1	1.31	0.97	1.32	0.99	1.67
Sp10	0.95	0.64	1.88	0.94	6.17	1.28	6.31	5.88	7.44	6.6	4.61	6.33
Sp11	0.32	0.64	0.63	0.94	1.3	0.32	2.99	1.63	4.53	2.64	3.62	4
Sp12	0.95	0.32	0.31	0.31	2.27	0.96	1.33	5.23	3.24	2.64	6.25	7
Sp13	0.95	0	0	0.94	0	0.32	1.66	0.98	0.32	0	1.97	0
Sp14	0	0.96	0.63	0	0.65	0	2.33	0.33	2.91	1.98	1.97	1
Sp15	0.63	1.27	2.81	0.94	3.25	2.24	7.31	5.23	11.33	5.94	7.89	9.67
Sp16	1.26	2.55	1.88	3.13	4.22	0.96	6.31	9.48	7.44	5.61	4.28	6
Sp17	0.63	0.96	0.63	0.63	0.65	0.64	2.99	1.63	0.97	0.66	2.63	1
Sp18	0.32	0.32	0.31	0	0	0	1.99	1.31	1.62	1.98	1.32	1
Sp19	0	0	0	0	0.65	0.96	1	1.63	0	1.98	1.64	1.33
Sp20	0.32	0.32	0.94	0.31	1.95	0.64	3.65	4.58	1.29	1.65	2.96	3.67
Sp21	3.15	3.18	2.81	4.08	4.55	1.6	5.32	7.19	3.88	6.6	5.59	4.33
Sp22	0	0	0	0	0	0	0	0	0	0	0	0
Sp23	0.32	0.32	0	0	0	0	0	0	0.32	0.33	0.33	0
Sp24	0	0	0	0	0	0	0	0	0	0.99	0	0.33
Sp25	0.63	0.96	1.88	0	1.62	1.92	1.66	4.58	4.85	8.58	4.28	7.33
Sp26	0.32	0	0	0	0	0.32	0	0	0	0.99	0.99	0.67
Sp27	0	0	0	0	0	0	0	0.33	0	0	0	0
Sp28	0.32	0.32	0	0	0.32	0	1.66	0.33	0.65	0.33	0.33	1.33
Sp29	0	0	0	0	0	0	0.33	0.65	0	0	0.33	0

Table A8-5 Diatom Counts for Lake Miski. Continued (9 of 12).

Sample	90	91	92	93	94	95	96	97	98	99	100	101
Age (ka)	8.18	8.21	8.25	8.28	8.31	8.34	8.38	8.41	8.44	8.47	8.51	8.54
Sp1	13.73	11.96	9.63	4.59	8.91	10.89	10.53	2.30	2.95	4.25	7.10	4.25
Sp2	0	0	0	0	0	0	0	0	0	0	0	0
Sp3	14.05	11.63	14.95	18.36	12.54	7.59	9.21	13.44	11.15	16.99	10	11.11
Sp4	14.05	20.6	21.59	21.97	18.81	17.49	16.12	20.66	21.97	20.26	20.65	21.57
Sp5	1.96	2.66	1.33	0.98	0.66	1.65	2.3	1.31	0.98	1.96	1.61	1.31
Sp6	0	0	0	0	0	0	0	0	0	0	0	0
Sp7	2.29	2.99	4.65	3.93	4.29	4.29	2.3	2.62	3.93	2.29	1.29	2.61
Sp8	1.31	1.66	0.66	1.64	3.63	2.31	2.3	1.64	1.31	0.65	1.29	1.96
Sp9	1.31	2.33	1.33	1.64	2.64	3.63	2.63	4.59	3.93	2.29	3.55	4.58
Sp10	4.58	2.66	6.98	2.95	1.98	6.93	5.26	3.61	2.62	6.86	4.19	3.92
Sp11	2.29	3.32	2.99	3.28	3.3	4.62	5.26	2.95	2.95	4.25	2.9	3.59
Sp12	6.21	3.65	4.32	3.93	7.59	8.25	9.21	5.9	10.82	5.23	6.77	8.82
Sp13	0.33	0.66	0.33	0.33	2.64	0	0	0.66	0.98	0	0.65	0.33
Sp14	1.31	1.33	1	2.3	4.29	2.64	0.66	4.59	2.62	1.63	3.23	2.61
Sp15	8.17	10.63	5.98	7.87	5.94	7.92	5.92	4.26	8.52	6.54	6.13	6.54
Sp16	10.13	7.31	10.3	7.21	6.27	11.55	13.49	5.9	5.9	5.56	6.45	7.52
Sp17	2.29	1.99	1.33	2.95	2.97	1.98	1.97	2.62	4.26	1.96	1.61	3.59
Sp18	1.31	1.99	1.66	0.66	1.32	0.99	1.32	1.31	1.97	1.96	0.65	1.31
Sp19	1.63	0.66	0.66	0.33	0.33	0	0.33	0.98	0	0.33	1.29	0
Sp20	1.63	2.33	2.99	1.64	2.64	0.99	2.96	3.28	3.61	2.94	1.61	3.59
Sp21	4.9	1	2.66	6.23	3.63	0.66	3.95	4.26	3.28	5.56	7.74	3.92
Sp22	0	0	0	0	0	0	0	0	0	0	0	0
Sp23	0.33	0	0	0.98	0	0	0	0.66	0.33	1.31	1.29	0.65
Sp24	0.65	0	0	0	0	0.33	0	0.33	0	0.33	0	0.65
Sp25	4.9	6.31	3.32	4.26	4.62	4.62	3.29	11.15	4.92	6.21	10	5.23
Sp26	0.65	1	0.66	0	0	0	0	0.66	0.66	0.33	0	0
Sp27	0	0	0	0.33	0.66	0.66	0.66	0	0.33	0	0	0
Sp28	0	0.33	0.66	1.64	0	0	0	0	0	0.33	0	0.33
Sp29	0	1	0	0	0.33	0	0.33	0.33	0	0	0	0

Table A8-5 Diatom Counts for Lake Miski. Continued (10 of 12).

Sample	102	103	104	105	106	107	108	109	110	111	112	113
Age (ka)	8.57	8.6	8.64	8.67	8.7	8.74	8.77	8.8	8.83	8.87	8.95	9.1
Sp1	5.52	8.50	3.63	5.43	6.56	3.24	6.13	5.26	11.58	7.57	3.96	2.45
Sp2	0	0	0	0	0	0	0	0	0	0	0	0
Sp3	18.18	8.82	10.56	12.78	10.49	13.27	13.87	9.54	13.5	11.67	19.31	22.06
Sp4	18.18	17.97	21.12	22.36	17.38	22.01	16.45	18.42	19.29	19.87	13.37	12.25
Sp5	0.32	1.31	1.98	1.28	0.98	0.97	1.61	1.97	1.29	1.26	0	1.96
Sp6	0	0	0	0	0	0	0	0.33	0	0	0	0
Sp7	2.6	4.25	2.64	5.75	2.3	2.27	2.9	3.62	1.93	3.79	2.48	1.96
Sp8	1.62	2.94	2.97	1.28	0.66	1.94	1.94	1.97	1.61	1.26	0.99	1.96
Sp9	3.25	4.25	2.97	2.88	2.95	2.27	3.23	3.95	1.93	0.95	1.98	3.43
Sp10	4.87	5.88	7.59	7.35	4.92	6.15	4.19	5.26	4.18	2.84	5.45	5.39
Sp11	2.27	4.25	3.96	3.19	3.28	3.56	2.58	2.3	2.57	0.63	6.93	3.92
Sp12	5.84	6.21	6.27	4.79	5.57	6.47	3.87	4.28	5.14	5.36	0	0.49
Sp13	0	0	0.33	2.56	1.31	0.97	0	0	0.64	0.63	1.49	0.49
Sp14	1.95	2.94	2.64	1.6	1.97	0.97	3.87	0.99	1.93	1.58	0	0
Sp15	6.82	7.84	6.6	5.11	8.85	7.77	6.77	8.88	9	11.67	7.92	5.39
Sp16	6.17	3.92	6.93	7.67	10.49	7.77	5.81	5.92	7.07	8.52	3.47	0.98
Sp17	2.6	2.61	2.97	1.6	2.95	1.94	3.55	2.63	0.64	1.26	3.96	1.96
Sp18	2.27	1.96	0.99	0.96	1.31	1.62	2.26	2.96	1.61	1.26	1.49	0.49
Sp19	0	0.65	0	0	1.31	0.65	0	0	1.93	0	0	1.47
Sp20	2.6	2.61	2.64	5.75	4.59	3.88	3.55	2.63	1.61	2.84	2.48	0.49
Sp21	5.52	4.58	4.95	2.24	2.3	6.47	8.71	7.89	6.43	9.15	0	6.37
Sp22	0	0	0	0	0	0	0	0	0	0	0.99	0
Sp23	0.65	0	0.99	0.64	0.98	0.32	0.97	0.33	0.64	0	0	0
Sp24	0	0	0	0	0	0	0.32	0.99	0.64	0	0	0
Sp25	6.49	7.19	5.61	4.15	8.2	5.5	5.81	8.22	3.54	7.26	2.48	0
Sp26	0	0.33	0.66	0	0.66	0	0.32	0.99	0	0.63	1.49	0.98
Sp27	0.65	0	0	0	0	0	0	0	0	0	16.34	21.57
Sp28	0.32	0.33	0.33	0	0	0	0.97	0	0.96	0	1.98	2.94
Sp29	1.3	0.65	0.66	0.64	0	0	0.32	0.66	0.32	0	1.49	0.98

Table A8-5 Diatom Counts for Lake Miski. Continued (11 of 12).

Sample	114	115	116	117	118	119	120	121	122	123	124
Age (ka)	9.25	9.39	9.54	9.68	9.83	9.98	10.12	10.27	10.41	10.56	10.7
Sp1	90.24	80.50	46.12	16.07	58.94	64.02	58.60	22.22	19.44	14.93	13.84
Sp2	0	0	0	0	0	0	0	0	0.93	0	0
Sp3	1.46	4.5	12.14	15.18	3.38	12.15	8.84	17.52	12.04	12.67	11.61
Sp4	1.95	5.5	9.71	11.61	6.76	4.21	7.44	8.12	8.8	6.79	8.93
Sp5	0	1	0.97	0.45	0	0	0	0	0	0	0
Sp6	0	0	0	0	0	0	0	0.43	2.78	1.81	0.45
Sp7	0	0	0.49	4.02	0	0.93	2.79	3.85	8.33	1.81	6.25
Sp8	0.49	0	1.46	3.57	0.97	1.4	0	0.85	2.31	2.71	2.68
Sp9	0	0	0	1.79	1.45	1.87	0.93	0.43	0	0	0
Sp10	0	1	1.46	3.57	0.97	0.47	1.4	1.71	0.46	0.9	1.79
Sp11	0.49	0	0.49	0.45	0.48	0	0	1.71	1.39	1.36	0
Sp12	0	0	2.91	0	0	0	0	0	0.46	0	0
Sp13	0.98	0	1.94	1.34	0	0	0.47	0	0.93	0.9	1.34
Sp14	0.98	0	1.46	1.79	0	0	0	0.43	0	0	0
Sp15	1.95	1	0.97	8.04	1.45	2.34	2.79	5.56	5.09	1.81	3.57
Sp16	1.46	1	9.22	5.36	1.93	3.27	5.58	2.99	3.24	3.62	0
Sp17	0	0	0	4.02	0	0	0	2.56	0.93	1.36	1.79
Sp18	0	1	0.97	8.04	1.45	0	0.47	0.85	3.24	4.52	3.13
Sp19	0	0	0	0.89	0	0.93	0	2.56	1.39	0	3.57
Sp20	0	0	0	2.23	1.93	0.93	0.93	0.85	0.93	1.81	2.68
Sp21	0	0	0.97	0	0	0	0	0.85	0	0.9	0
Sp22	0	0	0	0	0	0	0	0	0	0	0
Sp23	0	0	0	0	0.97	0	0.47	0	0	0	0
Sp24	0	0	0	0.89	0	0	0	0	2.31	3.62	2.68
Sp25	0	0	0.49	0.45	0	0	0	0	0	1.81	1.79
Sp26	0	0	0	0	0	0	0	0	0	0	0
Sp27	0	4.5	5.34	7.59	18.84	6.54	8.37	25.64	24.07	34.39	31.7
Sp28	0	0	0.97	0.89	0	0.93	0.93	0	0	0.9	0
Sp29	0	0	1.94	1.79	0.48	0	0	0.85	0.93	1.36	2.23

Table A8-5 Diatom Counts for Lake Miski. Continued (12 of 12).

Sample	125	126	127	128	129	130
Age (ka)	10.85	11	11.36	11.72	12.09	12.61
Sp1	3.56	25.24	3.65	4.73	0.33	0.66
Sp2	0	0	0	0	0	0.99
Sp3	29.78	9.9	22.59	11.04	13.58	11.22
Sp4	7.11	12.46	11.96	18.61	21.52	20.79
Sp5	0	1.92	0.66	2.84	1.32	0.33
Sp6	5.33	2.24	0.33	1.26	0	1.65
Sp7	6.22	2.88	2.99	5.36	6.29	6.27
Sp8	1.33	0.96	1	2.21	0.99	0.66
Sp9	0	0.64	5.98	1.58	1.32	5.28
Sp10	0	1.92	10.3	1.26	0.66	0.33
Sp11	0	0.64	0.66	0.63	1.32	0.99
Sp12	0.44	0	1.33	0.95	0	0
Sp13	0	0.96	2.99	5.99	2.98	1.32
Sp14	0.89	0	0.66	2.52	4.3	5.94
Sp15	1.33	2.24	4.65	6.62	6.29	11.88
Sp16	0.89	3.51	3.65	5.68	2.32	4.95
Sp17	0.44	2.24	1.66	2.21	2.98	2.31
Sp18	1.33	1.6	3.65	4.73	2.32	2.64
Sp19	6.22	4.15	1.99	0.95	2.32	1.65
Sp20	0	2.24	1.33	4.42	2.65	6.27
Sp21	0	17.57	1.66	7.57	14.24	0
Sp22	0	0	0	0.32	0	0
Sp23	0	0.32	0	0	0	1.98
Sp24	0.89	0.64	0	0.32	0.99	0.99
Sp25	0.89	3.19	11.96	4.73	1.99	4.29
Sp26	0	0.32	0.66	0.32	1.99	1.65
Sp27	33.33	0.64	1.33	1.89	3.64	2.97
Sp28	0	0.96	1.99	0.95	2.98	0.99
Sp29	0	0.64	0.33	0.32	0.66	0.99

Table A8-6 DCA axis scores for diatom data from Lakes Pacucha and Miski, 1 of 5

Site	Age (ka)	DCA1	DCA2	DCA3	DCA4
Pacucha	0	3.911	1.565	1.508	1.444
Pacucha	0.14	3.819	1.542	1.498	1.43
Pacucha	0.28	3.907	1.565	1.505	1.445
Pacucha	0.42	3.924	1.572	1.51	1.446
Pacucha	0.57	3.865	1.562	1.492	1.446
Pacucha	0.75	2.651	1.269	1.192	1.28
Pacucha	0.94	3.914	1.591	1.546	1.462
Pacucha	1.26	2.715	1.315	1.134	1.178
Pacucha	1.61	3.88	1.59	1.495	1.45
Pacucha	1.85	3.844	1.548	1.491	1.429
Pacucha	2.08	3.953	1.584	1.511	1.445
Pacucha	2.31	3.97	1.586	1.522	1.456
Pacucha	2.54	3.957	1.586	1.526	1.452
Pacucha	2.77	3.947	1.586	1.537	1.46
Pacucha	2.98	2.73	1.299	1.167	1.199
Pacucha	3.06	3.744	1.533	1.453	1.406
Pacucha	3.14	2.278	1.096	1.078	1.117
Pacucha	3.22	3.801	1.573	1.463	1.446
Pacucha	3.38	3.939	1.587	1.529	1.455
Pacucha	3.46	3.966	1.59	1.533	1.462
Pacucha	3.53	2.195	1.169	1.012	1.172
Pacucha	3.61	3.96	1.59	1.534	1.463
Pacucha	3.69	3.914	1.584	1.503	1.459
Pacucha	3.77	3.954	1.591	1.538	1.464
Pacucha	3.85	3.946	1.588	1.524	1.461
Pacucha	4.01	3.929	1.575	1.514	1.449
Pacucha	4.09	3.942	1.583	1.509	1.446
Pacucha	4.19	3.712	1.58	1.591	1.468
Pacucha	4.3	2.293	1.77	0.711	1.221
Pacucha	4.41	2.222	1.104	1.061	1.134
Pacucha	4.51	3.516	1.542	1.43	1.391
Pacucha	4.62	3.698	1.568	1.511	1.433
Pacucha	4.75	3.965	1.591	1.514	1.464
Pacucha	4.83	1.923	2.384	2.353	1.906
Pacucha	4.92	2.203	1.146	1.106	1.125
Pacucha	5.15	2.895	1.28	1.375	1.214
Pacucha	5.5	2.169	1.01	1.1	1.072
Pacucha	5.86	1.821	0.859	1.391	0.872
Pacucha	6.22	2.016	0.939	1.233	0.977
Pacucha	6.57	1.371	1.578	1.332	1.484
Pacucha	6.96	2.157	1.182	1.306	1.153
Pacucha	7.17	2.133	1.084	1.215	1.09
Pacucha	7.38	2.146	1.132	1.013	1.196
Pacucha	7.59	2.064	1.134	1.141	1.161
Pacucha	7.8	2.251	1.496	1.253	1.06
Pacucha	8.01	1.731	2.461	1.409	2.076
Pacucha	8.23	1.385	0.497	1.561	0.53

Table A8-6 DCA axis scores for diatom data from Lakes Pacucha and Miski. Continued (2 of 5)

Site	Age (ka)	DCA1	DCA2	DCA3	DCA4
Pacucha	8.45	3.812	1.57	1.506	1.442
Pacucha	8.67	2.318	1.15	1.243	0.989
Pacucha	8.89	0.886	0.179	1.853	0.193
Pacucha	9.11	1.614	1.89	2.106	1.516
Pacucha	9.33	1.958	1.477	1.238	1.322
Pacucha	9.55	1.794	1.713	1.223	1.437
Pacucha	9.77	2.141	1.421	1.199	1.046
Pacucha	9.99	2.352	1.492	1.618	1.378
Pacucha	10.2	2.082	1.762	1.792	1.436
Pacucha	10.4	1.989	1.976	2.324	1.411
Pacucha	10.6	2.154	1.511	1.59	1.174
Pacucha	10.8	1.945	1.122	1.203	1.129
Pacucha	10.9	1.773	2.299	0.366	2.304
Pacucha	11.1	2.19	1.417	1.022	0.834
Pacucha	11.3	2.249	1.624	0.953	0.971
Pacucha	11.5	2.415	1.541	0.891	0.71
Pacucha	11.7	2.416	1.582	0.985	0.846
Pacucha	11.8	2.087	1.142	1.239	1.031
Pacucha	12	2.311	1.468	1.099	0.913
Pacucha	12.2	2.231	1.333	1.16	0.961
Pacucha	12.4	2.206	1.307	1.123	0.976
Pacucha	12.5	3.146	1.578	1.27	1.457
Pacucha	12.7	2.193	1.267	1.164	0.985
Pacucha	12.9	2.153	1.282	1.129	1.017
Miski	0	0.787	2.231	0.36	1.942
Miski	0.02	0.788	2.348	0.232	2.071
Miski	0.1	0.797	2.111	0.507	1.8
Miski	0.17	0.612	2.612	0.061	2.304
Miski	0.24	0.746	2.122	0.412	1.861
Miski	0.31	0.675	2.248	0.345	1.927
Miski	0.39	0.589	2.666	0.021	2.341
Miski	0.46	0.773	2.41	0.255	2.096
Miski	0.53	0.485	2.584	0.076	2.213
Miski	0.61	0.158	2.552	0.098	2.09
Miski	0.68	0.026	2.664	0.025	2.151
Miski	0.75	0.274	2.431	0.184	2.002
Miski	0.83	0.119	2.475	0.171	1.98
Miski	0.9	0.186	2.44	0.182	1.953
Miski	0.97	0.293	2.479	0.205	1.956
Miski	1.04	0.409	2.621	0.05	2.215
Miski	1.12	0.245	2.457	0.146	2.076
Miski	1.26	0.054	2.683	0	2.177
Miski	1.41	0.083	2.529	0.114	2.047
Miski	1.56	0	2.656	0.038	2.13
Miski	1.7	0.111	2.419	0.213	1.925
Miski	1.85	0.064	2.56	0.101	2.041
Miski	1.99	0.04	2.578	0.097	2.077

Table A8-6 DCA axis scores for diatom data from Lakes Pacucha and Miski. Continued (3 of 5)

Site	Age (ka)	DCA1	DCA2	DCA3	DCA4
Miski	2.14	0.201	2.427	0.197	1.974
Miski	2.29	0.13	2.403	0.229	1.885
Miski	2.46	0.246	2.485	0.21	1.988
Miski	2.62	0.34	2.507	0.181	1.941
Miski	2.78	0.512	2.097	0.57	1.549
Miski	2.94	0.464	2.358	0.379	1.897
Miski	3.11	0.08	2.524	0.118	2.019
Miski	3.27	0.172	2.491	0.163	1.957
Miski	3.43	0.137	2.52	0.204	2.044
Miski	3.6	0.362	2.623	0.019	2.316
Miski	3.76	0.244	2.485	0.33	2.025
Miski	3.92	0.146	2.648	0.084	2.17
Miski	4.09	0.361	2.6	0.093	2.227
Miski	4.25	0.223	2.532	0.169	2.101
Miski	4.42	0.139	2.401	0.236	1.951
Miski	4.59	0.317	2.352	0.276	1.997
Miski	4.75	0.542	2.603	0.086	2.229
Miski	4.92	0.261	2.6	0.064	2.194
Miski	5.08	0.793	2.375	0.256	2.145
Miski	5.17	0.662	2.434	0.27	2.174
Miski	5.25	0.733	2.262	0.449	2.051
Miski	5.33	0.62	2.375	0.359	2.114
Miski	5.41	0.523	2.488	0.247	2.171
Miski	5.5	0.627	2.464	0.32	2.198
Miski	5.58	0.557	2.509	0.231	2.206
Miski	5.66	0.581	2.287	0.334	2.069
Miski	5.75	0.583	2.444	0.36	2.174
Miski	5.83	0.671	2.25	0.418	2.016
Miski	5.91	0.472	2.401	0.313	2.096
Miski	5.99	0.566	2.406	0.315	2.175
Miski	6.08	0.501	2.433	0.296	2.141
Miski	6.16	0.601	2.376	0.269	2.132
Miski	6.24	0.753	2.13	0.605	1.923
Miski	6.33	0.667	2.28	0.503	2.026
Miski	6.41	0.785	2.355	0.248	2.21
Miski	6.49	0.558	2.363	0.353	2.099
Miski	6.57	0.571	2.064	0.612	1.823
Miski	6.66	0.601	2.097	0.58	1.844
Miski	6.74	0.681	2.276	0.419	2.051
Miski	6.82	0.651	2.38	0.36	2.127
Miski	6.91	0.172	2.203	0.393	1.8
Miski	6.99	0.493	2.191	0.468	1.895
Miski	7.07	0.547	1.991	0.613	1.763
Miski	7.16	0.231	1.924	0.548	1.591
Miski	7.24	0.759	1.974	0.6	1.845
Miski	7.32	1.058	1.91	0.813	1.779
Miski	7.4	0.355	2.737	0.057	2.352

Table A8-6 DCA axis scores for diatom data from Lakes Pacucha and Miski. Continued (4 of 5)

Site	Age (ka)	DCA1	DCA2	DCA3	DCA4
Miski	7.49	0.462	2.019	0.487	1.736
Miski	7.57	0.428	2.218	0.368	1.914
Miski	7.63	0.533	1.658	0.748	1.389
Miski	7.66	0.996	2.543	0.242	2.425
Miski	7.69	0.929	2.298	0.444	2.07
Miski	7.73	0.809	2.435	0.333	2.246
Miski	7.76	0.914	2.449	0.453	2.279
Miski	7.79	1.061	2.276	0.372	2.166
Miski	7.82	1.083	2.417	0.353	2.324
Miski	7.86	0.943	2.182	0.414	2.083
Miski	7.89	1.164	2.516	0.26	2.449
Miski	7.92	0.796	2.558	0.246	2.34
Miski	7.95	0.731	2.232	0.642	1.987
Miski	7.99	1.127	2.567	0.245	2.444
Miski	8.02	0.824	2.385	0.432	2.193
Miski	8.05	0.956	2.454	0.34	2.279
Miski	8.08	1.04	2.441	0.431	2.255
Miski	8.12	0.988	2.301	0.452	2.099
Miski	8.15	0.821	2.503	0.264	2.264
Miski	8.18	0.956	2.495	0.386	2.293
Miski	8.21	0.993	2.315	0.509	2.112
Miski	8.25	0.917	2.439	0.399	2.23
Miski	8.28	1.012	2.442	0.29	2.317
Miski	8.31	0.959	2.299	0.353	2.137
Miski	8.34	0.687	2.339	0.417	2.098
Miski	8.38	0.657	2.474	0.31	2.235
Miski	8.41	0.945	2.396	0.346	2.173
Miski	8.44	0.852	2.375	0.335	2.136
Miski	8.47	0.883	2.538	0.232	2.349
Miski	8.51	0.854	2.432	0.354	2.208
Miski	8.54	0.739	2.493	0.219	2.287
Miski	8.57	0.957	2.591	0.199	2.424
Miski	8.6	0.757	2.316	0.439	2.067
Miski	8.64	0.776	2.403	0.299	2.151
Miski	8.67	0.815	2.354	0.302	2.177
Miski	8.7	0.841	2.507	0.287	2.264
Miski	8.74	0.857	2.559	0.286	2.345
Miski	8.77	0.967	2.389	0.331	2.234
Miski	8.8	0.869	2.364	0.415	2.148
Miski	8.83	1.003	2.511	0.396	2.337
Miski	8.87	0.969	2.383	0.348	2.208
Miski	8.95	1.002	2.672	0.087	2.478
Miski	9.1	1.017	2.597	0.172	2.411
Miski	9.25	1.738	1.944	0.619	1.968
Miski	9.39	1.4	2.522	0.45	2.475
Miski	9.54	1.218	2.556	0.329	2.469
Miski	9.68	1.455	2.375	0.719	2.286

Table A8-6 DCA axis scores for diatom data from Lakes Pacucha and Miski. Continued (5 of 5)

Site	Age (ka)	DCA1	DCA2	DCA3	DCA4
Miski	9.83	0.961	2.81	0.11	2.629
Miski	9.98	1.233	2.779	0.15	2.71
Miski	10.12	1.047	2.471	0.307	2.416
Miski	10.27	1.247	2.533	0.489	2.424
Miski	10.41	1.334	2.077	0.77	2.063
Miski	10.56	1.421	2.614	0.37	2.656
Miski	10.7	1.297	2.289	0.751	2.234
Miski	10.85	1.489	2.501	0.59	2.461
Miski	11	1.221	2.295	0.823	2.165
Miski	11.36	1.154	2.484	0.426	2.288
Miski	11.72	1.383	1.973	0.823	1.902
Miski	12.09	1.386	2.011	0.701	1.893
Miski	12.61	1.282	2.137	0.629	1.973

Appendix VIII

Table A8-7 Charcoal data from Lakes Miski and Huamanmarca, 1 of 3

Site	Depth (cm)	Age	Particle number	Charcoal area/cc	Site	Depth (cm)	Age	Particle number	Charcoal area/cc
Huamanmarca	0	0	222	12.9033	Miski	0	0	35	0.08064
Huamanmarca	5	322.26	202	13.49	Miski	5	132.476	65	11.1907
Huamanmarca	10	694.513	106	4.80122	Miski	10	314.912	92	9.92806
Huamanmarca	15	1066.77	364	17.3097	Miski	15	497.347	118	15.435
Huamanmarca	20	1439.02	178	11.3695	Miski	20	679.783	174	26.9475
Huamanmarca	25	1811.27	106	20.7046	Miski	25	862.219	300	39.829
Huamanmarca	30	2183.52	122	13.5261	Miski	30	1044.65	232	31.0735
Huamanmarca	35	2555.77	258	34.7251	Miski	35	1227.09	151	22.7953
Huamanmarca	40	2608.14	156	10.3688	Miski	40	1409.53	140	26.2737
Huamanmarca	45	2660.5	132	7.59565	Miski	45	1591.96	91	12.0982
Huamanmarca	50	2712.86	116	5.37139	Miski	50	1774.4	211	30.828
Huamanmarca	55	2765.22	184	13.4536	Miski	55	1956.83	93	10.8436
Huamanmarca	60	2817.58	100	7.55994	Miski	60	2139.27	188	24.9308
Huamanmarca	65	2869.95	238	22.404	Miski	65	2334.28	168	18.9268
Huamanmarca	70	2922.31	170	8.25306	Miski	70	2537.69	193	19.7494
Huamanmarca	75	2974.67	130	6.58982	Miski	75	2741.09	98	11.7795
Huamanmarca	80	3027.03	132	9.73069	Miski	80	2944.49	78	10.6399
Huamanmarca	85	3079.4	264	14.1107	Miski	85	3147.89	197	20.61
Huamanmarca	90	3131.76	110	6.43238	Miski	90	3351.29	47	7.70701
Huamanmarca	95	3184.12	174	8.62016	Miski	95	3554.69	205	19.4367
Huamanmarca	100	3236.48	154	11.2614	Miski	100	3758.09	101	14.9151
Huamanmarca	105	3288.84	232	13.2909	Miski	105	3963.79	167	26.6004
Huamanmarca	110	3341.21	250	14.3644	Miski	110	4171.03	262	34.9946
Huamanmarca	115	3393.57	296	11.1379	Miski	115	4378.26	230	37.7549
Huamanmarca	120	3445.93	246	13.4806	Miski	120	4585.49	276	30.1458
Huamanmarca	125	3498.29	246	16.8268	Miski	125	4792.73	417	35.4679
Huamanmarca	130	3550.66	200	13.5375	Miski	130	4999.96	304	35.1654
Huamanmarca	135	3603.02	214	12.0988	Miski	135	5207.19	104	11.5945
Huamanmarca	140	3655.38	320	15.4621	Miski	140	5414.43	66	10.3933
Huamanmarca	145	3707.74	128	6.19712	Miski	145	5621.66	102	14.7832
Huamanmarca	150	3760.1	252	15.8322	Miski	150	5828.89	98	12.6888
Huamanmarca	155	3812.47	140	7.52	Miski	155	6036.13	233	22.3702
Huamanmarca	160	3864.83	292	13.436	Miski	165	6450.59	148	10.7232
Huamanmarca	165	3917.19	204	8.39744	Miski	170	6657.83	195	16.8433
Huamanmarca	170	3969.55	160	10.2534	Miski	175	6865.06	138	13.6175
Huamanmarca	175	4021.92	486	26.8518	Miski	180	7072.29	220	19.6091

Table A8-7 Charcoal data from Lakes Miski and Huamanmarca. Continued (2 of 3)

Site	Depth (cm)	Age	Particle number	Charcoal area/cc	Site	Depth (cm)	Age	Particle number	Charcoal area/cc
Huamanmarca	180	4074.28	596	41.3233	Miski	185	7279.53	139	11.1567
Huamanmarca	185	4126.64	128	7.85254	Miski	190	7486.76	80	5.89926
Huamanmarca	190	4179	796	35.4616	Miski	195	7643.68	181	13.3164
Huamanmarca	195	4231.36	148	7.30906	Miski	200	7725.12	93	6.6025
Huamanmarca	200	4283.73	228	10.5446	Miski	205	7806.57	112	8.75546
Huamanmarca	205	4391.11	292	20.1106	Miski	210	7888.01	72	7.2521
Huamanmarca	210	4535.17	172	9.07546	Miski	215	7969.46	98	9.48198
Huamanmarca	215	4679.24	180	14.6299	Miski	220	8050.9	148	11.4847
Huamanmarca	220	4823.3	148	7.50925	Miski	235	8295.24	158	16.5486
Huamanmarca	225	4967.37	152	9.40186	Miski	255	8621.02	126	13.7088
Huamanmarca	230	5111.43	224	10.2733	Miski	273	9027.44	58	5.85011
Huamanmarca	235	5255.49	280	14.3675	Miski	285	9902.25	98	13.8584
Huamanmarca	240	5399.56	152	8.35354	Miski	290	10266.7	100	12.6862
Huamanmarca	245	5543.62	200	16.831	Miski	295	10631.2	121	17.0363
Huamanmarca	250	5687.68	284	16.0141	Miski	300	10995.8	111	12.886
Huamanmarca	255	5831.75	236	12.6072	Miski	305	11360.3	187	19.3139
Huamanmarca	260	5975.81	308	13.2997	Miski	310	11724.8	40	5.09005
Huamanmarca	265	6119.88	164	11.7563	Miski	315	12089.3	14	1.81389
Huamanmarca	270	6263.94	192	11.3782	Miski	320	12607.5	6	0.638208
Huamanmarca	275	6408	360	23.7642	Miski	325	12621.2	4	0.507904
Huamanmarca	280	6552.07	308	20.6203	Miski	330	12635	6	0.879744
Huamanmarca	285	6696.13	524	41.6051	Miski	335	12648.7	3	0.424576
Huamanmarca	290	6866.22	348	19.7138	Miski	340	12662.5	2	0.586496
Huamanmarca	295	7053.66	260	20.8376	Miski	345	12676.2	2	0.299264
Huamanmarca	300	7241.09	240	13.152	Miski	350	12690	1	0.036096
Huamanmarca	305	7428.53	116	6.57792	Miski	355	12703.8	0	0
Huamanmarca	310	7615.97	260	22.559	Miski	360	12717.5	1	0.186112
Huamanmarca	315	7803.4	180	13.4612	Miski	365	12731.3	0	0
Huamanmarca	320	7990.84	156	12.6044	Miski	370	12745	0	0
Huamanmarca	325	8178.28	100	5.06573	Miski	375	12758.8	0	0
Huamanmarca	330	8692.58	136	13.9999	Miski	380	12772.5	0	0
Huamanmarca	335	9697.19	16	0.837376	Miski	385	12786.3	0	0
Huamanmarca	340	10701.8	30	1.53485	Miski	390	12800	0	0
Huamanmarca	345	11706.4	0	0	Miski	395	12813.8	0	0
Huamanmarca	350	12711	0	0	Miski	398	12822	0	0
Huamanmarca	355	13715.6	2	0.009344					

Table A8-7 Charcoal data from Lakes Miski and Huamanmarca. Continued (3 of 3)

Site	Depth (cm)	Age	Particle number	Charcoal area/cc
Huamanmarca	360	14720.3	0	0
Huamanmarca	365	15724.9	0	0
Huamanmarca	370	16729.5	0	0
Huamanmarca	375	17734.1	4	0.132736
Huamanmarca	380	18738.7	0	0
Huamanmarca	385	19743.3	0	0
Huamanmarca	390	20747.9	0	0
Huamanmarca	395	21752.5	0	0
Huamanmarca	400	22757.1	0	0
Huamanmarca	405	23761.8	0	0

Table A8-8 Loss-on-ignition data for Lake Miski, 1 of 5

Age	Depth (cm)	Organics	CaCO3	Silica
0	0	39.4977	0	60.5023
23.0144	2	41.8981	0	58.1019
95.9886	4	39.2019	0.704225	60.0939
168.963	6	38.6256	0.473934	60.9005
241.937	8	38.3693	2.15827	59.4724
314.912	10	37.6652	0.220264	62.1145
387.886	12	37.5839	0.894855	61.5213
460.86	14	37.7729	4.36681	57.8603
533.834	16	35.5972	1.63934	62.7635
606.809	18	43.1034	0.862069	56.0345
679.783	20	45.7565	0.369004	53.8745
752.757	22	40.1302	11.2798	48.59
825.732	24	41.7722	1.89873	56.3291
898.706	26	41.7373	1.90678	56.3559
971.68	28	39.6018	1.32743	59.0708
1044.65	30	38.2576	1.32576	60.4167
1117.63	32	42.7419	1.20968	56.0484
1190.6	34	37.0968	1.79211	61.1111
1263.58	36	36.1769	1.57978	62.2433
1336.55	38	39.4444	1.11111	59.4444
1409.53	40	41.8426	0.191939	57.9655
1482.5	42	42.3301	1.16505	56.5049
1555.47	44	45.7565	1.84502	52.3985
1628.45	46	46.771	0.978474	52.2505
1701.42	48	40	2.5	57.5
1774.4	50	38.5246	1.63934	59.8361
1847.37	52	41.357	1.61551	57.0275
1920.35	54	47.0588	0.519031	52.4221
1993.32	56	45.9807	0.96463	53.0547
2066.29	58	45.0088	1.05079	53.9405
2139.27	60	40.4568	0.978793	58.5644
2212.24	62	41.4075	0.981997	57.6105
2293.6	64	38.9803	0.986842	60.0329
2374.96	66	40.6855	0.745156	58.5693
2456.32	68	34.6327	1.7991	63.5682
2537.69	70	33.7313	1.04478	65.2239
2619.05	72	39.9682	1.27389	58.758
2700.41	74	35.6037	1.23839	63.1579
2781.77	76	39.0551	1.88976	59.0551
2863.13	78	33.6957	1.63043	64.6739
2944.49	80	34.0496	2.31405	63.6364
3025.85	82	34.2199	2.12766	63.6525
3107.21	84	37.9747	1.44665	60.5787
3188.57	86	45.1554	2.74223	52.1024
3269.93	88	39.8551	3.62319	56.5217

Table A8-8 Loss-on-ignition data for Lake Miski. Continued (2 of 5)

Age	Depth (cm)	Organics	CaCO3	Silica
3351.29	90	43.0328	3.27869	53.6885
3432.65	92	39.3715	1.84843	58.78
3514.01	94	44.856	0	55.144
3595.37	96	72.5464	0.331565	27.122
3676.73	98	44	0.210526	55.7895
3758.09	100	38.8792	0.350263	60.7706
3839.45	102	39.7119	0	60.2881
3922.35	104	46.3074	0.798403	52.8942
4005.24	106	42.8811	0.335008	56.7839
4088.13	108	42.7256	2.76243	54.512
4171.03	110	46.7188	1.5625	51.7188
4253.92	112	39.5161	3.70968	56.7742
4336.81	114	40.8037	2.47295	56.7233
4419.71	116	45.2135	2.20913	52.5773
4502.6	118	47.9228	2.07715	50
4585.49	120	40.5689	2.09581	57.3353
4668.39	122	45.2899	5.43478	49.2754
4751.28	124	34.8966	2.06897	63.0345
4834.17	126	33.4161	2.23602	64.3478
4917.07	128	31.6794	3.05344	65.2672
4999.96	130	33.871	2.78592	63.3431
5082.85	132	33.2882	3.51827	63.1935
5165.75	134	48.7346	1.68722	49.5782
5248.64	136	34.7885	1.63711	63.5744
5331.53	138	39.5946	2.56757	57.8378
5414.43	140	39.9188	3.51827	56.5629
5497.32	142	39.2279	3.36239	57.4097
5580.21	144	42.8025	0.509554	56.6879
5663.11	146	33.7871	3.09406	63.1188
5746	148	38.9105	3.24254	57.847
5828.89	150	38.8889	2.77778	58.3333
5911.79	152	40.8788	3.06258	56.0586
5994.68	154	39.4507	2.74657	57.8027
6077.57	156	37.0513	1.92308	61.0256
6160.47	158	37.1295	1.87207	60.9984
6243.36	160	38.2192	2.46575	59.3151
6326.25	162	35.2368	3.48189	61.2813
6409.15	164	35.3247	2.85714	61.8182
6492.04	166	36.1823	1.9943	61.8234
6574.93	168	35.5781	2.1601	62.2618
6657.83	170	34.907	2.86123	62.2318
6740.72	172	36.7847	3.26975	59.9455
6823.61	174	34.122	2.24159	63.6364
6906.51	176	25.4766	1.38648	73.1369
6989.4	178	34.4221	1.88442	63.6935

Table A8-8 Loss-on-ignition data for Lake Miski. Continued (3 of 5)

Age	Depth (cm)	Organics	CaCO3	Silica
7072.29	180	29.959	0.957592	69.0834
7155.19	182	21.3187	2.1978	76.4835
7238.08	184	16.8966	1.63793	81.4655
7320.97	186	21.6135	1.79283	76.5936
7403.87	188	19.147	1.81488	79.0381
7486.76	190	18.9379	1.60321	79.4589
7569.65	192	18.8	1.6	79.6
7627.39	194	25.8696	1.95652	72.1739
7659.97	196	25.6773	1.88457	72.4382
7692.55	198	27.8912	3.80952	68.2993
7725.12	200	28.9916	3.78151	67.2269
7757.7	202	28.9398	3.58166	67.4785
7790.28	204	29.5794	3.25645	67.1642
7822.86	206	21.8679	2.50569	75.6264
7855.43	208	31.454	2.96736	65.5786
7888.01	210	25.7831	2.53012	71.6867
7920.59	212	27.8049	2.80488	69.3902
7953.17	214	31.1453	2.51397	66.3408
7985.75	216	36.0709	3.05958	60.8696
8018.32	218	30	3.52941	66.4706
8050.9	220	33.0289	3.19635	63.7747
8083.48	222	31.6017	2.0202	66.3781
8116.06	224	31.686	2.61628	65.6977
8148.64	226	29.8013	2.25166	67.947
8181.21	228	29.9868	3.17041	66.8428
8213.79	230	32.9609	3.07263	63.9665
8246.37	232	31.7872	1.90996	66.3029
8278.95	234	32.1285	2.1419	65.7296
8311.53	236	25.3286	2.38949	72.282
8344.1	238	38.088	2.27618	59.6358
8376.68	240	34.1463	3.44333	62.4103
8409.26	242	33.6913	2.41611	63.8926
8441.84	244	34.0397	1.8543	64.106
8474.42	246	32.7827	1.39771	65.8196
8506.99	248	31.7905	2.55786	65.6516
8539.57	250	17.9913	1.01156	80.9971
8572.15	252	24.5455	2.72727	72.7273
8604.73	254	29.6104	1.55844	68.8312
8637.31	256	31.3158	2.5	66.1842
8669.88	258	35.6742	1.96629	62.3596
8702.46	260	33.1586	2.22805	64.6134
8735.04	262	31.0667	2.53333	66.4
8767.62	264	29.434	2.26415	68.3019
8800.2	266	32.1526	2.17984	65.6676
8832.77	268	28.066	3.18396	68.75

Table A8-8 Loss-on-ignition data for Lake Miski. Continued (4 of 5)

Age	Depth (cm)	Organics	CaCO3	Silica
8865.35	270	17.0972	2.82903	80.0738
8954.54	272	28.5554	2.23964	69.2049
9100.34	274	20.8448	0.183655	78.9715
9246.14	276	21.2274	1.20724	77.5654
9391.94	278	17.3679	1.43241	81.1996
9537.74	280	14.029	1.03663	84.9343
9683.54	282	33.8014	0.501505	65.6971
9829.35	284	19.2509	0.696864	80.0523
9975.15	286	16.3043	0.334448	83.3612
10120.9	288	16.0281	1.40735	82.5645
10266.7	290	17.3913	1.02302	81.5857
10412.5	292	14.3264	0.285103	85.3885
10558.3	294	14.4298	0.310318	85.2599
10704.1	296	17.4249	0.0858369	82.4893
10850	298	13.0564	0.222552	86.7211
10995.8	300	22.4558	0.110619	77.4336
11141.6	302	12.9231	1.53846	85.5385
11287.4	304	14.8718	0	85.1282
11433.2	306	29.4057	0	70.5943
11579	308	14.3266	0.0716332	85.6017
11724.8	310	21.1245	0.481928	78.3936
11870.6	312	12.8311	0.353149	86.8158
12016.4	314	14.2779	0	85.7221
12162.2	316	13.297	0.653951	86.049
12307.9	318	15.3104	0.241109	84.4485
12607.5	320	13.074	0.127551	86.7985
12613	322	6.00264	0.296834	93.7005
12618.5	324	5.07766	0.388292	94.5341
12624	326	5.65013	0.543281	93.8066
12629.5	328	4.61334	0.69698	94.6897
12635	330	2.9368	0.553309	96.5099
12640.5	332	2.61342	0.439055	96.9475
12646	334	2.22805	0.374462	97.3975
12651.5	336	1.61957	0.465196	97.9152
12657	338	1.97684	0.499201	97.524
12662.5	340	1.97875	0.541554	97.4797
12668	342	1.89619	0.517142	97.5867
12673.5	344	2.23529	0.333333	97.4314
12679	346	2.50836	0.397157	97.0945
12684.5	348	3.10811	0.189189	96.7027
12690	350	2.04538	0.464077	97.4905
12695.5	352	2.01908	0.238474	97.7424
12701	354	1.51808	0.163715	98.3182
12706.5	356	1.79825	0.205515	97.9962
12712	358	1.56019	0.2135	98.2263

Table A8-8 Loss-on-ignition data for Lake Miski. Continued (5 of 5)

Age	Depth (cm)	Organics	CaCO3	Silica
12717.5	360	1.82155	0.231553	97.9469
12723	362	1.607	0.159109	98.2339
12728.5	364	1.67419	0.244545	98.0813
12734	366	1.38601	0.127449	98.4865
12739.5	368	1.54025	0.264988	98.1948
12745	370	1.67761	0.182349	98.14
12750.5	372	1.64374	0.357334	97.9989
12756	374	1.53756	0.486571	97.9759
12761.5	376	1.49254	0.39675	98.1107
12767	378	1.30772	0.274459	98.4178
12772.5	380	1.31313	0.252525	98.4343
12778	382	2.43741	0.265296	97.2973
12783.5	384	2.29312	0.697906	97.009
12789	386	2.46454	0.514184	97.0213
12794.5	388	2.52129	0.233762	97.2449
12800	390	2.45289	0.22742	97.3197
12805.5	392	2.20181	0.190084	97.6081
12811	394	2.46159	0.453911	97.0845
12816.5	396	1.54993	0.298063	98.152
12822	398	2.04965	0.0866051	97.8637

Table A8-9 Magnetic Susceptibility data for Lake Miski. 1 of 4

Age ka	Depth (cm)	MS1 SI	Age ka	Depth (cm)	MS1 SI	Age ka	Depth (cm)	MS1 SI	Age ka	Depth (cm)	MS1 SI
-0.05	0	-0.543	0.753	22	-1.042	1.555	44	-1.467	2.375	66	-1.595
-0.032	0.5	-0.594	0.771	22.5	-1.074	1.574	44.5	-1.446	2.395	66.5	-1.617
-0.013	1	-0.6	0.789	23	-1.023	1.592	45	-1.487	2.416	67	-1.612
0.005	1.5	-0.618	0.807	23.5	-1.069	1.61	45.5	-1.591	2.436	67.5	-1.575
0.023	2	-0.6	0.826	24	-1.037	1.628	46	-1.491	2.456	68	-1.635
0.041	2.5	-0.705	0.844	24.5	-1.057	1.647	46.5	-1.507	2.477	68.5	-1.595
0.06	3	-0.601	0.862	25	-1.137	1.665	47	-1.506	2.497	69	-1.625
0.078	3.5	-0.716	0.88	25.5	-1.148	1.683	47.5	-1.471	2.517	69.5	-1.647
0.096	4	-0.631	0.899	26	-1.246	1.701	48	-1.5	2.538	70	-1.7
0.114	4.5	-0.682	0.917	26.5	-1.113	1.72	48.5	-1.437	2.558	70.5	-1.742
0.132	5	-0.719	0.935	27	-1.091	1.738	49	-1.514	2.578	71	-1.688
0.151	5.5	-0.791	0.953	27.5	-1.233	1.756	49.5	-1.479	2.599	71.5	-1.598
0.169	6	-0.709	0.972	28	-1.203	1.774	50	-1.567	2.619	72	-1.516
0.187	6.5	-0.805	0.99	28.5	-1.183	1.793	50.5	-1.576	2.639	72.5	-1.534
0.205	7	-0.766	1.008	29	-1.202	1.811	51	-1.476	2.66	73	-1.68
0.224	7.5	-0.779	1.026	29.5	-1.356	1.829	51.5	-1.427	2.68	73.5	-1.633
0.242	8	-0.809	1.045	30	-1.24	1.847	52	-1.403	2.7	74	-1.732
0.26	8.5	-0.867	1.063	30.5	-1.202	1.866	52.5	-1.52	2.721	74.5	-1.685
0.278	9	-0.791	1.081	31	-1.288	1.884	53	-1.54	2.741	75	-1.71
0.297	9.5	-0.876	1.099	31.5	-1.292	1.902	53.5	-1.55	2.761	75.5	-1.777
0.315	10	-0.899	1.118	32	-1.198	1.92	54	-1.569	2.782	76	-1.767
0.333	10.5	-0.89	1.136	32.5	-1.268	1.939	54.5	-1.552	2.802	76.5	-1.809
0.351	11	-0.964	1.154	33	-1.214	1.957	55	-1.628	2.822	77	-1.671
0.37	11.5	-0.885	1.172	33.5	-1.309	1.975	55.5	-1.531	2.843	77.5	-1.81
0.388	12	-0.968	1.191	34	-1.296	1.993	56	-1.522	2.863	78	-1.75
0.406	12.5	-0.902	1.209	34.5	-1.331	2.012	56.5	-1.546	2.883	78.5	-1.788
0.424	13	-0.891	1.227	35	-1.423	2.03	57	-1.544	2.904	79	-1.776
0.443	13.5	-0.986	1.245	35.5	-1.268	2.048	57.5	-1.648	2.924	79.5	-1.783
0.461	14	-0.946	1.264	36	-1.324	2.066	58	-1.586	2.944	80	-1.847
0.479	14.5	-0.965	1.282	36.5	-1.426	2.085	58.5	-1.561	2.965	80.5	-1.822
0.497	15	-0.974	1.3	37	-1.412	2.103	59	-1.543	2.985	81	-1.956
0.516	15.5	-0.966	1.318	37.5	-1.249	2.121	59.5	-1.65	3.006	81.5	-1.926
0.534	16	-0.984	1.337	38	-1.389	2.139	60	-1.626	3.026	82	-1.855
0.552	16.5	-0.974	1.355	38.5	-1.363	2.158	60.5	-1.641	3.046	82.5	-1.888
0.57	17	-1.039	1.373	39	-1.353	2.176	61	-1.608	3.067	83	-1.842
0.589	17.5	-0.962	1.391	39.5	-1.38	2.194	61.5	-1.623	3.087	83.5	-1.979
0.607	18	-0.963	1.41	40	-1.412	2.212	62	-1.655	3.107	84	-1.973
0.625	18.5	-0.972	1.428	40.5	-1.396	2.233	62.5	-1.588	3.128	84.5	-1.982
0.643	19	-1.036	1.446	41	-1.386	2.253	63	-1.667	3.148	85	-2.109
0.662	19.5	-1.033	1.464	41.5	-1.366	2.273	63.5	-1.608	3.168	85.5	-2.028
0.68	20	-1.051	1.483	42	-1.498	2.294	64	-1.625	3.189	86	-2.083
0.698	20.5	-1.007	1.501	42.5	-1.42	2.314	64.5	-1.642	3.209	86.5	-2.01
0.716	21	-1.012	1.519	43	-1.495	2.334	65	-1.558	3.229	87	-2.044
0.735	21.5	-0.935	1.537	43.5	-1.513	2.355	65.5	-1.531	3.25	87.5	-1.982

Table A8-9 Magnetic Susceptibility data for Lake Miski. Continued (2 of 4)

Age ka	Depth (cm)	MS1 SI	Age ka	Depth (cm)	MS1 SI	Age ka	Depth (cm)	MS1 SI	Age ka	Depth (cm)	MS1 SI
3.27	88	-2.052	4.171	110	-2.283	5.083	132	-2.29	5.995	154	-2.427
3.29	88.5	-2.061	4.192	110.5	-2.219	5.104	132.5	-2.274	6.015	154.5	-2.539
3.311	89	-2.044	4.212	111	-2.246	5.124	133	-2.263	6.036	155	-2.449
3.331	89.5	-2.085	4.233	111.5	-2.306	5.145	133.5	-2.204	6.057	155.5	-2.447
3.351	90	-2.063	4.254	112	-2.222	5.166	134	-2.242	6.078	156	-2.509
3.372	90.5	-2.003	4.275	112.5	-2.197	5.186	134.5	-2.252	6.098	156.5	-2.493
3.392	91	-2.172	4.295	113	-2.146	5.207	135	-2.283	6.119	157	-2.427
3.412	91.5	-2.126	4.316	113.5	-2.291	5.228	135.5	-2.255	6.14	157.5	-2.5
3.433	92	-2.155	4.337	114	-2.301	5.249	136	-2.357	6.16	158	-2.546
3.453	92.5	-2.161	4.358	114.5	-2.355	5.269	136.5	-2.307	6.181	158.5	-2.459
3.473	93	-2.216	4.378	115	-2.281	5.29	137	-2.401	6.202	159	-2.454
3.494	93.5	-2.153	4.399	115.5	-2.21	5.311	137.5	-2.369	6.223	159.5	-2.367
3.514	94	-2.165	4.42	116	-2.344	5.332	138	-2.324	6.243	160	-2.509
3.534	94.5	-2.107	4.44	116.5	-2.296	5.352	138.5	-2.215	6.264	160.5	-2.474
3.555	95	-2.155	4.461	117	-2.337	5.373	139	-2.186	6.285	161	-2.575
3.575	95.5	-2.153	4.482	117.5	-2.32	5.394	139.5	-2.272	6.306	161.5	-2.544
3.595	96	-2.092	4.503	118	-2.35	5.414	140	-2.411	6.326	162	-2.569
3.616	96.5	-2.222	4.523	118.5	-2.319	5.435	140.5	-2.266	6.347	162.5	-2.619
3.636	97	-2.2	4.544	119	-2.218	5.456	141	-2.356	6.368	163	-2.521
3.656	97.5	-2.149	4.565	119.5	-2.364	5.477	141.5	-2.29	6.388	163.5	-2.467
3.677	98	-2.114	4.585	120	-2.309	5.497	142	-2.301	6.409	164	-2.49
3.697	98.5	-2.126	4.606	120.5	-2.282	5.518	142.5	-2.432	6.43	164.5	-2.583
3.717	99	-2.12	4.627	121	-2.343	5.539	143	-2.359	6.451	165	-2.464
3.738	99.5	-2.11	4.648	121.5	-2.384	5.559	143.5	-2.405	6.471	165.5	-2.594
3.758	100	-2.275	4.668	122	-2.296	5.58	144	-2.354	6.492	166	-2.506
3.778	100.5	-2.139	4.689	122.5	-2.415	5.601	144.5	-2.386	6.513	166.5	-2.427
3.799	101	-2.197	4.71	123	-2.405	5.622	145	-2.405	6.533	167	-2.593
3.819	101.5	-2.144	4.731	123.5	-2.327	5.642	145.5	-2.341	6.554	167.5	-2.395
3.839	102	-2.038	4.751	124	-2.328	5.663	146	-2.449	6.575	168	-2.463
3.86	102.5	-2.105	4.772	124.5	-2.356	5.684	146.5	-2.346	6.596	168.5	-2.572
3.881	103	-2.068	4.793	125	-2.405	5.705	147	-2.4	6.616	169	-2.58
3.902	103.5	-2.138	4.813	125.5	-2.348	5.725	147.5	-2.35	6.637	169.5	-2.478
3.922	104	-2.102	4.834	126	-2.253	5.746	148	-2.517	6.658	170	-2.369
3.943	104.5	-2.172	4.855	126.5	-2.174	5.767	148.5	-2.478	6.679	170.5	-2.526
3.964	105	-2.209	4.876	127	-2.29	5.787	149	-2.454	6.699	171	-2.457
3.985	105.5	-2.055	4.896	127.5	-2.21	5.808	149.5	-2.51	6.72	171.5	-2.382
4.005	106	-2.176	4.917	128	-2.368	5.829	150	-2.385	6.741	172	-2.432
4.026	106.5	-2.173	4.938	128.5	-2.384	5.85	150.5	-2.555	6.761	172.5	-2.373
4.047	107	-2.171	4.959	129	-2.242	5.87	151	-2.546	6.782	173	-2.353
4.067	107.5	-2.083	4.979	129.5	-2.374	5.891	151.5	-2.48	6.803	173.5	-2.292
4.088	108	-2.227	5	130	-2.253	5.912	152	-2.542	6.824	174	-2.287
4.109	108.5	-2.258	5.021	130.5	-2.354	5.933	152.5	-2.452	6.844	174.5	-2.238
4.13	109	-2.165	5.041	131	-2.248	5.953	153	-2.551	6.865	175	-2.341
4.15	109.5	-2.182	5.062	131.5	-2.41	5.974	153.5	-2.546	6.886	175.5	-2.33

Table A8-9 Magnetic Susceptibility data for Lake Miski. Continued (3 of 4)

Age ka	Depth (cm)	MS1 SI	Age ka	Depth (cm)	MS1 SI	Age ka	Depth (cm)	MS1 SI	Age ka	Depth (cm)	MS1 SI
6.907	176	-2.235	7.693	198	-2.696	8.051	220	-2.636	8.409	242	-2.497
6.927	176.5	-2.266	7.701	198.5	-2.742	8.059	220.5	-2.623	8.417	242.5	-2.476
6.948	177	-2.256	7.709	199	-2.615	8.067	221	-2.494	8.426	243	-2.347
6.969	177.5	-2.342	7.717	199.5	-2.725	8.075	221.5	-2.607	8.434	243.5	-2.3
6.989	178	-2.497	7.725	200	-2.804	8.083	222	-2.577	8.442	244	-2.451
7.01	178.5	-2.63	7.733	200.5	-2.76	8.092	222.5	-2.502	8.45	244.5	-2.549
7.031	179	-2.642	7.741	201	-2.914	8.1	223	-2.593	8.458	245	-2.369
7.052	179.5	-2.578	7.75	201.5	-2.849	8.108	223.5	-2.531	8.466	245.5	-2.342
7.072	180	-2.66	7.758	202	-2.82	8.116	224	-2.623	8.474	246	-2.457
7.093	180.5	-2.555	7.766	202.5	-2.81	8.124	224.5	-2.646	8.483	246.5	-2.47
7.114	181	-2.598	7.774	203	-2.833	8.132	225	-2.665	8.491	247	-2.372
7.134	181.5	-2.644	7.782	203.5	-2.863	8.14	225.5	-2.7	8.499	247.5	-2.407
7.155	182	-2.695	7.79	204	-2.835	8.149	226	-2.652	8.507	248	-2.402
7.176	182.5	-2.605	7.798	204.5	-2.82	8.157	226.5	-2.57	8.515	248.5	-2.375
7.197	183	-2.605	7.807	205	-2.885	8.165	227	-2.579	8.523	249	-2.333
7.217	183.5	-2.658	7.815	205.5	-2.77	8.173	227.5	-2.699	8.531	249.5	-2.319
7.238	184	-2.637	7.823	206	-2.804	8.181	228	-2.725	8.54	250	-2.275
7.259	184.5	-2.707	7.831	206.5	-2.745	8.189	228.5	-2.724	8.548	250.5	-2.179
7.28	185	-2.771	7.839	207	-2.818	8.198	229	-2.74	8.556	251	-2.227
7.3	185.5	-2.779	7.847	207.5	-2.733	8.206	229.5	-2.783	8.564	251.5	-2.075
7.321	186	-2.657	7.855	208	-2.8	8.214	230	-2.76	8.572	252	-2.048
7.342	186.5	-2.812	7.864	208.5	-2.81	8.222	230.5	-2.802	8.58	252.5	-2.034
7.362	187	-2.607	7.872	209	-2.687	8.23	231	-2.825	8.588	253	-1.99
7.383	187.5	-2.76	7.88	209.5	-2.787	8.238	231.5	-2.733	8.597	253.5	-1.917
7.404	188	-2.777	7.888	210	-2.74	8.246	232	-2.765	8.605	254	-1.889
7.425	188.5	-2.79	7.896	210.5	-2.733	8.255	232.5	-2.685	8.613	254.5	-1.892
7.445	189	-2.605	7.904	211	-2.661	8.263	233	-2.735	8.621	255	-1.837
7.466	189.5	-2.701	7.912	211.5	-2.725	8.271	233.5	-2.679	8.629	255.5	-1.718
7.487	190	-2.783	7.921	212	-2.74	8.279	234	-2.837	8.637	256	-1.69
7.507	190.5	-2.694	7.929	212.5	-2.593	8.287	234.5	-2.91	8.645	256.5	-1.617
7.528	191	-2.756	7.937	213	-2.706	8.295	235	-2.749	8.654	257	-1.663
7.549	191.5	-2.787	7.945	213.5	-2.687	8.303	235.5	-2.733	8.662	257.5	-1.575
7.57	192	-2.587	7.953	214	-2.657	8.312	236	-2.636	8.67	258	-1.562
7.59	192.5	-2.683	7.961	214.5	-2.724	8.32	236.5	-2.683	8.678	258.5	-1.502
7.611	193	-2.71	7.969	215	-2.654	8.328	237	-2.792	8.686	259	-1.542
7.619	193.5	-2.628	7.978	215.5	-2.577	8.336	237.5	-2.683	8.694	259.5	-1.637
7.627	194	-2.727	7.986	216	-2.695	8.344	238	-2.645	8.702	260	-1.639
7.636	194.5	-2.752	7.994	216.5	-2.616	8.352	238.5	-2.587	8.711	260.5	-1.665
7.644	195	-2.709	8.002	217	-2.68	8.36	239	-2.719	8.719	261	-1.9
7.652	195.5	-2.731	8.01	217.5	-2.654	8.369	239.5	-2.577	8.727	261.5	-2.133
7.66	196	-2.688	8.018	218	-2.687	8.377	240	-2.618	8.735	262	-2.134
7.668	196.5	-2.826	8.026	218.5	-2.766	8.385	240.5	-2.582	8.743	262.5	-2.191
7.676	197	-2.703	8.035	219	-2.659	8.393	241	-2.594	8.751	263	-2.043
7.684	197.5	-2.694	8.043	219.5	-2.544	8.401	241.5	-2.466	8.759	263.5	-2.13

Table A8-9 Magnetic Susceptibility data for Lake Miski. Continued (4 of 4)

Age ka	Depth (cm)	MS1 SI	Age ka	Depth (cm)	MS1 SI	Age ka	Depth (cm)	MS1 SI	Age ka	Depth (cm)	MS1 SI
8.768	264	-2.069	9.975	286	-1.51	11.579	308	-1.236	12.635	330	4.848
8.776	264.5	-2.107	10.012	286.5	-1.546	11.615	308.5	-1.146	12.636	330.5	5.413
8.784	265	-2.095	10.048	287	-1.589	11.652	309	-1.201	12.638	331	5.83
8.792	265.5	-2.023	10.085	287.5	-1.609	11.688	309.5	-1.131	12.639	331.5	6.155
8.8	266	-2.066	10.121	288	-1.658	11.725	310	-0.933	12.641	332	6.501
8.808	266.5	-1.992	10.157	288.5	-1.683	11.761	310.5	-0.857	12.642	332.5	6.745
8.816	267	-2.021	10.194	289	-1.767	11.798	311	-0.785	12.643	333	7.053
8.825	267.5	-2.015	10.23	289.5	-1.747	11.834	311.5	-0.668	12.645	333.5	7.748
8.833	268	-1.978	10.267	290	-1.675	11.871	312	-0.744	12.646	334	7.58
8.841	268.5	-2.039	10.303	290.5	-1.715	11.907	312.5	-0.707	12.647	334.5	8.019
8.849	269	-1.942	10.34	291	-1.684	11.944	313	-0.669	12.649	335	8.313
8.857	269.5	-2.013	10.376	291.5	-1.656	11.98	313.5	-0.602	12.65	335.5	8.406
8.865	270	-2.023	10.413	292	-1.608	12.016	314	-0.433	12.652	336	8.445
8.874	270.5	-2.044	10.449	292.5	-1.642	12.053	314.5	-0.364	12.653	336.5	8.843
8.882	271	-1.919	10.485	293	-1.679	12.089	315	-0.147	12.654	337	8.983
8.918	271.5	-2.017	10.522	293.5	-1.697	12.126	315.5	-0.073	12.656	337.5	9.004
8.955	272	-2.065	10.558	294	-1.707	12.162	316	0.073	12.657	338	8.957
8.991	272.5	-2.034	10.595	294.5	-1.818	12.199	316.5	0.147	12.658	338.5	9.095
9.027	273	-1.901	10.631	295	-1.933	12.235	317	0.291	12.66	339	8.807
9.064	273.5	-2.206	10.668	295.5	-1.928	12.272	317.5	0.305	12.661	339.5	8.85
9.1	274	-2.074	10.704	296	-1.951	12.308	318	0.377	12.663	340	8.96
9.137	274.5	-1.885	10.741	296.5	-2.146	12.456	318.5	0.451	12.664	340.5	8.752
9.173	275	-1.844	10.777	297	-2.18	12.605	319	0.505	12.665	341	8.876
9.21	275.5	-1.786	10.814	297.5	-2.157	12.606	319.5	0.579	12.667	341.5	8.859
9.246	276	-1.766	10.85	298	-2.28	12.608	320	0.69	12.668	342	9.084
9.283	276.5	-1.68	10.886	298.5	-2.356	12.609	320.5	0.758	12.669	342.5	9.06
9.319	277	-1.558	10.923	299	-2.342	12.61	321	0.831	12.671	343	9.161
9.355	277.5	-1.518	10.959	299.5	-2.471	12.612	321.5	0.901	12.672	343.5	9.048
9.392	278	-1.654	10.996	300	-2.442	12.613	322	0.94	12.674	344	8.647
9.428	278.5	-1.697	11.032	300.5	-2.257	12.614	322.5	1.081	12.675	344.5	8.545
9.465	279	-1.515	11.069	301	-2.158	12.616	323	1.276	12.676	345	8.701
9.501	279.5	-1.494	11.105	301.5	-2.261	12.617	323.5	1.429	12.678	345.5	8.1
9.538	280	-1.354	11.142	302	-2.201	12.619	324	1.634	12.679	346	7.673
9.574	280.5	-1.268	11.178	302.5	-2.421	12.62	324.5	1.852	12.68	346.5	7.403
9.611	281	-1.448	11.215	303	-2.318	12.621	325	1.868	12.682	347	7.9
9.647	281.5	-1.571	11.251	303.5	-2.235	12.623	325.5	2.081	12.683	347.5	8.187
9.684	282	-1.632	11.287	304	-2.152	12.624	326	2.021	12.685	348	8.401
9.72	282.5	-1.662	11.324	304.5	-2.166	12.625	326.5	2.163	12.686	348.5	8.413
9.756	283	-1.736	11.36	305	-1.871	12.627	327	2.234	12.687	349	8.747
9.793	283.5	-1.708	11.397	305.5	-1.792	12.628	327.5	2.771	12.689	349.5	8.91
9.829	284	-1.639	11.433	306	-1.606	12.63	328	3.187	12.69	350	9.466
9.866	284.5	-1.693	11.47	306.5	-1.434	12.631	328.5	3.615	12.691	350.5	10.272
9.902	285	-1.706	11.506	307	-1.368	12.632	329	3.971	12.693	351	10.671
9.939	285.5	-1.552	11.543	307.5	-1.339	12.634	329.5	4.165	12.694	351.5	10.764